Geostatistical and Stochastic Approaches to Incorporation of Heterogeneity in Mill Tailings Hydraulic Properties into Numerical Models: Implications for Seepage Prediction Uncertainty

by

James A. Beach

Submitted in Partial Fulfillment
of the Requirements for the Degree
of Master of Science in Hydrology

New Mexico Institute of Mining and Technology
Socorro, New Mexico

July, 1989

ABSTRACT

A numerical modeling study is completed in order to address the uncertainty in seepage predictions from a variably saturated tailings impoundment. Spatial variability in hydraulic properties is treated in both a deterministic and stochastic framework. A deterministic approach is taken to implement uncertainty in boundary conditions for the model. In contrast to most deterministic studies of mill tailings seepage, an effort is made to incorporate the spatial heterogeneity of hydraulic properties observed in the field. Multiple regression and kriging are used to determine hydraulic property fields which are used as input into the numerical model. The results of numerous simulations suggest that incorporation of major spatial trends in hydraulic properties into numerical models is of vital importance in correctly predicting seepage distributions from tailings impoundments. One and two-dimensional modeling approaches of the tailings impoundment result in enormous differences in seepage predictions. Two-dimensional deterministic simulations show that proper incorporation of boundary conditions into the mathematical model is a very important but difficult step in the modeling process. The results suggest that hydraulic gradients exhibiting even a small horizontal component can lead to significant horizontal flux rates in heterogeneous, anisotropic porous media. Uncertainty in hydraulic properties is handled by incorporating a stochastic conceptualization in order to produce several realizations of the saturated hydraulic conductivity field. "Quasi" Monte Carlo simulations show that variance and correlation structure in the hydraulic property fields indeed affects the uncertainty in the seepage predictions; however, variance in output parameters is also highly dependent on the boundary conditions implemented in the model. Under many field conditions, uncertainty in boundary conditions is expected to be the primary source of uncertainty in model output. In general, the random nature of the saturated hydraulic conductivity does not impart substantial variance in the output parameters if relatively small hydraulic gradients exist in the flow domain. On the other hand, given the same uncertainty in hydraulic property fields, model output variance increases in the variably saturated flow regime when fluid is being forced through the system under higher hydraulic gradients. Therefore, in delineating flow phenomena under some unsaturated flow conditions, it may be more important to consider major spatial trends in hydraulic properties and uncertainty in boundary conditions than to consider small scale heterogeneities and the associated uncertainty in the hydraulic properties. Conditioning hydraulic property data through geostatistical kriging is shown to reduce the variability in seepage predictions when hydraulic properties are correlated over significant distances. Results of the study suggest that relatively simple procedures may be used to reduce seepage from prospective and abandoned waste impoundments.

TABLE OF CONTENTS

LIST OF FIGURES

LIST OF FIGURES (continued)

LIST OF FIGURES (continued)

LIST OF FIGURES (continued)

LIST OF FIGURES (continued)

LIST OF FIGURES (continued)

LIST OF TABLES

ACKNOWLEDGEMENTS

Funds for this research were provided by the U.S. Bureau of Mines Generic Research Center on Waste Treatment and Recovery at the University of Nevada Reno under Project No. 3504 entitled "Characterization of Spatial Variability in Mill Tailings Hydraulic Properties".

The following individuals contributed to this research: Deborah McElroy, Gregory Lewis, Alva Parsons–Mattson, Robert Mace, Dr. Peter Huyakorn, Dr. John L. Wilson, Dr. Dave Peterson, Annette Schafer–Perini, and Dr. Jim McCord.

ACKNOWLEDGMENTS

Acknowledgment for funding of this research goes to U.S. Bureau of Mines Generic Research Center on Waste Treatment and Recovery at the University of Nevada Reno under Project No. 3504 entitled "Characterization of Spatial Variability in Mill Tailings Hydraulic Properties".

I wish to express thanks to my research advisors and friends Dr. Daniel Stephens and Dr. Allan Gutjahr. Their support and superior guidance made this a more organized and beneficial report. I want to especially thank them for allowing me to pursue my own ideas as I learned from their advice and consultation.

Thanks also to Dr. Peter Huyakorn and Dr. John Wilson for their helpful suggestions during the course of this research. Dr. Dave Peterson, Annette Schafer-Perini, and Dr. Jim McCord frequently offered valuable assistance which allowed this research to progress on a day to day basis.

My many friends at New Mexico Tech made the stay in Socorro a crazy and memorable experience. Thanks to all!

A special thanks to my entire family for their love and support from the very beginning.

CHAPTER 1

INTRODUCTION

Mill tailings are crushed ore which have been largely depleted of the profitable minerals. Tailings impoundments are often used to store the tailings which are by-products of a series of crushing and chemical treatments designed to extract minerals from the ore. After the extraction process, tailings are generally delivered to an impoundment site in the form of a slurry which is then deposited in such a way that the slurry liquid can be decanted and reused in the milling process. Disposal techniques include placing the slurry in a tailings dam *[Johnson (1987), Kealy (1970)]* or nozzling the slurry under pressure into the impoundment *[Lewis, 1985]*. Figure 1.1 shows a cross-section of a conceptualized mill tailings impoundment in which the slurry is placed at the edges of the impoundment and allowed to deposit sediment as the fluid flows under gravity forces toward the center of the impoundment. This technique initially allows sedimentation of the coarsest particles at the point of origin and successively finer factions of the slurry migrate to the interior portions of the impoundment. This type of depositional system produces significant heterogeneity but also some degree of correlation in the grain size distribution throughout the impoundment. This spatial variability in particle size causes a large variation in the hydraulic properties which are a key parameter in determining seepage and the spatial variability in the seepage from these impoundments.

Numerical models may be used to quantify the seepage rates from mill tailings impoundments. These numerical models are implemented in computer codes which are designed to solve the mathematical equations which govern the

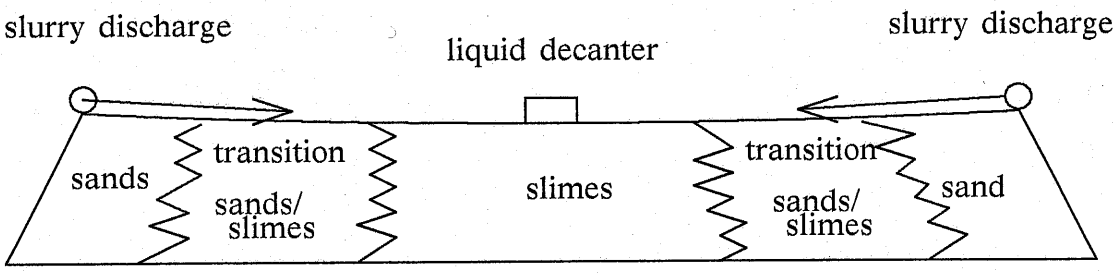

Figure 1.1 Conceptual model of porous media variation within a tailings impoundment.

flow of fluids in porous media. In order to accurately simulate seepage from waste impoundments, some knowledge of the spatial distribution of the hydraulic properties is required. Insight into the nature of the spatial variability in hydraulic properties allows a more accurate prediction of the quantity of seepage from the impoundment as well as the spatial variability of the seepage. Knowledge of the spatial distribution of the seepage rates is a very important factor which can aid in efficient design of remedial action programs in abandoned impoundments as well as in the proper design of prospective impoundments in order to minimize seepage from the impoundments and possible groundwater contamination.

Another important aspect of seepage prediction which should be addressed in any model study is the uncertainty associated with the prediction. Modeling a field scale system with a mathematical model demands that many assumptions be incorporated into the conceptual model. How does one verify that the assumptions made in the conceptual model do not invalidate the prediction from the model? If the assumptions made in the conceptual model do not agree with the true field conditions, some uncertainty is introduced into the prediction. It is critical to realize that any conceptual model contains inherent

weaknesses which will lead to an uncertainty in the prediction obtained from the model. Obviously, it is impossible to fully mimic true field conditions in any mathematical model. However, when a mathematical model is incorporated to predict present or future conditions based on data assumed to be representative of past conditions, it is important to understand how the model assumptions will affect the final predictions. If the hydraulic properties are assumed to be uncertain, analysis can be completed to determine the sensitivity of the model output to the uncertainty of the hydraulic properties. *McLauglin [1988]* identifies four factors which determine model accuracy: natural heterogeneity, input estimation, data collection, and model structure. The first part of this study will concentrate mainly on outlining the important aspects of incorporating heterogeneity of hydraulic properties into numerical models and to determine other input variables which have a significant effect on the model predictions. Another goal of the this study is to determine the usefulness of stochastic approaches for incorporation of spatial variability of hydraulic properties into conceptual models designed to predict seepage rates and saturation profiles in waste impoundments.

Prediction of the magnitude and direction of moisture movement from waste impoundment sites is the first step in determining the propensity for groundwater contamination. *Narasimhan [1986]* and *Smith and Schwartz [1981c]* emphasize the importance of determination of the dynamics of the flow system prior to analyzing transport phenomena. Without accurate predictions of velocity distributions and saturation profiles, the accuracy of contaminant transport predictions from these impoundments is limited. Accurate representation of transport phenomena in mill tailings and other impoundments containing high concentrations of chemical constituents is a very complex issue. It would be valuable to understand the flow phenomena prior to undertaking any studies

concerning transport of chemical constituents. Of course, the flow and transport processes are not completely separate phenomena; for example, it may be possible for chemical reactions to alter hydraulic conductivity at some impoundments. However, a good understanding of the spatial variability of the seepage in these impoundments is a prerequisite to accurate predictions of contaminant transport.

Motivation for Study

Hydrologists and engineers involved in numerical modeling exercises aimed at determining the amount of seepage from waste impoundment sites are often faced with the problem of accurately characterizing and incorporating heterogeneity in hydraulic properties into mathematical models. In groundwater hydrology studies, there is almost always a need for more data concerning the spatial distribution of hydraulic properties in the domain being studied. More often than not, a very limited amount of information concerning spatial distribution of hydraulic properties is available, and most often extensive amounts of data can not be obtained due to budget restrictions. Given these restraints, modelers must design a field of hydraulic properties that serves as a reasonable representation of actual field properties so that accurate estimates of seepage can be obtained. Regardless of the methods used to characterize and incorporate the spatial variability into the model, there is always some degree of uncertainty associated with the prediction of the hydraulic property field. Though the final prediction sought is that of the seepage magnitude and spatial distribution along the base of an impoundment, it is important to realize what effect the prediction of the hydraulic property field has on the predicted seepage field.

Approach of the Study

Most modeling studies of tailings impoundments to date have been deterministic in nature. In other words, the predictions were obtained from simulations which were performed with a given set of input parameters (e.g. hydraulic properties). In the present study, conceptual models will be implemented which are based on a three different model approaches: a deterministic conceptualization, a stochastic–deterministic conceptualization, and a conditional simulation approach. This approach will allow comparison of different conceptual models which may be used in an effort to delineate flow phenomena in a variably saturated impoundment.

In deterministic simulations, the hydraulic properties of the domain are assumed to be known at all points. The numerical model is then used to obtain a steady–state solution to the problem with the given hydraulic property field and boundary conditions. This approach is often taken to determine flow phenomena and seepage rates from waste impoundments. However, since deterministic simulations do not incorporate uncertainty in hydraulic properties, regulators and operators of mill tailings impoundments can not gain insight into the uncertainty of the seepage field.

Stochastic–deterministic simulations assume hydraulic properties of the domain can be defined according to certain stochastic behavior. Hydraulic properties are assumed to exhibit some mean value in space as well as some random behavior about the mean. Under these assumptions, "unconditional" realizations of hydraulic property fields can produced from measured or assumed statistical properties of the media. With this approach, many realizations of the hydraulic property field can be generated which have the same statistical properties which are assumed or estimated from field data. These fields can then

be used as input into numerical models. The statistical properties of the seepage field from many simulations can then be calculated to illuminate the uncertainty of the model prediction at any point in the impoundment. This procedure is known as Monte Carlo simulation. Due to the immense size and complexity of the problem in this study, a full Monte Carlo approach is not feasible. Therefore, a relatively small number of simulations will be performed in order to determine the statistics of the model output variables.

The conditional simulation approach, like the stochastic–deterministic conceptualization assumes that the statistical moments of the hydraulic properties are known. Unlike stochastic–deterministic simulations however, the hydraulic properties at "measured points" are held at their respective values while the properties at other points in the domain are given a stochastic distribution according to the assumed or measured covariance structure. A geostatistical technique known as kriging is used to implement this procedure. With this approach, many "conditioned" hydraulic property fields can be determined and used as input into a numerical model to determine the effect of the spatial distribution of the hydraulic properties. The statistical properties of the model predictions from several simulations can then be determined in order to quantify the variation in model output parameters given the uncertainty in the hydraulic property field, while at the same time incorporating the data that is observed in the field. Once again, due to the immense size and complexity of the problem in this study, a full Monte Carlo approach is not feasible, therefore only a few simulations will be performed using different conditioned hydraulic property fields to determine statistics for model output.

Many designs have been proposed to combat the possible contamination problems of seepage originating from tailings impoundments and other waste storage facilities. Some of these designs involve relocation of the pile

while others involve using artificial or natural covers to decrease the quantity of infiltration into the impoundment and thus decrease the amount of contaminated seepage emanating from the impoundment. Reshaping the surface of the abandoned impoundment is also another option to decrease the quantity of infiltration into the impoundment. The results of the study also reveal important practical implications which should be considered in remedial design. In an effort to impart more practicality in this study, I also address issues which are important in waste impoundment remediation and groundwater protection.

CHAPTER 2

PREVIOUS WORK ON MILL TAILINGS

Much of the work concerning tailings impoundments and seepage through tailings dams has come from a geotechnical perspective in which the main concern was determining the safety and stability of tailings dams. Only in the past decade have serious efforts been made to determine the quantity of seepage from tailings disposal impoundments and the propensity for this effluent to degrade groundwater quality. Many waste impoundments are several decades old but have only recently come to the attention of the public sector because they may threaten the quality of valuable groundwater resources. The time delay for possible contaminants from these impoundments to reach groundwater resources and the misconceptions about the flow and transport phenomena governing these processes has allowed a "play now and pay later" attitude amongst regulators and site operators. In this chapter, a brief description of some of the previous work pertinent to this study is reviewed.

Previous Characterization of Mill Tailings Hydraulic Properties

Previous to this study, extensive characterization of a mill tailings impoundment had been completed. Due to legal and professional considerations, the correct name and exact location of the mill tailings impoundment will not be mentioned in this work. Comprehensive field work included sampling the impoundment along horizontal and vertical transects so that a complete vertical cross-section could be characterized. The main focus of the sampling procedure

was characterization of hydraulic properties which are important as input into numerical models. Another objective of the sampling procedure was to determine the in situ moisture content of the tailings so that some practical insight could be gained as to the conditions present in the pile during different seasons of the year. The hydraulic properties determined in the previous study were saturated hydraulic conductivity, porosity, moisture content at 1.5 and 15 bars of negative pressure, soil moisture characteristic curves, and particle size distribution. For a complete description of the sampling procedures, lab and field methods, as well as a complete presentation of the results of the characterization, the reader is referred to the Independent Studies in Hydrology by *Johnson [1987]* and *Harris [1987]*.

A brief presentation of the results of the previous characterization work is given here in order to familiarize the reader with the type of spatial variability present in the hydraulic properties of mill tailings impoundments. In general, the conceptual models used in the present study will attempt to incorporate the general heterogeneity found in mill tailings impoundments but will avoid the total dependence on the acquired data since some conceptual models used in this study will rely on statistical properties of the data which were not determined in past studies. We expect most of the generalizations made about the heterogeneity of these tailings are applicable to other impoundments which are deposited in a similar fashion as the mill tailings impoundment studied by Johnson *[1987]*.

The mill tailings impoundment was a relatively small tailings enclosure. The full vertical cross section which was sampled and characterized is 104 meters long and about 5 meters deep. The small size of the impoundment and relatively cheap graduate research assistant labor costs allowed sampling to be completed on a fairly dense grid. In order to characterize the vertical

saturated hydraulic conductivity along a transect through the center of the pile, shelby tubes were used to obtain samples laterally at a separation distance of 4–5 meters and at several depths. Lab analysis of the shelby tubes was then completed in order to determine the saturated conductivity over 13 cm. ranges using a constant head permeameter. Continuous vertical transects at six different locations across the impoundment were also obtained using shelby tubes. One hundred cubic centimeter ring samples were then extracted from these tubes at 50 centimeter intervals and soil moisture characteristic curves were determined in the lab using hanging column and pressure plate methods.

Figure 2.1 shows the cross section of the impoundment and the position of neutron probe access tubes. As a brief summary of the moisture conditions present in the impoundment throughout the year, Figures 2.2 – 2.4 shows the moisture conditions in three vertical transects in which neutron probe access tubes were placed. These graphs were generated from data taken from *Johnson [1987].* This data from these transects was chosen because they represent the relative zones described in the conceptual model shown in Figure 1.1. These figures show moisture content throughout the year for the three major zones of media present in the impoundment. Note that the moisture content at all levels of the transect in the transition zone (Figure 2.3) are relatively higher than in the sand zone or the slime zone. This phenomena is due to the layering of coarse and fine grained media which occurs in this portion of the pile. The alternating coarse and fine grain layers set up an effective barrier to vertical moisture flow in the unsaturated zone because the hydraulic conductivity of the coarser media is much lower then the fine grained media under unsaturated conditions. It is important to point out that at distances greater than 50cm below the impoundment surface, the moisture contents in the slime zone (Figure 2.4) are relatively low (roughly 50% saturated). This is especially interesting when we

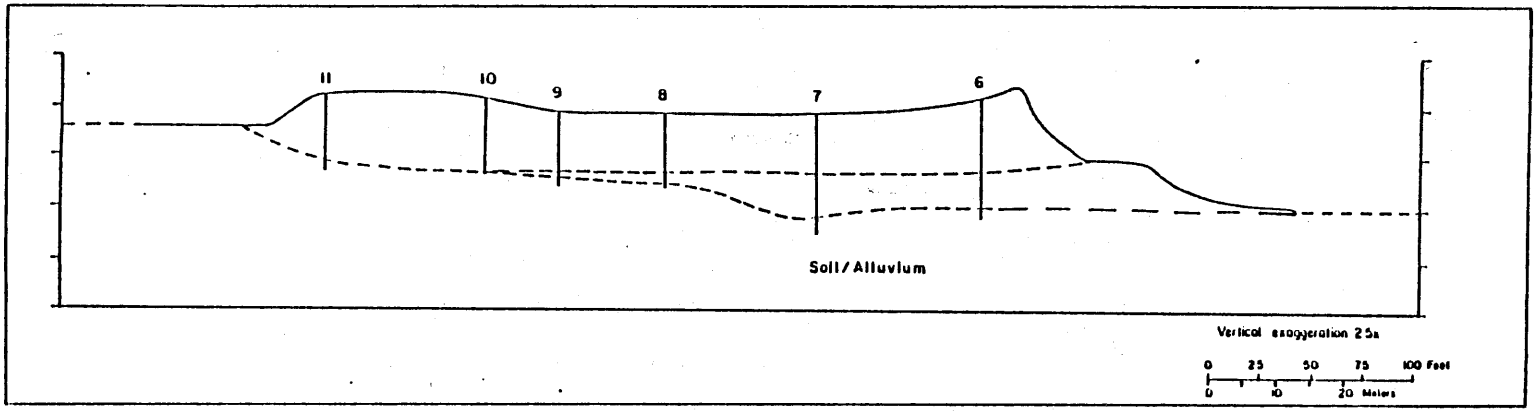

Figure 2.1. Cross section of tailings impoundment showing location of neutron-probe access tubes. (after *Johnson [1987]*)

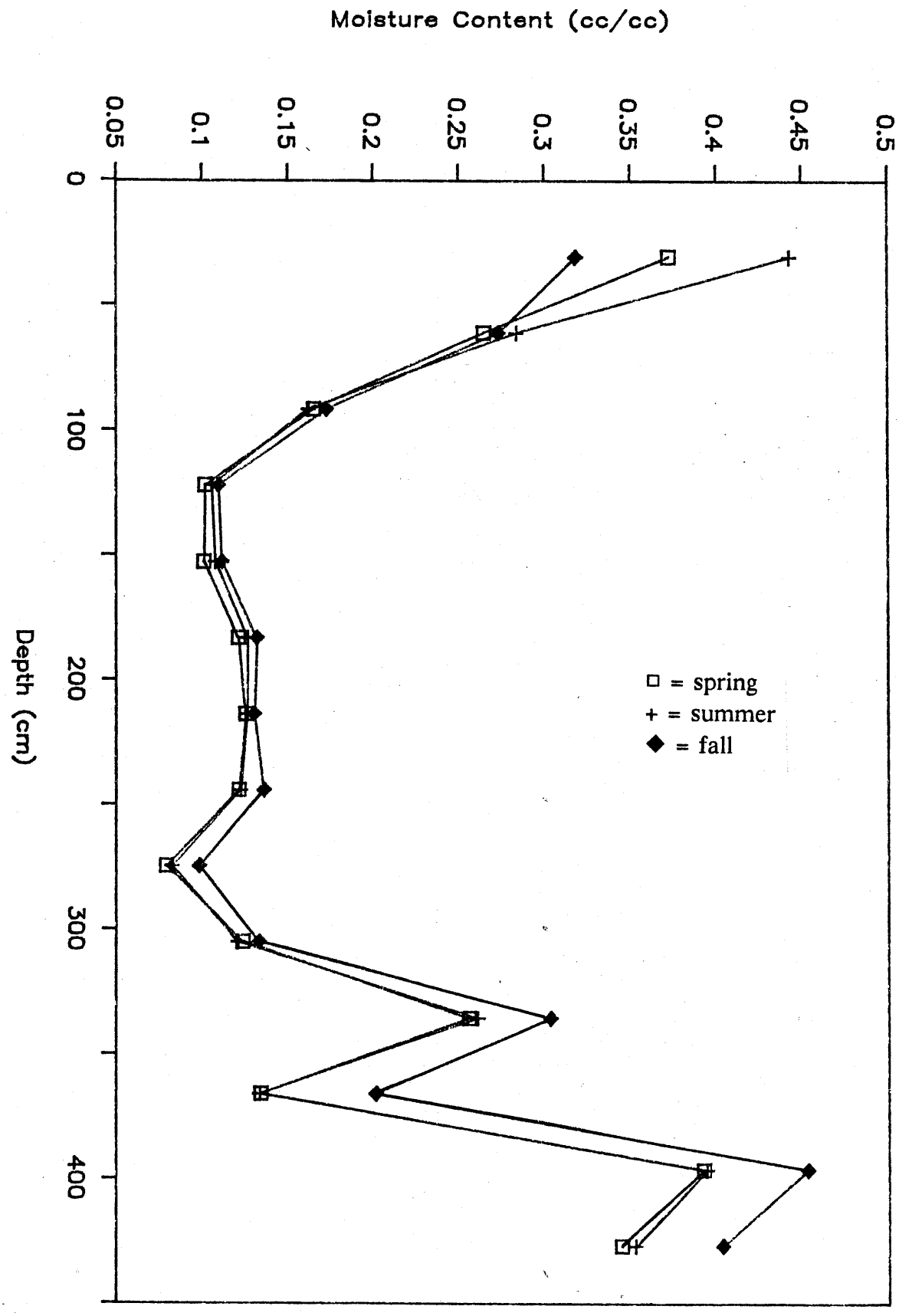

Figure 2.2 Moisture profile of the sand zone at different times of the year.

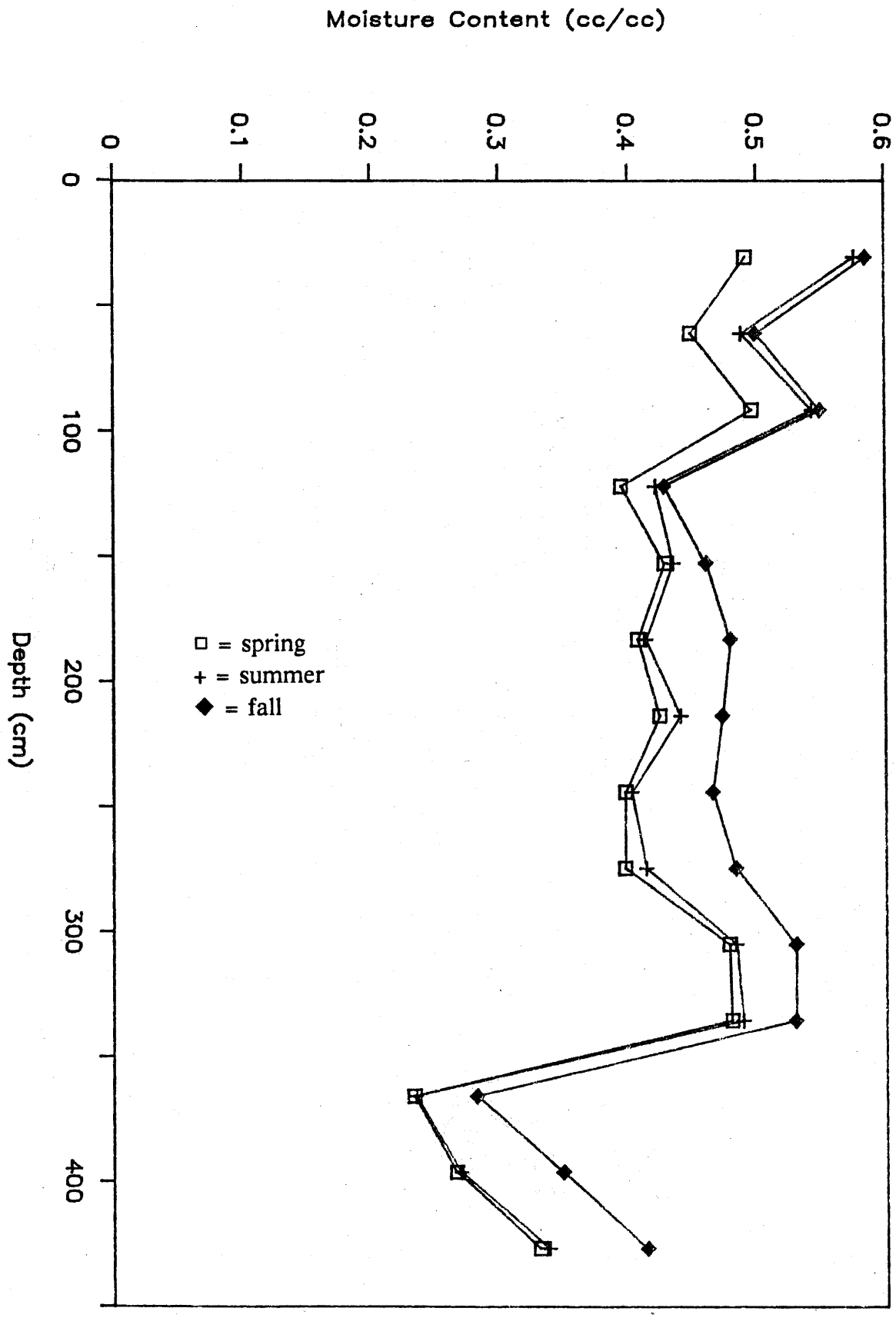

Figure 2.3. Moisture profile of the transition zone at different times of the year.

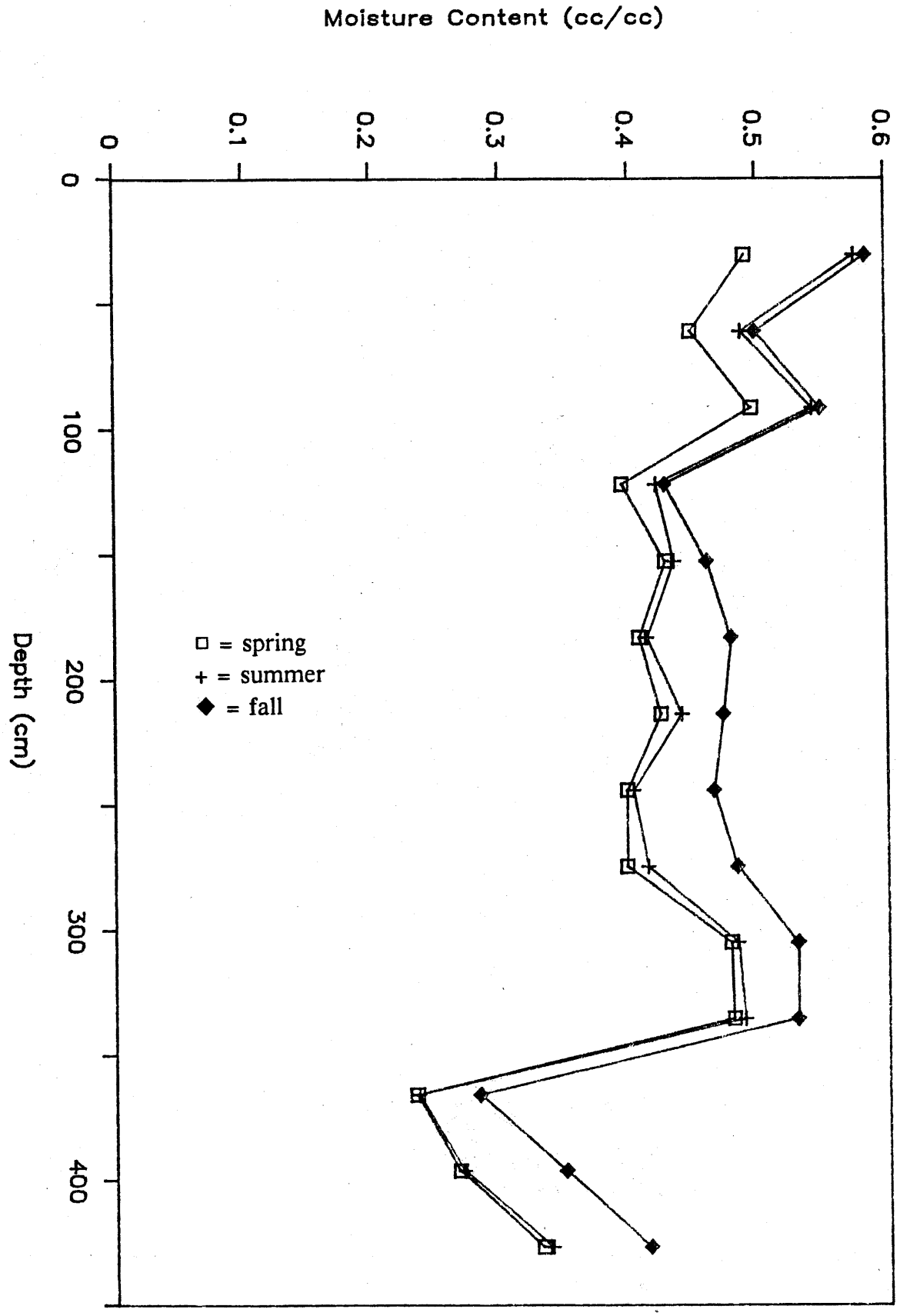

Figure 2.3. Moisture profile of the transition zone at different times of the year.

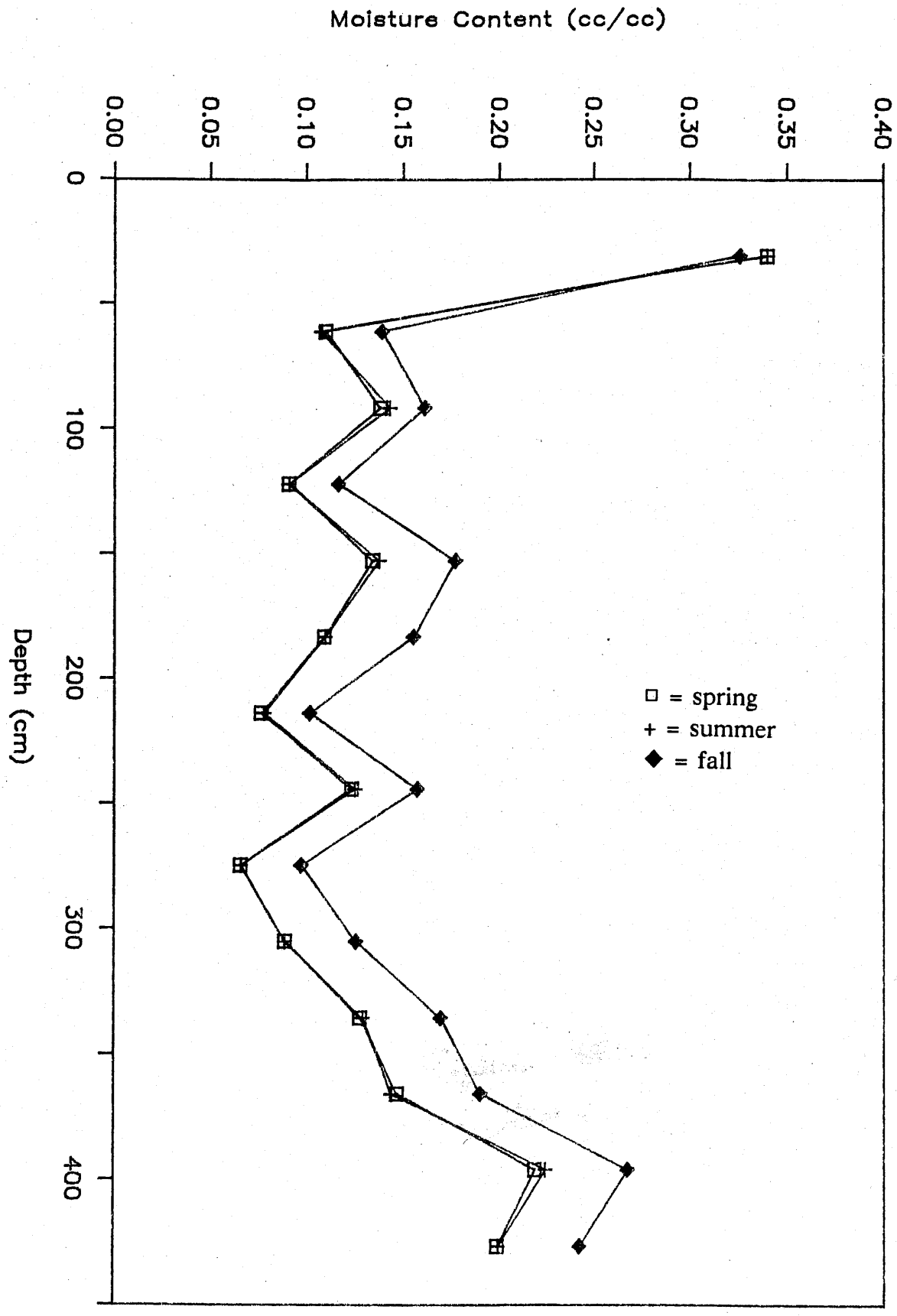

Figure 2.4. Moisture profile of the slime zone at different times of the year.

consider that a pond existed at the surface of the slime zone for extended periods of the spring and summer seasons. It is also apparent from these figures that the moisture content at different points in the tailings impoundment is relatively constant throughout the year. This result does not imply that the pile is in a constant steady state of equilibrium but it does suggest that it is possible to gain insight into the seepage rates at the base of the impoundment by determining the flux rates in the impoundment under steady state conditions.

Particle size distribution throughout the impoundment exhibited very drastic changes, both laterally and vertically. Figure 2.5 shows the extreme particle size distributions exhibited in the impoundment across the vertical cross section that was sampled. This figure shows that the particle sizes vary by four orders of magnitude and description of the media range from clay to sands. One simple but interesting artifact of the data is shown in Figure 2.6. The coefficient of variation for different parameters in each vertical transect is plotted as a function of distance along the vertical cross section. The coefficient of variation is defined as the ratio of the mean to the standard deviation for a given data set. The figure shows that the coefficient of variation for the 50% particle size is relatively constant across the entire cross section. However, the coefficient of variation for the moisture content and saturated hydraulic conductivity show significantly lower values in the center of the cross section which contains the "slime" zone. Even though the particle size of the "slime" zone contains roughly the same variation as the other portions of the impoundment (figure 2.6), the hydraulic properties and moisture content distributions show less variation. This is expected since the relative size of the particles and the particle size variation are smaller than the size and particle size variation in the sandy portions of the pile. Thus, the relative effect of the particle size variation has less significant effects on hydraulic properties at this smaller scale. This result is

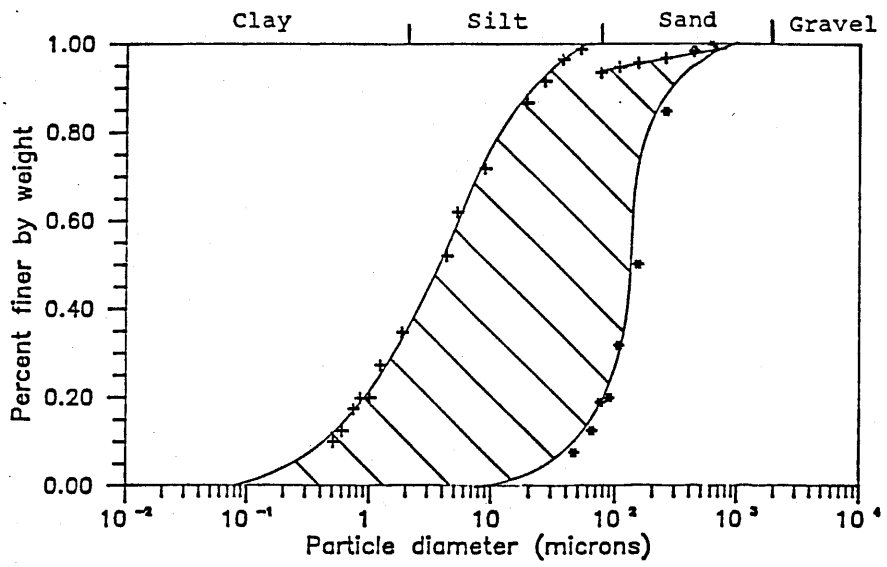

Figure 2.5. Range of grain size curves exhibited throughout an impoundment cross section. (after *Johnson [1987]*)

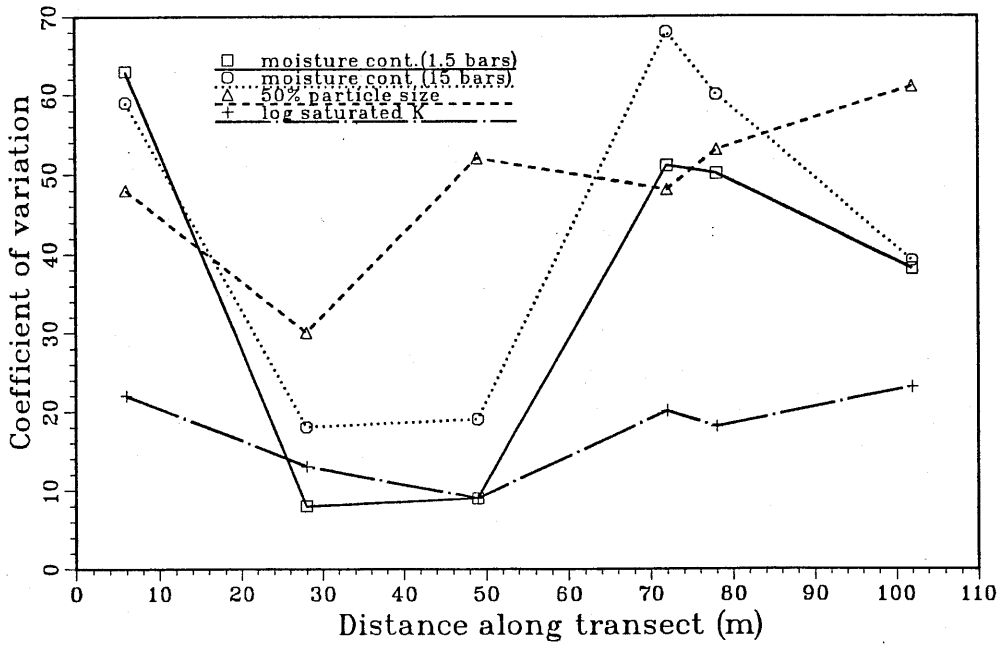

Figure 2.6 Coefficient of variation for various properties throughout an impoundment.

important to consider when defining the variability of hydraulic properties for the slime zone, especially if this variability is based on the particle size variation.

Soil moisture characteristic curves determined from tailings samples exhibit large variations due to the enormous contrast in the particle size distribution in the impoundment. Figure 2.7 shows various soil moisture characteristic curves for tailings samples taken in different portions of the impoundment. Proper characterization of the spatial variability in the soil moisture characteristic relationships is very important when numerical models are used to determine the spatial variability in unsaturated flow components.

Saturated hydraulic conductivity is a fundamental media property and one of the most important variables needed for numerical modeling studies of the vadose zone. Therefore, great effort was taken to properly identify the spatial variability in this property. Figures 2.8 and 2.9 show the distribution of the log of the saturated hydraulic conductivity along the horizontal transects for different depths. In general, it was discovered that the hydraulic conductivity shows less variation at greater depths. This is most likely due to the chemical processes that have altered the properties of the tailings at the surface of the impoundment by partial cementation of the particles. Figures 2.10 and 2.11 show the vertical distribution of saturated hydraulic conductivity at two locations in the pile. Obviously, tremendous changes in the saturated conductivity occur over very short distances in the vertical direction. The saturated hydraulic conductivity changes much more quickly than in the vertical direction than in the horizontal direction. These variations in the hydraulic conductivity will be greatly amplified as the media becomes less saturated. This phenomena is shown in Figure 2.12 for various types of media present in tailings impoundments. Figure 2.12 shows that the hydraulic conductivity of the sand decreases very rapidly as the capillary pressure increases and thus the moisture content in the soil decrease. The slime

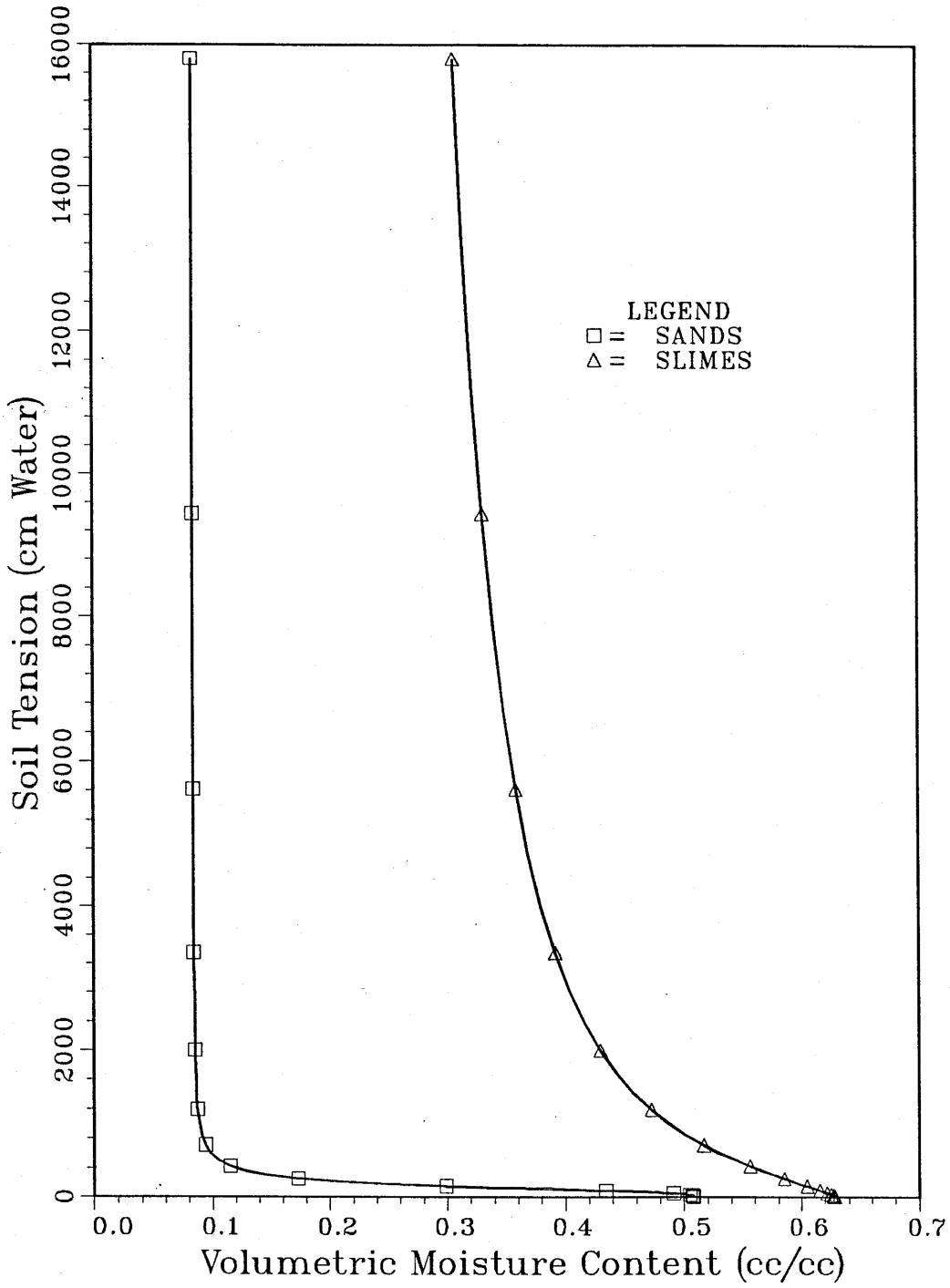

Figure 2.7. Soil moisture characteristic curves typical of mill tailings deposits.

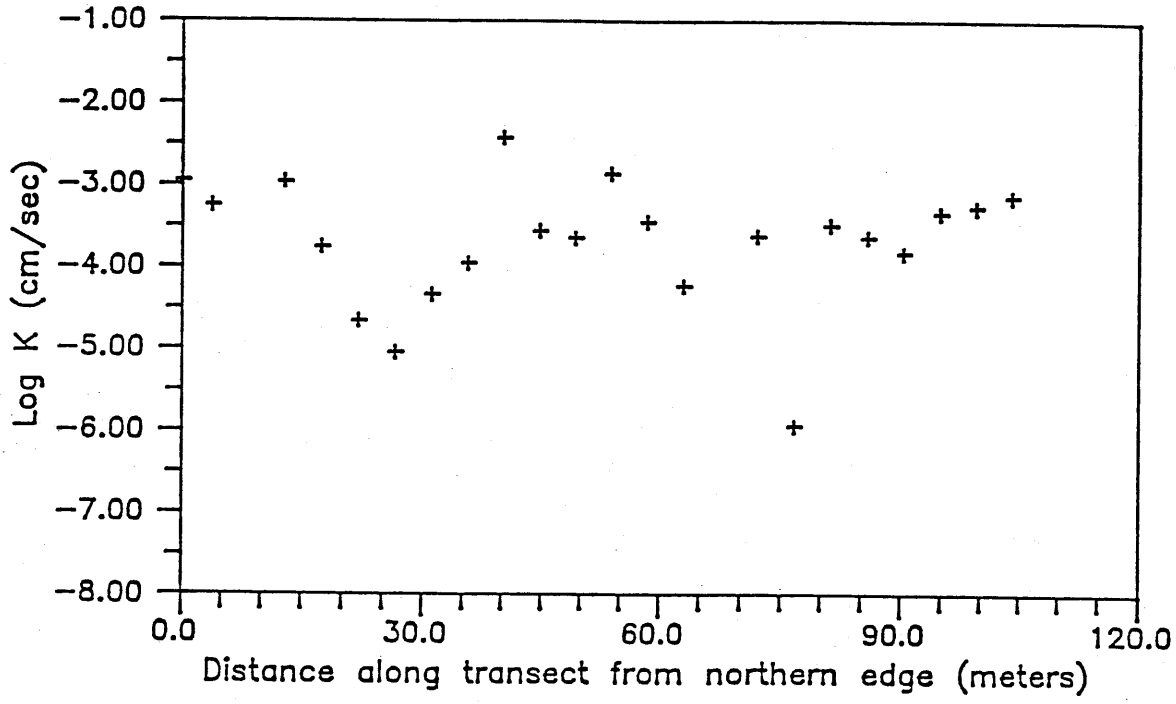

Figure 2.8. Distribution of log K laterally at 28 cm. depth. (after *Johnson [1987]*)

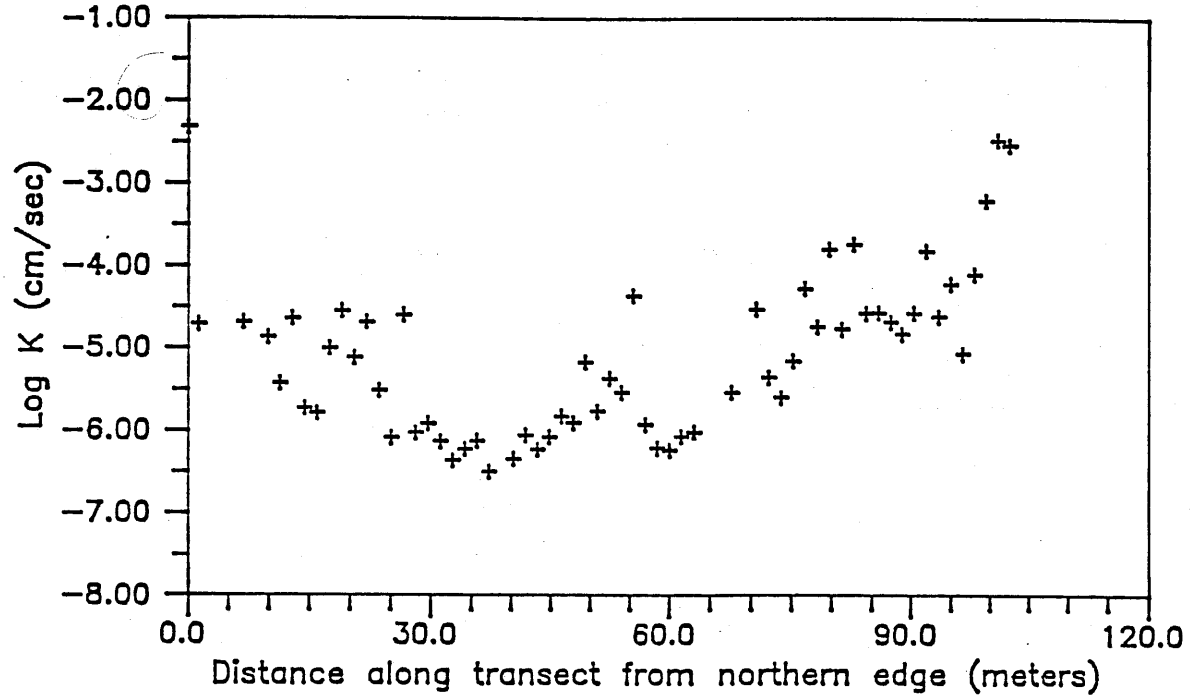

Figure 2.9. Distribution of log K laterally at 205 cm. depth. (after *Johnson [1987]*)

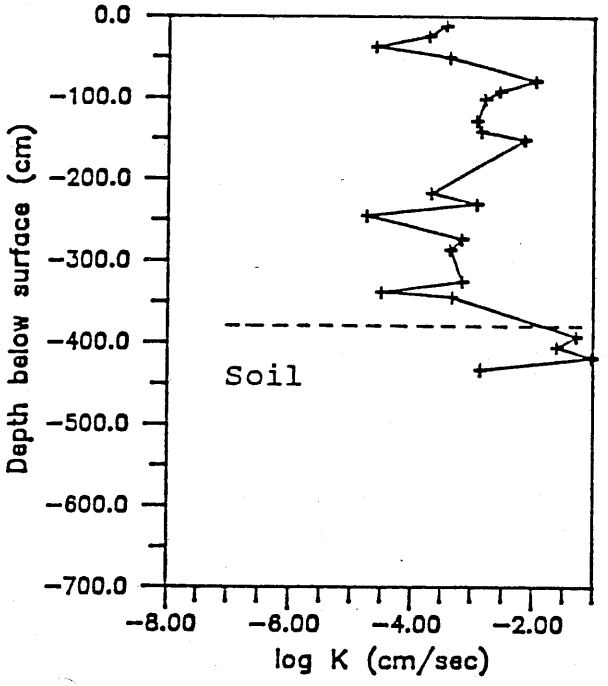

Figure 2.10. Log K with depth. Sand zone.

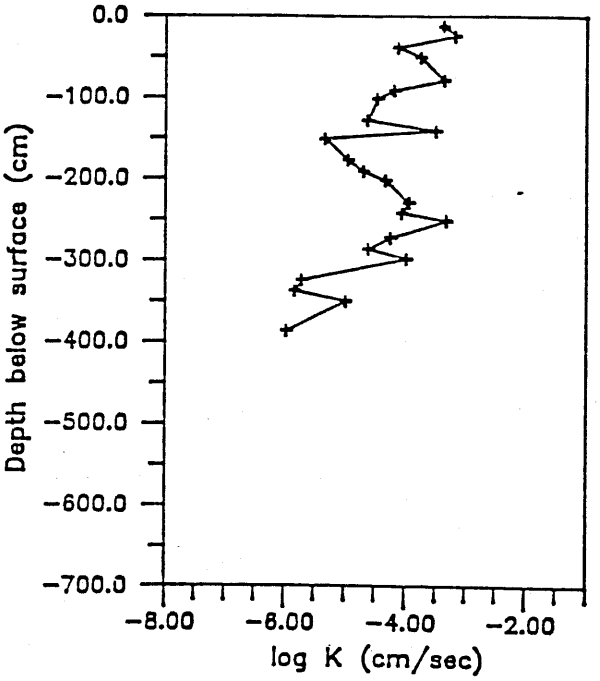

Figure 2.11. Log K with depth. Transition zone.

(after *Johnson [1987]*)

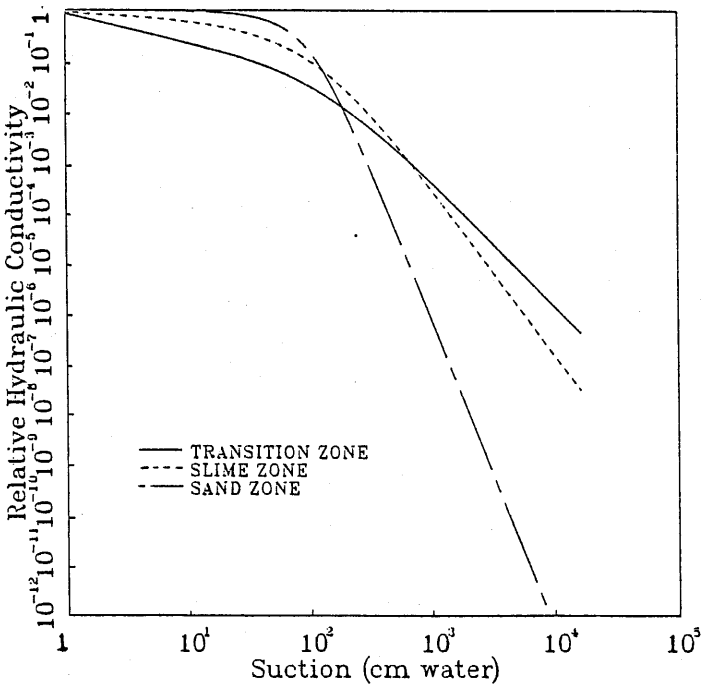

Figure 2.12. Relative hydraulic conductivities for various tailings materials.

zone retains higher hydraulic conductivities at lower pressures and moisture contents and thus will conduct more moisture at the same capillary pressure under the equal hydraulic gradients.

Once again, this summary of the hydraulic property distribution is given only to offer the reader some insight into the spatial variability present in the mill tailings impoundments and is not meant to give a full description of the results and conclusions reached by *Johnson [1987]*. The data and results from the previous study will be used sparingly in this study and will be incorporated more as a guide to the construction of conceptual models which will be used to investigate the results and effectiveness of alternate approaches for incorporation of spatial variability of hydraulic properties into numerical models.

Previous Work on Mill Tailings Seepage

Previous studies aimed at seepage prediction from mill tailings impoundments have focused on conceptual models which fail to account for the true heterogeneity present in the hydraulic property field. These studies have improved our understanding of the major components which govern the seepage rates from these waste impoundments. In recent years however, several studies by *Stephens et al. [1988]*, *Parsons [1988]*, *Siegel and Stephens [1980]*, and *Stephens and Heerman [1988]* have shown that the flow phenomena present in and around waste impoundment sites can not be sufficiently described by simple one–dimensional conceptual models which assume the media is homogeneous and isotropic.

Mill tailings impoundments and the unsaturated zone located beneath these impoundments are often incorrectly perceived as permanent storage facilities for the waste materials and potential contaminants they contain. *Stephens and Knowlton [1986]* show that recharge can occur even at arid sites in which the annual evapotranspiration greatly exceeds the precipitation. *Stephens [1985]* reemphasizes that permanent storage of waste seepage in the vadose zone is not possible if recharge occurs under natural conditions. Some scientists hold the misconception that moisture contents in the unsaturated zone below some theoretical "irreducible moisture content" implies that a certain amount of moisture seepage from waste impoundments can be permanently stored in the vadose zone below these impoundments. This conceptualization totally ignores recharge from natural processes and also incorrectly incorporates the ill–defined term known as "irreducible moisture content". *Lewis and Stephens [1985]* used bromide tracers in order to determine the movement of moisture in unsaturated tailings in an arid environment. These authors concluded that moisture

movement in tailings impoundments is predominantly downward. They also show that downward moisture movement can occur under soil moisture conditions that some scientists consider drier than some irreducible moisture content.

These results suggest that site specific hydrologic characterization should be completed if any impoundment site is to be properly analyzed, whether the purpose be for evaluation of future construction of an impoundment or for remedial action purposes. Proper design of potential waste impoundment sites and intelligent reclamation of abandoned impoundments is crucial in protecting groundwater supplies in the region of the impoundments. Because groundwater contamination may not be detected for years or possibly decades after the impoundment is in active use, it is essential that we understand basic flow phenomena in and around the impoundment before the construction of impoundments is undertaken. For remedial action purposes, it is essential that we understand the flow phenomena so that effective and efficient abatement procedures can be pursued.

Previous models used to predict seepage from tailings impoundments

Two main approaches have been used predict and analyze the seepage from mill tailings impoundments; analytical solutions and numerical modeling. A limited number of analytical solutions are available to analyze seepage from impoundments due to the nonlinear nature of governing equations for unsaturated flow which make analytical solutions impossible. Therefore, most analytical solutions that do exist assume that flow dynamics can be modeled by simple one–dimensional infiltration equations. These solutions may not be valid in many cases, especially where the phreatic water surface is far below the bottom of the impoundment. Numerical models are much more adaptable to difficult boundary

conditions and structure of the solution domain, and most importantly can account for multidimensional flow and anisotropic media. Several numerical modeling studies have been completed for mill tailings impoundments which focus on location of the phreatic surface in the impoundment so that safety of tailings dams or distribution of moisture in and around the tailings impoundment can be accessed. A brief review of previous work on mill tailings impoundments is given below.

Analytical Solutions

A simple one-dimensional model proposed by *McWhorter and Nelson [1979]* assumes that the tailings impoundment is under constant ponding and the advance of the wetting front is determined by the hydraulic conductivity of the liner and the capillary properties of the foundation material. As seen in Figure 2.13, several distinct layers of the impoundment are defined and an associated hydraulic conductivity is assigned to each layer. Seepage from beneath the impoundment is assumed to take place in distinct stages. These stages are conceived as follows: (1) a wetted zone which may or may not be saturated progresses vertically downward until it reaches the water table or an impervious boundary. (2) A saturated groundwater mound will form and rise toward the impoundment and the groundwater mound will continue to rise until a complete zone beneath the impoundment is saturated and flow from the impoundment occurs under saturated conditions toward the water table. (3) The mound spreads laterally and declines in height as the supply of water is removed. Equations are derived in order to describe the downward movement of water during the stages.

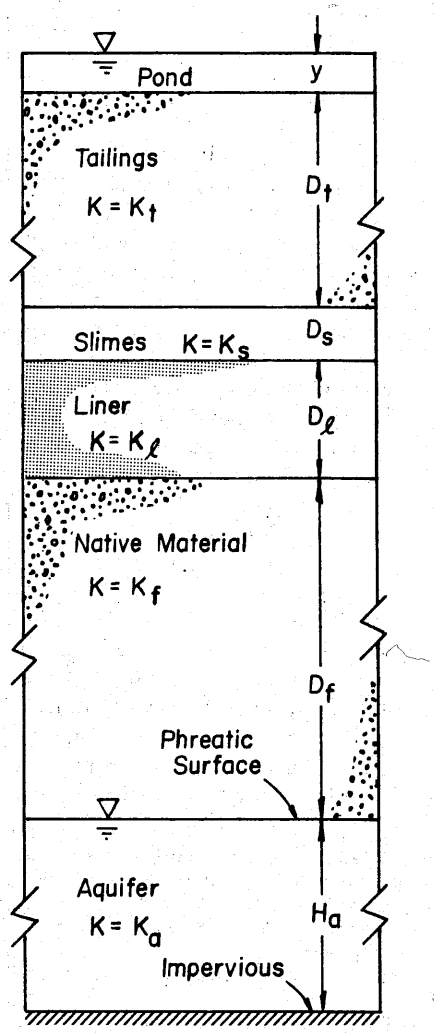

Figure 2.13. Illustration of conceptual model proposed by McWhorter and Nelson. (after *McWhorter and Nelson [1979]*)

During the first stage of seepage, the seepage rate q at the base of the impoundment is given by

$$q = \frac{(y + D_t + D_s + D_l) - h_d}{\frac{D_t}{K_t} + \frac{D_s}{K_s} + \frac{D_l}{K_l}} \qquad (2.1)$$

and $$\beta = y + D_t + D_s + D_l - K_f \left(\frac{D_t}{K_t} + \frac{D_s}{K_s} + \frac{D_l}{K_l} \right) \qquad (2.2)$$

The region under the impoundment is considered unsaturated if $\beta < h_d$ and is saturated if $\beta > h_d$ where h_d is a negative pressure head representing the pressure at which water is displaced by air. D_l and K_l are thickness and hydraulic conductivity of the liner material respectively, D_t and K_t are thickness and hydraulic conductivity of the coarse tailings material above the slime zone, and D_s and K_s are thickness and hydraulic conductivity of the slime zone respectively. The authors also develop several other equations to analyze the flow during different stages of seepage. The authors conclude that the major controls on the seepage rate from the impoundment in this model are the hydraulic conductivities of the liner and the foundation material. For a complete description of the equations, see *McWhorter and Nelson [1979]. McIntosh and van Zyl [1985]* use this model in a probabilistic study to access the variation in seepage based on the variance of the input parameters.

The conceptualized model described above is relatively simple. However, in some cases the simple model may not accurately predict the field environment and the boundary conditions present at a tailings impoundment. The weakest point of this model may be the assumption of one–dimensional vertical flow, especially in layered, unsaturated media. Several studies including *Siegel and Stephens [1980], Yeh and Gelhar [1982], Yeh et.al. [1985a,b,c], Stephens et.al. [1987], Mantoglou and Gelhar [1987a,b,c],* and *Stephens and Heerman [1988]* stress the importance of considering lateral flow components when modeling flow and transport in layered, heterogeneous, unsaturated media. The one–dimensional model does not allow lateral movement of moisture which will

significantly affect the seepage prediction. This is especially true when tailings and foundation materials exhibit significant anisotropy which tend to enhance lateral flow components and thus provide more water for surface evaporation and horizontal movement to other portions of the tailings. This model is designed mainly to provide simple engineering solutions to a problem which fits the conceptual model closely. The assumptions made in this conceptual model may be invalid at many tailings impoundments. The assumption of one–dimensional vertical flow beneath the impoundment will not only have a great impact on the model approach and predictions but also on the monitoring system and procedures which will be used in delineating seepage rates and contaminant transport in the region around the impoundment. For instance, if significant unsaturated lateral flow is present under a tailings impoundment, monitoring techniques installed to detect saturated vertical flow may not be adequate to obtain accurate assessment of the quantity and quality of effluent from the impoundment and thus drastic misconceptions can be formulated concerning the flow and transport phenomena present in and around the impoundment. This point can not be overemphasized for studies aimed at determining seepage from abandoned impoundments where the final goal is to incorporate proper remedial action schemes to combat groundwater contamination.

Numerical Modeling Studies

As mentioned earlier, recent studies have shown that complex flow phenomena can take place in and around mill tailings impoundments. It is important to understand these phenomena so that any particular conceptual model can be evaluated for inherent weaknesses which occur due to the simplifying assumptions imposed on the problem. In order to implement a more accurate model of tailings impoundments, numerical approaches are often

employed so that more realistic boundary conditions and natural heterogeneities can be incorporated into the model. Several researchers have applied numerical models in the past to assess moisture retention and locate the free water table surface in active tailings impoundments. A brief description of this previous work is given here.

Kealy [1970] used a numerical model to predict the location of the phreatic surface in an active mill tailings impoundment. The conceptual model used in the study assumed the mill tailings impoundment was situated directly over a permeable base. Zones exhibiting various conductivity were then incorporated into the model in order to determine their affect on the location of the phreatic surface. This author concluded that for prediction of the phreatic surface, the anisotropy ratio is relatively unimportant in saturated soils, and that the conductivity of the dam material is by far the most important determinant of the phreatic surface location. This result suggest that the unsaturated hydraulic conductivities of tailings materials will also be important for prediction of seepage from mill tailings impoundments when most of the flow occurs under unsaturated conditions.

Siegel and Stephens [1980] compare the results of a simple one dimensional approach to those obtained from two dimensional numerical modeling techniques which allowed incorporation of anisotropy of the media and lateral flow components. They conclude that the simple one dimensional approach may be sufficient to describe the flow phenomena occurring in isotropic media but state that the results of the one dimensional solution may differ significantly from models which incorporate multidimensional flow, especially when the media is considered anisotropic. Figure 2.14 – 2.17 illustrate the variability in saturation profiles under a lined pond for different anisotropy ratios. These authors also concluded that a slightly larger amount of seepage would

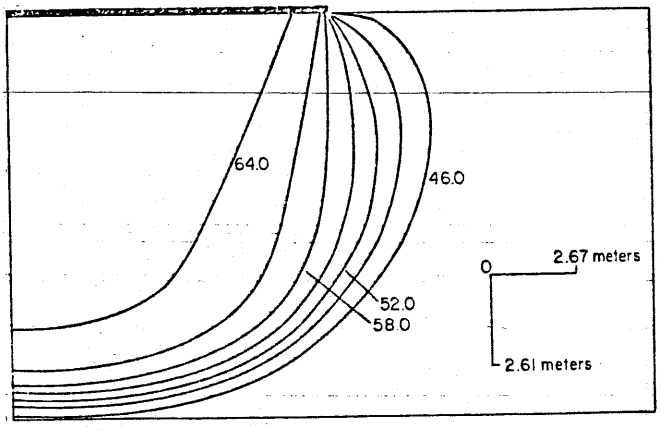

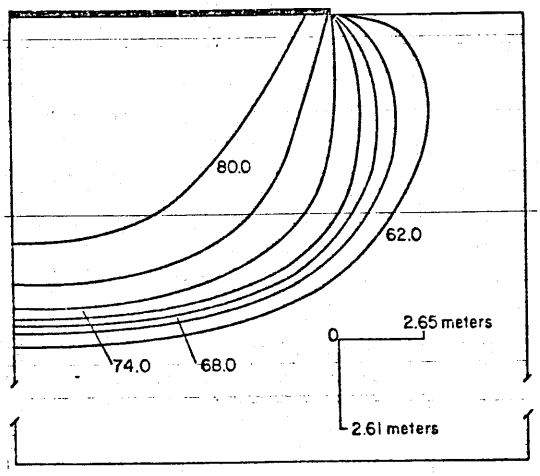

Figure 2.14 and 2.15. Saturation profiles in isotropic sand and loam respectively after one year under a lined pond. (After *Siegel and Stephens [1980]*)

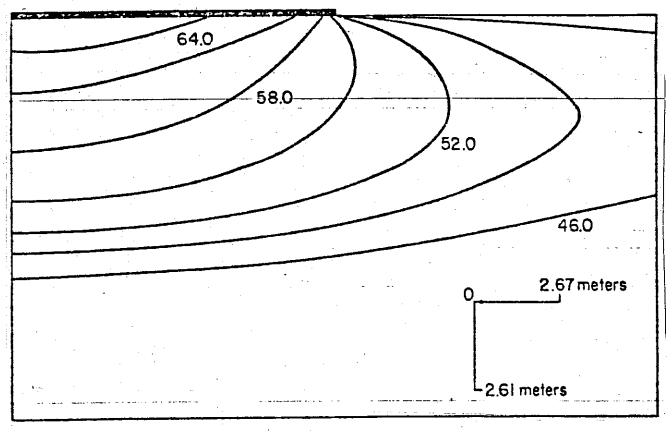

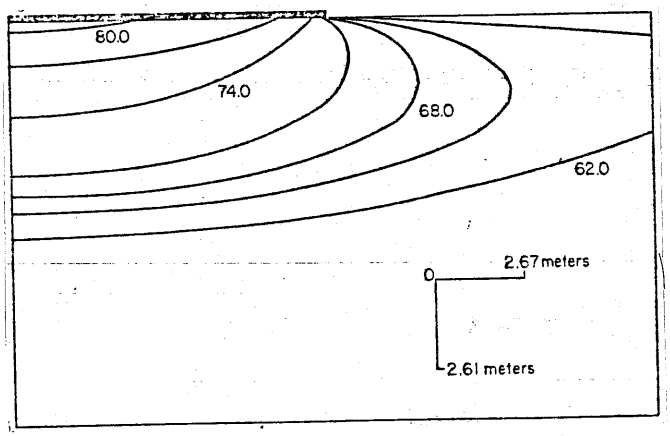

Figure 2.16 and 2.17. Saturation profiles in anisotropic sand and loam respectively after one year under lined pond . (After *Siegel and Stephens [1980]*)

occur from the pond when the underlying material was considered anisotropic but that lateral spreading and evaporation tended to slow the vertical rate of advance of the wetting front from the pond due to the lateral spreading and evapotranspiration. These phenomena are not considered in the one–dimensional model. Once again, the results reemphasize the importance of considering the lateral flow components in and around tailings impoundments.

Lam and Barbour [1985] used a finite–element model in order to assess the movement of contaminants through a mill tailings impoundment under transient conditions. They show that a bentonite cutoff wall significantly inhibits the travel times of contaminants in the impoundment. They also conclude that significant flow can occur in the unsaturated zone and stress that both the unsaturated and saturated zones of soil must be considered to accurately model the flow regime. Incorporation of a sand zone among other lower permeability zones is shown to affect the seepage and transport processes significantly.

Harris [1987] used a numerical model to incorporate the heterogeneity in the mill tailings hydraulic properties in order to observe the saturation profiles and hydraulic head distribution in an abandoned impoundment. The results of this study show that the saturation profiles are strongly influenced by the incorporation of the natural heterogeneity in the impoundment. Figure 2.18 shows the zoned regions of the finite element model in which the saturated and unsaturated hydraulic properties were different. Figures 2.19 and 2.20 show the results of the numerical simulations which incorporated heterogeneity in the soil moisture characteristic relationship and the saturated and unsaturated hydraulic conductivity. Figure 2.19 and 2.20 are virtually the same, suggesting that the anisotropic nature of the media does not significantly alter pressure and thus saturation profiles. Harris does not present data indicating fluid movement within the impoundment. A strong correlation can be seen in the zoned regions

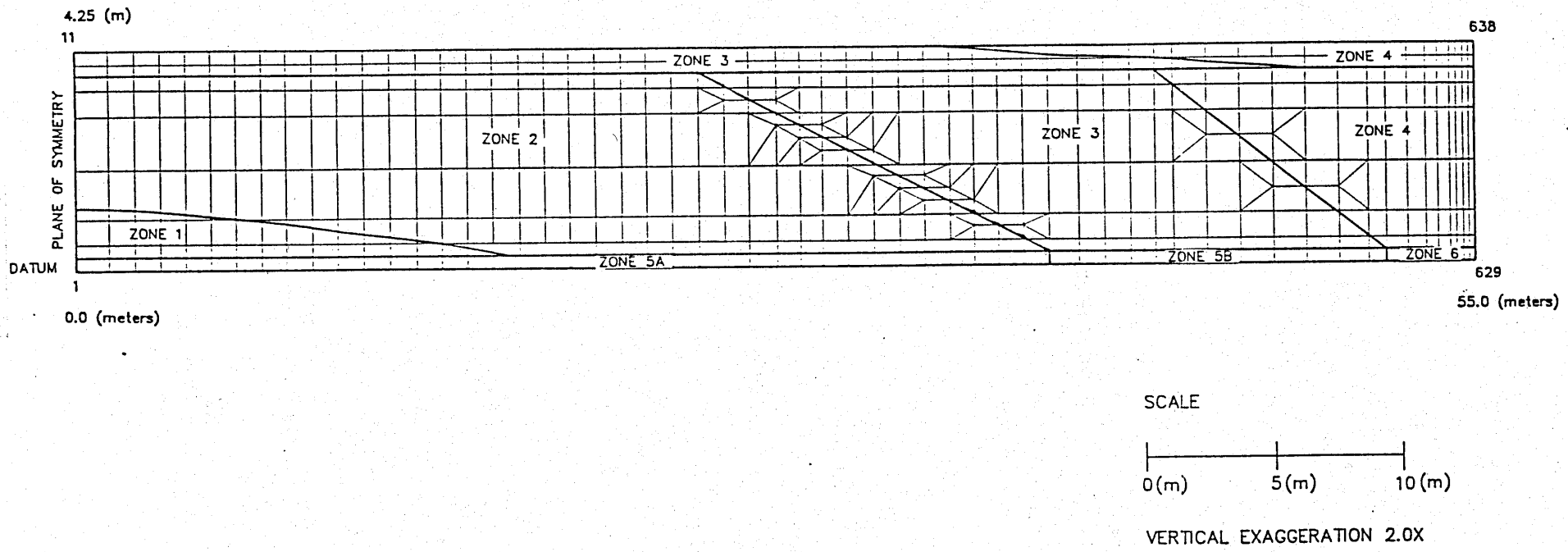

Figure 2.18. Finite element grid showing the incorporated zones of materials having different saturated and unstaurated hydraulic properties. (After *Harris [1987]*)

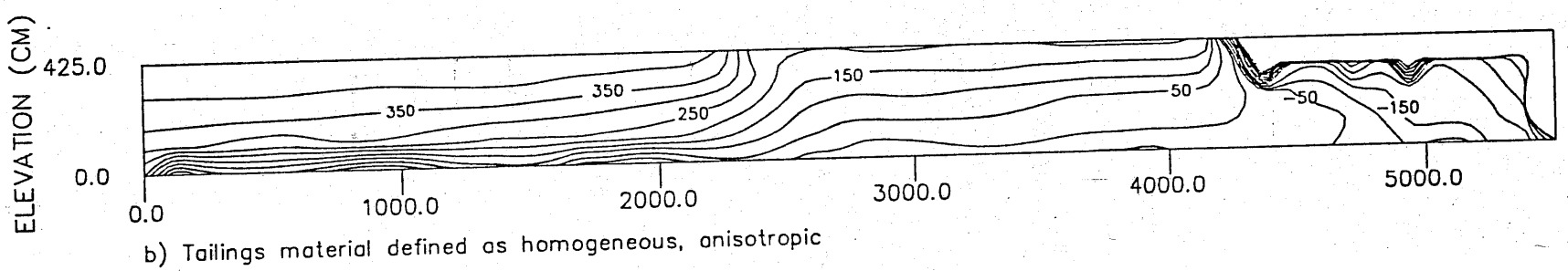

Hydraulic head field.

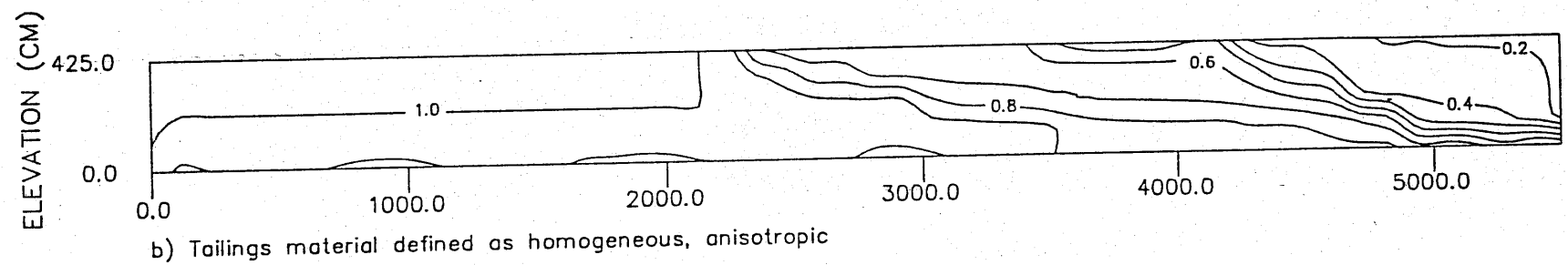

Saturation field.

Figure 2.20. Results of simulation incorporating spatial variability in hydraulic properties. Media is given a horizontal to vertical anisotropy ratio ranging from two to four. (After *Harris [1987]*)

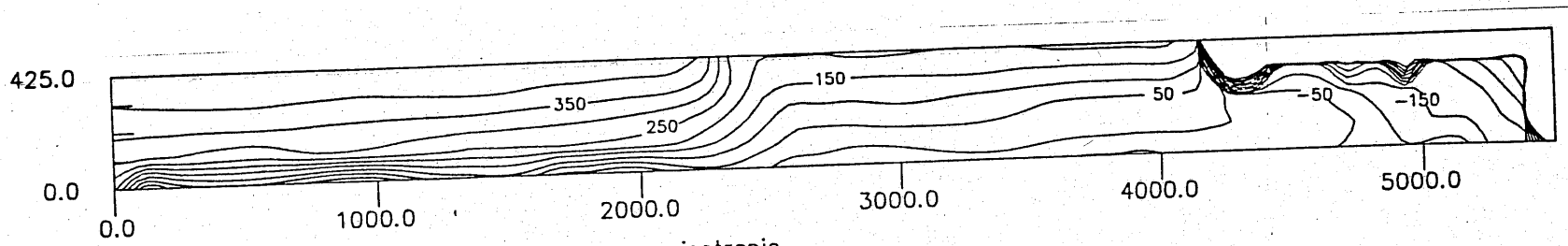

Hydraulic head field.

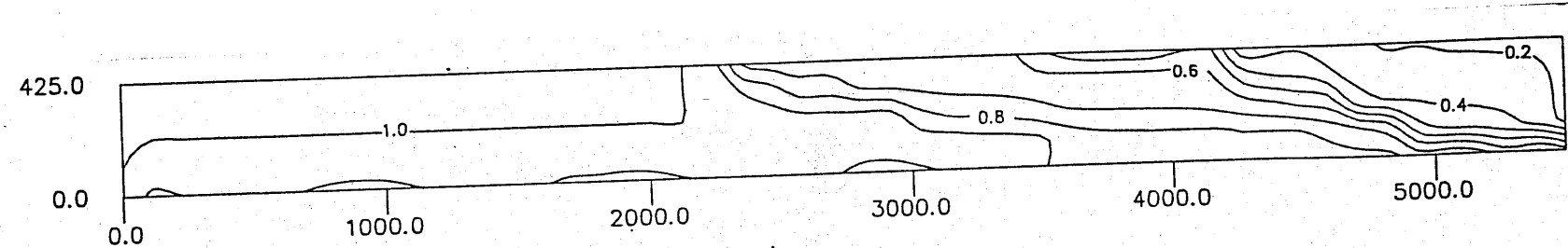

Saturation field.

Figure 2.19. Results of simulation incorporating spatial variability in hydraulic properties. Isotropic media. (After *Harris [1987]*)

and the saturation profiles, thus it seems plausible that the seepage rate would also be somewhat dependent on the incorporation of the hydraulic properties into the model.

All of the numerical modeling studies discussed above imply that the incorporation of natural heterogeneity and the consideration of lateral flow components is very important in correctly analyzing and predicting seepage rates from tailings impoundments or any naturally heterogeneous flow system. In the following chapters, several approaches are implemented in order to incorporate the natural heterogeneity of the hydraulic properties present in mill tailings impoundments into numerical models so that seepage predictions and the uncertainty in these seepage predictions can be assessed.

CHAPTER 3

NUMERICAL MODELING

Numerical modeling is a problem solving technique which has gained wide use in many areas of science and engineering since the advent of what we consider "high speed" computers. In particular, finite difference and finite element methods have been applied extensively in groundwater hydrology for purposes such as groundwater resource evaluation, prediction of seepage through dams, delineation of groundwater flow paths, and moisture flow in the unsaturated zone just to mention a few. Most recent applications of these numerical methods have focused on modeling contaminant transport in porous media. Numerical codes are now available for analysis of a multitude of physical problems including saturated and unsaturated fluid movement in porous media, flow of fluids in fractured media, multiphase flow in porous media, heat transfer and the dynamics of deformable media. Many codes attempt to simulate a combination of these physical problems. In the following section, I give a brief and general description of the numerical model used in this study and discuss the assumptions of the conceptual model and the possible weaknesses of the numerical implemention. It is not my intention to give a full description of the development of the numerical scheme since other authors are much better qualified to do so. *Wang and Anderson [1980]* give a very basic introduction to finite difference and finite element methods as applied to groundwater modeling. A few of the many other texts available which examine more realistic problems include *Huyakorn and Pinder [1983]*, *Pinder and Gray [1977]*, and *de Marsily [1986]*.

Description of the Numerical Model Used in the Study

At the time this results of this study were written, the numerical code used in the work was proprietary in nature. Details of the code are not available to the general public. Therefore, only general statements about the code and the numerical scheme incorporated can be discussed in this thesis. The name of the code as it is marketed is VAM2D. It is available through HydroGeologic Inc. and was developed by P.S. Huyakorn, H.O. White, and L.L. Wadsworth.

When undertaking any modeling exercise in which the objective is to simulate physical processes, certain assumptions must be made in order to facilitate the construction of a suitable model which is feasible for the study. Any type of model incorporates assumptions which may or may not be valid for a particular case of study. For example, correct implementation of micromodels or Hele–Shaw models requires the assumption that physical phenomena and flow dynamics of the system being simulated can be accurately represented by a physical model of the situation which may be hundreds or thousands of times smaller than the actual size of the physical problem. Many analytical mathematical models assume that the porous media properties are homogeneous in the entire domain of study. As with the above mentioned models, numerical models also incorporate simplifying assumptions which vary in validity from one physical situation to another. In numerical modeling, it is important to realize the assumptions which are integrated into the conceptual model and the assumptions and weaknesses of the numerical scheme used to evaluate the problem so that some insight can be gained into the validity of the model predictions.

The first step in numerical modeling involves representing the physical process mathematically. In other words, the physical process must be represented by mathematical equations which properly define the physical problem. In the

physical problem studied in this research, the mathematical expression is a partial differential equation written in equation 3.1 below. The development of this equation without source and sink terms can be found in *Bear [1979]*.

$$\frac{\partial}{\partial x_i}\left[\varrho_w K_{ij} k_{rw}\left(\frac{\partial \psi}{\partial x_j} + g_j\right)\right] = \frac{\partial}{\partial t}\left(\varrho_w \phi S_w\right) - \varrho_w q \qquad (3.1)$$

where ϱ_w = density of water, $[M/L^3]$

K_{ij} = hydraulic conductivity tensor, $[L/T]$

k_{rw} = relative hydraulic conductivity as a function of pressure, $\left[\frac{(L/T)}{(L/T)}\right]$

ψ = pressure head (taken negative when media is unsaturated), $[L]$

x_i = spatial coordinates (i = 1, 2), $[L]$

g_j = unit vector gravity component, [ ]

t = time $[T]$

ϕ = effective porosity, $[L^3/L^3]$

S_w = water phase saturation, $[L^3/L^3]$

q = volumetric flow rate via source or sinks per unit volume porous media, $[L^3/L^3T]$

The equation above describes the fluid flow in porous media and the change in the pressure of the fluid as it changes in time due to changes in the compressibility of the matrix and the fluid. A more common form is shown in equation 3.2.

$$\frac{\partial}{\partial x_i}\left[K_{ij}\, k_{rw} \left(\frac{\partial \psi}{\partial x_j} + g_j\right) \right] = \eta \frac{\partial \psi}{\partial t} - q \qquad (3.2)$$

where

$$\eta = S_w S_S + \phi \frac{\partial S_w}{\partial \psi} \qquad (3.3)$$

and

$$S_s = \varrho_w\, g\, (\phi\beta + \alpha) \qquad (3.4)$$

where S_s = specific storage, $[L^{-1}]$

g = gravitational constant, $[L/T^2]$

β = compressibility of water, $[M/LT^2]$

α = compressibility of matrix, $[M/LT^2]$

For this particular study, most simulations performed where "steady state" in nature. In other words, the storage of the system and the changes in pressure that would occur due to the compressibility of the matrix and the water where not considered. This assumption simplifies the governing partial differential equation even further and it can be written as in equation 3.5 below.

$$\frac{\partial}{\partial x_i}\left[K_{ij}\, k_{rw} \left(\frac{\partial \psi}{\partial x_j} + g_j\right) \right] = 0 \qquad (3.5)$$

If x_1 is taken to be in the horizontal direction and x_2 is taken in the vertical

direction, the equation can be used to simulate saturated and unsaturated flow in a two dimensional vertical plane.

In order to solve equation 3.5, relationships must be specified for the relative permeability versus water saturation, and pressure head versus water saturation. Various relationships are available for this purpose. A review of some of the models used to characterize these relationships as related to mill tailings hydraulic properties can be found in *Larson and Stephens [1985]*. For this particular study, the method described by *Brooks and Corey [1966]* as used to define the relative conductivity versus water saturation relationship.

$$k_{rw} = \frac{(S_w - S_{wr})^n}{(1 - S_{wr})^n} = S_e{}^n \qquad (3.6)$$

where

$$S_e = \frac{S_w - S_{wr}}{1 - S_{wr}} \qquad (3.7)$$

and

$$n = \frac{(2 + 3\lambda)}{\lambda} \qquad (3.8)$$

and

S_w = water saturation, $[L^3/L^3]$

S_{wr} = residual water saturation, $[L^3/L^3]$

λ = pore size distribution index,
slope of log S_e versus log capillary pressure line

The simple functional form of the relationship makes it attractive for use in numerical models because the derivative of the relationship can be determined analytically. The relationship chosen for water saturation versus pressure head relationship was the model proposed by *Mualem [1976]*. This model has been

widely adopted in recent years since the development *[van Genuchten, 1980]* of a curve fitting algorithm to determine physical parameters to define the soil moisture characteristic curve. The model can be defined as follows:

$$S_e = \frac{1}{[\,1 + (\,\alpha\,|\,\psi - \psi_a\,|\,)^{n}\,]^{m}} \qquad \text{for } \psi < \psi_a \qquad (3.9a)$$

$$S_e = 1 \qquad \text{for } \psi > \psi_a \qquad (3.9b)$$

where

α = fitting parameter which is inversely related to the air entry pressure of the media, $[L^{-1}]$

ψ = pressure head, $[L]$

ψ_a = air entry pressure head, $[L]$

n = fitting parameter defining the magnitude of shift in the soil moisture characteristic curve, [ ]

m = $1 - 1/n$, [ ]

The iterative numerical scheme used to solve the system of non–linear equations resulting from this implementation is described by *Huyakorn et al [1984]*.

Assumptions implemented in the numerical model

When using any mathematical model, is it important to be aware of the physical assumptions which are adopted in the development of the model. The model used for this study contains several assumptions which come about due to the conceptualization of the physical problem and the implementation of numerical scheme to analyze the problem. These assumptions are listed and discussed below.

- Only single phase flow of the fluid is considered. Flow of the vapor phase is assumed negligible. The validity of this assumption is problem specific and it's

accuracy may even vary within a specific domain being studied, however, vapor flow is generally neglected with only minimum error in the analysis provided that the moisture content of the porous media is high enough so the mass transport in the fluid phase is significantly higher than that of the vapor phase.

- Flow is considered isothermal and governed by Darcy's law. Isothermal conditions are obviously very seldom seen in field conditions but the variations in the temperature and the gradient caused by this temperature variation is considered minor compared to the hydraulic gradient caused by pressure variation and gravity forces present in the impoundment. Darcy's law should be valid except for very low moisture contents when the flow of moisture may be governed by the vapor phase.
- Hysteresis effects in the relationships of relative hydraulic conductivity and pressure head versus saturation are assumed to be negligible. Since steady state conditions are less dependent on hysteretic phenomena then are transient conditions, this assumption is not restrictive for this study.
- Flow in fractures is not accounted for in the model. Once again, this assumption should not be restrictive for the present analysis because only a very small portion of the tailings surface exhibits cracking and thus flow in fractures is considered negligible relative to the flow of moisture in the continuous porous media.

Model Verification

It is always important to insure that numerical models correctly solve the governing partial differential equation used to mathematically define a physical process. Often, this is done by comparing results of the numerical solution to that of an analytic solution. It may also be be important to insure that the correct partial differential equation has been chosen to model a given process. For

situations where no analytic solutions exist due to difficult boundary conditions, heterogeneity, etc., field or lab data are often used in an effort to verify numerical models.

The numerical model used in this study had been previously verified by the authors of the code. The results of those verification exercises will not be presented here. Verification tests show that VAM2D does produce very similar results to analytic solutions when simulating moisture flow in unsaturated media. VAM2D was also benchmarked against several other numerical codes for various problems. These exercises show that VAM2D is capable of producing numerical solutions very similar to other numerical models which have been validated and used in the public domain. Therefore, verification studies were not completed in this research due to the work previously completed by the authors of the code.

Problems Associated with Numerical Modeling

As with any mathematical model designed to depict a physical phenomena, numerical modeling has difficulties. For the flow problem studied herein, problems lie in properly estimating and implementing physical boundary conditions and obtaining a solution to the non–linear problem. Some of these problems and the approaches taken to deal with them are discussed below.

Boundary conditions

Estimation and implementation of boundary conditions in such a fashion so the mathematical model is a reasonably correct representation of the physical situation is a very difficult but important step in the modeling process. Obviously, the boundary conditions placed on the solution domain can have a major impact on the predictions obtained from the model. Therefore, it is important to realize the

impact of the boundary conditions on the model predictions. Below, I discuss some of the problems associated with estimating boundary conditions for physical situations exhibiting variable saturation.

Estimating Evaporation

Evaporation from the surface of a porous media is a very difficult process to accurately quantify, because the amount of water taken from the surface is a function of the atmospheric demand and the soil moisture availability. Evaporation is a coupled phenomena. The amount of water evaporated from the surface is not only dependent on the evaporation potential of the atmosphere but also on the liquid and vapor phase conductivity of the porous media. In numerical models, one way to implement this phenomena is discussed by *Neuman et al. [1974]*. Proper implementation of this technique requires accurate estimates of the maximum evaporation potential and an estimate of the minimum pressure head the porous media will acquire in an evaporative environment. However, the method is not used without added computational burden and an additional aspect of non–linearity to the already difficult problem.

Numerous solutions have been proposed to calculate the evaporative flux through of porous media using both analytical and numerical approaches, including those investigated by *Poulovassilis and Psychyou [1985], Staple [1974], Gardner and Hillel [1962], Gardner [1958]*. No simple analytical solution exists to relate the evaporation rate to soil and atmosphere conditions when the water table is far below the evaporation surface. *Chandler et.al [1985]* discuss observations of field evaporation of uranium tailings solution. Van Zyl *[1987]* discusses the results of numerical simulations which suggest that upward flux due to evaporation in mill tailings is restricted to a certain depth below the surface depending on the hydraulic characteristics of media. In a fine textured tailings, surface evaporation

will cause upward flux from a greater depth. In coarse textured tailings, the same atmospheric demand will cause a quicker depletion of the water close to the surface but will not dry the tailings to as great a depth.

No evaporation data is available for mill tailings. Therefore, different scenarios were implemented in order to determine the effect of evaporation on the steady state seepage rates at the base of the impoundment. In most simulations, a prescribed head boundary was implemented at the surface of the impoundment. However, this method is not error free, because the determination of pressure heads in porous media, especially at an evaporation surface, is very difficult. Some of the problems associated with this technique are discussed below.

Estimating Soil Moisture Conditions

Typically, the pressure head at a point in porous media is estimated either by tensiometers or by first determining the moisture content of the soil and then relating it to the pressure head at that moisture content according to some soil moisture characteristic relationship as depicted in Figure 2.7. The soil moisture characteristic curve is usually determined through lab methods utilizing hanging column and pressure plate methods. The soil moisture content is generally determined by neutron attenuation methods or other techniques which are generally difficult to verify. The uncertainty of the pressure head prediction is especially increased at the surface of the media because most moisture measurement techniques are difficult or impossible to use at the surface of the porous media, therefore making pressure head predictions at that point very difficult. Thus, implementation of a prescribed head boundary at an evaporation surface is certainly open to tremendous uncertainty.

One main objective of this study is to assess the effects of incorporating the spatial variability in hydraulic properties through different approaches, and not

to directly assess the effects of uncertainty in boundary conditions on the domain, prescribed pressure head boundaries were generally used in the numerical simulations in this study. The data is not available for this study to perform model calibration, therefore it would be the emphasis remains on determining uncertainty in model output induced from uncertainty in hydraulic properties. Incorporation of prescribed pressure head boundaries also leads to faster convergence of the numerical solution or in some cases makes a solution obtainable, when solving a highly non-linear set of equations resulting from a problem in which variations in the hydraulic properties are relatively drastic from element to element. In the next section, I discuss the problems associated with obtaining a numerical solution for the non-linear system of equations which results from implementation of finite element methods in an unsaturated heterogeneous media.

Convergence of numerical solution

When dealing with flow in unsaturated media, the system of equations resulting from the finite element discretization is non-linear. This non-linearity can best be seen if we look closely at the governing flow equation for variably saturated media shown in equation 3.10. This is the same equation as shown in equation 3.5 except it has been rewritten assuming that the coordinates are aligned with the principle flow directions so that the off diagonal terms K_{zx} and K_{xz} in the conductivity tensor are zero.

$$\frac{\partial}{\partial x}\left[K_{xx}\, k_{rw}\, \frac{\partial \psi}{\partial x} \right] + \frac{\partial}{\partial z}\left[K_{zz}\, k_{rw} \left(\frac{\partial \psi}{\partial z} + 1 \right) \right] = 0 \qquad (3.10)$$

where K_{xx} = hydraulic conductivity in the x direction, (horizontal), $[L/T]$

K_{zz} = hydraulic conductivity in the z direction (vertical), $[L/T]$

k_{rw} = relative hydraulic conductivity, $\left[\frac{(L/T)}{(L/T)}\right]$

The numerical scheme solves for the dependent variable ψ , but as shown in equation 3.10 and illustrated in Figure 2.12, the relative conductivity is a function of ψ , therefore the problem becomes non–linear. The numerical algorithm handles this non–linearity by solving for the dependent variable through an iterative process. In the code used for this study, two iterative procedures were available for this purpose, a Newton–Raphson scheme and a Picard scheme. Both of the procedures are discussed in *Huyakorn and Pinder [1983]*. *Huyakorn et al. [1984]* suggest that the Newton–Raphson scheme may converge more quickly for highly non–linear systems of equations.

The degree of the non–linearity the system of equations entails is dependent on the type of heterogeneity incorporated in the mathematical model via the finite element grid. The unsaturated problem is always non–linear, but the "degree" of non–linearity may change from element to element due to changes in the unsaturated properties of the media incorporated for each element. The phenomena which induces this added degree of non–linearity is illustrated in Figure 2.7. As an extreme case to illustrate this point, assume two adjacent elements in the grid are assigned unsaturated properties similar to those of the two soil moisture characteristic curves seen in Figure 2.7. Since the dependent variable the numerical scheme is "iterating on" is ψ , the pressure head at the nodes, it is easily seen that at a given pressure head, the saturation and the relative hydraulic conductivity of the two elements will vary greatly. This will induce still a higher degree of non–linearity in the system of equations than when a

homogeneous unsaturated soil is incorporated in the model. In this case, even the best iterative scheme may fail to converge on the correct solution. One way to combat this problem is to incorporate a smooth field of unsaturated hydraulic properties; however, this may not always be realistic as compared to the physical problem being studied. I will further discuss this problem and the steps taken to alleviate it in the section describing the approach used in the deterministic simulations.

Steady–State versus Transient Analysis

As mentioned previously, most simulations performed in this study were steady state in nature. The effects of change of storage due to compressibility of the water and matrix as well as temporal changes in boundary conditions are not considered. In this study steady state analysis is a necessity due to the nature of the problem. Since the problem is unsaturated, relatively large scale, and generally incorporates very heterogeneous media into the finite element grid, transient analysis would require extensive computer time. For the main objective of this study however, which is to study the effects of incorporation of heterogeneity on the uncertainty of seepage predictions, steady state analysis is not a limitation. Although hydrologic systems are almost never in a steady state condition in nature, observation of steady state seepage rates from the model predictions are the most feasible and sensible approach to the observing the uncertainty in this prediction given the uncertainty in the input parameters. Of course, whether or not the observations obtained in the steady state analysis are applicable to transient situations is always a point of debate. However, the assumption of steady state conditions in mill tailings impoundments may be fairly correct if the "time constant" for the system is relatively small. The time constant is some representative length of time in which transient occurences are expected to

"travel" or are transmitted through the physical system. In unsaturated media, the time constant is dependent on the specific moisture capacity of the system, the physical dimensions of the system, and the ability of the system to conduct (K_{sat} and $K(\psi)$) the changing boundary condition. Thus, for relatively small impoundments, it may be reasonable to study model predictions under steady state conditions.

Computer Resources

Solving multi-dimensional unsaturated flow and transport problems is a very computer-intensive undertaking. The non-linear nature of the flow equations allows only a very few linearized forms of the equation to be solved analytically. Therefore, numerical methods must be used to solve the problems exhibiting irregular boundaries, difficult boundary conditions, non-linearity, and heterogeneity. The computer resources and time needed to solve the problem is mainly dependent on the size and non-linear nature of the problem, the types of boundary conditions imposed, and the temporal nature of the problem, either steady state or transient.

In this study, the relatively large size of the field problem examined and the nature of the heterogeneity and non-linearity incorporated into the model required the use of a relatively fine finite element grid in order to insure convergence of the numerical solution. At this time in many non-research working environments, the use of multidimensional models for evaluating flow and transport in unsaturated porous media is not feasible due to the limited computer resources and time which are available to solve the problem. It is therefore important to determine when and where conceptual models must incorporate the true heterogeneity and multi-dimensional nature of flow and transport processes in

order to correctly model and understand these complex phenomena. Only then can hydrologists and engineers develop feasible working models for field applications.

DETERMINISTIC APPROACH TO INCORPORATION OF SPATIAL VARIABILITY INTO NUMERICAL MODELS

Introduction

A purely deterministic approach was initially implemented to determine the seepage distribution from the impoundment. This method assumes the hydraulic properties of the tailings are known at all points in the impoundment. The main purpose of the simulations was to determine the effect of boundary conditions and anisotropy of the tailings hydraulic properties on the seepage predictions from the impoundment. Because all the hydraulic properties are considered constant in each simulation, the effect of uncertainty in the hydraulic properties cannot be directly examined with this approach. In this section, description of the deterministic approach is given and results of simulations will be presented.

Hydraulic properties of the tailings are held constant in deterministic simulations; therefore, the only significant remaining variable is the boundary conditions imparted on the domain. In general, limited soil moisture data, rainfall data, and evaporation data exist for mill tailings impoundments, therefore several scenarios were implemented in the boundary conditions in order to assess several scenarios which portray a reasonable degree of likeness to true field conditions and to show the effects of each set of boundary conditions on the seepage prediction. This analysis also allows for more intelligent incorporation of the boundary conditions in conditional and stochastic–deterministic simulations as well. *Johnson [1987]* presents soil moisture data from neutron probe readings which were taken while field sampling was completed. Based on these soil moisture conditions and the observations that were made in the field during the

time of sampling, typical scenarios have been established which cover a broad range of possible conditions which are present at an impoundment during the year. Since the simulations performed considered only steady-state conditions, a variety of simulations are needed in order to observe the variations in the seepage predictions at various times of the year.

Finite Element Grid

The finite element grid used in the deterministic simulations was constructed in a fashion to enhance convergence of the numerical solution even if stringent boundary conditions and highly nonlinear hydraulic properties were incorporated into the model. In some simulations, a coarser grid would have made the problem less computationally burdensome; however, when strigent evaporative and input fluxes were incorporated into the steady state model, the fine grid was a necessity for convergence. Convergence rates generally decrease as the grid is coarsened and at some point the coarseness of the grid eventually causes convergence failure in the numerical scheme. Of course, as the number of nodes in the finite element grid increase, so does the amount of c.p.u. time needed to solve the larger number of nonlinear equations, even though it may take a fewer number of iterations to converge to a solution. Therefore, there is a trade-off between the number of iterations needed to obtain the solution and the number of nodes in the grid so long as the numerical scheme converges on the correct solution for both grids.

Since various boundary conditions were placed on the domain, a consistent grid of square elements was constructed for the entire domain. Each element was 17 centimeters on a side and the grid contained 25 elements in the vertical direction and 323 elements in the horizontal direction. The dimensions of the grid were thus 4.25 meters high by 54.91 meters long. The total number of

nodes was 8424 and the number of finite elements was 8075. Linear quadrilateral elements were used in the finite element implementation.

Approach of deterministic simulations

The saturated hydraulic conductivity and some of the unsaturated hydraulic property fields used in the deterministic simulations are those described by the multiple regression equations developed using the data which gathered in the field are determined in the laboratory by *Johnson [1987]* and *Harris [1987]*. The regression equations were developed using the hydraulic property as the dependent variable and the horizontal and vertical location of the measurement point in the cross section as the independent variables. Therefore, each dependent variable is associated with two or more independent variables defining the position of the measurement within the impoundment. In this manner, hydraulic property fields can be estimated for the entire impoundment based solely on the location of the point in the impoundment and thus the element location in a finite element grid. Of course, these hydraulic property fields are only one "hypothetical" recreation of field conditions. Regression analysis inherently smoothes the data due to the "fitting" technique of least squares analysis. Therefore, multiple regression analysis is a useful tool for determining the major trends in the data but lacks the ability to define a spatial variability present in areas of the impoundment where the large changes in the properties occur over relatively small distances. One such example of this is the transition zone shown in Figure 1.1 where significant layering occurs over relatively small distances due to the depositional environment at this point in the impoundment.

The contoured fields of the saturated and unsaturated hydraulic properties obtained from regression analysis are shown in Figures 3.1–3.5. The nonlinear nature of contour lines in the hydraulic property fields in Figure 3.1,

3.3, and 3.4 is an artifact of the quadratic nature of the regression equations. In other words, one of the independent variables in the regression equations was the square of the x location of the measurement point, therefore the relative magnitude of the model regression parameter (regression coefficient) defines the nonlinear nature of the equations. A summary of the regression equations developed for each of the hydraulic properties is given in Appendix A.

Figure 3.1 shows the contoured field of the log saturated hydraulic conductivity which was developed by *Johnson [1987]*. The trends predicted by the multiple regression analysis are consistent expected variations in the saturated hydraulic conductivity for this type of depositional environment.

Figure 3.2 shows the contoured field of the Brooks/Corey n–parameter (equation 3.6) which determines the relative hydraulic conductivity. The distribution of this parameter within the domain was determined from other published data on media exhibiting similar texture as the tailings in as much as this data was not available for this study. As the value of n increases, the relative hydraulic conductivity decreases more slowly with increasing capillary pressure (Figure 3.6). Therefore, as depicted in Figure 3.2, the media toward the outer edge of the impoundment (right side of the contour plot) will show unsaturated hydraulic properties similar to sands and the media in the center of the impoundment (the left side of the contoured plot) will show hydraulic properties similar to clays. Unfortunately, the smoothness of the contoured field does not exhibit the true heterogeneity in the unsaturated hydraulic properties exhibited in the tailings, especially in the transition zone.

Figure 3.3 shows the contoured field of the van Genuchten n parameter appearing in equation 3.9. *van Genuchten [1980]* relates the fitting parameter n to the magnitude of the horizontal shift in the soil moisture characteristic relationship as shown in Figure 2.7. For instance, the soil moisture characteristic

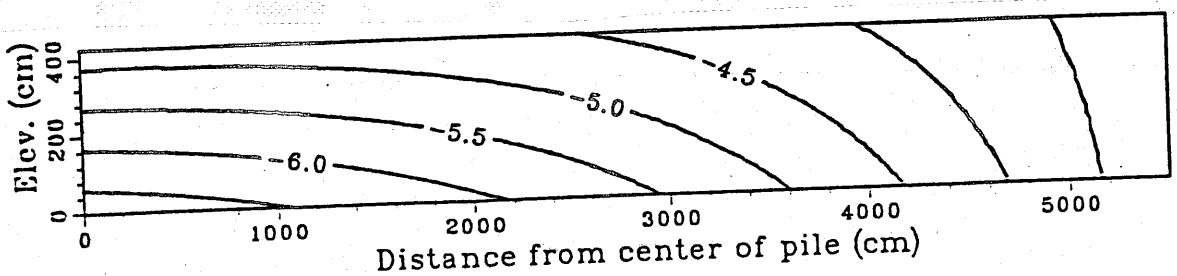

Figure 3.1. Contoured field of the log saturated hydraulic conductivity from multiple regression. (After *Johnson [1987]*)

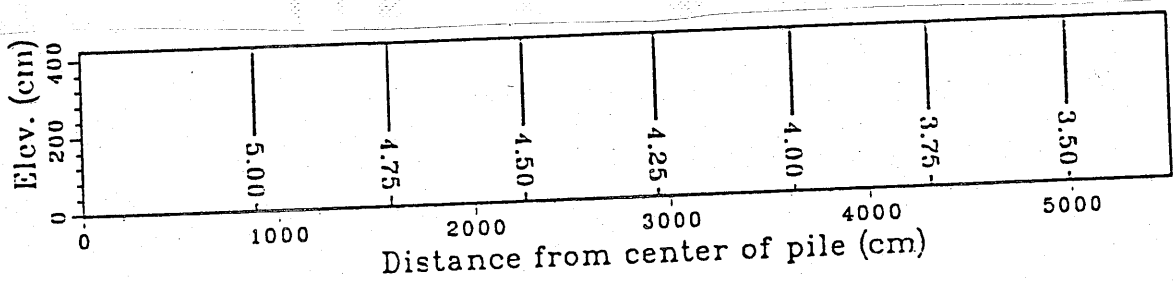

Figure 3.2. Contoured field of Brooks/Corey parameter describing unsaturated hydraulic conductivity.

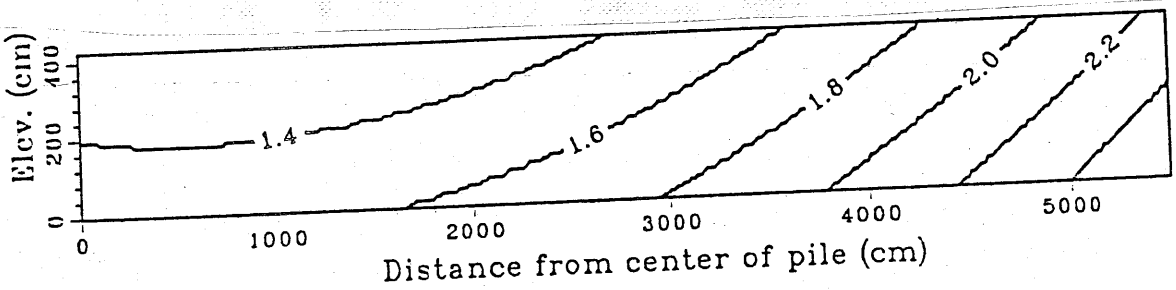

Figure 3.3. Contoured field of van Genuchten n parameter from multiple regression.

curve for a sandy material exhibits a larger horizontal shift and thus this soil would have a larger n value according to equation 3.9. On the other hand, a clay type material would have a smaller n value. Comparison of the this contour plot to the contoured field of porosity from regression equations developed by *Johnson [1987]* in Figure 3.7 shows the two properties have very similar trends. Figure 3.8 shows the contoured field of the moisture content at 1.5 bars pressure based on regression equations developed by Johnson. Once again, the same trend appears in this hydraulic characteristic. This comparison implies that porosity of the tailings is correlated to the soil moisture characteristic relation.

Figure 3.4 shows the contoured field of the van Genuchten α parameter in equation 3.9 as determined by multiple regression analysis. The van Genuchten parameters predicted by the regression equations are consistent with observations of the data and expected trends in this depositional environment. The α parameter defines the inverse of the height of capillary rise in a media *[van Genuchten, 1980]*. As seen in the contour plot, the α parameter is smaller in the center of the pile and becomes larger in the outer portions of the impoundment. This is consistent with capillary theory which states that the height of capillary rise in a media is inversely proportional to the size of the grains. *[Hillel, 1980]*. The data needed for the regression analysis shown in Figures 3.3 and 3.4 was taken from *Johnson [1987]*.

Figure 3.5 shows the contoured plot of the residual water saturation values assumed for the domain. The m parameter in equation 3.9 is not shown since it is a simple relationship (see equation 3.9) dependent only on the n parameter which is shown in Figure 3.3. Figure 3.9 shows three soil moisture characteristic curves developed for the sand, transition, and slime zones from the parameters shown in Figures 3.3 and 3.4.

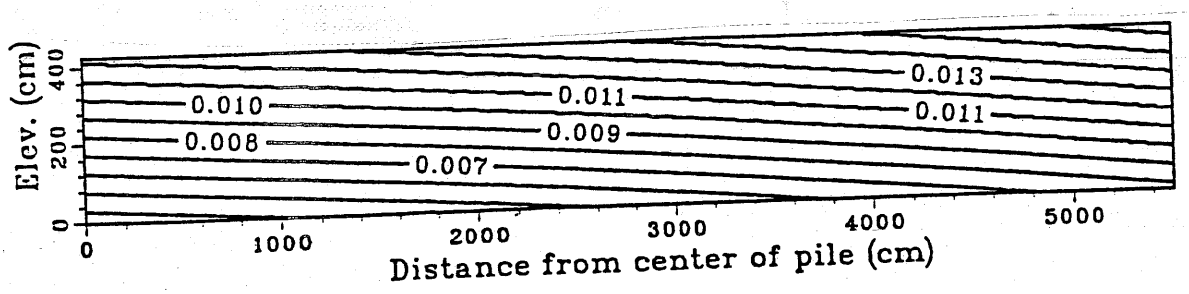

Figure 3.4. Contoured field of van Genuchten a parameter from multiple regression.

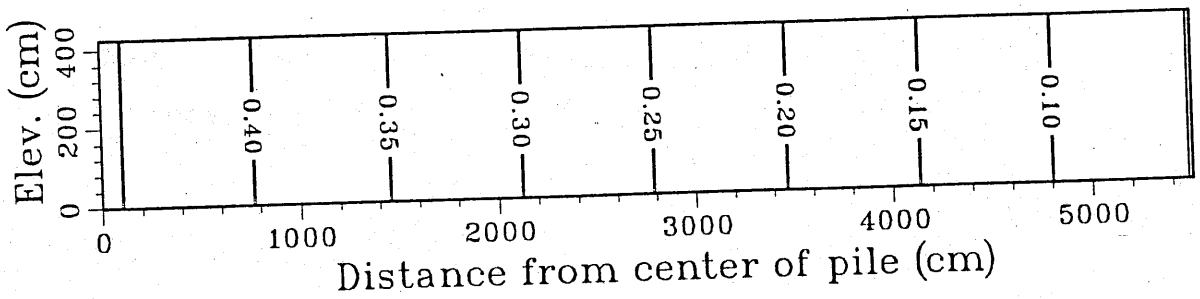

Figure 3.5. Contoured field of residual saturation.

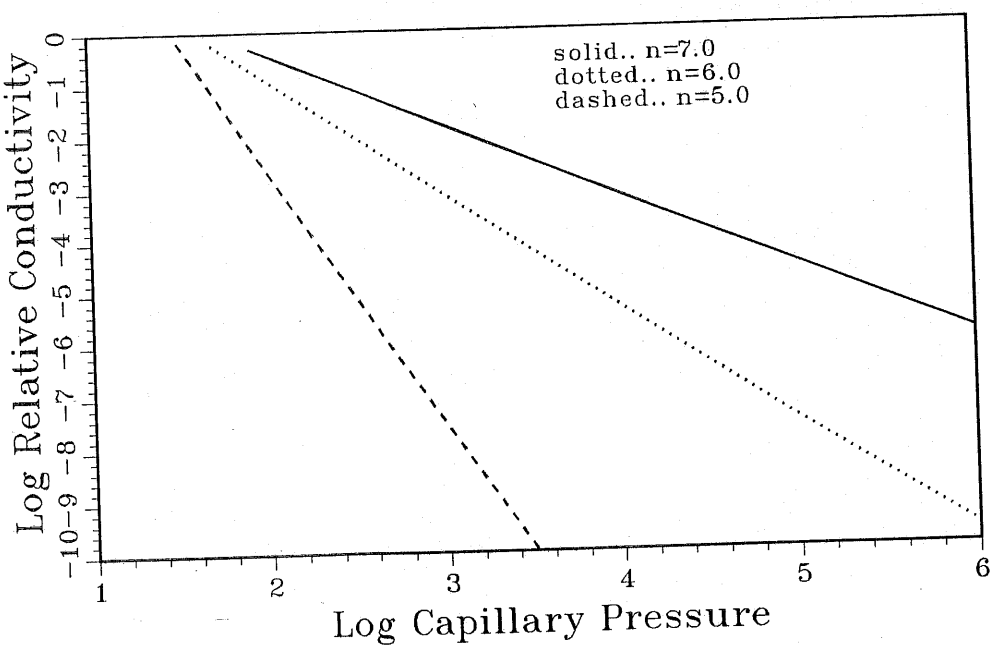

Figure 3.6. Relative hydraulic conductivity versus capillary pressure for different values of n in the Brooks/Corey model.

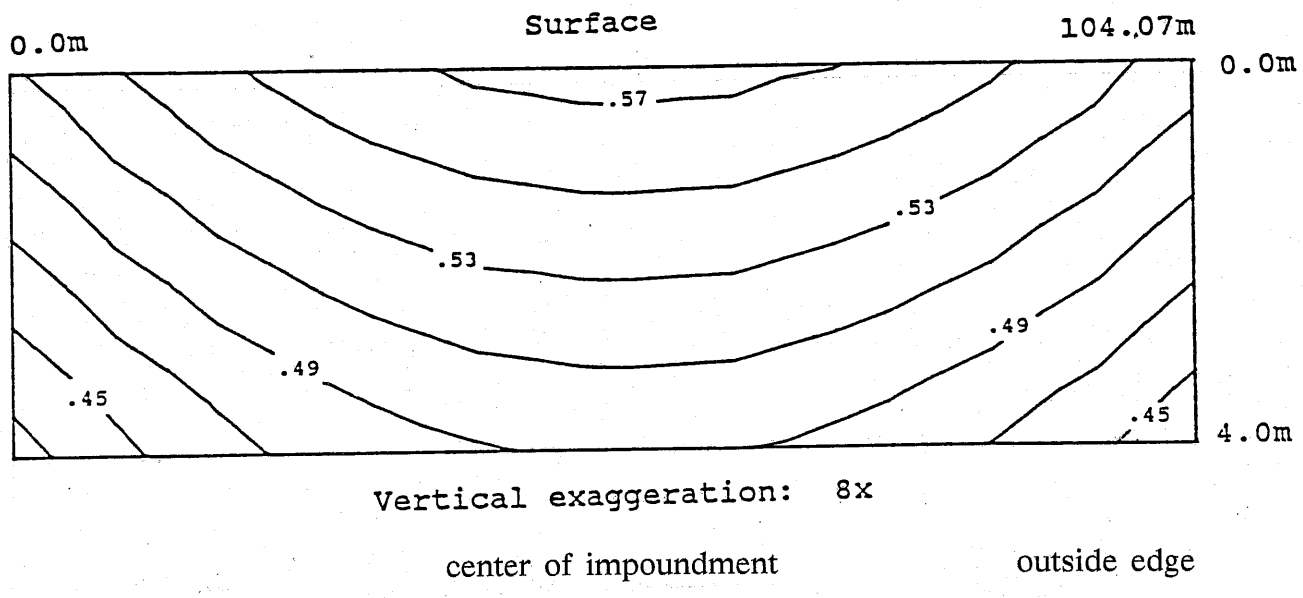

Figure 3.7. Contoured cross-section of porosity from multiple regression analysis. (After *Johnson [1987]*)

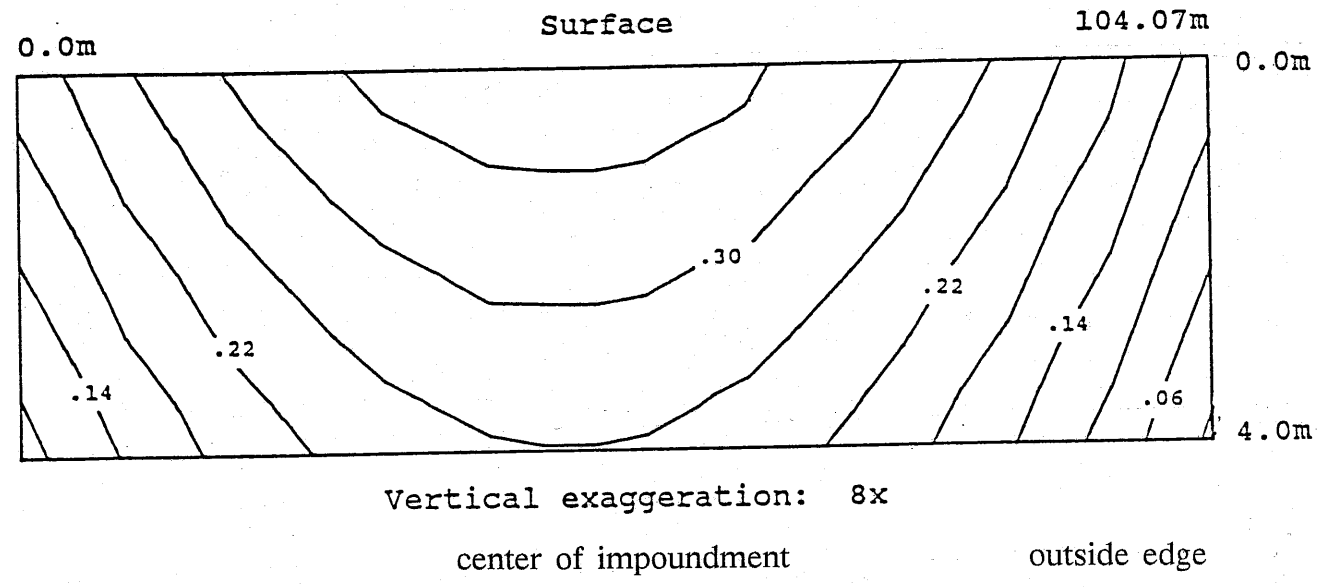

Figure 3.8. Contoured cross-section of moisture content at 1.5 bars capillary pressure from multiple regression model. (after *Johnson [1987]*)

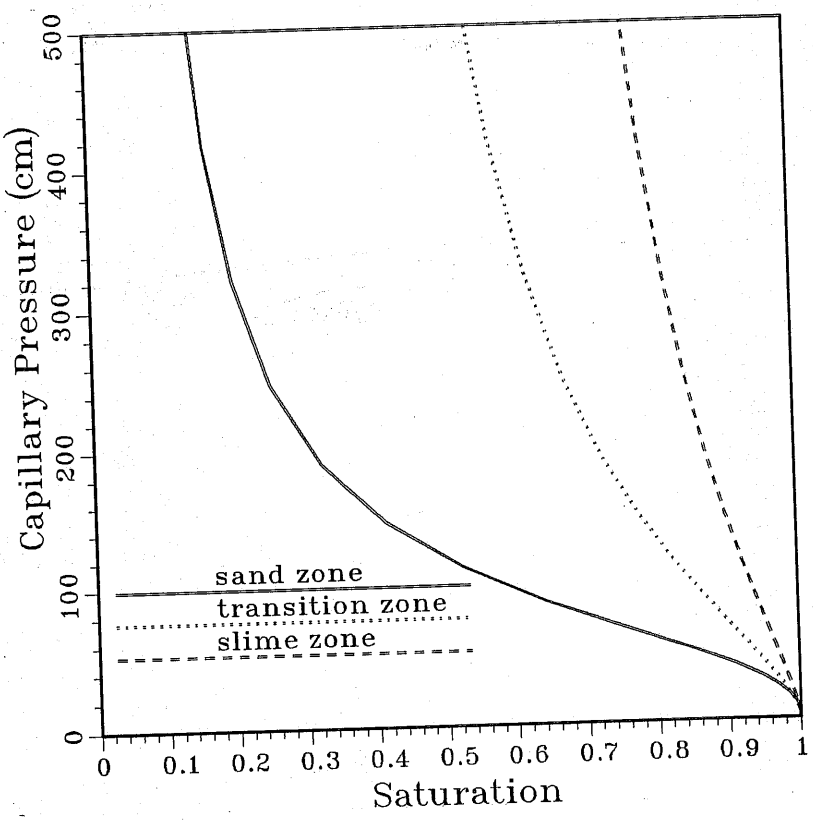

Figure 3.9. Soil moisture characteristic curves for conceptualized zones of sand, transition, and slime from hydraulic parameters shown in Figures 3.3 and 3.4.

One measure of the ability of the multiple regression model to describe the trends in the data is the multiple correlation coefficient. The multiple correlation coefficient equals one if the model is able to define all of the variability in the values. This coefficient is closer to zero if the model fails to predict the variability in the values. As shown in Appendix A, the multiple correlation coefficient for the saturated hydraulic conductivity is higher than those calculated for the unsaturated van Genuchten parameters shown in Figures 3.3 and 3.4. The ability of the multiple regression model to describe the trends in the physical parameters is dependent on several factors including the number of values in the two-dimensional domain, the spatial location of these values, and the type of regression equations employed to represent the trends. According to the multiple correlation coefficients obtained from the analysis by *Johnson [1987]*, the regression equations define the spatial variability in the saturated hydraulic conductivity relatively well. However, the multiple correlation coefficient determined in this study for the unsaturated hydraulic properties that determine the soil moisture characteristic curve show that the regression equations fail to predict much of the variability in the physical parameters. Nevertheless, the general trends depicted in the predictions from the regression equations are consistent with observations made in the field and the data which was analyzed. This analysis is not intended to reproduce the true field conditions. In this analysis, we are only interested in predicting the major trends in the data. Therefore, regression analysis is very useful.

One very helpful attribute of the regression model predictions is the smoothed property fields which result from the least squares analysis in order to determine the coefficients for the regression equations. The smooth trends inherent in the two-dimensional regression fields is very helpful in promoting convergence of the numerical solution as discussed in Chapter 2. Therefore,

regardless of the inability of the regression equations to completely define the spatial variability in the hydraulic properties, these property fields were used in the deterministic simulations because the general trends of the predictions were consistent with the trends seen in the data determined in the field and laboratory.

As a first approach, the contoured fields were broken into zones within which the hydraulic properties were considered homogeneous. This approach was abandoned because of numerical difficulties encountered obtaining a solution for the system of highly non–linear equations resulting from to the incorporation of the zones. These homogeneous zones actually created a layering effect in the model. These problems eventually produced an even simpler and more correct approach to incorporate the spatial variability in the hydraulic properties defined by the regression equations. Instead of artificially producing homogeneous zones within the domain which were not predicted by the regression model, the regression equations were used to determine a smooth field of saturated and unsaturated hydraulic properties throughout the domain. In other words, the hydraulic properties were allowed to change from element to element so that each element in the domain has it's own set of hydraulic properties defined by the regression equations.

Appropriate changes were made in the numerical code in order to incorporate this approach and simple algorithms were written to produce the values of the hydraulic properties for each element in the domain according to the regression equations. This method is more consistent with the predictions made by the regression equations and also serves to greatly smooth the unsaturated hydraulic properties. This smoothing is a very important factor in decreasing the nonlinear nature of the system of equations which result from the finite element formulation in unsaturated media. Incorporating hydraulic property distributions in this fashion produces an essentially homogeneous media

over the small scale encompassing several nodes. Therefore, the nonlinear nature of the problem is decreased. This implication is very advantageous when solving large systems of equations which result from the fine grid size needed for unsaturated problems. Not only does this smoothing allow a solution to be obtained for the system of equations but also reduces the central process unit (c.p.u.) time needed to obtain the solution.

Results of deterministic simulations

A complete set of results is given for each numerical simulation. Included in the results are contour fields of pressure head, hydraulic head, saturation, darcy velocity vector field, flux rate at the base of the tailings, and the cumulative flux as a function of the distance from the center of the pile. In addition, the complete set of boundary conditions, including prescribed pressure head boundaries and prescribed flux boundaries are stated or shown graphically for each simulation. The hydraulic head field, analogous to the total potential field, determines the directional component of the total energy gradient (not including thermal, electrical, and chemical gradients, which are not considered in this analysis). The velocity vector field gives the direction and relative magnitude (relative to all other vectors in the plot) of the mean darcy velocity of fluid particles at the finite element centroid. In general, only one of every 20 vectors is plotted. The saturation field is very important in determining the type of chemical processes that will occur in the tailings as well determining the location of the "free water table surface" in the tailings impoundment. The seepage rate at the base of the tailings is perhaps one of the most important results of the simulations, because this prediction actually shows where the seepage rates are greatest. Consequently, the distribution of seepage rate indicates which areas of the impoundment could contribute to groundwater contamination. This flux rate

at the base of the impoundment was assumed equal to the vertical velocity at the centroid of each element along the bottom row in the grid. Cumulative downward flux as a function of distance from the center of the pile is another way to gain insight about locations in the pile which are contributing significantly to seepage. In most cases, relative seepage magnitude across the pile is also plotted on the same graph as cumulative downward flux. This curve is a scaled version of the flux distribution at the base of the pile, but is presented as a relative percentage of flux from 0 to 100 percent.

In order to help the reader clarify and distinguish various boundary conditions for each simulation, Table 3.1 provides as a summary of boundary conditions and other important information. Table 3.1 shows when boundary conditions for different simulations are identical in order to aid the reader in comparing the effects of incorporated anisotropy.

Mass Balance Calculations for Steady-State Simulations

One method used to check the validity of numerical solutions is by applying mass balance principles. Mass balance computations can be carried out for steady-state simulations by equating the total mass entering the system to the total mass leaving the system. If these quantities are very close to being equal, one can have some confidence that the solution is correct, provided that proper verification and validation of the numerical scheme has been completed. *Huyakorn et al. [1984]* discuss efficient and accurate techniques for mass balance computations.

Computations for the steady-state simulations performed in this study always showed excellent mass balance. After experimentation, the convergence criteria for the numerical scheme was set at 1 cm pressure head. When implementing this convergence criteria, mass balance computations always

Simulation	Anistropy (K_h/K_v)	Explaination of boundary conditions	
		Surface	Base
DS1	1	0–2200cm, ψ =15cm 2200–5500cm, ψ =–100cm	ψ =–55cm
DS2	1	0–2200cm, ψ =15cm 2200–5500cm, ψ =–400cm	"
DS3	1	0–5500cm, downward flux of 12.7 cm/yr	"
DS4	1	0–5500cm, downward flux of 51 cm/yr	"
DS5	20	identical to DS1	"
DS6	20	identical to DS2	"
DS7	100	identical to DS2	"
DS8	20	identical to DS3	"
DS9	100	identical to DS3 and DS8	"
DS10	20	identical to DS4	"

Table 3.1. Summary of boundary conditions and anisotropy ratios used in deterministic simulations.

showed errors to be less than .01% of the total flow into the system. For steady-state simulations, this computation involves calculating nodal fluxes at all the boundary nodes and equating them equal to zero. Given these results, and the previous verification and benchmarking of VAM2D, I feel that much confidence can be placed in the numerical solutions obtained in this study.

Results of simulations considering isotropic tailings

In the first set of simulations performed, the media is considered isotropic. In other words, for each element in the grid, the saturated hydraulic conductivity in the vertical direction is assumed equal to saturated hydraulic conductivity in the horizontal direction. Boundary conditions for the domain were chosen to depict soil moisture conditions which were observed in the field throughout the year of sampling.

A brief description of the boundary conditions and the reasoning used to determine them is discussed for each simulation. Soil moisture conditions at the base of the pile are consistent with those measured in the field by *Harris [1987]* using a neutron moisture probe to determine moisture content. This moisture content value was then correlated to a pressure head determined by the soil moisture characteristic curve for the media. The soil moisture conditions from the edge of the pond to the edge of the pile are difficult to estimate since the neutron moisture probe can only be used with confidence approximately 20-30 cm below the surface depending on moisture conditions. Prescribed pressure head boundaries along this surface were generally implemented in an effort to depict soil moisture conditions present under different scenarios. Obviously, this method of estimating boundary conditions has inherent weaknesses which can lead to gross miscalculations in the boundary conditions used for the simulation. However, the information gained from these simulations

can nevertheless be very helpful in determining the sensitivity of the model to different boundary conditions. Once again, one purpose of the deterministic simulations is to gain insight into the effect of boundary conditions on the seepage from the pile and hopefully determine boundary conditions that reflect the conditions present at the impoundment at different times of the year. Therefore, more meaningful boundary conditions can be incorporated into the conditional and stochastic–deterministic simulations that will follow the deterministic simulations. Unless otherwise stated, the inside and outside edge of the pile are considered no flow boundaries.

Figure 3.10 graphically displays the boundary conditions for the steady–state scenario depicted in deterministic simulation #1 (DS1). A fifteen centimeter depth of ponding exists to 22 meters outward from the center of the impoundment and a condition of partial saturation in incorporated from the edge of the pond to the edge of the pile. The sides of the impoundment are considered no flow boundaries. This simulation is not an attempt to recreate boundary conditions present at the impoundment described by *Harris [1987]*. The status of the impoundment for DS1 are shown in Figures 3.11 a,b,c,d. Figures 3.12–3.13 show the seepage distribution and the cumulative downward flux at the base of the impoundment. In this simulation, the boundary conditions were chosen to depict the conditions present at an abandoned impoundment in the rainy season or at an active impoundment when fresh tailings slurry is being placed in the impoundment daily.

Since the capillary pressure at the surface of the impoundment is relatively low, the sandy portions of the pile exhibit the largest downward seepage even though the tailings are unsaturated in this portion of the impoundment. Figure 3.12 shows that the seepage rate at the base of the tailings continuously increases from the center of the pile to the outer edge. In fact, the seepage rate

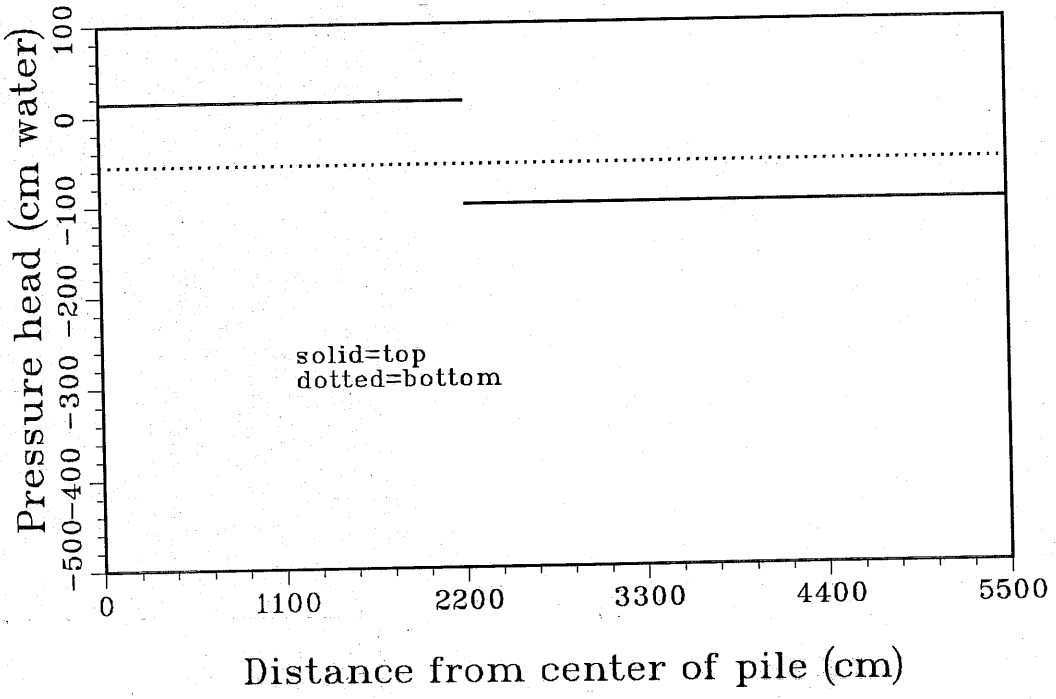

Figure 3.10. Graphical representation of boundary conditions for DS1.

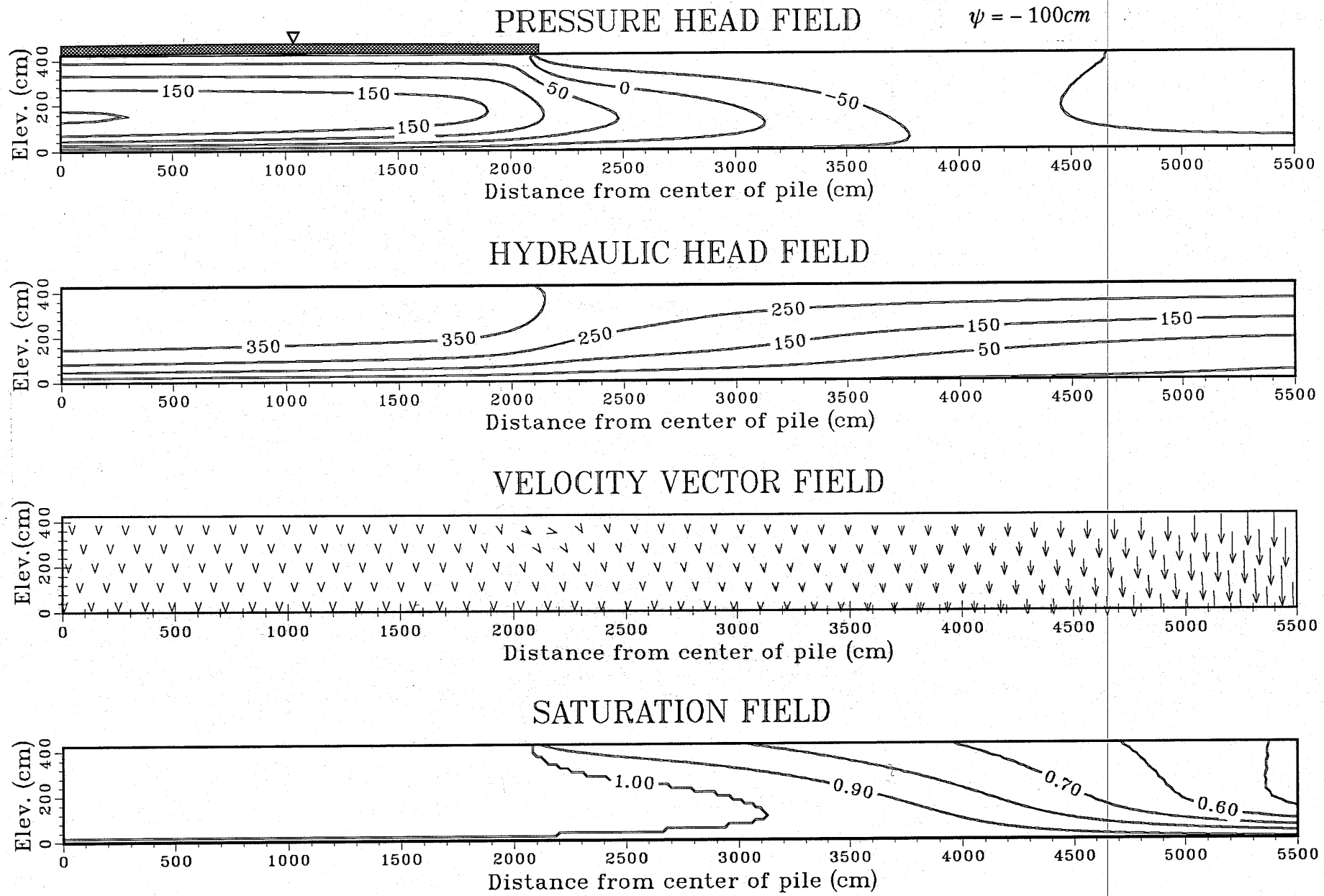

Figure 3.11(a,b,c,d). Steady-state results from deterministic simulation 1. Isotropic media.

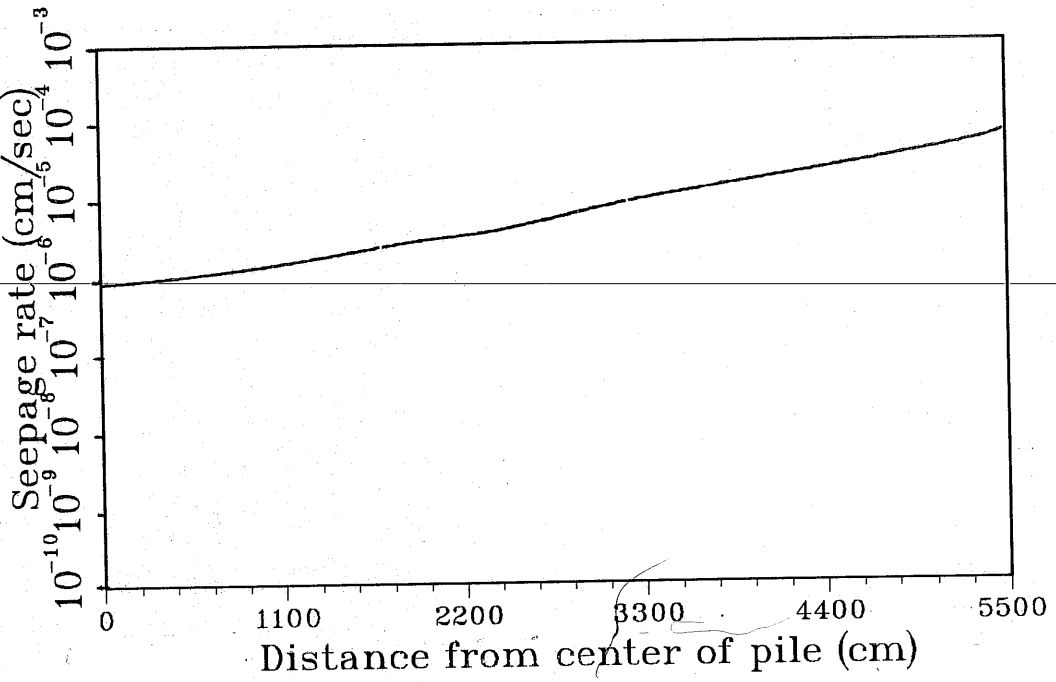

Figure 3.12. Flux distribution at the base of the impoundment for DS1.

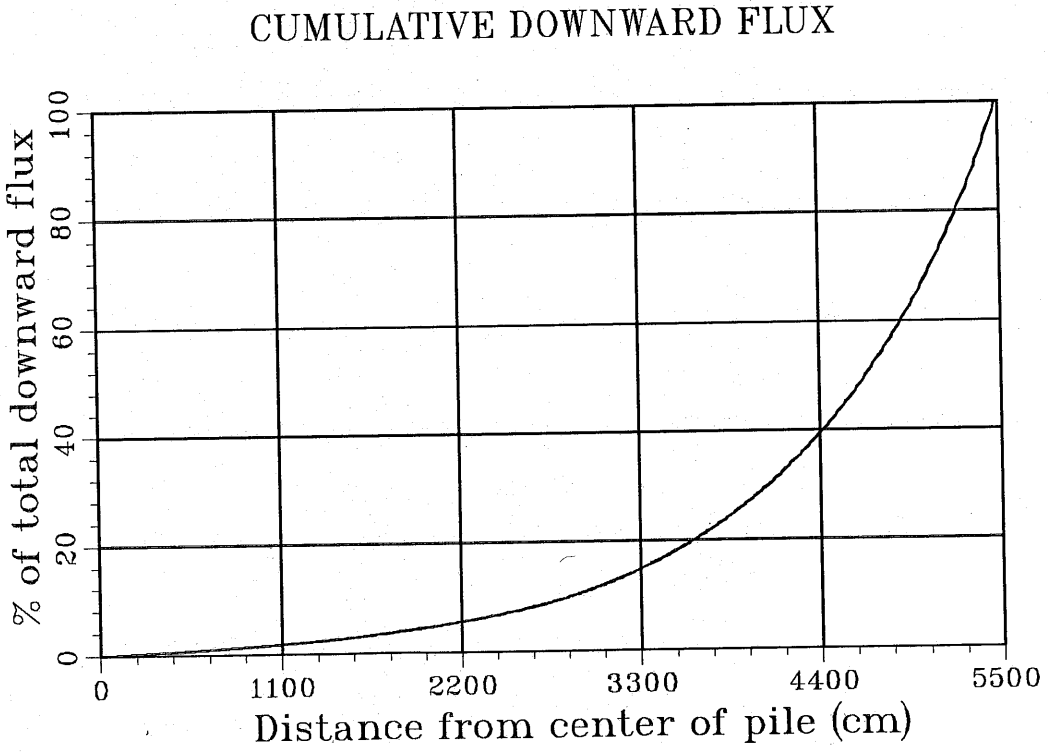

Figure 3.13. Cumulative flux curve and relative flux distribution at the base of the impoundment for DS1.

at the outside of the pile is approximately 100 times greater than the seepage rate under the ponded region. It should be noted that the ponded depth of 15cm at the very edge of the pond may be somewhat unrealistic. One would expect the pond depth to decrease at the edge of the pond. The greater depth of ponding may slightly increase the seepage rate at the edge of the pond due to increased hydraulic gradients but the results are expected to be very similar to those shown here. In Figure 3.13 it can be seen that 50% of the downward flux from the impoundment seeps from the outside 9 meters of the tailings. The tailings exhibit a high degree of saturation even in the sandy portions of the pile. This result is inconsistent with field observations during anytime of the year. This suggests that the prescribed head boundary condition at the surface of the impoundment is either too "wet" or may be inconsistent with field conditions. The hydraulic gradient is generally downward in most portions of the pile with the exception of the area in the vicinity of the edge of the pond. In this area, the hydraulic gradient shows significant horizontal components to accommodate the horizontal movement of water from the pond to the outer area which exhibits a smaller total fluid potential.

The boundary conditions for DS2 are intended to depict a situation after the rainy season has passed when the outer portions of the pile have dried out significantly. This scenario could also represent a portion of the impoundment which is drier because tailings are being deposited on the opposite side of the impoundment. The impoundment is still ponded from the center of the impoundment outward to 22 meters. Figure 3.15 a,b,c,d show the state of the impoundment under steady state conditions for the boundary conditions given in Figure 3.14. Once again, the majority of the flux is vertically downward except for the upper portion of the pile close to the boundary between the pond and the unsaturated region where some evaporation is shown due to the discontinuous

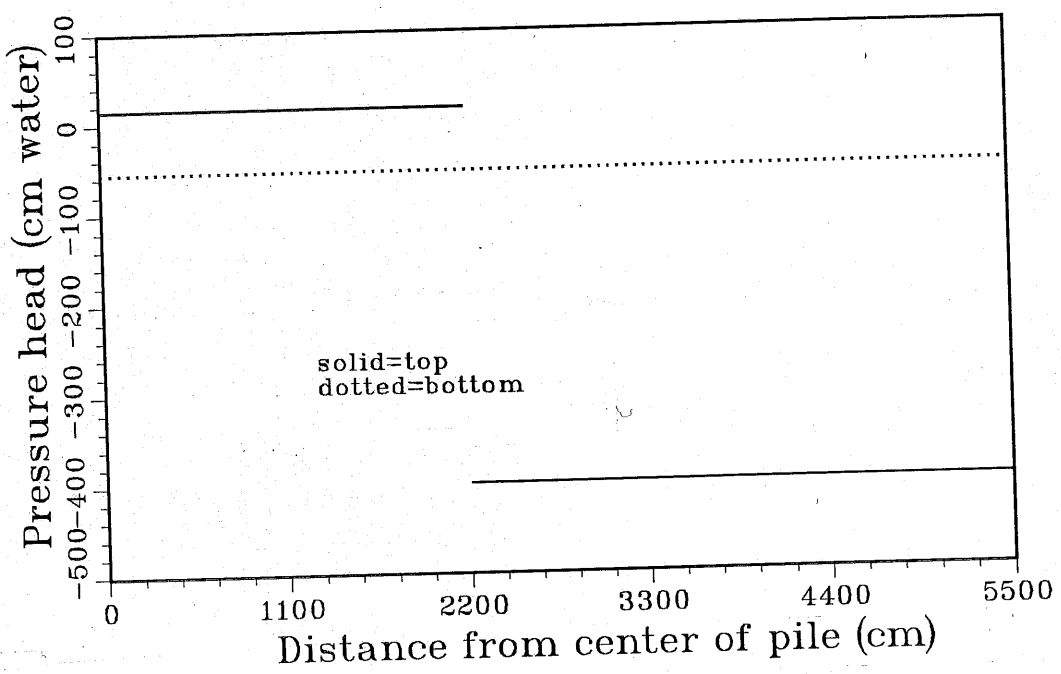

Figure 3.14. Graphical representation of boundary conditions for DS2.

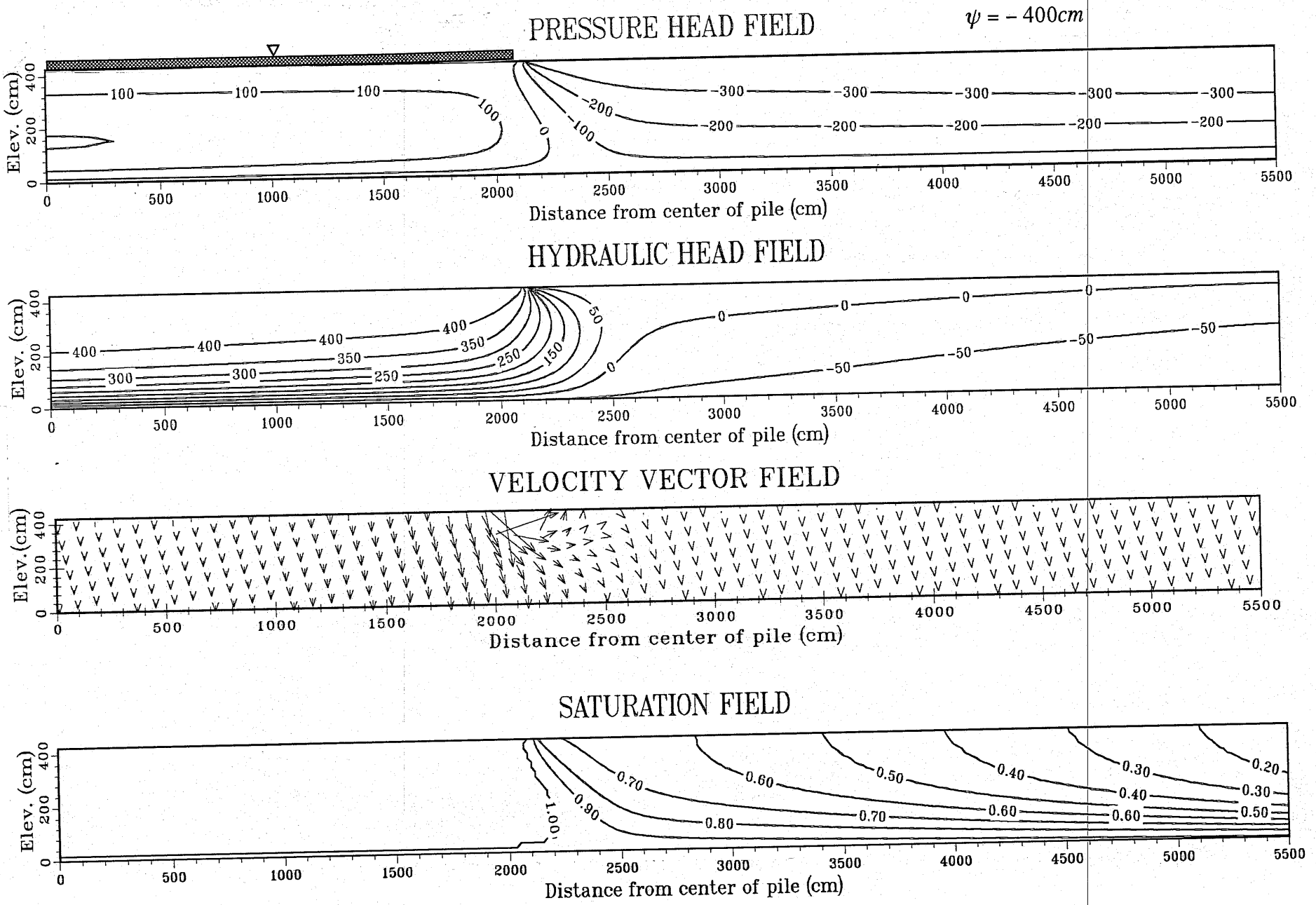

Figure 3.15(a,b,c,d). Steady-state results from deterministic simulation 2. Isotropic media.

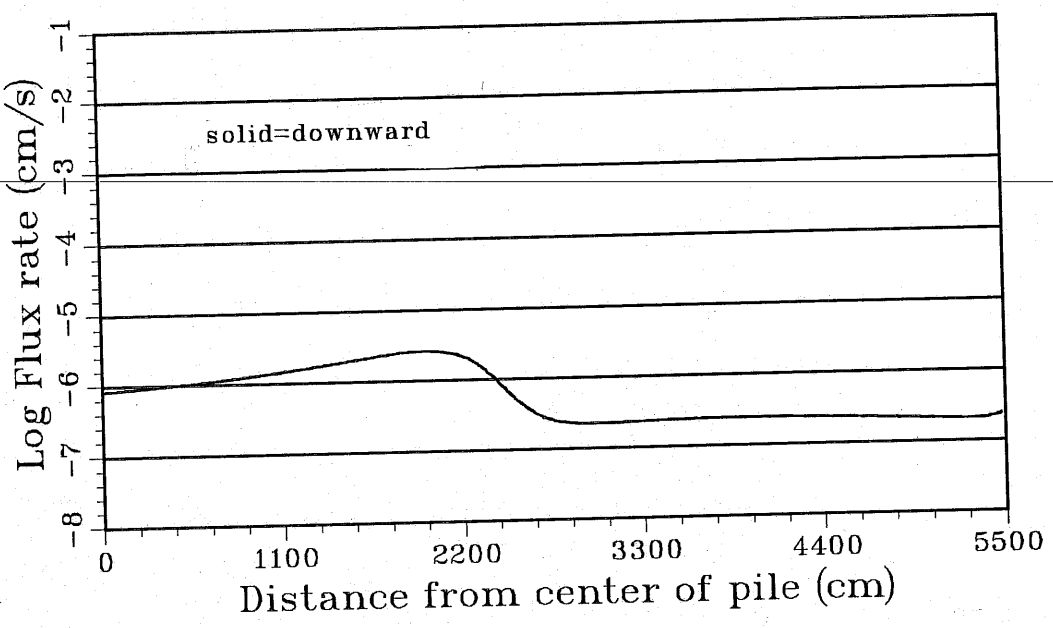

Figure 3.16 Flux distribution at the base of the impoundment for DS2.

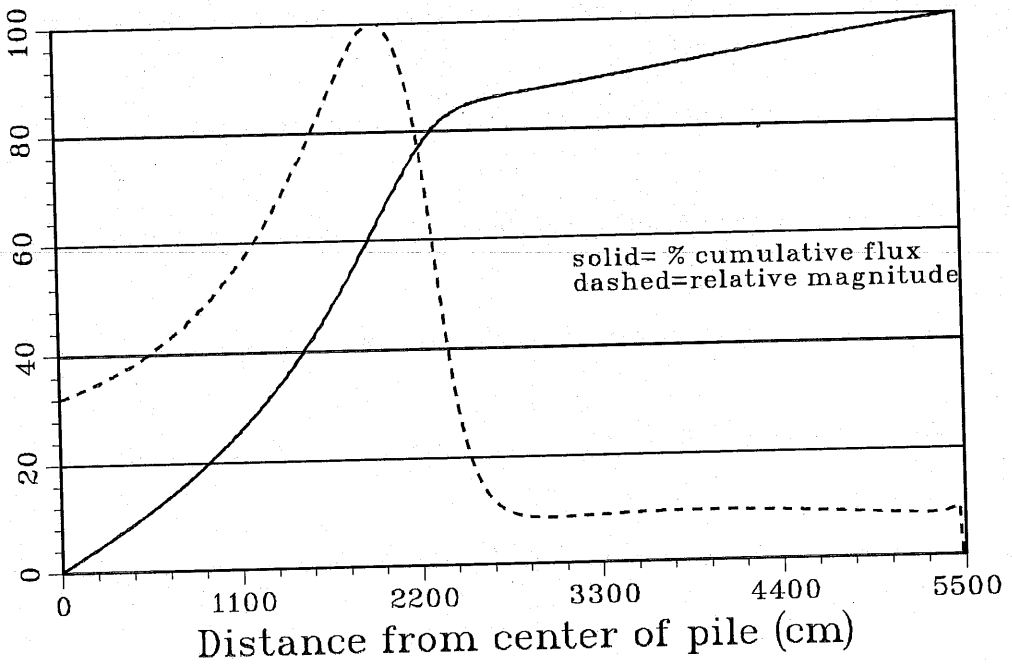

Figure 3.17. Cumulative flux curve and relative flux distribution at base of the impoundment from DS2.

boundary conditions at the edge of the pond. The extension of the saturated zone is limited to the region directly under the ponded region. Compared to Figure 3.11b from DS1, the hydraulic gradient shows a larger horizontal component in order to satisfy the larger variation in the total fluid potential in the horizontal direction. Although the saturation profile shown in Figure 3.15b exhibits a closer resemblance to observed field data, the results are inconsistent with the moisture content profiles shown in chapter 2. This is due to the uncertainty in boundary conditions and the incorporation of the smoothed hydraulic property fields. The smoothed fields from the regression equations do not depict the natural layering present in the impoundment. Therefore, seepage is not inhibited in the deterministic models as is seen in the moisture profile observed in the field. Figure 3.16 shows that the flux distribution across the tailings impoundment has changed dramatically as compared to the steady state conditions determined for the "wetter" conditions depicted in DS1. The seepage rate the base of the pond is now greatest at the edge of the ponded region and least at the outer edge of the pile. The downward flux increases consistently from the center of the impoundment to the edge of the pond because the saturated hydraulic conductivity is slowly increasing according to the predictions made by the regression equations. The simulation predicts that over 80% of the downward seepage from the impoundment now originates directly from the ponded region. Comparison of Figures 3.16 and 3.12 display the large variation in the seepage distribution as a function soil moisture conditions and weather conditions at the surface of the impoundment.

Deterministic simulation #3 (DS3) and was performed in an effort to determine the flow dynamics of the impoundment in the winter months when snow is present on the surface of the tailings. Daytime heating causes a slow melting and thus an relatively constant influx of moisture through the surface of

the tailings. In DS3, the relatively wet boundary condition at the base of the impoundment corresponds to a situation where a phreatic water table exists a short distance below the pile. The influx rate at the surface of the impoundment is approximately 0.0015 cm/day or 12.7 cm/year. Figure 3.18 a,b,c,d reveal the variation in capillary pressure and saturation due to the incorporation of the heterogeneity in the unsaturated hydraulic properties in this model. Figures 3.19 and 3.20 show that the flux distribution at the base of the impoundment is very similar to the input flux at the surface of the impoundment at these low infiltration rates.

DS4 was completed in order to evaluate the distribution of seepage when a relatively high rate of precipitation is falling on the impoundment. The influx rate of precipitation for DS4 was 51 cm/year and the bottom boundary is still prescribed at 55 cm capillary pressure. Figure 3.21a shows that the pressure head at the top-center of the impoundment is greater than zero and thus under these steady state conditions, ponding would occur on the impoundment. The hydraulic head field exhibits non-vertical directional components from the center to the outer portions of the impoundment. Since the media is considered isotropic, these gradients do not significantly alter the spatial distribution of flux at the base of the pile, as exhibited in Figures 3.22 and 3.23. However, if the media were, in fact, considered anisotropic, these horizontal flow components would be amplified and could have a significant impact on movement of moisture in the impoundment. We shall investigate the effect of anisotropy in the next section.

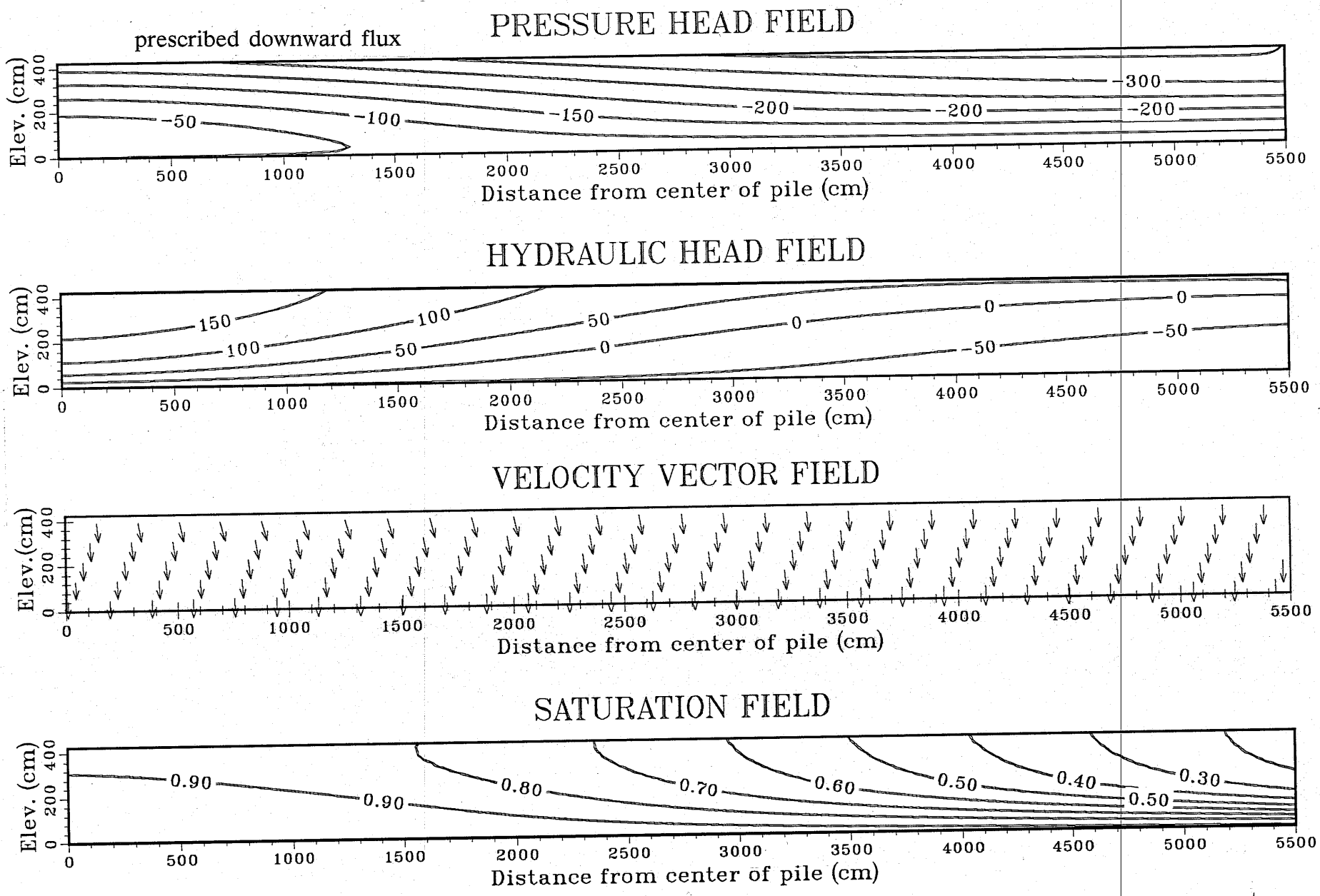

Figure 3.18(a,b,c,d). Steady-state results from deterministic simulation 3. Isotropic media.

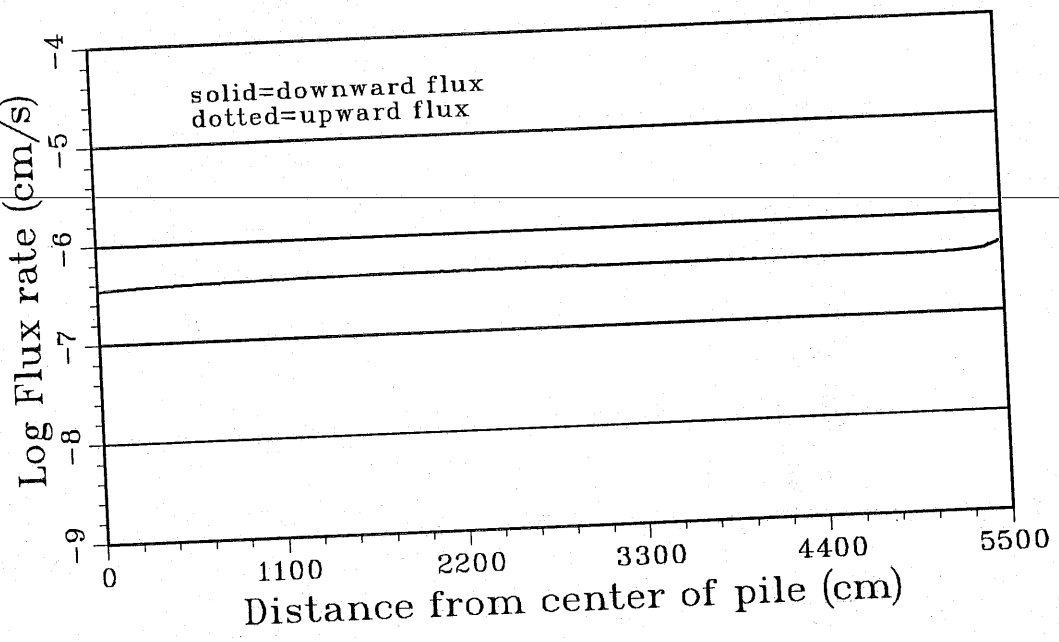

Figure 3.19. Flux distribution at the base of the impoundment for DS3.

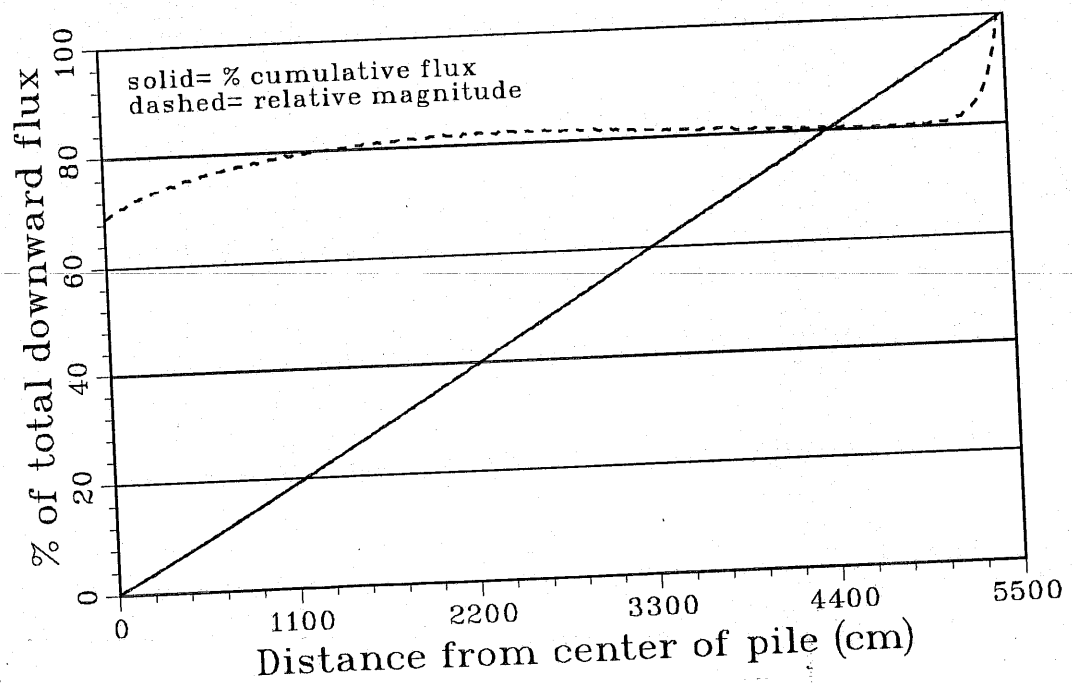

Figure 3.20. Cumulative flux curve and relative flux distribution at the base of the impoundment for DS3.

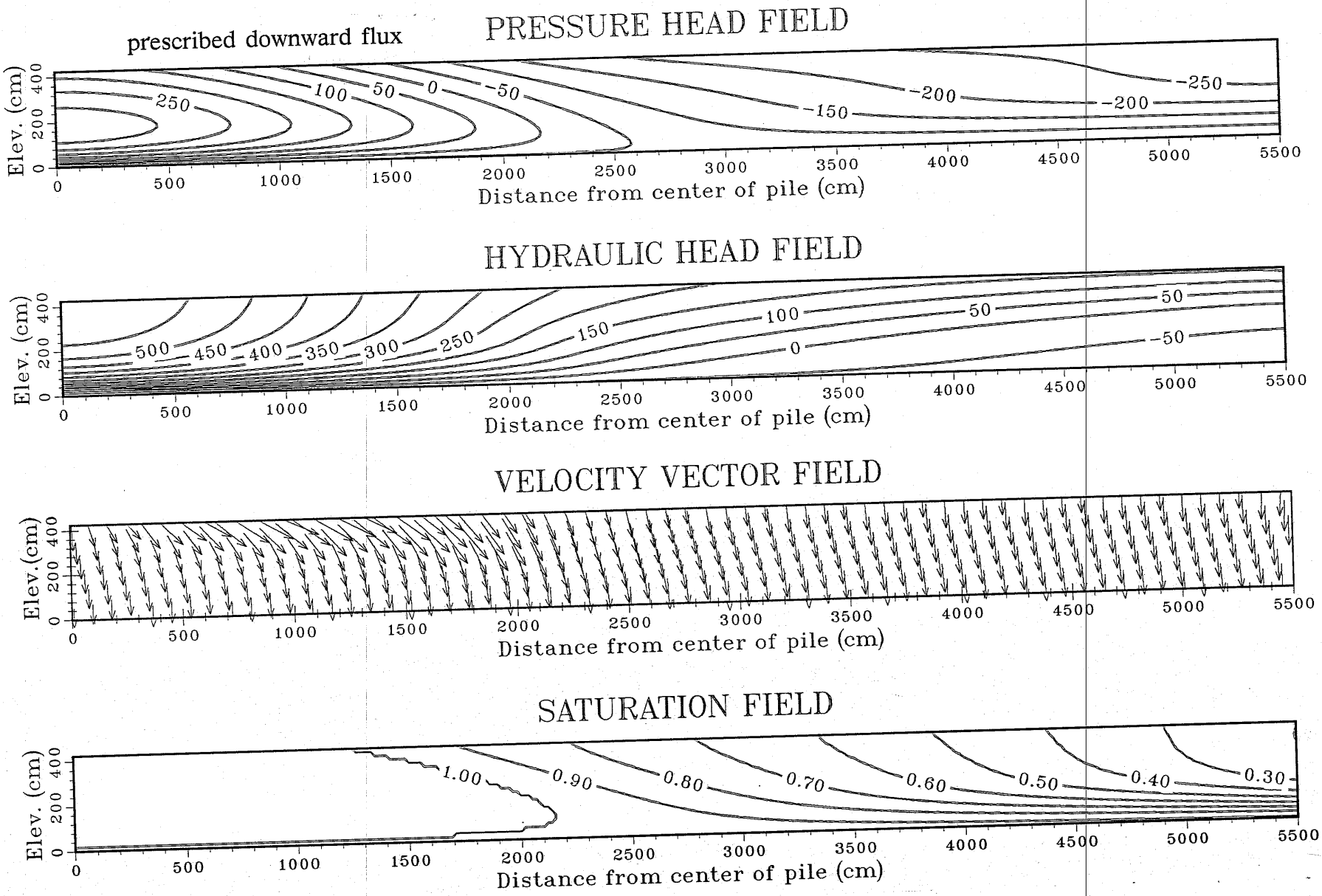

Figure 3.21(a,b,c,d). Steady-state results from deterministic simulation 4. Isotropic media.

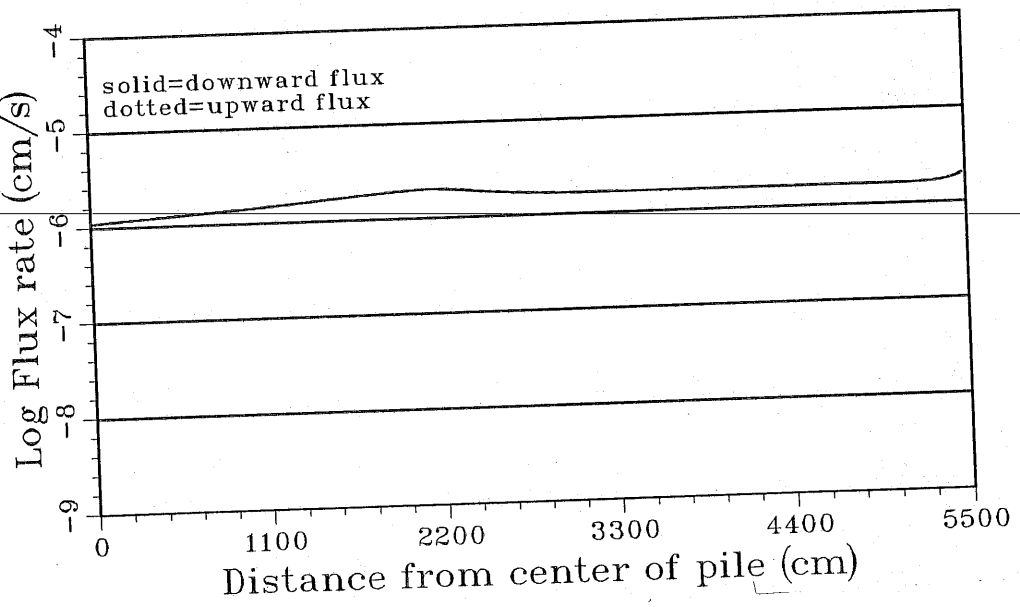

Figure 3.22. Flux distribution at the base of the impoundment for DS4.

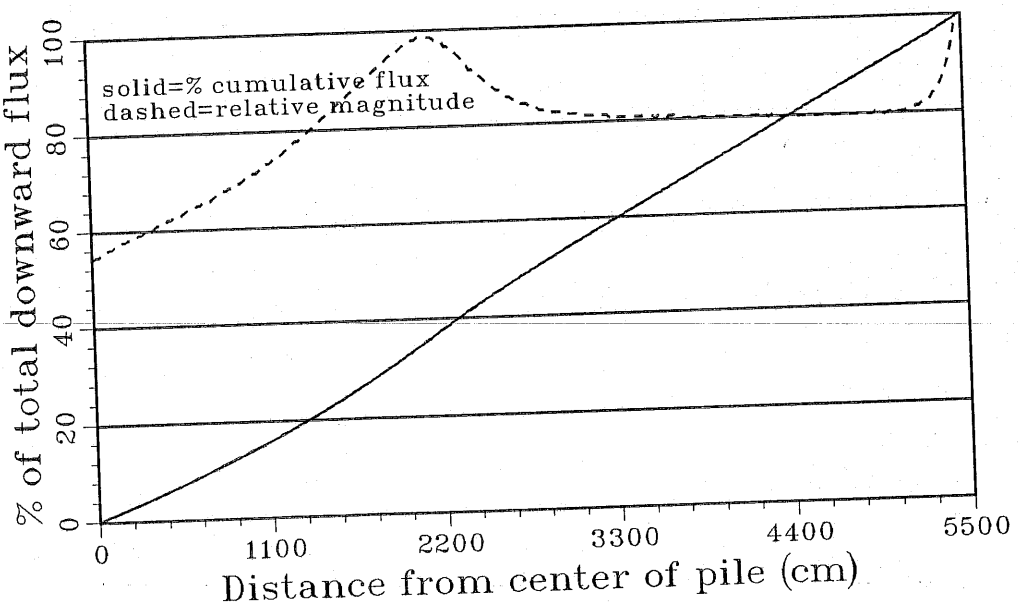

Figure 3.23. Cumulative flux curve and relative flux distribution at the base of the impoundment for DS4.

Results of Simulations Considering Constant Anisotropy

Siegel and Stephens [1980] have shown the effects of anisotropy on the saturation distribution under a lined mill tailings impoundment. *Johnson [1987]* presents pictures of tailings cores which exhibit extensive layering, especially in portions of the pile where the depositional environment is changing rapidly due to variations in the amount and type of tailings slurry being placed in the impoundment. Therefore in this section, results of simulation will be presented which consider the anisotropic nature of the tailings material. In the following simulations, the anisotropy ratios considered were 20 and 100. The anisotropy ratio refers to the ratio of the horizontal to vertical saturated hydraulic conductivities. In order to obtain anisotropy in the media, the horizontal conductivity was simply multiplied by the anisotropy ratio. The simulations were performed under the same boundary conditions as the isotropic simulations so that meaningful comparisons of simulations are possible.

DS5 was performed under the same boundary conditions as DS1. The major difference in the steady state predictions from the simulations are found in Figure 3.24c where the flux exhibits significant lateral components which leads to a shift in the cumulative flux curve in Figure 3.26. The incorporated anisotropy ratio of 20 induces significant lateral flow components in the saturated and unsaturated zones which is an important consideration in modeling contaminant movement from waste impoundments. Figure 3.24c also shows that the lateral extent of complete saturation is now extended further from the ponded region.

DS6 and DS7 were completed assuming identical boundary conditions as DS2. The anisotropy ratio was 20 and 100, respectively, for DS6 and DS7. Figures 3.27a,b,c,d, 3.28, and 3.29 show the results of DS6. Figure 3.29 clearly shows that a significant amount of seepage from the impoundment originating

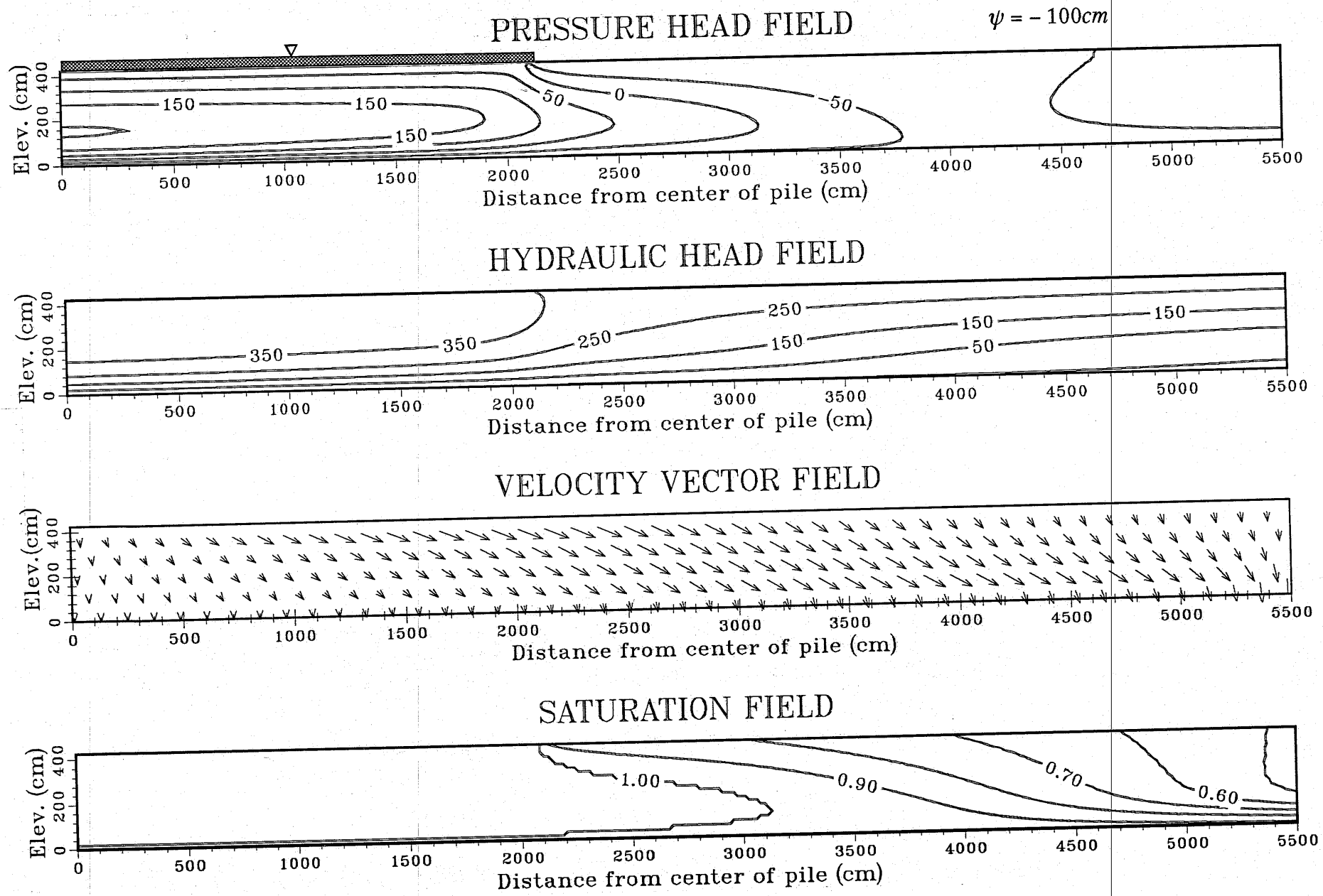

Figure 3.24(a,b,c,d). Steady-state results from deterministic simulation 5. Anisotropy ratio equals 20.

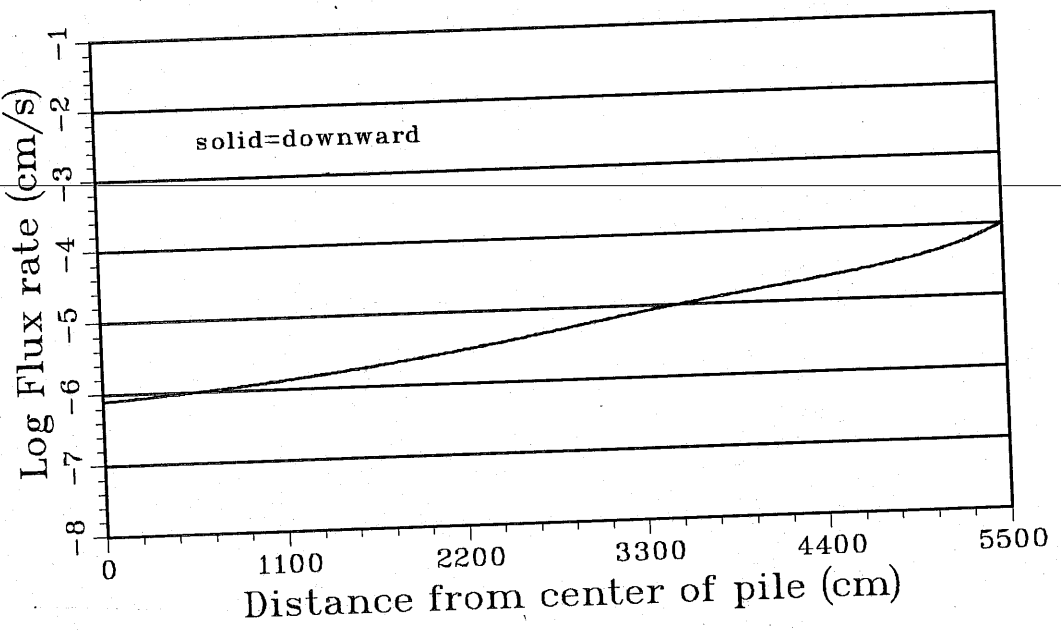

Figure 3.25. Flux distribution at the base of the impoundment for DS5.

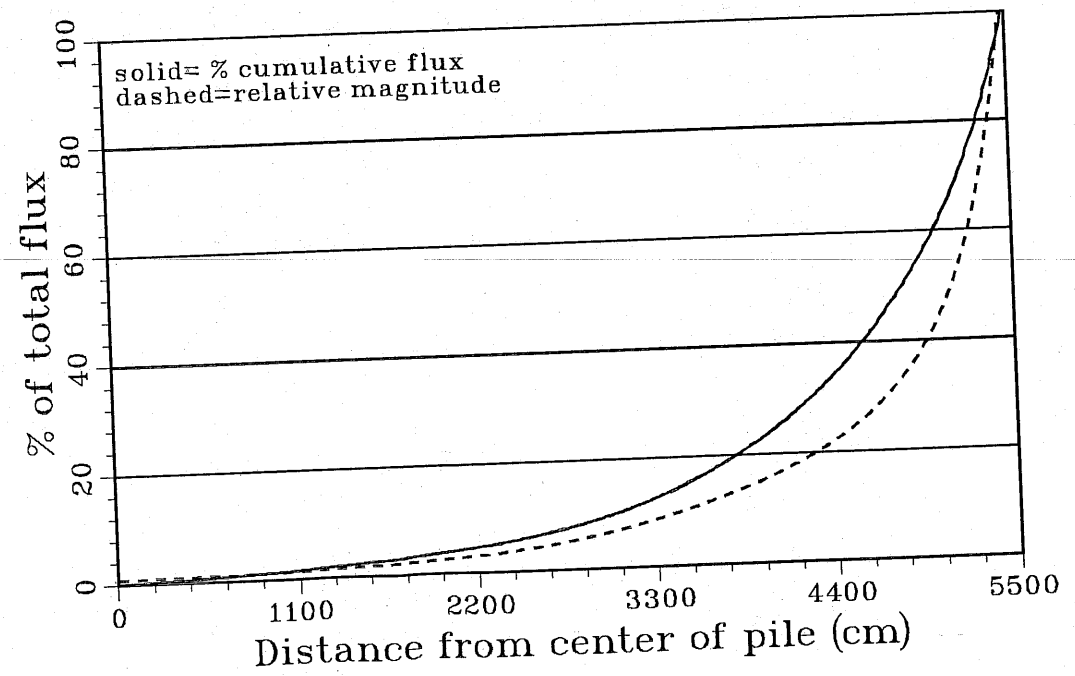

Figure 3.26. Cumulative flux curve and relative flux distribution at the base of the impoundment for DS5.

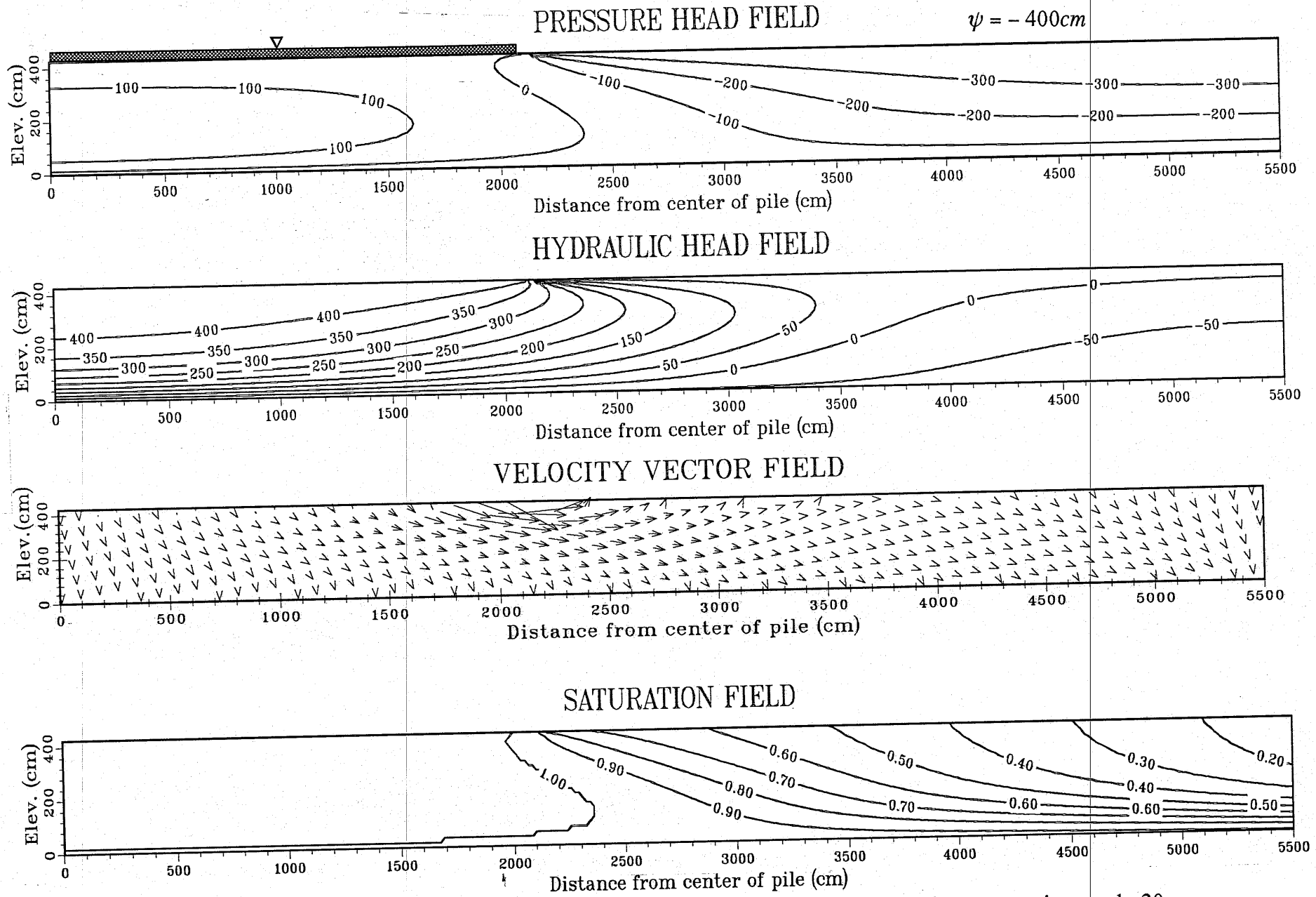

Figure 3.27(a,b,c,d). Steady–state results from deterministic simulation 6. Anisotropy ratio equals 20.

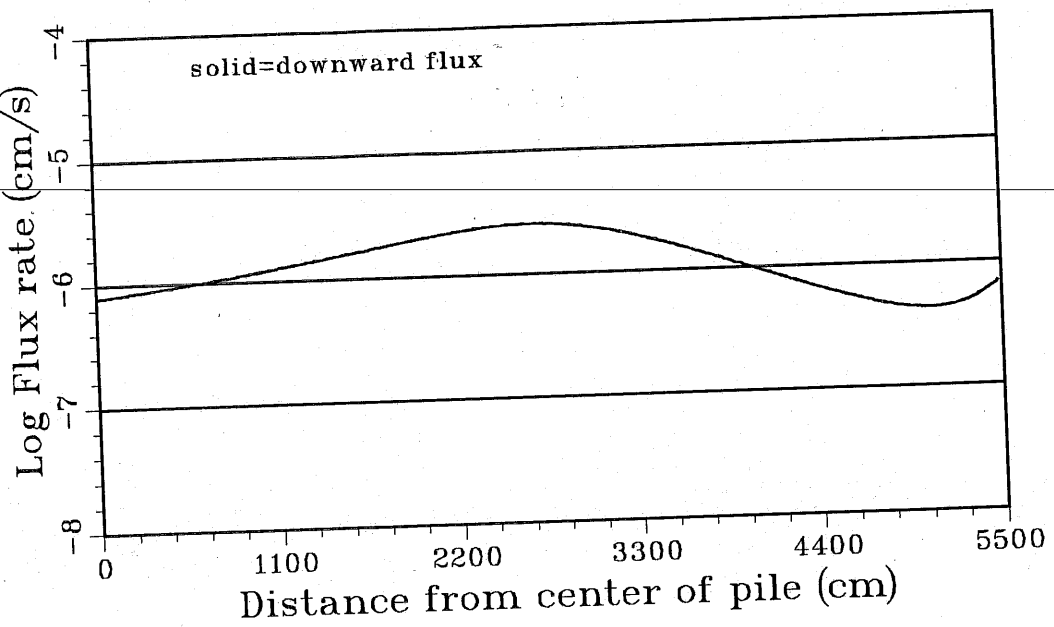

Figure 3.28. Flux distribution at the base of the impoundment for DS6.

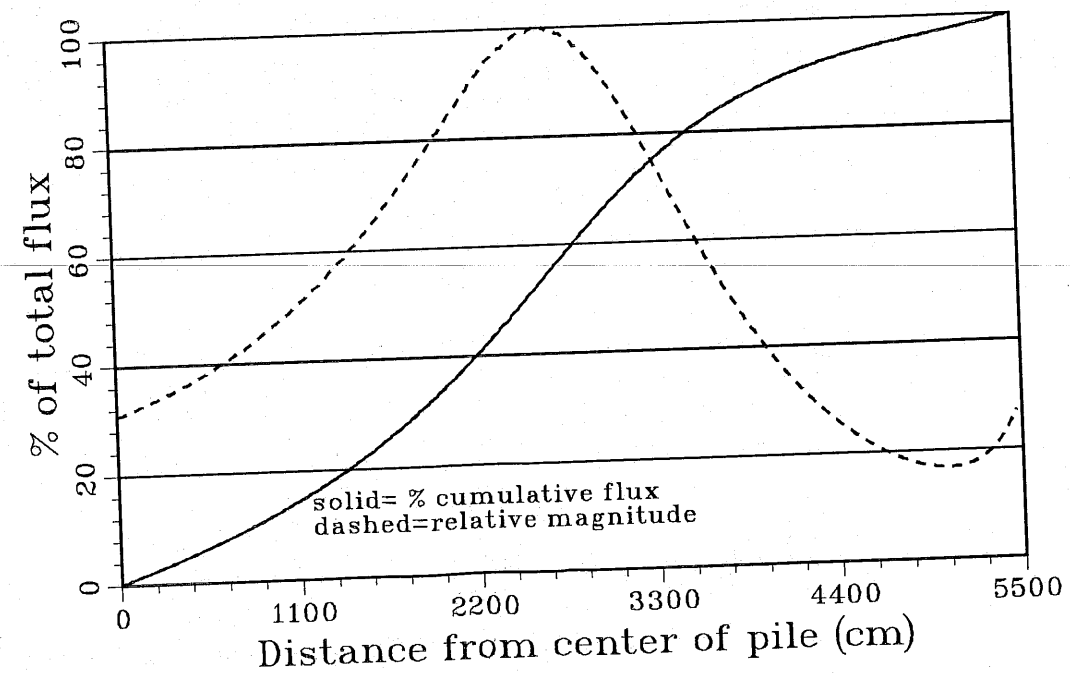

Figure 3.29. Cumulative flux curve and relative flux distribution at the base of the impoundment for DS6.

from the pond is distributed to the outer portions of the impoundment due to the anisotropic nature of the tailings materials. Also note that the velocity vectors near the surface of the pile are upward for a greater distance from the pond. This increased evaporation out of the system due to the lateral flow components is consistent with the findings of *Siegel and Stephens [1980]*.

Figures 3.30a,b,c,d, 3.31, and 3.32 show the state of the impoundment from DS7. Figures 3.30c and 3.31 show how the increase in the anisotropy ratio increases the lateral flow components in the impoundment, which in turn significantly affects the seepage distribution at the base of the pile. The increased anisotropy once again increases the availability of fluid for evaporation and thus more water is lost through the impoundment surface. But as will be discussed later, the increased anisotropy will also increase the total seepage from the impoundment under the ponded conditions.

DS8 was performed using the same boundary conditions as DS3. The media is assumed to have an anisotropy ratio of 20. Figure 3.33a,b,c,d depicts the steady state conditions for the impoundment under the prescribed boundary conditions. Figure 3.33c shows the increase in lateral flow components due to the incorporated anisotropy. The relative flux distribution curve in Figure 3.35 shows the downward flux rate at the base of the pile is doubled in the outer portions of the impoundment due to the lateral flow components. Once again, the saturation and pressure head distributions are almost identical to those for when the media is considered isotropic. It is apparent from Figures 3.34 and 3.35 that the no-flow boundary on the outer edge of the pile is forcing the moisture to move downward as it comes closer to the edge of the pile. In reality, some flow would occur through this boundary, but consideration of the flux rate at the base of the impoundment at this location proves that even if the maximum

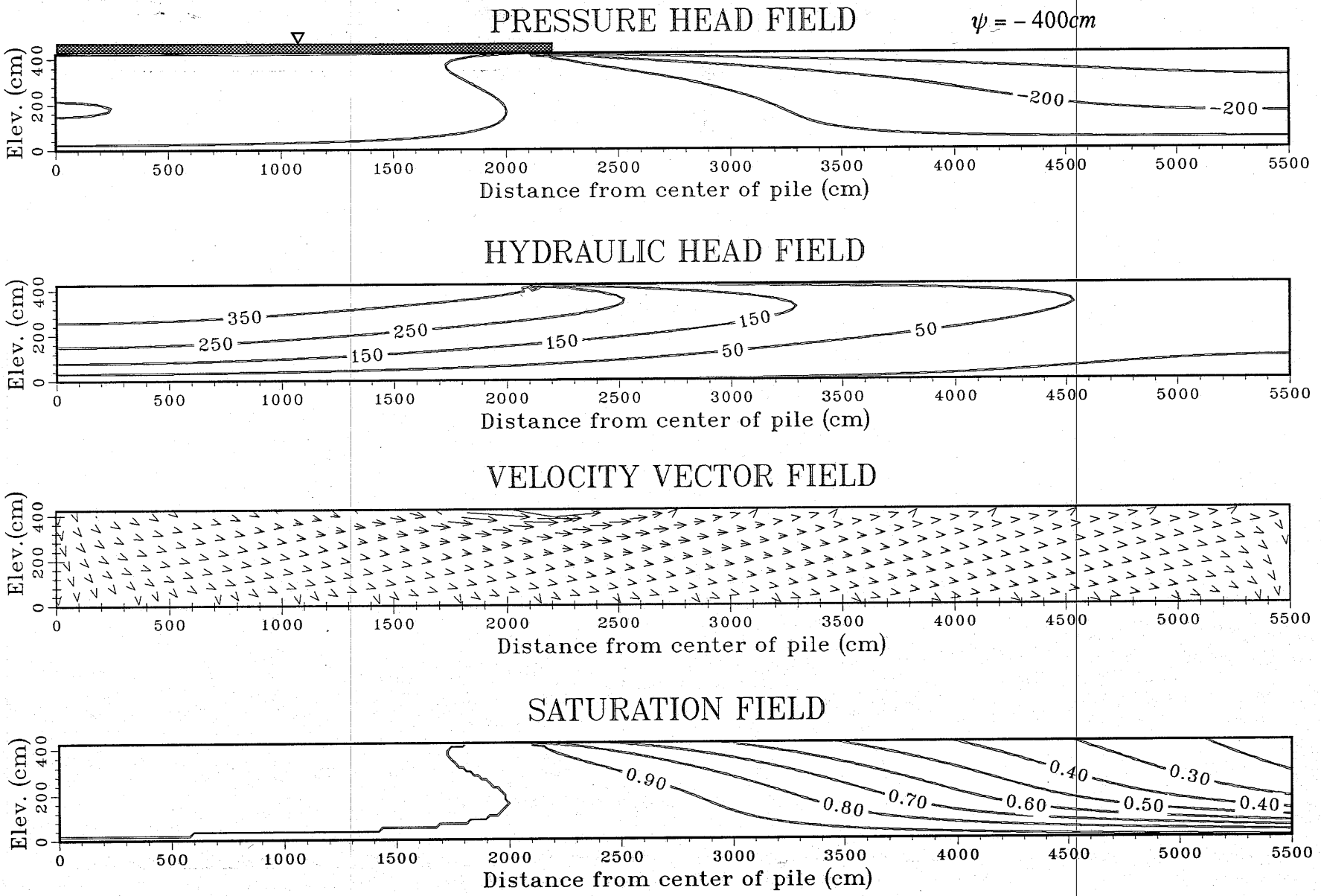

Figure 3.30(a,b,c,d). Steady-state results from deterministic simulation 7. Anisotropy ratio equals 100.

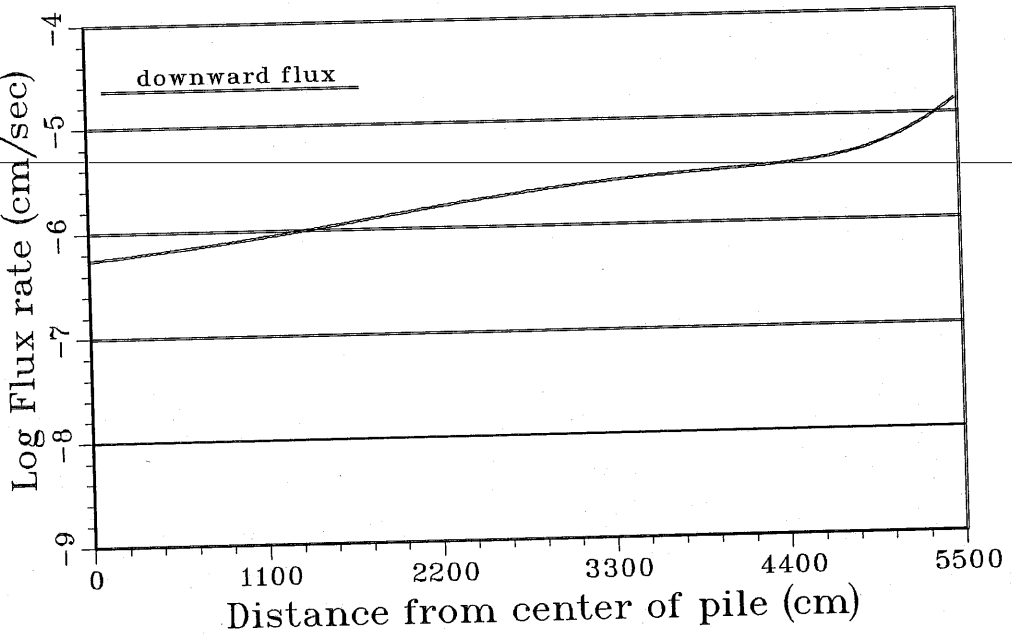

Figure 3.31. Flux distribution at the base of the impoundment for DS7.

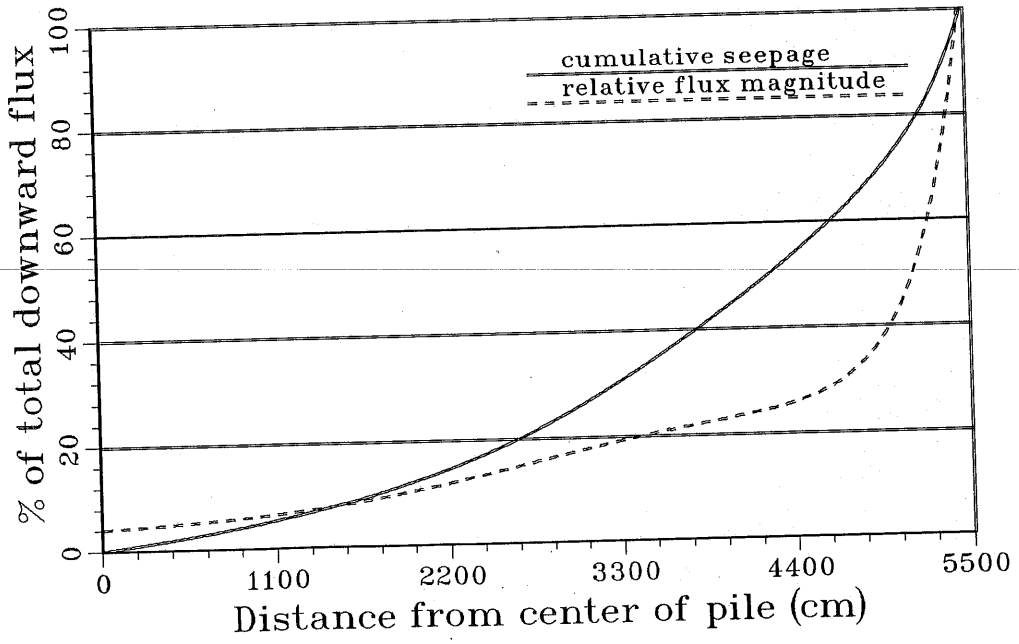

Figure 3.32. Cumulative flux curve and relative flux distribution at the base of the impoundment for DS7.

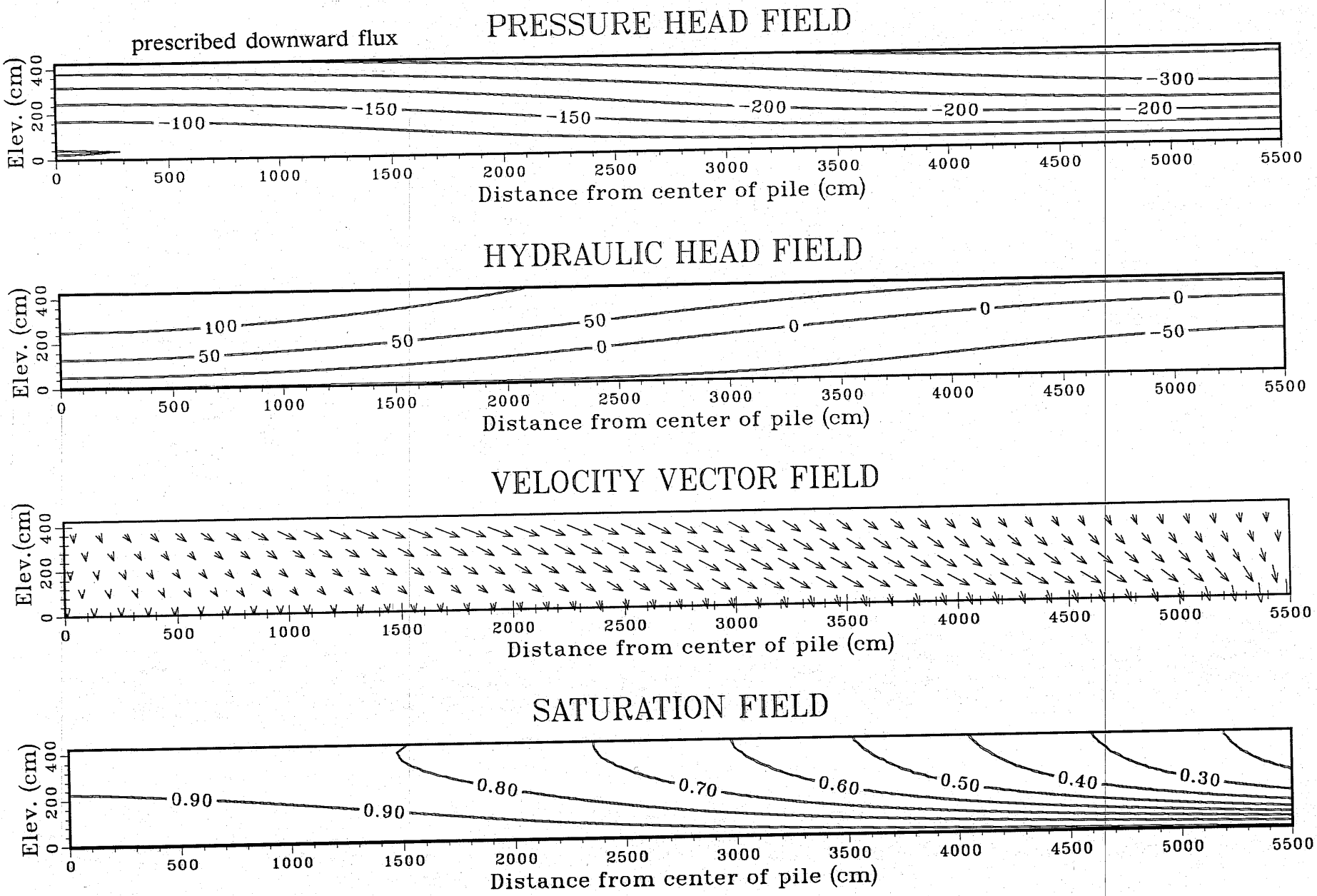

Figure 3.33(a,b,c,d). Steady-state results from deterministic simulation 8. Anisotropy ratio equals 20.

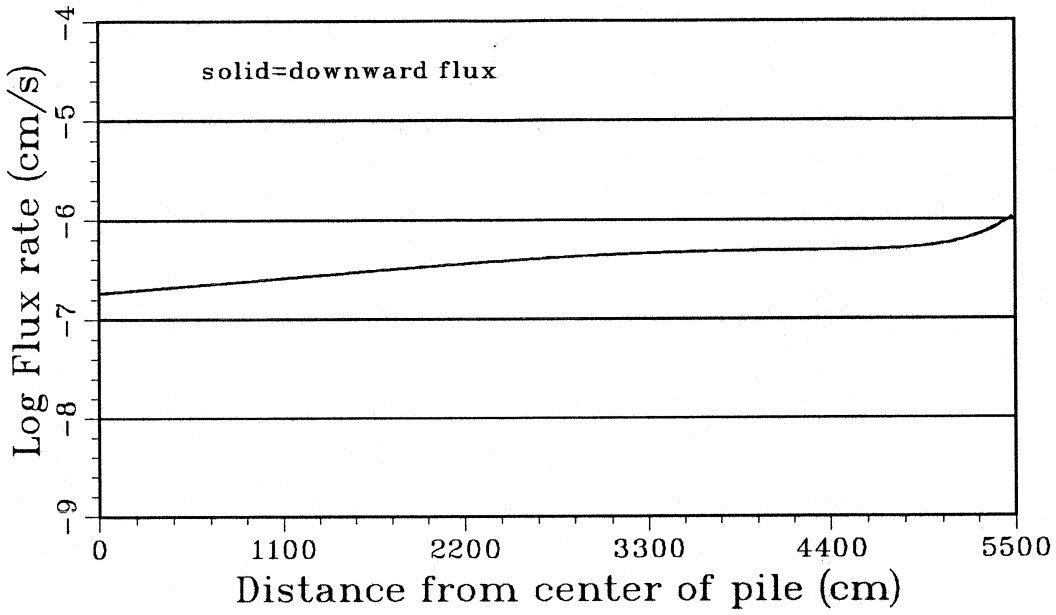

Figure 3.34. Flux distribution at the base of the impoundment for DS8.

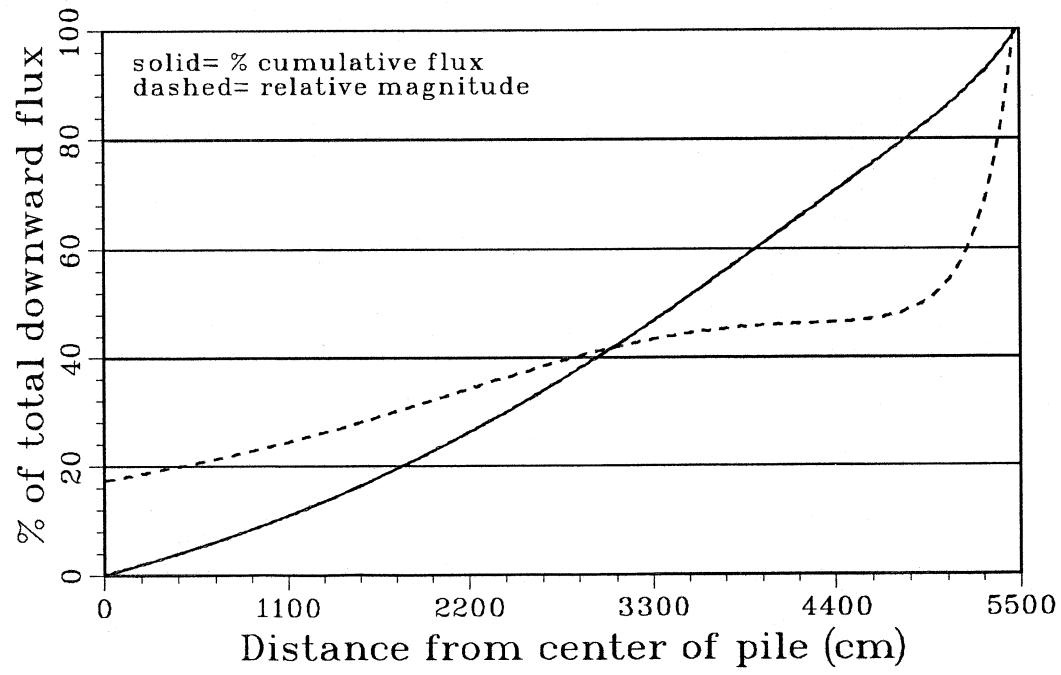

Figure 3.35. Cumulative flux curve and relative flux distribution at the base of the impoundment for DS8.

potential evaporation escaped the no flow boundary, the flux rates at the base of the pile would still continue to increase to the edge of the impoundment.

DS9 was performed under the same boundary conditions as DS3 and DS8 (12.7 cm/year influx at the surface of the impoundment) but incorporated an anisotropy ratio of 100 for the porous media. Figure 3.36a,b,c,d shows the status of the impoundment at steady state. Figure 3.36c shows even more pronounced lateral flow components than DS8 due to the larger anisotropy ratio. Figure 3.37 shows that the downward flux rate from the outer portions of the pile is now at least 10 times greater than the flux rate at the center of the pile. The implications of this result could be a very important consideration when designing selective remedial action schemes to treat only those portions of the pile which exhibit significant downward seepage. Figure 3.38 clearly displays that 50% of the seepage from the impoundment exits in the outer 10 meters of the impoundment due to the lateral flow components induced by the anisotropic media.

Figure 3.39a,b,c.d show the results of DS10 in which a downward flux of 20 inches per year is prescribed at the surface and the anisotropy ratio is 20 for the porous media. These boundary conditions are identical to those of DS4. Comparison of Figure 3.39a,c and 3.21a,c show that the incorporated anisotropy allows for much more lateral flow and therefore the center of the pile no longer exhibits ponding. The anisotropy allows the significant fluid to flow to the outer portion of the pile under relatively minor hydraulic head gradients. The total seepage is the same for both scenarios, but the seepage distribution shows large variation.

Figure 3.42a,b shows the comparison of seepage at the base of the impoundment considering boundary conditions shown in Figures 3.12 and 3.17 respectively and incorporating different anisotropy ratios. As the anisotropy

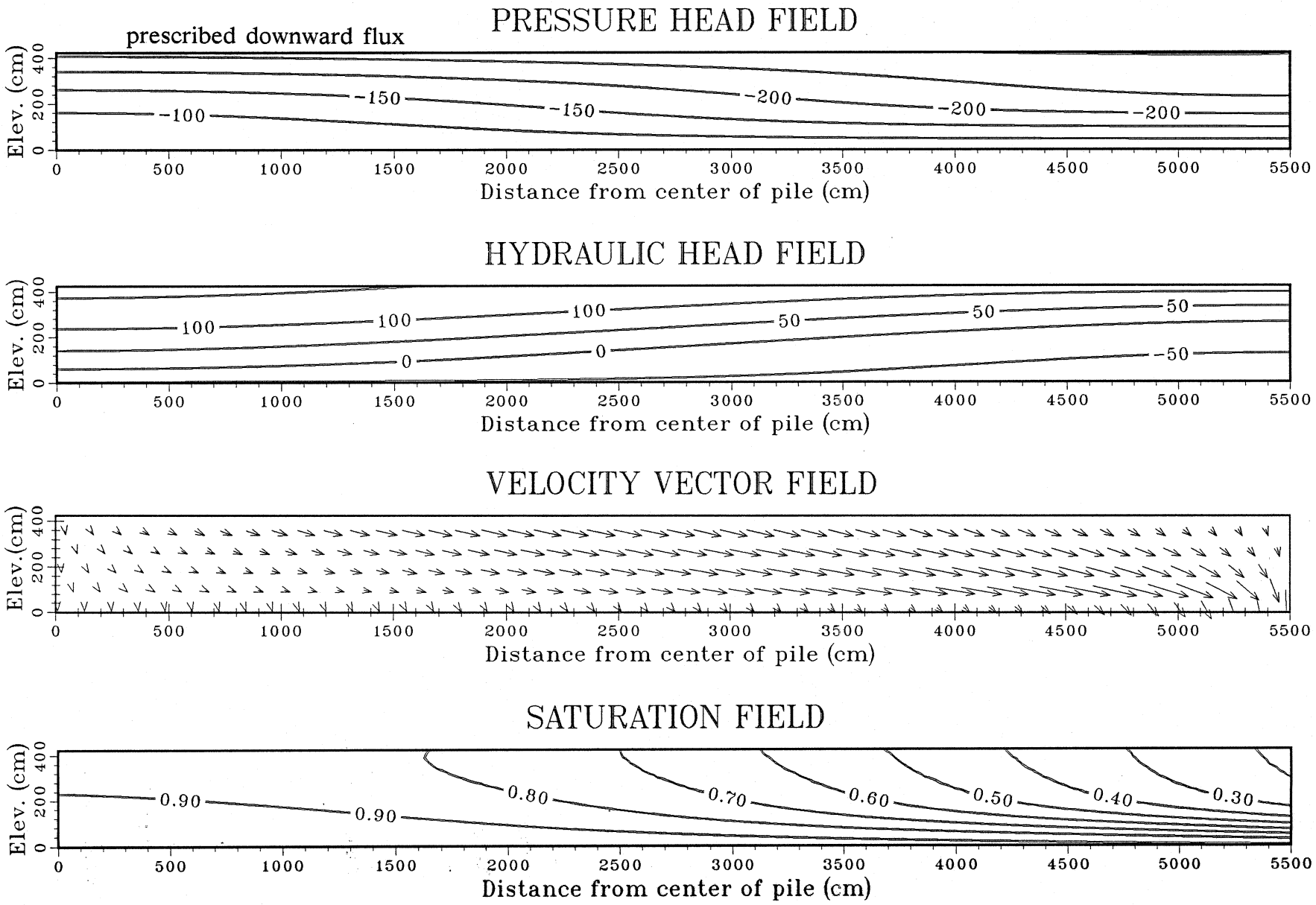

Figure 3.36(a,b,c,d). Steady-state results from deterministic simulation 9. Anisotropy ratio equals 100.

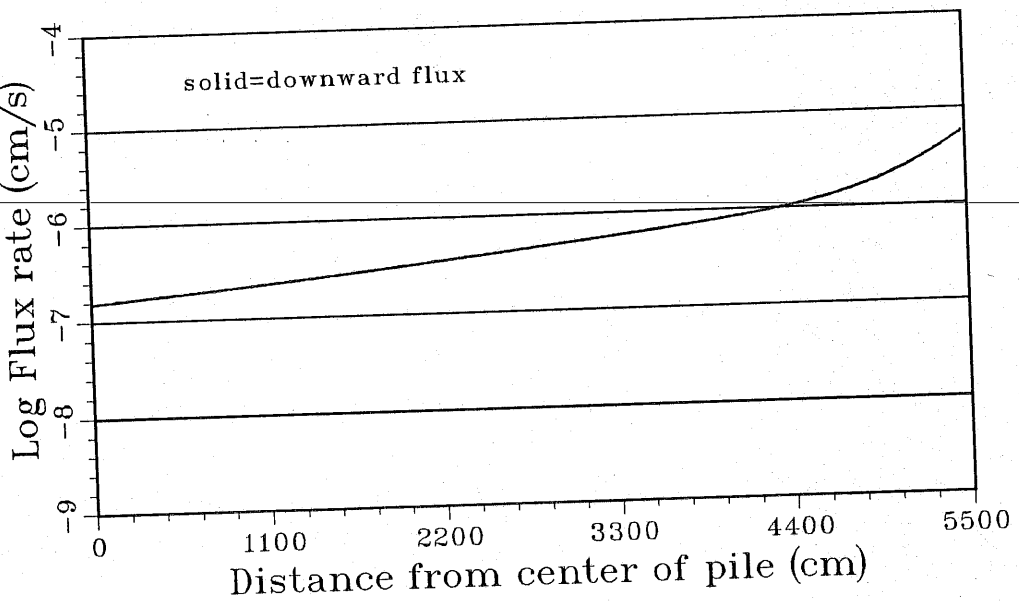

Figure 3.37. Flux distribution at the base of the impoundment for DS9.

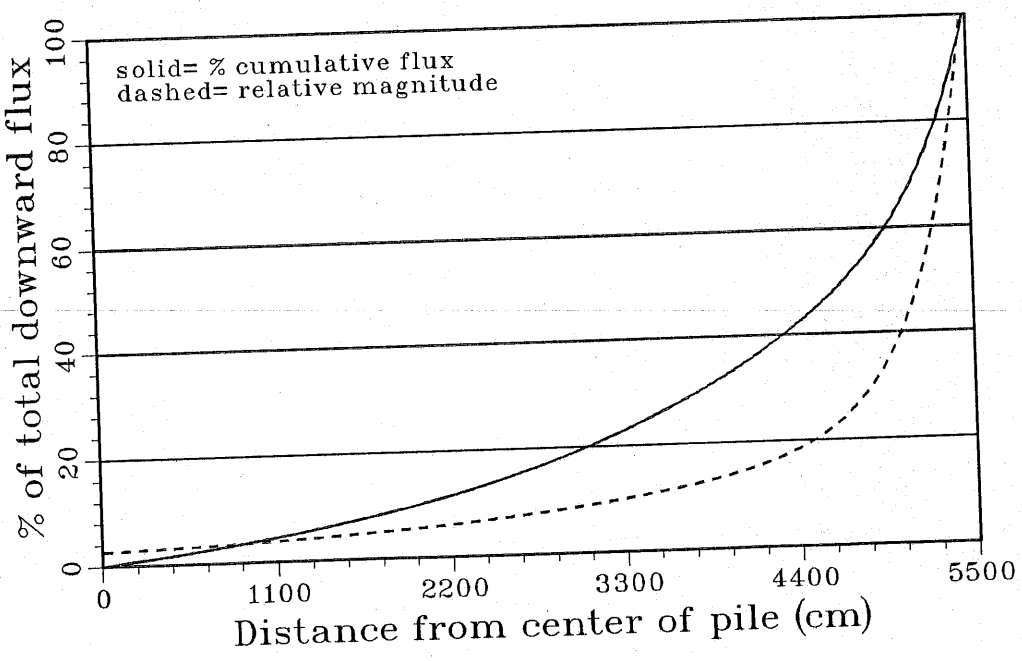

Figure 3.38. Cumulative flux curve and relative flux distribution at the base of the impoundment for DS9.

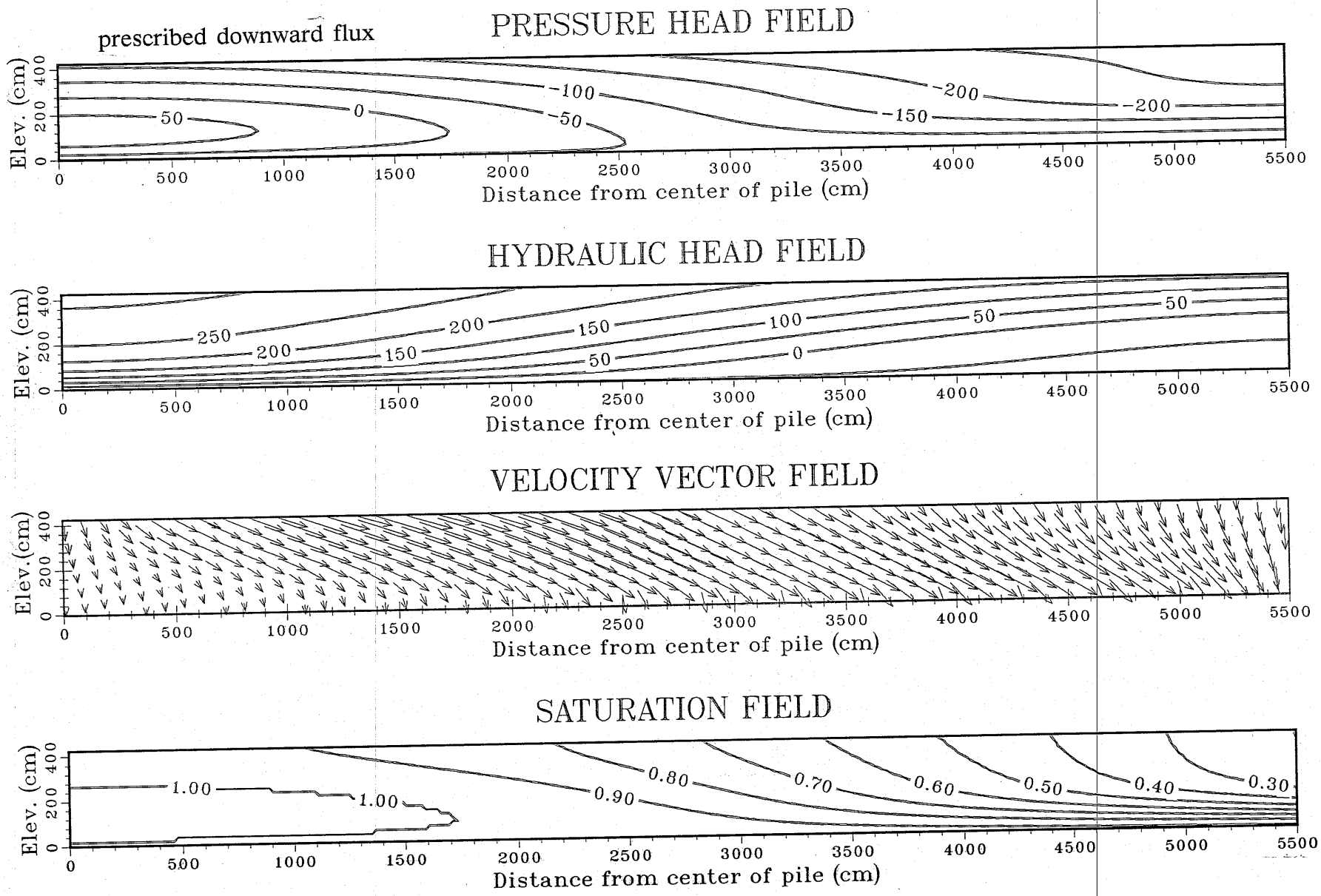

Figure 3.39(a,b,c,d). Steady-state results from deterministic simulation 10. Anisotropy ratio equals 20.

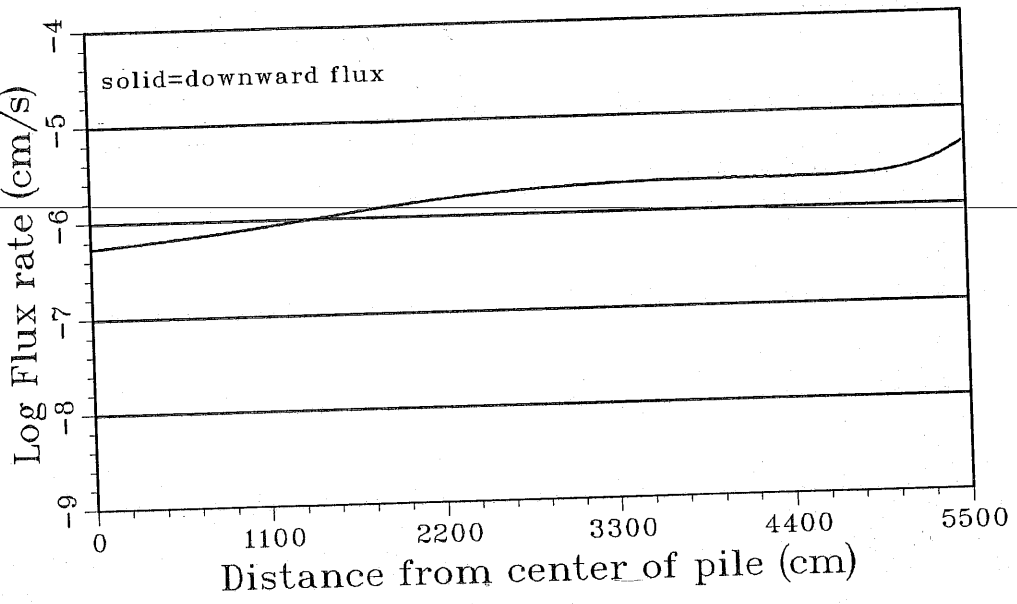

Figure 3.40. Flux distribution at the base of the impoundment for DS10.

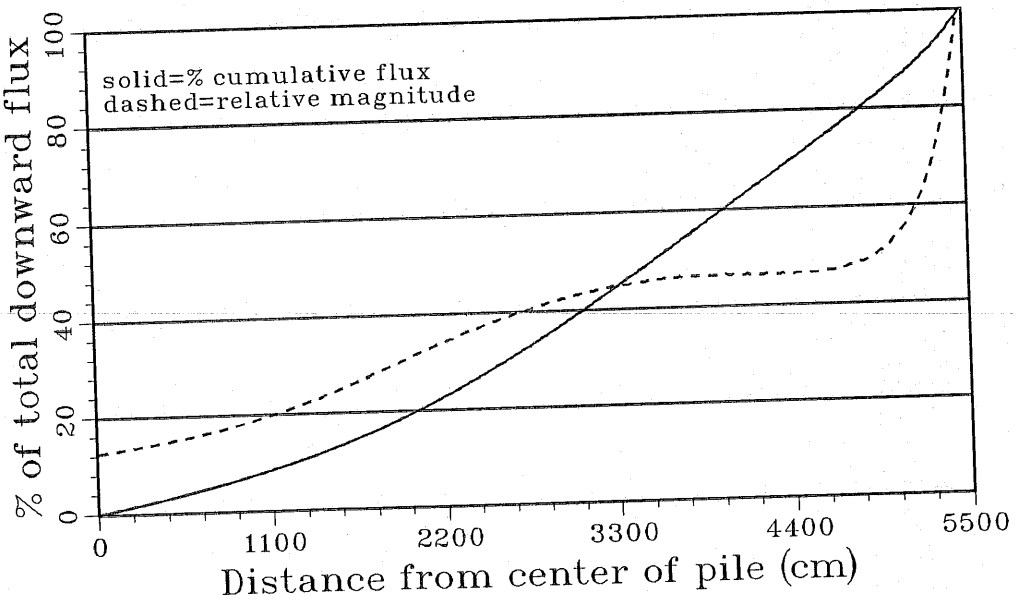

Figure 3.41. Cumulative flux curve and relative flux distribution at the base of the impoundment for DS10.

increases, the distribution of flux is shifted to the outer portions of the impoundment. Evaporation and total seepage from the impoundment are increased as anisotropy increases, especially when the outer portion of the impoundment are "drier" as depicted by seepage distributions in Figure 3.42b. The implications of these results can not be overemphasized when determining effective monitoring schemes to delineate the propensity for groundwater contamination through seepage from waste impoundments.

It is important to point out here that the size of the impoundment will have an effect on the relative importance of the lateral flow components. In this analysis, the impoundment was relatively small. Therefore, horizontal flow components significantly affect the distribution of the seepage from the impoundment. In larger impoundments, horizontal flow components from the ponded region will not be transmitted as far from the pond. Thus, the consideration of impoundment dimensions is an important factor in model approach, characterization of the impoundment, and design of layout for instrumentation in the vadose zone.

It is clear from the deterministic simulations that incorporation of any existing anisotropy into the conceptual model is an important factor in determining the magnitude and distribution of seepage from the base of tailings impoundments. It is important to consider the "true" anisotropy of the media even when the flow system exhibits only minor horizontal gradients because these gradients may cause significant lateral flow components.

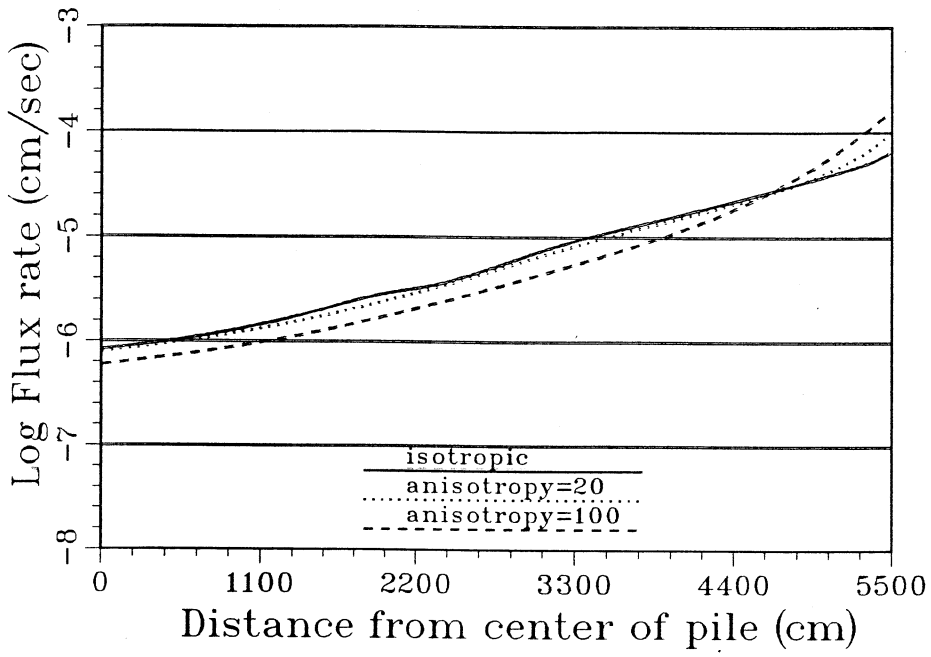

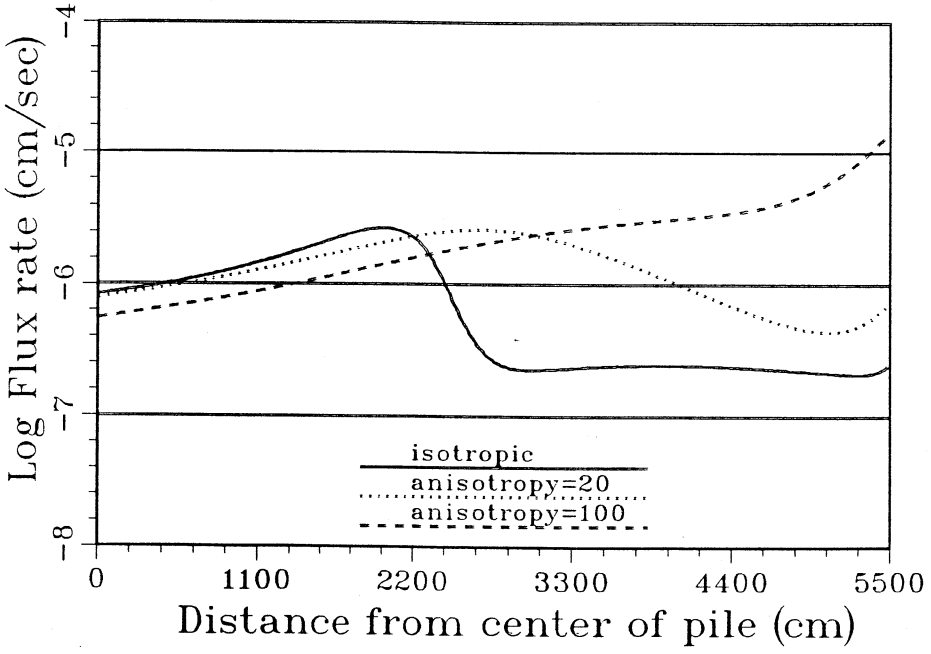

Figure 3.42(a,b). Flux distribution at the base of the impoundment for different simulations assuming various anisotropy ratios under boundary conditions shown in Figures 3.10 and 3.14 respectively.

Simulations of Evaporation from Tailings Seepage Model

Active waste impoundments, whether mill tailings or other types of waste impoundments, are often referred to as evaporation ponds. In fact, it is often assumed that seepage from these impoundments is negligible due to evaporation at the surface of the impoundment. In order to assess the effect of evaporation on seepage predictions from unlined tailings impoundments, steady-state simulations were performed which considered different evaporation scenarios and anisotropy ratios for the tailings. The objectives of the simulations were to:

1. discern the importance of correctly determining evaporation rates from impoundments
2. determine the effect of anisotropy on seepage predictions when an impoundment is experiencing evaporation
3. delineate the effect of various evaporation scenarios on the seepage rate at the base of the impoundment.

The conceptual model used is shown in Figure 3.43. The impoundment is ponded from the center outward to 22 meters. The three evaporation scenarios used for the simulations are shown in Figure 3.44, which displays graphically the evaporation distribution as a function of distance from edge of the pond. Three scenarios are used in order to determine the effect of each on the seepage distribution at the base of the impoundment. The exponential decrease in evaporation from the edge of the pond to the edge of the impoundment as depicted in Scenario #1 and #2 is indicative of the quantity of fluid available for evaporation at the surface of the pile due to the lateral flow components. Scenario #3 incorporates a constant evaporation rate in order to compare the effect of this evaporation scheme as compared to the more realistic exponential decrease in evaporation away from the pond.

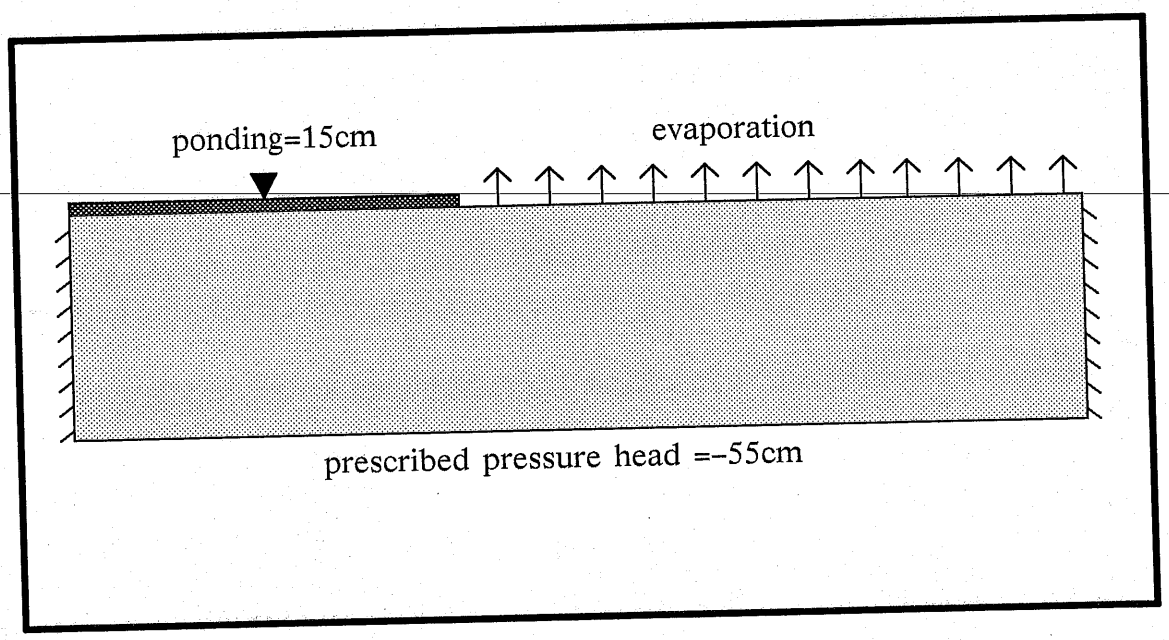

Figure 3.43. Conceptualization of steady-state evaporation model.

In order to compare evaporation scenarios with previous deterministic simulations which implemented prescribed pressure head boundaries at the surface of the impoundment, the same boundary conditions for the pond and base of the impoundment as were identical to previous simulations. With the exception of the evaporation boundary condition, evaporation simulations 1 through 5 (ES1-5) were performed with the same prescribed boundary conditions as was DS1. The prescribed pressure boundary at the base of the impoundment was -55cm, and the ponding depth was 15cm.

Evaporation simulation 1 (ES1) incorporates evaporation scenario #2 (exponential decay from 10 inches per year at pond to 2 inches per year at edge of impoundment). The tailings material is considered isotropic. Figure 3.45 a,b,c,d show the state of the impoundment at steady-state under the prescribed boundary conditions. Figure 3.45c clearly shows that the moisture movement is

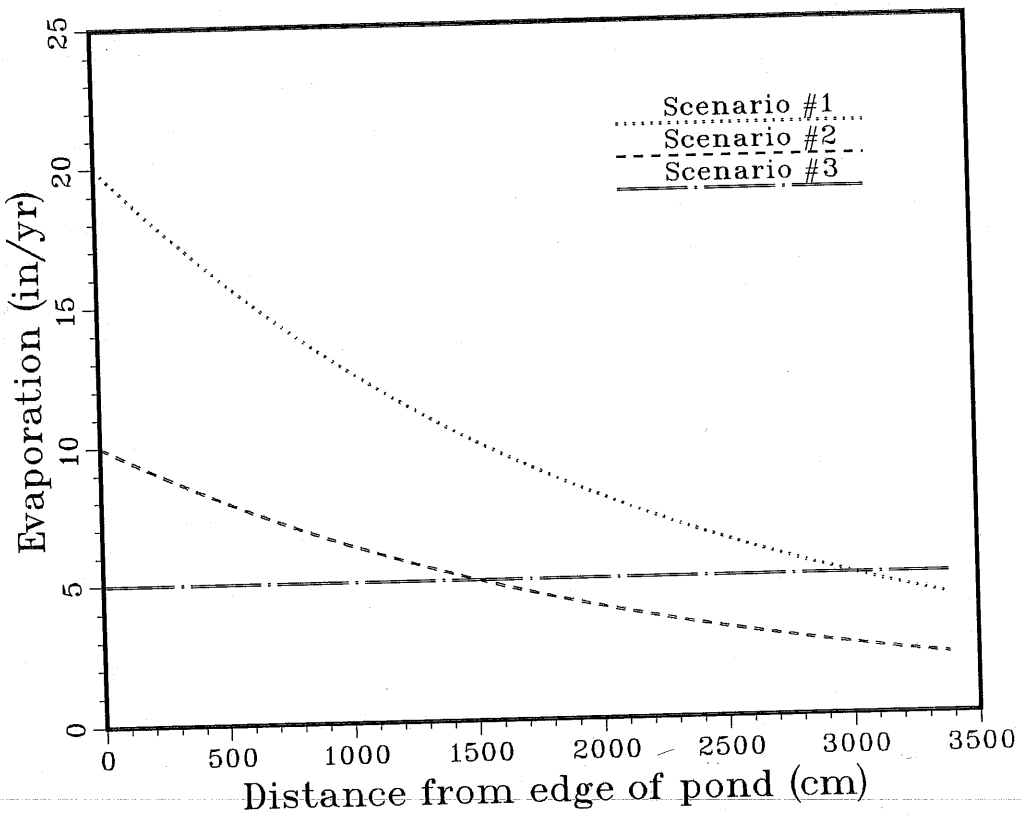

Figure 3.44. Graphical representation of the three evaporation scenarios as a function of distance from the edge of the pond.

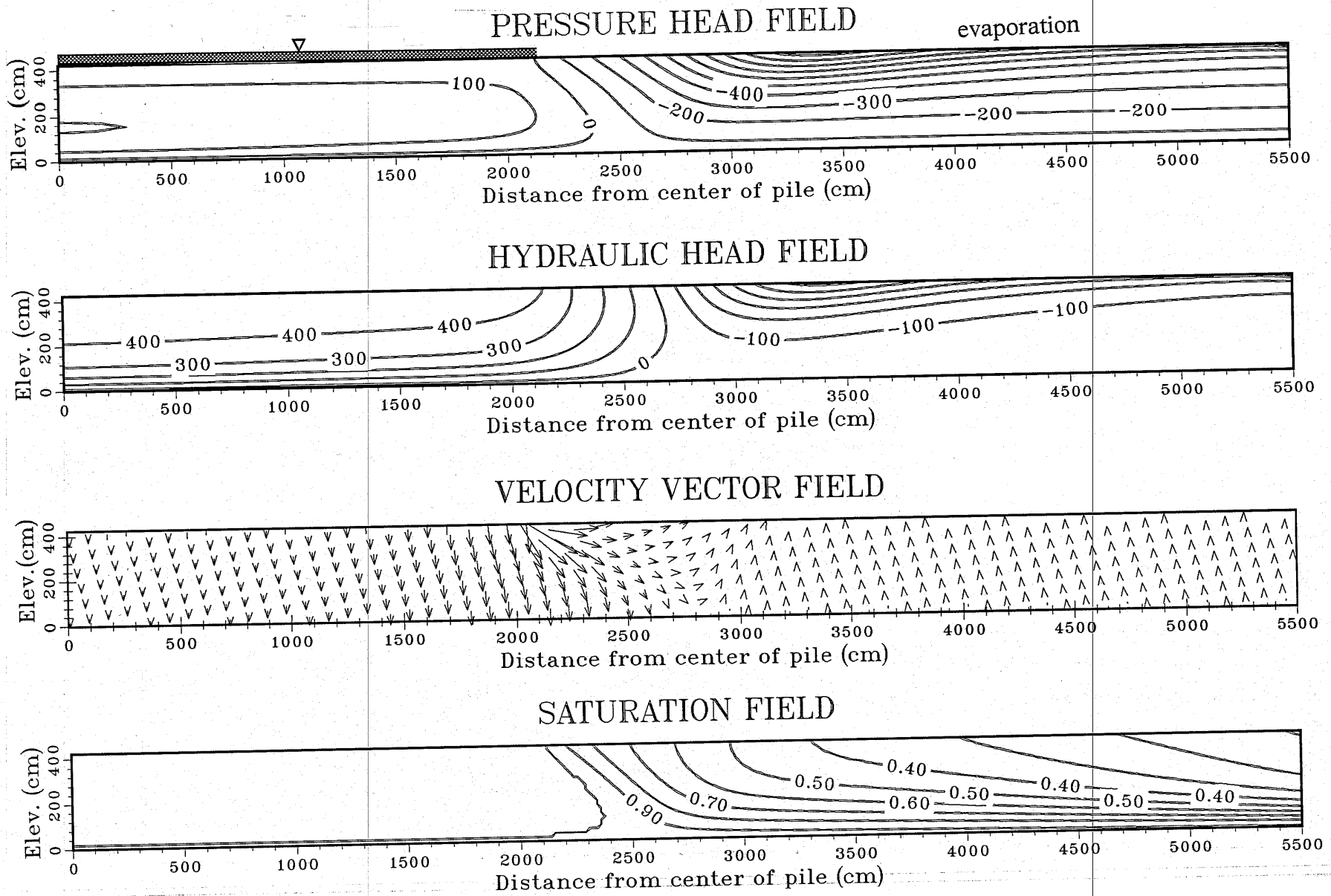

Figure 3.45(a,b,c,d). Steady-state results from evaporation simulation 1. Isotropic media.

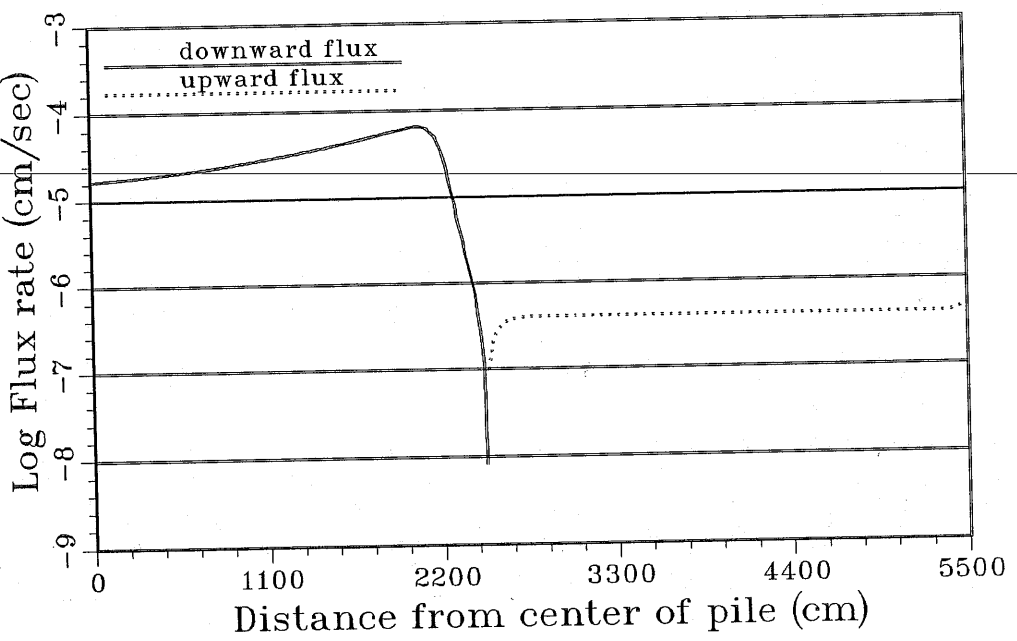

Figure 3.46. Flux distribution at the base of the impoundment for ES1.

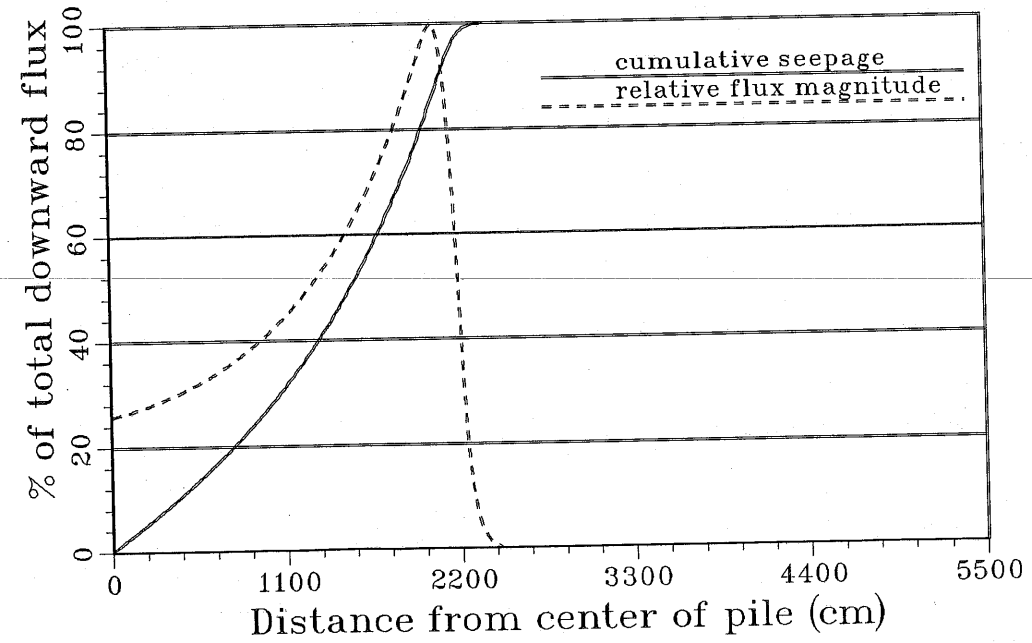

Figure 3.47. Cumulative flux curve and relative flux distribution at the base of the impoundment for ES1.

vertically upward in the portions of the impoundment which are not ponded. The hydraulic gradients exhibit strong horizontal components, but the isotropic nature of the tailings material assumed in this simulation allows only minimal horizontal fluid movement. The minimum pressure head of approximately -1100cm exists about 35m from the center of the impoundment at the surface of the pile. Figure 3.46 shows the seepage at the base of the impoundment terminates about 3 meters from the edge of the pond.

Evaporation simulation #2 (ES2) incorporates the same boundary conditions as ES1 but the tailings material is assumed to have an anisotropy ratio of 20. Figure 3.48a,b,c,d represents the status of the impoundment with the incorporated anisotropy. Comparison of Figure 3.45c to Figure 3.48c clearly illustrate the enormous influence the incorporated anisotropy induces in the flow regime. The assumed anisotropy allows lateral flow components to propagate to the edge of the impoundment over 30m away. As compared to Figure 3.45a, a minimum pressure head of -550cm is now located at the outermost portions of the impoundment surface. The saturation is also greater in the outer portions of the impoundment. Due to the incorporated anisotropy, seepage now exists along the entire base of the impoundment. This result can not be overemphasized when modeling flow and transport in heterogeneous, anisotropic systems. The proper incorporation of porous media anisotropy in flow and transport modeling is a very fundamental factor in determining the fate of contaminants in the vadose zone and, consequently in the saturated zone.

The saturation in the sandy region (for all deterministic simulations) always increases with depth due to the imposed pressure head boundary at the base of the impoundment. This constant increase in saturation with depth was not always observed in the moisture contents measured in the field. The inconsistency in observed and simulated profiles lies mainly in the difference in

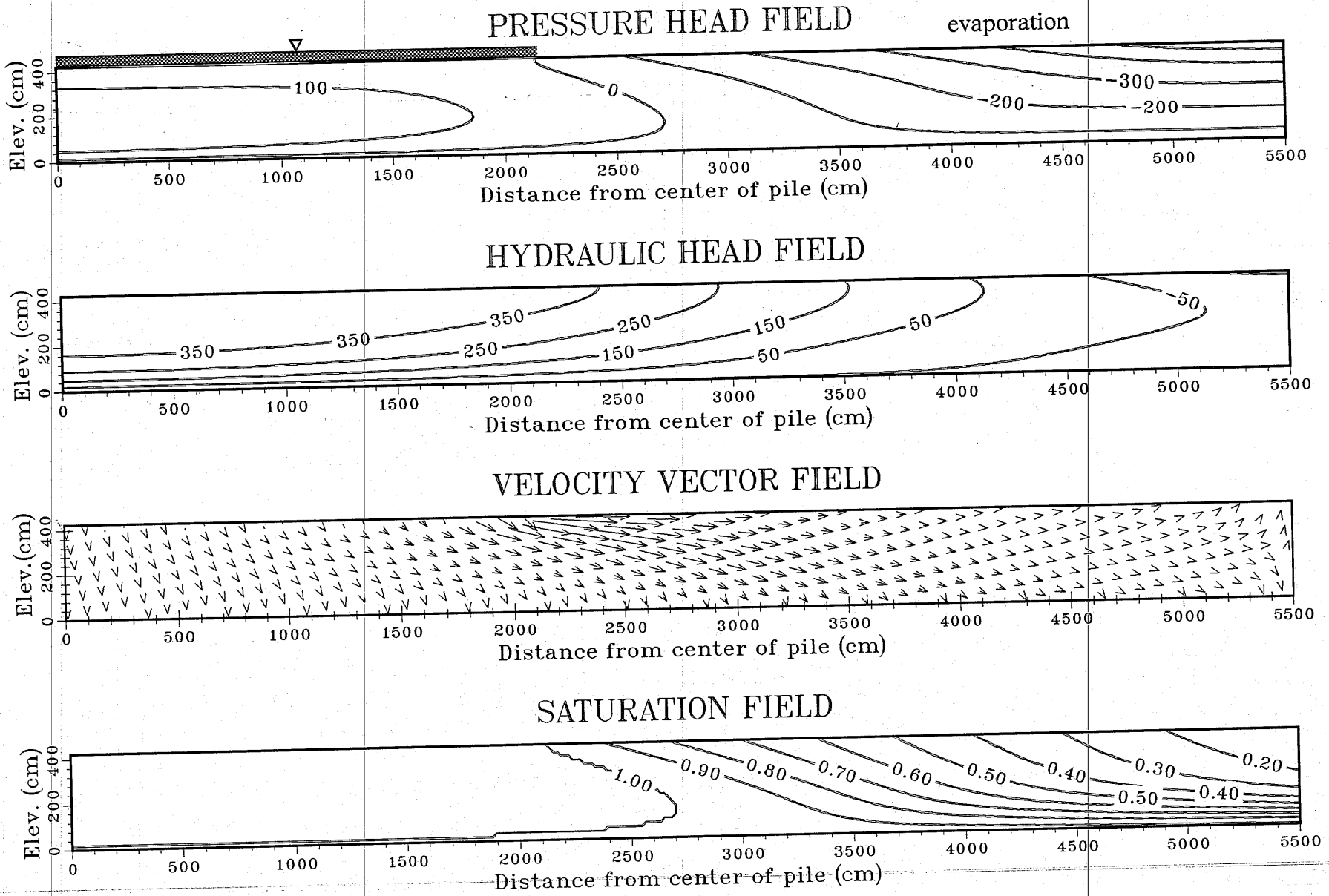

Figure 3.48(a,b,c,d). Steady-state results from evaporation simulation 2. Anisotropy ratio equals 20.

boundary conditions and the incorporation of the hydraulic properties. For steady-state simulations, the bottom boundary condition is the most important factor determining the saturation profile in the sandy region. This is because the flux rates in this region are relatively small in comparison to the saturated hydraulic conductivity. If the sandy zone exhibits very small moisture movement, the saturation profile is determined by the "near" static conditions present due to the prescribed head boundary condition at the base of the impoundment. These results suggest that the simulations may not be a good representation of actual field conditions. However, as stated earlier, the hydraulic property fields incorporated in the deterministic simulations are not consistent with field observations; and boundary conditions are very uncertain. Therefore, some deviation from the observed conditions is certainly expected. Keep in mind that the simulations are not an attempt to reproduce the moisture content profiles shown in Chapter 2. Rather, incorporation of various boundary conditions and hydraulic anisotropy ratios allows a qualitative analysis to be performed. This analysis is important in determining those factors which play an important role in flow processes for this conceptual model.

Evaporation simulations #3 incorporated the same porous media properties as ES2 but implemented evaporation scenario #3 (constant evaporation of 5 in/yr). Figure 3.49 shows the steady-state flux distribution at the base of the impoundment under the two scenarios. The difference in the two flux distributions is very small, considering the difference in the evaporation schemes. Obviously the incorporated anisotropy plays an important role in reducing the effects of the different evaporation schemes. The fluid evaporated in the outer portions of the impoundment is made available by the lateral flow components originating at the pond. As observed in the previous simulations, the lateral flow components are most definitely a partial product of the incorporated anisotropy.

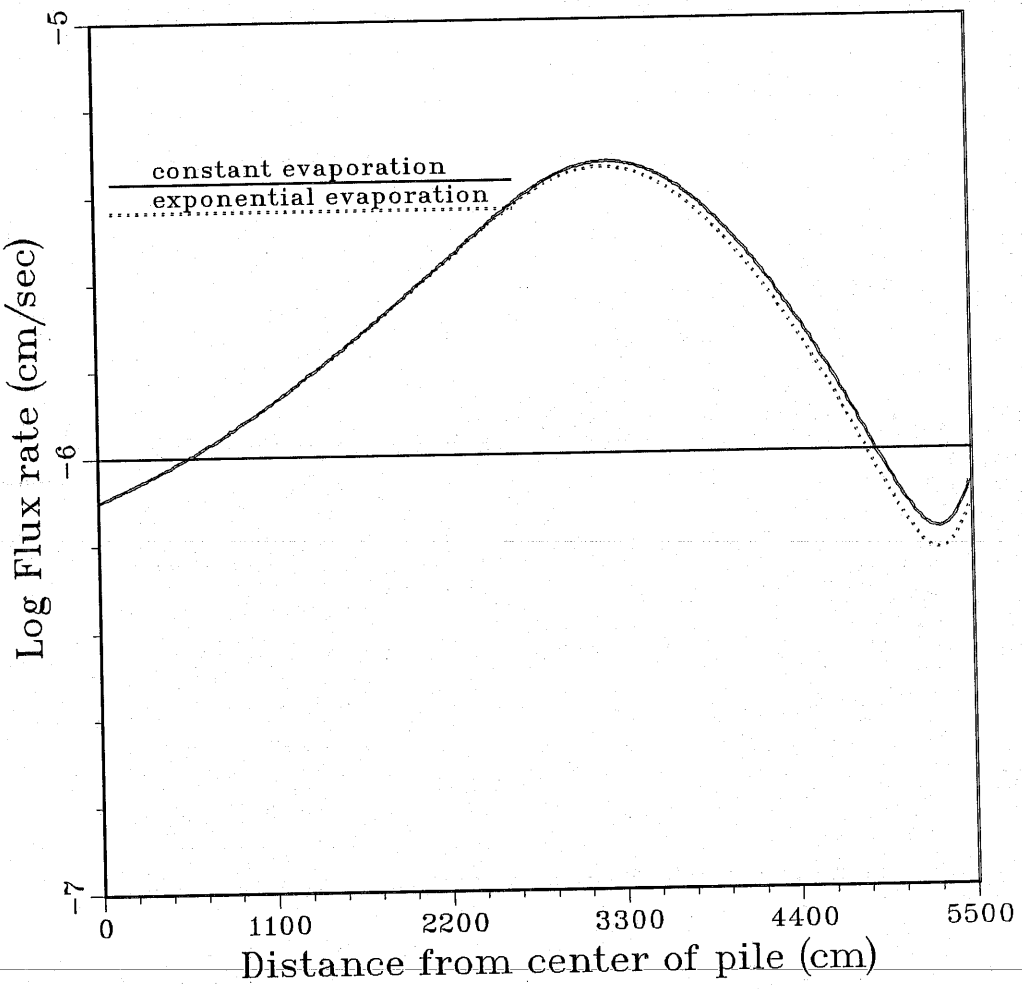

Figure 3.49. Comparison of flux distributions at the base of the impoundment for ES2 and ES3 which incorporate evaporation scenarios #2 and #3 respectively.

ES4 and ES5 were performed to investigate the effects of media exhibiting a very strong hydraulic anisotropy. In both simulations, an anisotropy ratio of 100 was incorporated. The evaporation schemes used for ES4 and ES5 were #1 and #3, respectively. The steady-state simulation results from ES4 are shown in Figure 3.50a,b,c,d. From Figure 3.50c, it is evident that the major component of the fluid velocity vectors is in the horizontal direction. Comparing the resulting pressure head field (Figure 3.50a) to Figure 3.48a will confirm that lower capillary pressures exist at the surface of the impoundment then in simulations considering lower anisotropy ratios. Figure 3.51 clearly demonstrates the significant change in the flux distribution at the base of the impoundment as compared to previous simulations. The anisotropic nature of the media permits large horizontal flow components which eventually travel to the outer edges of the impoundment where most of the fluid flows through the base of the impoundment and a small portion is evaporated from the surface of the impoundment. The variation in results from ES5 and ES4 are almost nonexistent, therefore ES5 results are not included.

From the simulations performed here, it would be difficult and unjustifiable to make broad conclusions concerning overall effects of evaporation on waste impoundment seepage. Perhaps the evaporation simulations have once again illustrated the importance of proper incorporation of anisotropy in flow and transport modeling; but, a few points should be stressed here.

1. Seepage from unlined waste impoundments may greatly exceed evaporation, especially when highly anisotropic media exist in the impoundment.
2. If the impoundment is under quasi steady-state conditions and the impoundment materials are significantly anisotropic, seepage rates

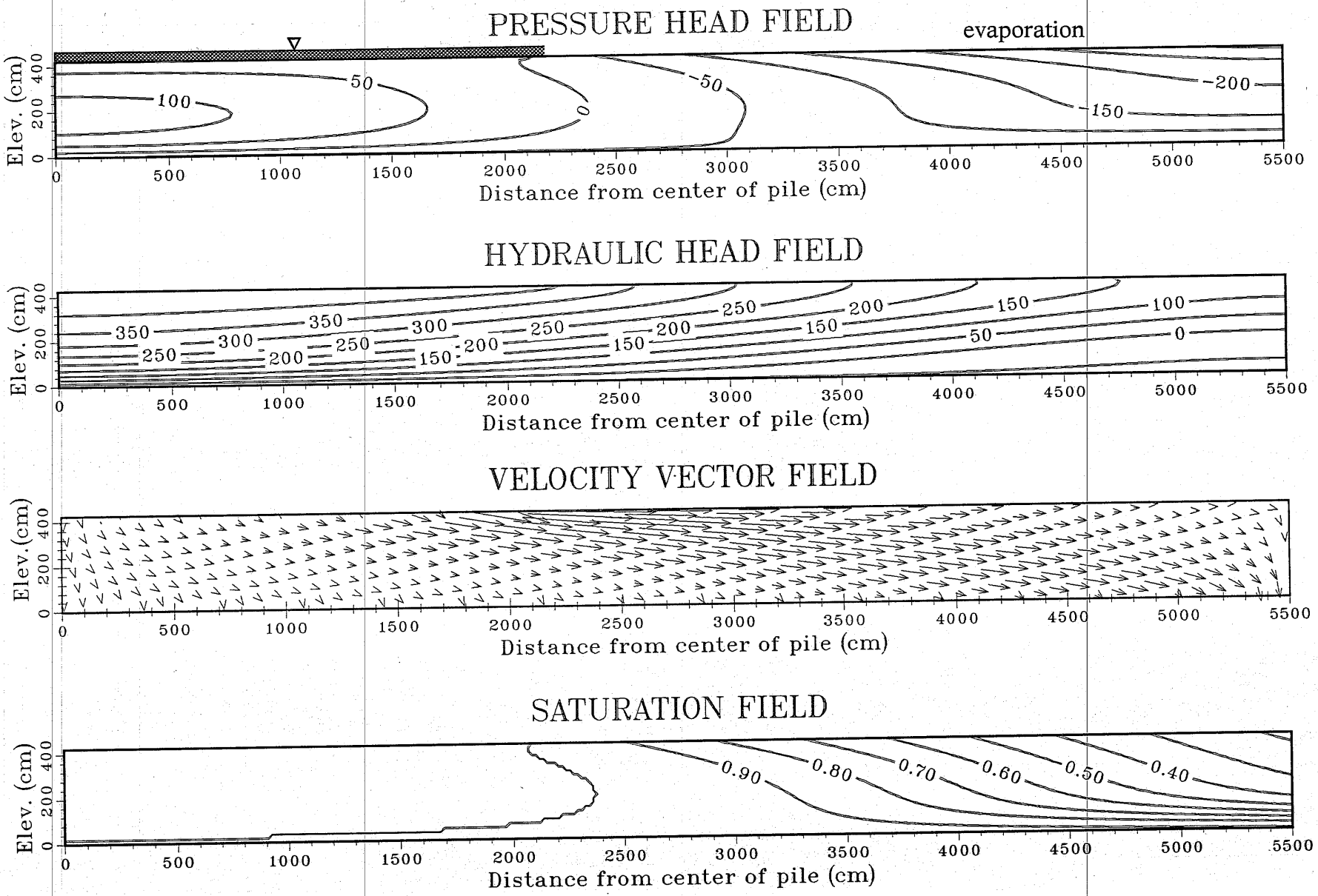

Figure 3.50(a,b,c,d). Steady-state results from evaporation simulation 4. Anisotropy ratio equals 100.

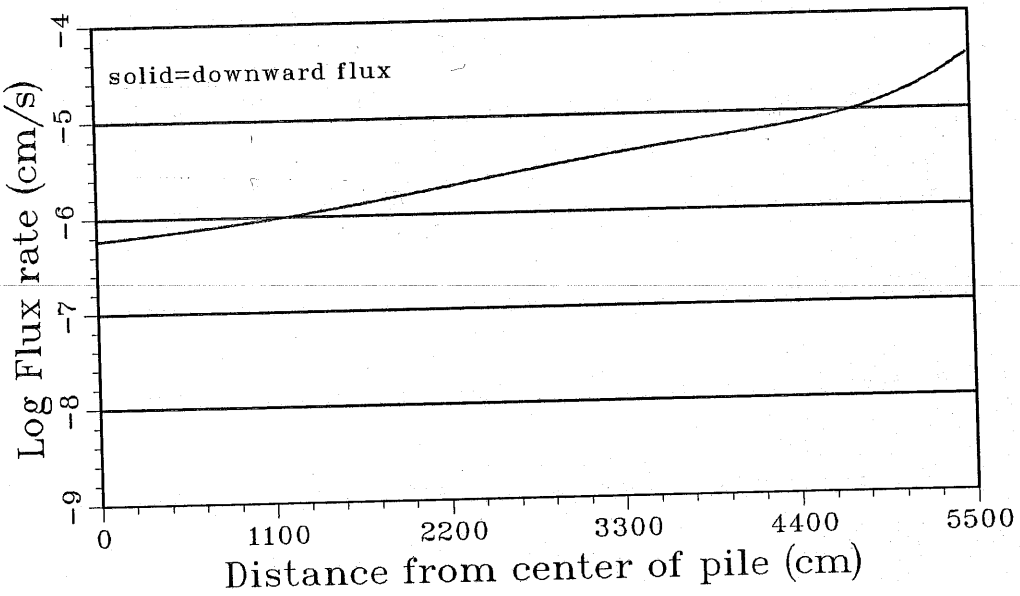

Figure 3.51. Flux distribution at the base of the impoundment for ES4.

from the impoundment are not significantly affected by the evaporation rates at the surface of the impoundment.

The validity of the suggestions pointed out above are of course subject to various factors, including impoundment depth, areal extent, and major trends in the hydraulic properties.

Volumetric Seepage from Deterministic Simulations

In order to properly assess the environmental impact of seepage from waste impoundments, it is important to correctly determine the total volume of seepage from an impoundment. As discussed earlier, seepage distribution is an important factor in determining the total seepage from an impoundment. Weather and soil moisture conditions as well as hydraulic properties of the tailings material define the seepage distribution and total seepage from impoundments. Therefore it is evident that the hydraulic properties incorporated into numerical models and boundary conditions imposed in the model are major factors in predicting seepage from modeled impoundments. In order to provide insight into the total volume of seepage from a small tailings impoundment under prescribed boundary conditions, the seepage rates obtained from the two-dimensional simulations were generalized to a three-dimensional scenario shown in figure 3.52. The two-dimensional modeled cross-section was used as the basis for a three-dimensional conceptualization. Predictions gained from the two-dimensional model were used to calculate total volumetric seepage rates from a rectangular tailings impoundment of width and depth equal to the those of the two-dimensional model. The conceptualized waste impoundment has a width of 54.91 meters, a height of 4.25 meters, and length of 100 meters. Equation 3.11 (shown in integral and discrete form) can be used to calculate the flux per unit width Q' ($units = [L^2/T]$) from the vertical cross-section of the two-dimensional model.

$$Q' = \int v(x)\, dx = \sum_{n=1}^{323} W(n)v(n) \qquad (3.11)$$

where: $v(x)$ =downward fluid velocity at x

$W(n)$=width of finite element over which fluid velocity is constant

$v(n)$ =constant fluid velocity over the distance $W(n)$

The total flow rate for any length of impoundment can then be calculated by simply multiplying the flux per unit Q' by the total length of the pile. If the impoundment is considered symmetric, (the left side of the model being the center of the impoundment) the total seepage calculated from the impoundment described above can simply be doubled in order to calculate the total seepage from the conceptualized impoundment.

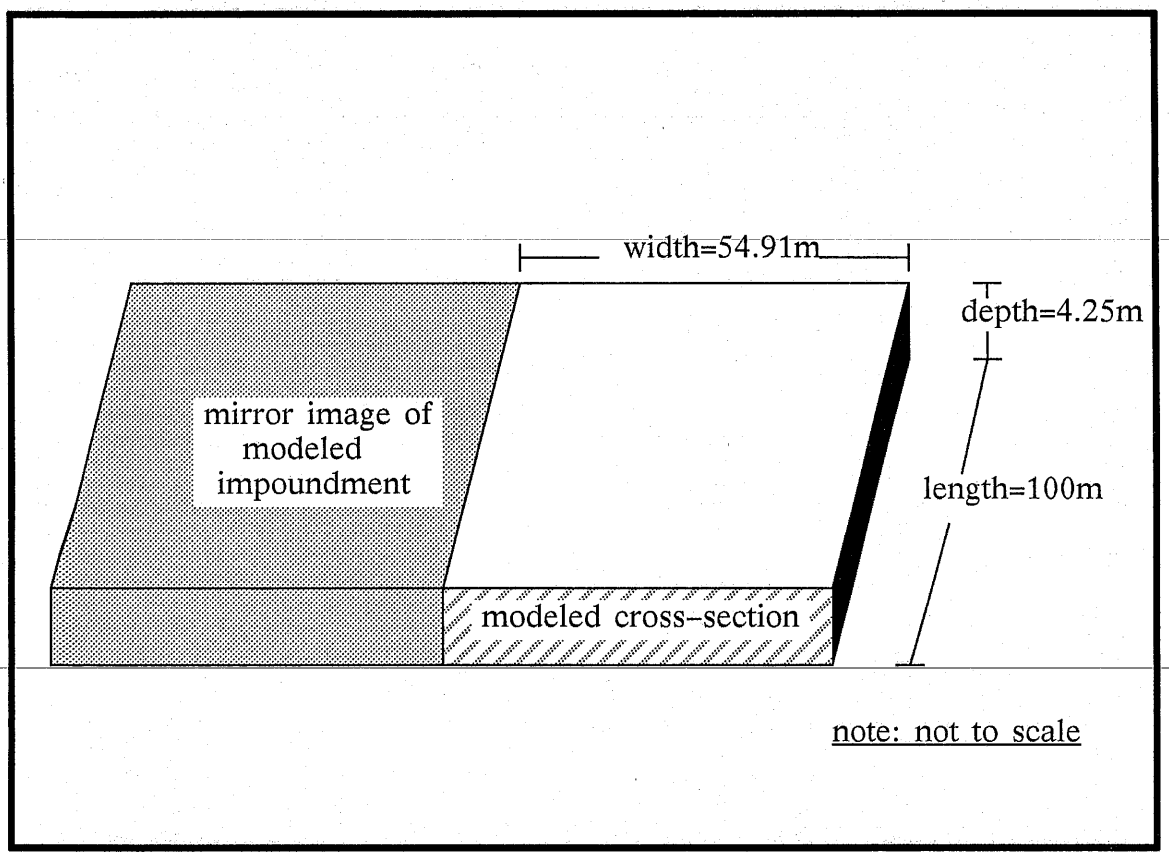

Figure 3.52 Three-dimensional conceptual model used to calculate total discharge from impoundment based on two-dimensional simulation results.

Table 3.2 shows the specific and volumetric discharges from this conceptualization for various simulations previously discussed. Large variation in seepage volumes exist for simulations incorporating different anisotropy ratios but identical boundary conditions. Under ponded conditions, anisotropy does not significantly increase the seepage in the outer portions of the impoundment if the sandy region is relatively wet. However, the seepage rate increases significantly under ponded conditions if the sandy portion of the impoundment is drier. Anisotropy is shown to be a very important factor in determining the seepage distribution and consequently the volumetric seepage from the impoundment.

boundary conditions	isotropic		anisotropy = 20		anisotropy = 100	
	total seepage cm^2/sec	volume m^3/day	total seepage cm^2/sec	volume m^3/day	total seepage cm^2/sec	volume m^3/day
Dirichlet = -100 cm	6.7 E-2	115.8	7.1 E-2	122.7	8.1 E-2	139.9
Dirichlet = -400 cm	4.7 E-3	8.2	7.5 E-3	13.2	1.4 E-2	24.8
Exponentially decaying evaporation	NA	NA	1.2 E-2 **	21.3 **	2.8E-2*	49.1*
Constant evaporation (13 cm/yr)	NS	NS	1.3 E-2 ***	21.9***	2.9 E-2***	50.6***

* Refers to evaporation scenario #1

** Refers to evaporation scenario #2

*** Refers to evaporation scenario #3

NS denotes no simulation was completed

NA denotes data is not available

Table 3.2. Total seepage rates for two-dimensional simulations and volumetric seepage rates for generalized three-dimensional impoundment ponded from the center outward to 22 meters. Boundary conditions refer to those applied from the edge of the pond to the edge of the impoundment. Bottom boundary condition is prescribed at -55 cm pressure head.

Comparison of One and Two-Dimensional Modeling Approaches

Seepage from mill tailings impoundments is often modeled as a one-dimensional process in which the porous media is considered homogeneous and isotropic. As discussed in chapter 2, recent evidence has shown that in many cases, movement of moisture and solutes in the vadose zone cannot be correctly modeled in a one-dimensional framework, especially if the porous media is heterogeneous and layered. In an effort to discern the importance of considering multi-dimensional flow effects in a mill tailings impoundment given various boundary conditions, one-dimensional steady-state simulations were completed for comparison to two-dimensional simulation seepage results. The conceptualized one-dimensional zones include the inner "slime" zone, a middle "transition" zone (due to the layering of fine and coarse media in this area), and an outer "sand" zone which are shown in Figure 1.1. The properties of the columns were taken as a vertical average of the properties in the two-dimensional model (shown in Figures 3.1-3.5) and are given in Table 3.3. The two-dimensional seepage rates were compared to the one-dimensional seepage rates by discretizing the two-dimensional system in the same fashion as would be done if only three zones of porous media were modeled. For comparison, the region from 0-2200 cm was considered the slime zone, 2200-4400 cm the transition zone, and 4400-5500 cm the sand zone. In order to compare the seepage results from the one and two-dimensional conceptualizations, the same boundary conditions were applied to the one-dimensional columns as were applied to the comparison region in the two-dimensional models. A comparison of the seepage velocities from the one and two-dimensional models can be found in Table 3.4. Table 3.4 shows the flux range which occurs in the impoundment in the zones defined above. The first value is the seepage rate at the inner portion

Hydraulic property	zone		
	slime	transition	sand
K_{sat} *(saturated conductivity)*	1.2E–7 cm/s	1.0E–5 cm/s	1.0E–3 cm/s
n (*Brooks/Corey*)	7.5	5.5	4.5
S_s *(specific storage)*	np	np	np
ϕ *(porosity)*	np	np	np
S_{rw} *(residual saturation)*	0.45	0.25	0.10
n *(van Genuchten)*	1.2	1.8	2.2
α *(van Genuchten)*	0.010	0.013	0.016
m *(van Genuchten)*	0.167	0.444	0.545

np – denotes the parameter was not pertinent to steady–state simulations

Table 3.3. Hydraulic properties incorporated into one–dimensional models for steady–state simulations.

of each range and the second value is the seepage rate at the outer portion of the defined range. Table 3.4 shows that significant variability can occur in the seepage predictions given from the one and two–dimensional steady–state models given uncertainty in the anisotropy ratio and the applied boundary conditions. The model predictions differ most in the transition zone where significant unsaturated horizontal flow components originating in the ponded zone increase the seepage from this region in the two–dimensional model. As is true of all mathematically imposed boundary conditions, the prescribed head boundary conditions implemented in this analysis may not be realistic in many situations; nevertheless, the influence of lateral flow components on the flux distribution

throughout the two-dimensional model can not be overlooked. The difference in seepage rates are most pronounced in the transition area because lateral flow components originating from the pond increase seepage in this region in the two-dimensional model. This is especially evident when the sand zone of the two-dimensional model is relatively dry due to prescribed boundary condition of -400cm at the surface of the impoundment. To illustrate the enormous difference in predictions from the models, we will compare volumetric seepage. Assume seepage from the transition zone of the one-dimensional model (for boundary conditions shown in column 3 of Table 3.4, or the second transition zone simulation) was used to calculate volumetric seepage from the impoundment. For the same conceptualized three-dimensional impoundment shown in Figure 3.52, the volumetric seepage is about 4.E-04 cubic meters per day. Compare that to the volumetric seepage rate of 8.2 cubic meters per day for the isotropic two-dimensional simulation. Although neither of the predictions is certain, it is apparent that the dimensionality of the model can play an important role in determining results of the analysis. It is important to remember that the boundary conditions imparted in the one-dimensional simulations play a very important role in the flux predictions at the base of the column. The drastic variation in the predictions from the one and two-dimensional models must be partly attributed to the difficulty in reproducing "identical" boundary conditions for the different models. However, this result does bring to light the importance of lateral flow components and proper model conceptualization in heterogeneous, anisotropic flow regimes.

zone	Dirichlet B.C.	1-d flux (cm/s)	ISOTROPIC		ANISTROPY = 20		ANISOTROPY=100	
			2-d flux range (cm/s)	% difference	2-d flux range (cm/s)	% difference	2-d flux range (cm/s)	% difference
slime	top=15 cm bot.=-55 cm	1.2E-7	9.0E-7 4.0E-6	650-3233	8.0E-7 2.8E-6	557-2233	7.9E-7 2.0E-6	558-2400
transition	top=-100 cm bot.=-55 cm	9.9E-7	7.0E-6 2.0E-5	607-1920	3.2E-6 1.6E-5	223-1516	2.0E-6 2.2E-5	102-2120
transition	top=-400 cm bot.=-55 cm	4.2E-9	5.6E-6 2.0E-6	118950-47520	2.5E-6 6.3E-7	59420-14900	2.5E-6 6.3E-7	59420-14900
sand	top=-100 cm bot.=-55 cm	4.9E-5	3.0E-5 8.0E-5	-38-63	1.6E-5 1.0E-4	-67-104	2.5E-5 2.0E-4	49-308
sand	top=-400 cm bot.=-55 cm	6.6E-8	2.5E-7 4.E-7	279-506	6.3E-7 4.0E-7	854-506	4.0E-6 1.6E-5	5960-24140

Table 3.4. Seepage prediction comparison from one and two-dimensional steady-state models.

STOCHASTIC–DETERMINISTIC APPROACH TO INCORPORATION OF SPATIAL VARIABILITY IN NUMERICAL MODELS

In the deterministic models studied up to this point, the hydraulic properties in the flow regime are assumed to be known at all points. The validity of this assumption is very dependent on the accuracy of the model used to define the hydraulic property distribution. Regardless of the sampling scheme implemented to characterize spatial heterogeneity in a flow regime, no deterministic model can completely duplicate the distribution of hydraulic properties present in the field. For all practical purposes, "fully" characterizing a highly heterogeneous flow system is virtually impossible. The uncertainty in the hydraulic properties for the flow simulation imparts some level of uncertainty in the model output predictions. One method of determining the relative levels of uncertainty in the model output parameters is by using a Monte Carlo approach. In this approach, observations of model output variance can be calculated based on uncertainty in input from numerous realizations of hydraulic conductivity. In the stochastic–deterministic approach used here, deterministic flow simulations are performed in which the saturated hydraulic conductivity distribution is considered a stochastic process. In this study, uncertainty in the prediction of hydraulic property fields is taken into account through a quasi Monte Carlo technique. In order to observe the variability in model output parameters due to the uncertainty in the input parameters, numerous simulations are performed using stochastic input fields. The model output statistics are then calculated in order to determine the relative variation in model output from various input models describing the distribution of saturated hydraulic conductivity.

Previous Work in Stochastic–Deterministic modeling

Freeze [1975] first attempted to incorporate the stochastic nature of the hydraulic properties of porous media into conceptual models for saturated groundwater flow. He conceptualized a purely random heterogeneous one–dimensional flow system composed of discrete blocks of homogeneous media. However, as pointed out by *Gelhar et al. [1976]*, it is important to consider the spatial correlation in the the hydraulic properties in this type of analysis. *Bakr et al. [1978]* showed the importance of incorporating the spatial correlation of the hydraulic properties into stochastic flow models.

Since the advent of these first papers which treated hydraulic properties as stochastic processes, extensive research has been completed in an effort to define the statistical nature of model predictions when the input processes to these models are considered stochastic. *Gelhar [1974], Gutjahr et al. [1978], Gelhar and Axness [1983], Mizell et al. [1982], and Yeh et al. [1985a,b,c]* use spectral methods to obtain solutions to stochastic perturbation equations in order to derive relationships between model input variation and model output variation. *Gelhar and Axness [1983]* develop an effective conductivity tensor based on the covariance structure and statistics of the media. *Mizell et al. [1982]* show that the multi–dimensional flow analysis results in significantly reduced head variances, and that head correlation will be greater than transmissivity correlation. *Yeh et al. [1985c]* conclude that variability in the capillary pressure increases as mean capillary pressure increases and that the anisotropy ratio increases when the mean capillary pressure increases. *Neuman [1982]* gives an overview of the approaches taken to date to statistically characterize heterogeneity in hydrogeologic systems.

The stochastic–deterministic approach has been used in the past decade to study the effects of hydraulic property correlation on model output. *Smith and Freeze [1979a,b]* use Monte Carlo techniques and a nearest–neighbor auto–regressive scheme to study the effects of different correlation scales on head fields in one– and two–dimensional saturated flow systems. These authors conclude that the correlation scale is a very important parameter in modeling the stochastic nature of a bounded media. Their study showed that the standard deviation of the hydraulic head field increased as the ratio of the correlation length to the size of the domain increased. They also point out the importance of recognizing a spatial trend in the mean hydraulic conductivity across the flow domain.

Smith and Schwartz [1981c] use a Monte Carlo approach to observe the effects of variation in particle arrival times due to uncertainty in the hydraulic conductivity data. They perform simulations using both conditioned and unconditioned data fields and conclude that a large number of hydraulic data may be neccesary in order to decrease the variance in the travel times.

Anderson and Shapiro [1983] compare Monte Carlo results to those of a perturbation approach to analyze one–dimensional unsaturated flow in a heterogeneous media. They conclude that the perturbation approach is valid for the cases they compared but warn that the one–dimensional conceptualization may be a severe restraint in truly multi–dimensional flow systems.

Most recently, *Hopmans et al. [1988]* studied two–dimensional unsaturated flow in heterogeneous soil with correlated hydraulic properties. In contrast to earlier findings with respect to saturated systems, these authors conclude that variability in the fluxes for the unsaturated system decrease with an increase in correlation length. They also state that the variability in the lateral

flow component at the layer boundary of a two layer system was significantly increased as compared to the single layer system.

Considering Mill Tailings Properties as Stochastic Processes

It may be unclear in some situations whether a certain process can be correctly defined by traditional stochastic methods. *Johnson [1987]* failed to find significant correlation in saturated hydraulic conductivity through variogram analysis in detrended measurements taken in a mill tailings impoundment. However, it is possible that the sampling procedure or methods of analysis used in the study were not performed in a manner which allowed an existing covariance structure to be recognized or calculated. One important step in the variogram analysis of data is removing the "trend" from the data. In variogram analysis, it is assumed that the mean or average of the data values is either known and constant in the domain, in which case the mean can be subtracted from the data values to obtain a "mean zero" process, or that the random process is assumed to be "second-order stationary" or "weakly stationary". A process is "second-order stationary" if the data does not exhibit a trend in space and if the covariance only depends on the separation distance and not the point of reference. Obviously, by nature of their depositional setting, mill tailings impoundments almost always exhibit trends in the hydraulic properties,, and thus if the classical geostatistical approach is taken to quantify the variability in the hydraulic properties, the data set must be detrended so that variogram analysis can be completed. Various methods are available which claim to properly detrend the data but, as pointed out by Davidoff *[1988]*, different methods of detrending data may not lead to equivalent outcomes from variogram analysis. Sampling procedure and methods of analysis must be incorporated in the stochastic conceptualization which allow detection of any existing covariance

structure. For instance, methods used to determine hydraulic conductivity must be performed on a scale which will allow variations in the property to be properly characterized. Various sampling schemes and data analysis (lab techniques, etc.) will play an important role in determining the "estimated" covariance structure.

Whether or not significant correlation exists in mill tailings hydraulic properties is a very important consideration when determining a conceptual approach taken to modeling flow and transport in and around tailings impoundments. If valid assumptions can not be incorporated concerning the stochastic conceptualization, the validity of the model approach is therefore uncertain from the beginning. Therefore it is always neccesary to assess the feasibility and accuracy of the conceptual model. *Byer and Stephens [1983]* show the significance of correlation structure in an alluvial sand and conclude that the correlation scale is on the order of one meter. The correlation scale in comparison to the scale of the overall problem domain is also a very important factor in the incorporation of a stochastic conceptual model. If the correlation scale is very small relative to the overall scale of the model, it may only be nessecary to incorporate the large scale trends in the domain and not the small scale heterogeneities, especially since this process can be very time consuming and expensive. At this point, the degree of certainty which can be imparted in a stochastic conceptualization of mill tailings properties is unknown. However, it is the purpose of this study is to assess the uncertainty in model predictions given uncertainty in the specific stochastic model, assuming that the overall stochastic conceptualization exhibits reasonable similarity to field conditions.

Elementary Introduction to the Stochastic Conceptualization

Deterministic modeling requires input of hydraulic property fields and boundary conditions for the flow model. In the stochastic-deterministic flow

simulations performed in this study, the saturated hydraulic conductivity fields are generated which have a given variance and correlation structure. Correlation structure refers to the nature of the "similarity" between measurements taken at different points in the domain. For instance, imagine a core which contains layers of sand and silt from a sedimentary formation. If the layers are of significant thickness, the porosity or hydraulic conductivity may show some spatial correlation or connection. In other words, the value of hydraulic conductivity at one point in the core shows some correlation to the value a short distance away and less correlation to values which are further away. If a significant number of values of hydraulic conductivity were determined throughout the core, analysis could be performed in order to evaluate the average distance over which the values were correlated. The variance over some incremental distance is referred to as the variogram and is defined as follows [see *Journal and Huljubrets (1979), de Marsily (1986)*]:

$$\gamma(\vec{h}) = \frac{1}{2}E\left\{\left[Z(\vec{x}+\vec{h}) - Z(\vec{x})\right]^2\right\} \tag{3.12}$$

where E denotes the mathematical expected value, Z is the value of the random variable, and $\vec{x}$ and $\vec{h}$ denote multi-dimensional vectors, $\vec{h}$ is the separation distance of the values. For the stationary case, the covariance structure $C(\vec{h})$ is simply a reflection of the variogram with respect to the horizontal axis with a vertical shift. This can be mathematically stated as:

$$C(\vec{h}) = C(0) - \gamma(\vec{h}) \tag{3.13}$$

where $C(0)$ is the covariance at zero separation distance, or the estimated variance of the random field. Graphical representation of these ideas are shown in Figure 3.53.

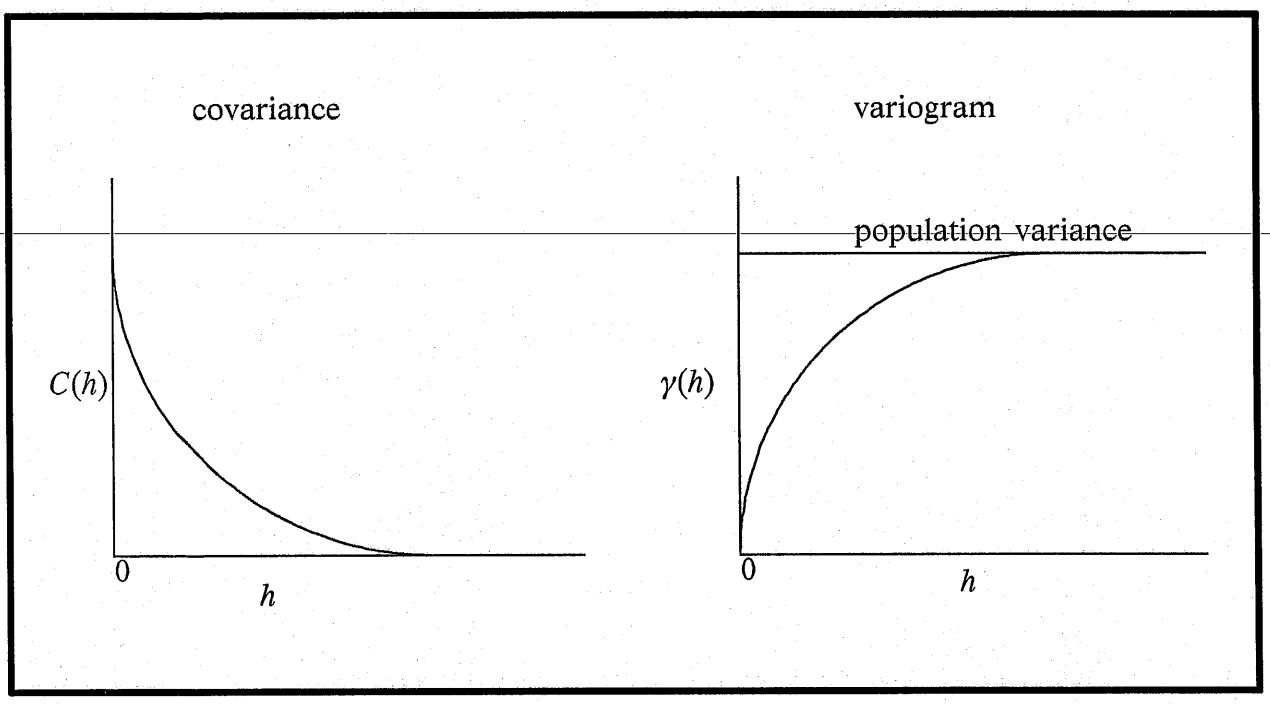

Figure 3.53. Hypothetical covariance and variogram.

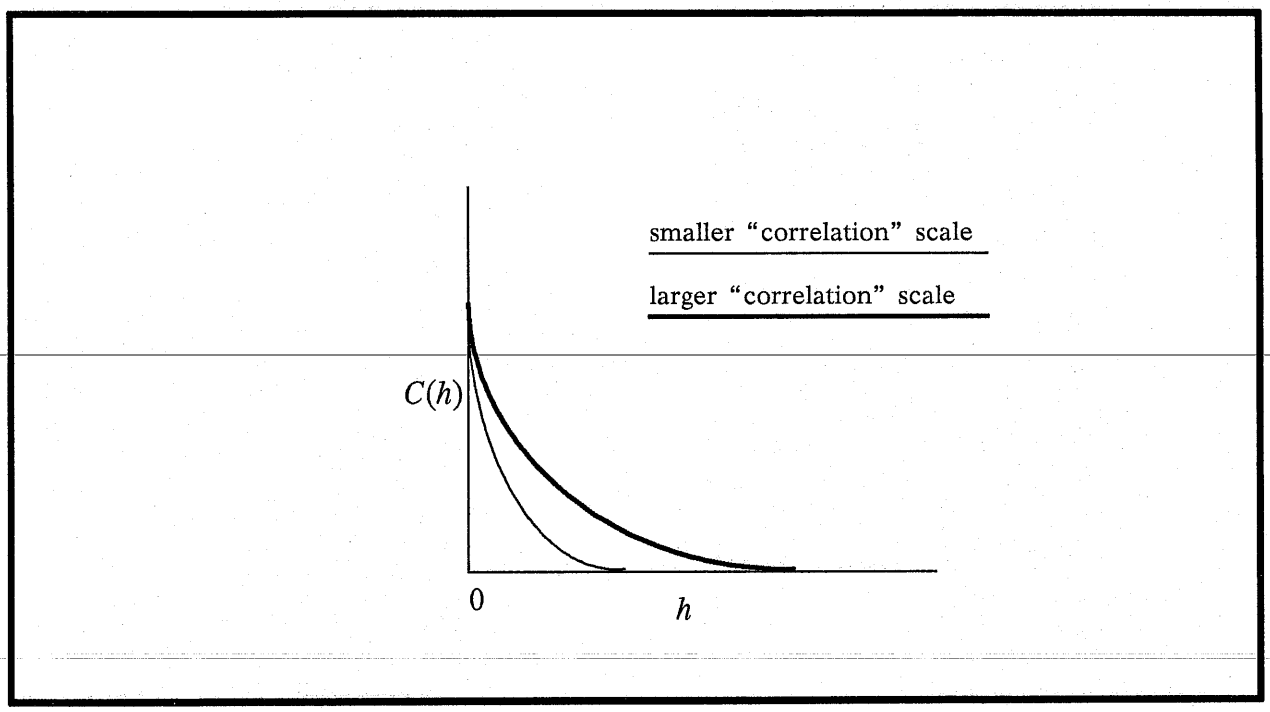

Figure 3.54. Hypothetical anisotropic covariance structure.

If the covariance structure can be defined, different methods could be used to generate many realizations of the core properties given the acquired statistical data. This procedure can also be carried out for multi-dimensional cases. As depicted in Figure 3.54, some fields do not exhibit the same correlation scales in different directions. This anisotropic covariance structure can also be accounted for in the model when generating realizations of the stochastic process.

Several methods are available to generate random fields of given covariance structure. The Turning Bands Method (TBM) *[Mantoglou and Wilson, 1981]*, Fast Fourier Transform method *[McKay, 1988]*, and the "nearest neighbor" autoregressive method *[Smith and Schwartz, 1981c, and Hopmans et al., 1988]* are a few which have been used in hydrologic studies in the past. However, consideration should be given to the size of the field and the covariance structure incorporated when choosing a method, since it has been shown that the TBM may produce preferential flow paths under certain conditions *(Wilson and Gutjahr, 1989)*. In this study, a Fast Fourier Transform (FFT) method was used to produce two-dimensional fields exhibiting anisotropic covariance structure. The code was developed by Dr. Allan Gutjahr and can be found in Appendix B of this paper. For a full description of the approach of the Fast Fourier Transform method, see *Mckay [1988]*. Since the method produces a mean zero stationary process, the trend or "known" mean in the saturated hydraulic conductivity was incorporated into the synthetic fields. The field of correct mean and stochastic behavior denoted by $S(\vec{x})$ is produced by assuming that the predictions from the regression model (denoted $R^*(\vec{x})$, where $\vec{x}$ denotes spatial coordinates), adequately approximate the trend or "mean" of the field.

$$S(\vec{x}) = S'(\vec{x}) + R^*(\vec{x}) \qquad (3.14)$$

The synthetic field produced via the FFT method denoted by $S'(\vec{x})$ is then simply added to $R^*(\vec{x})$ as shown in equation 3.14 to produce the field $S(\vec{x})$ of correct mean and proper stochastic properties.

Description of Simulations Performed using Stochastic Fields

The degree of nonlinearity in the system of equations which results from implementing the finite element method in unsaturated, heterogeneous media is very dependent on the variance and type of covariance structure which is incorporated into the random fields. As an illustration of this point, consider the anisotropic covariance structures shown in Figure 3.55 and 3.56. The covariance structures depicted in the figure are defined by different analytical functions and thus show slight variation in both horizontal and vertical directions. Equation 3.15 gives a mathematical description of the exponential covariance structure shown in Figure 3.55.

$$C(\xi) = \sigma^2 \exp\left\{-\left[\left(\frac{\xi_x}{\beta_x}\right)^2 + \left(\frac{\xi_z}{\beta_z}\right)^2\right]^{\frac{1}{2}}\right\} \qquad (3.15)$$

where:

$C(\xi)$ = covariance at separation distance ξ

σ^2 = variance of the stochastic process

ξ_x and ξ_z = separation distance in the horizontal and vertical directions respectively

β_x and β_z = parameter defining the distance over which the properties are "significantly" correlated in the x and z directions respectively; sometimes refers to as the "correlation scale"

Equation 3.16 gives a mathematical description of the "double exponential" covariance structure shown in Figure 3.56.

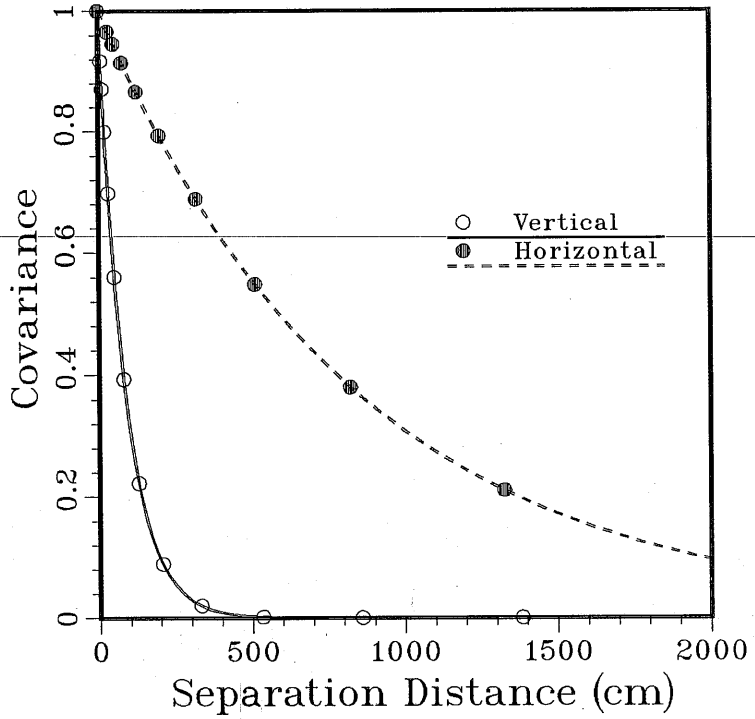

Figure 3.55. Exponential covariance structure used to generate the log saturated conductivity fields shown in Figure 3.57.

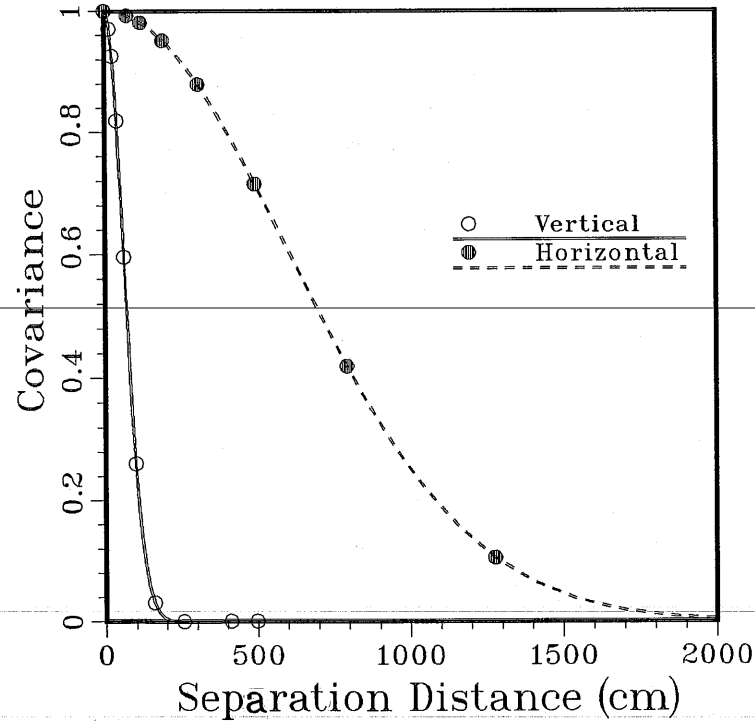

Figure 3.56. Double exponential covariance structure used to generate the log saturated conductivity fields shown in Figure 3.58.

$$C(\xi) = \sigma^2 \exp\left(-\left\{\frac{\xi_x^2}{\beta_x^2} + \frac{\xi_z^2}{\beta_z^2}\right\}\right) \qquad (3.16)$$

The parameters for both covariance equations are σ^2 = 1.0, β_x = 850cm, and β_z = 85cm. Four realizations of log saturated hydraulic conductivity fields produced from each covariance structure shown in Figures 3.55 and 3.56 via the Fast Fourier Transform method are shown in Figures 3.57 and 3.58 respectively. Notice that the mean field of log saturated hydraulic conductivity shown in Figure 3.1 has been incorporated in the field according to equation 3.16. Obviously, small changes in the covariance structure can produce significant changes in the resulting synthetic fields. The fields resulting from the exponential covariance structures are more "noisy" than those from the double exponential covariance structure. This increased small scale variability in the exponential fields increases the nonlinearity in the system of equations resulting from the finite element implementation. The increased nonlinearity may cause convergence problems in the iterative scheme used to solve the system of nonlinear equations.

In the following section, we examine several "quasi" Monte Carlo unconditional simulations which were performed to investigate the results of incorporating various types of stochastic hydraulic property fields into numerical models. Different sets of boundary conditions are applied in order to delineate the variation in steady-state results under various soil moisture flow conditions. In this fashion, it will be possible to delineate which types of boundary conditions lead to major uncertainty in flow phenomena. Table 3.5 gives a summary of the covariance structures and boundary conditions used in the Monte Carlo and conditional simulations.

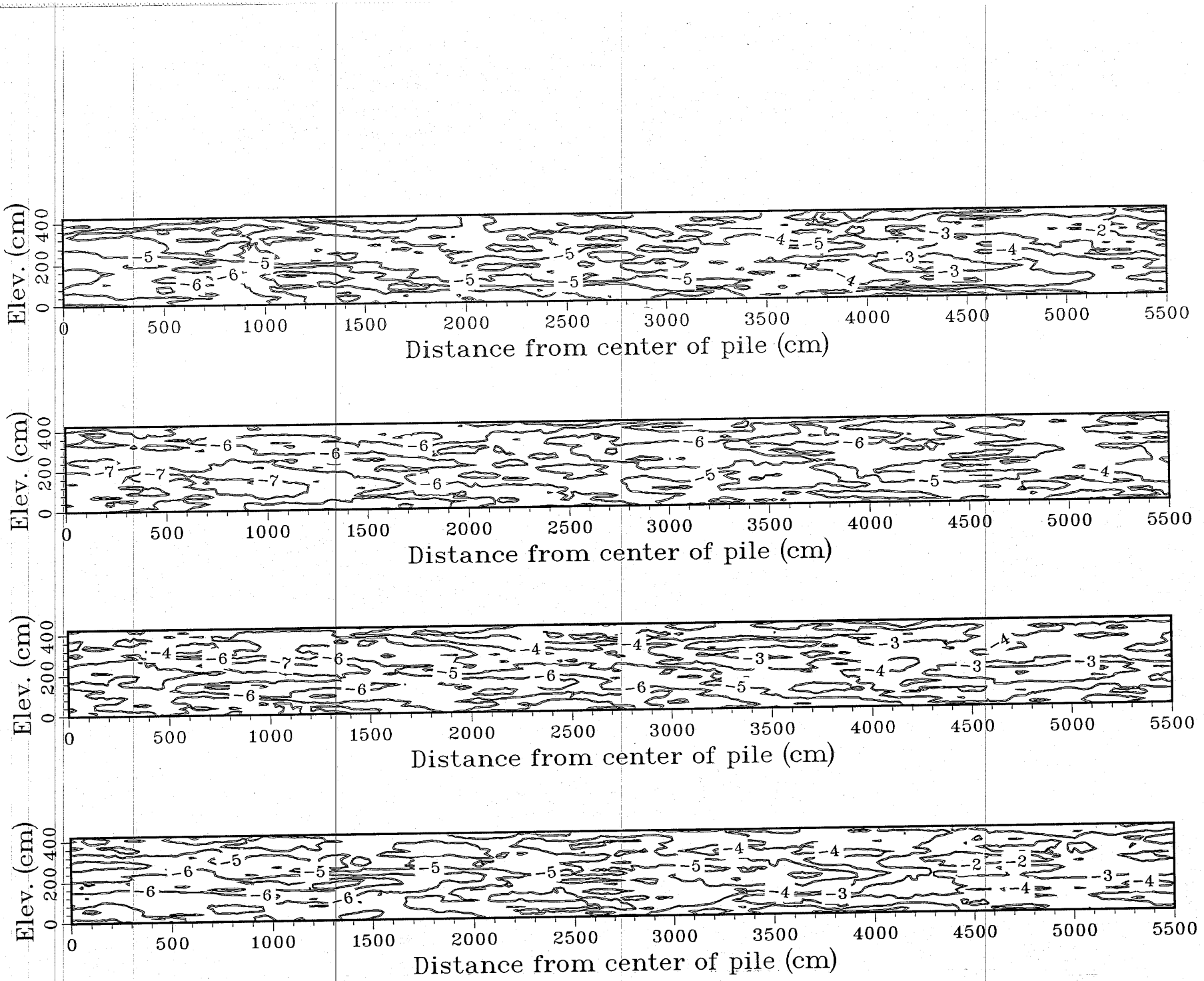

Figure 3.57. Four realizations of log saturated hydraulic conductivity generated via the FFT method using covariance structure shown in Figure 3.55.

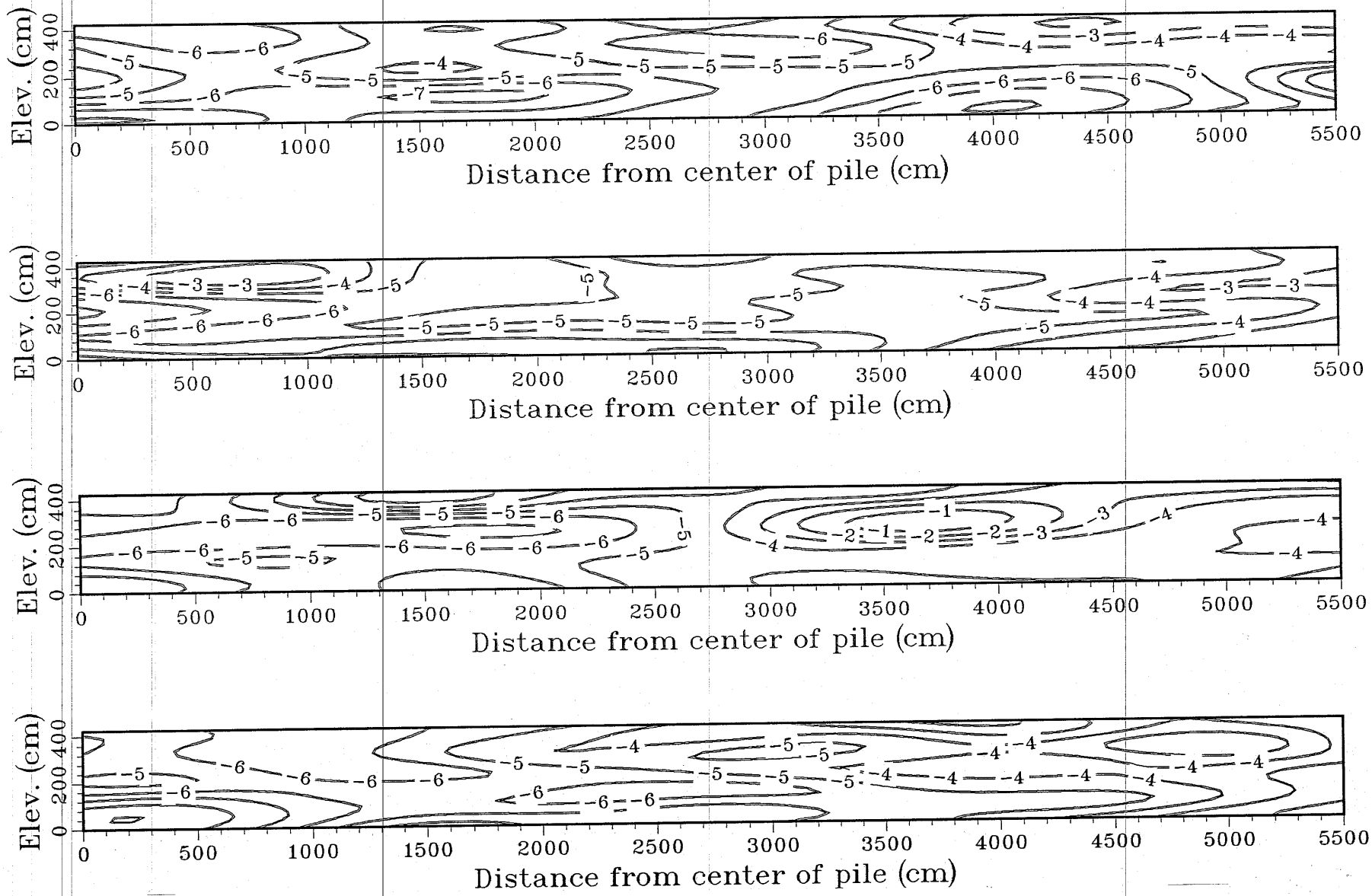

Figure 3.58. Four realizations of log saturated hydraulic conductivity generated via the FFT method using covariance structure shown in Figure 3.56.

Simulation Set	Covariance Structure	$\sigma^2_{\log K}$	β_z	β_x	Boundary Conditions
MC#1	see equation 3.15	.25	85cm	850cm	Surface: constant flux = 51 cm/yr Base: prescribed pressure head = −55cm.
MC#2	"	.50	85cm	850cm	"
MC#3	"	.50	85cm	850cm	15cm ponding from 0–22m prescribed pressure head=−100 from 22–55m Base: prescribed pressure head = −55cm.
MC#4	see equation 3.16	.50	75cm	753cm	"
MC#5	see equation 3.15	.50	170cm	1700cm	"
CS#1	"	.50	170cm	1700cm	"

Table 3.5. Summary of covariance structure and boundary conditions used in Monte Carlo and conditional Simulations.

Discussion of Model Output Statistics from "Quasi" Monte Carlo Simulations

Let us first examine the results of quasi Monte Carlo simulations which were performed under the same boundary conditions but with different variance in the saturated hydraulic conductivity field. The boundary conditions for Monte Carlo simulations #1 and #2 (MC1 and MC2 respectively) are as follows: a prescribed pressure head at the base of the impoundment (-55cm), and a prescribed downward flux rate at the surface of the impoundment (51 cm/yr). These boundary conditions may also be indicative of a system in the deep vadose zone in which there is a constant vertical recharge rate from the surface. MC1 and MC2 were performed using log saturated hydraulic conductivity fields which exhibited a variance of 0.25 and 0.50, respectively. Figure 3.59 shows the exponential covariance structure used produce the log saturated hydraulic conductivity fields for MC1 and MC2. Four realizations of the log saturated hydraulic conductivity field used in MC1 are shown in Figure 3.60. Since the variance of the fields is relatively small, the major trends in the hydraulic conductivity shown in Figure 3.1 are still quite visible in the contour lines of the stochastic fields.

Seepage statistics from MC1 are shown in Figure 3.61. A hydraulic anisotropy ratio of 20 was also incorporated into the porous media in each finite element. This anisotropy was constant at any given pressure. The variation in seepage about the mean as described by the standard deviation is relatively small. The variability across the domain in the standard deviations about the mean may be partially due to the small number of runs (10) completed for the Monte Carlo study. It is worthwhile at this point to compare Figure 3.61 to Figure 3.40 which displays the seepage rate at the base of the impoundment from deterministic simulation #10. All hydraulic properties for these two sets of simulations were

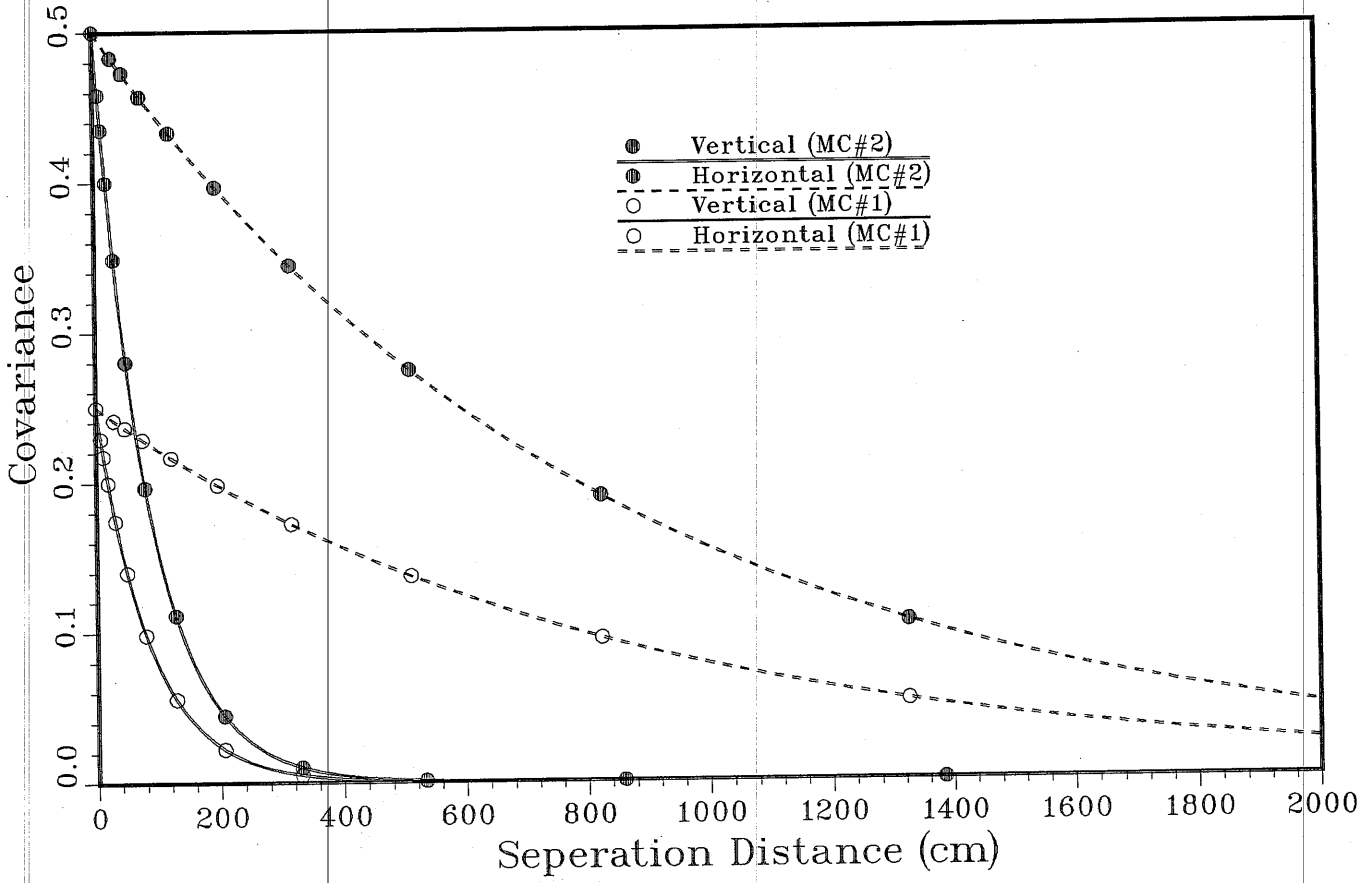

Figure 3.59. Exponential covariance structure used to generate the log saturated hydraulic conductivity fields for MC1 and MC2.

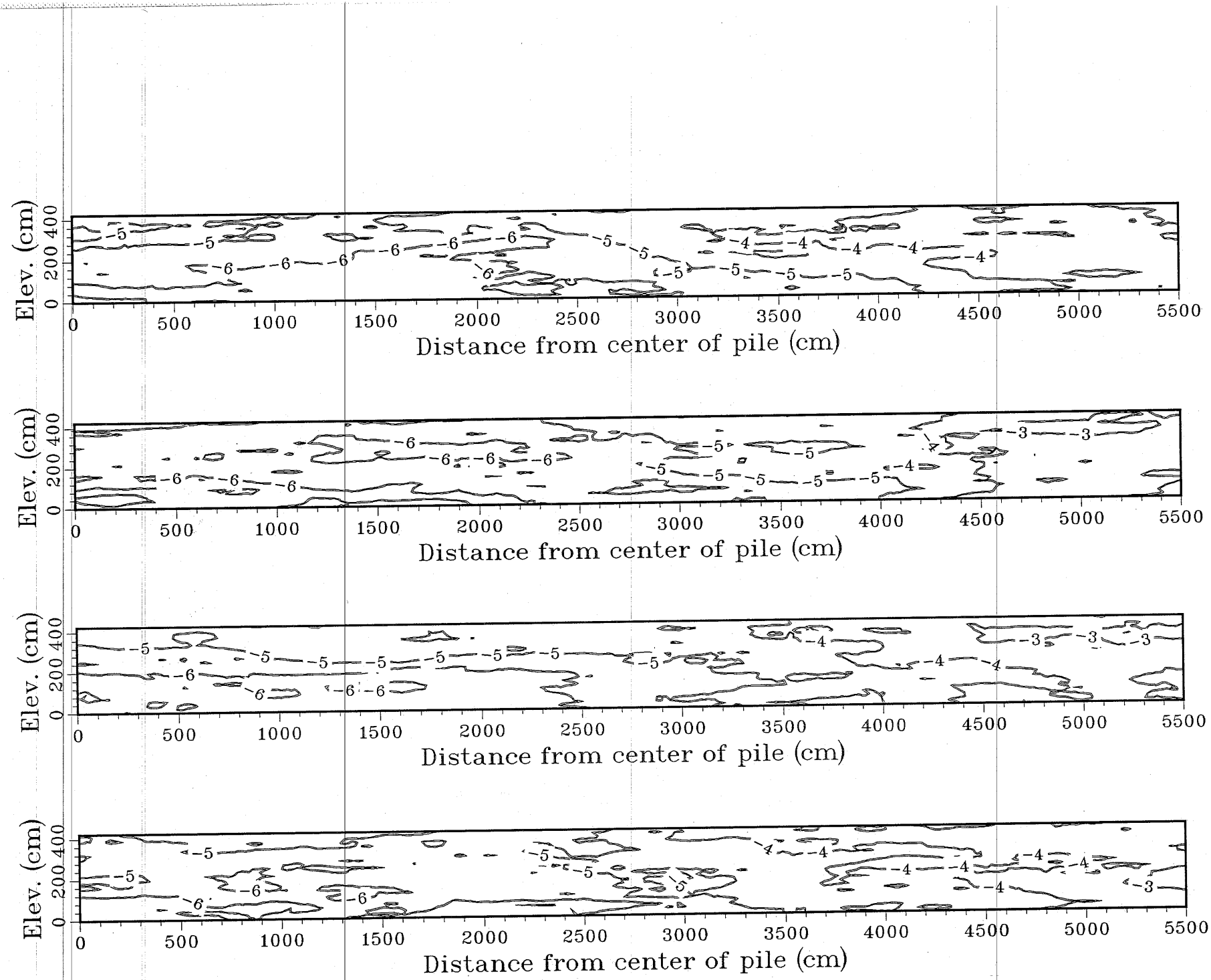

Figure 3.60. Four realizations of log saturated hydraulic conductivity generated by the Fast Fourier Transform method for use in MC1.

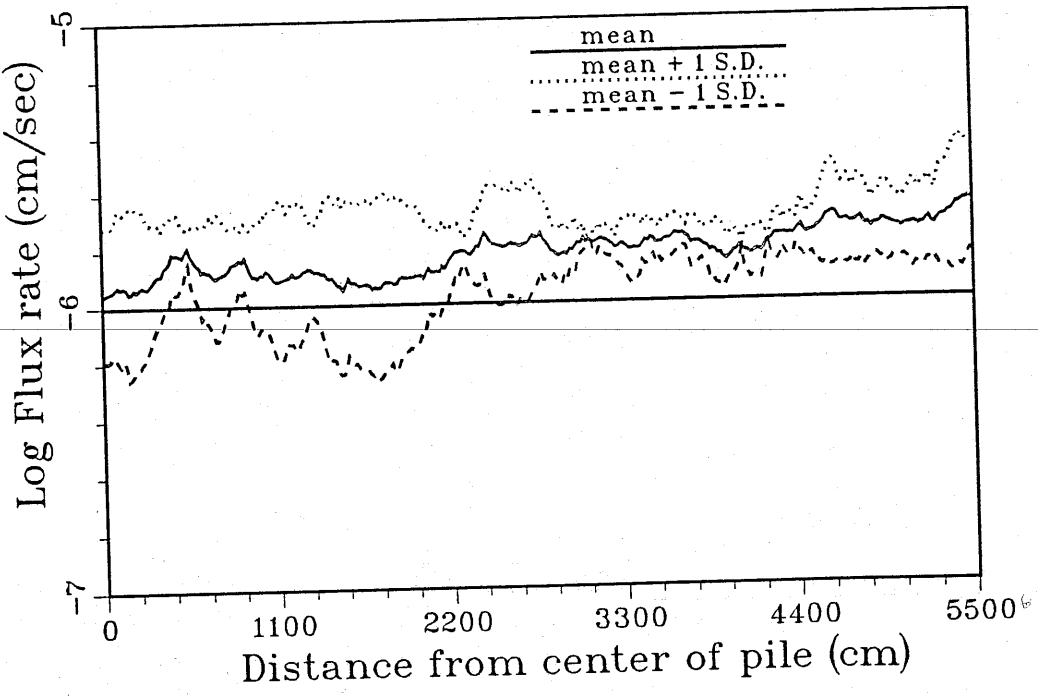

Figure 3.61. Seepage statistics for Monte Carlo simulation 1 (MC1).

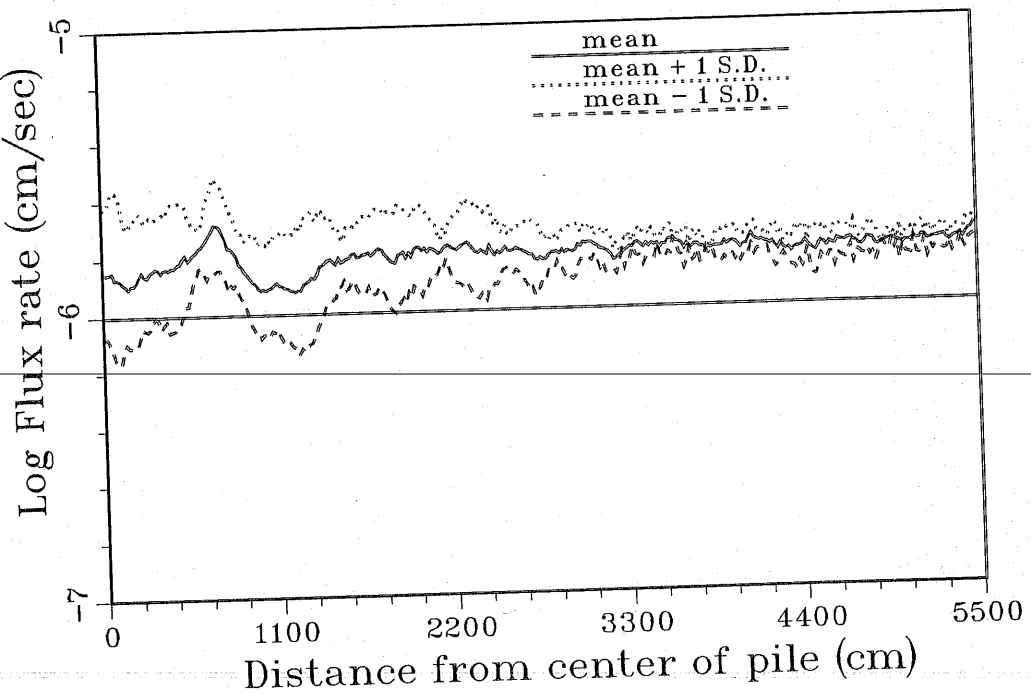

Figure 3.62. Seepage statistics for Monte Carlo simulation 2 (MC2).

identical with the exception of the random distribution of saturated hydraulic conductivity given in MC1. Comparison of the mean seepage distribution in Figure 3.61 to the deterministic seepage rate in Figure 3.40 shows that the mean seepage is more constant across the domain whereas the deterministic flux rate shows a much more persistent increase from the center of the impoundment to the edge. The difference in flux distribution is caused by the lateral heterogeneity which impedes flow in the horizontal direction. The impeding layers restrict lateral flow and since the hydraulic gradient is vertically downward, fluid is forced downward. This result carries significant implications for conceptualizing models for solute transport delineation. For instance, using "effective" or constant hydraulic properties to define heterogeneity based on the statistical properties of the porous media may not be sufficient to define flow phenomena and is perhaps a more questionable approach in determining transport processes.

Seepage statistics from MC2 are shown in Figure 3.62. As in MC1, the hydraulic anisotropy ratio is 20, but the variance for the saturated hydraulic conductivity fields used for the simulations is doubled to 0.50. As seen in Figure 3.62, the increased variance in the conductivity field is not reflected in the variation of seepage rate at the base of the impoundment. This result may be partially explained by realizing the variation in conductivity zones in the impoundment due to the incorporated randomness and by analyzing the hydraulic head field. It is apparent that lateral flow components are diminished in areas of the impoundment where the hydraulic gradients show smaller lateral components, as can be seen in the mean hydraulic head field shown in Figure 3.63a. In the outer edge of the impoundment, the hydraulic gradients are generally vertically downward, whereas in the center of the impoundment, the gradients exhibit a larger lateral component toward the outer portion of the impoundment.

Movement of fluid particles in the outer portions of the impoundment will tend to be more inhibited laterally by the zones of low conductivity then those in the center of the impoundment because the lateral hydraulic gradients are less significant. As for comparison of MC1 and MC2, the seepage variance at the base of the impoundment is less for MC2 because the hydraulic gradients are essentially equal in both scenarios (see Figures 3.63a and 3.64a), but the resistance to lateral flow is greater in MC2 since the variance of the hydraulic conductivity is greater and thus fluid particles have a greater chance of encountering low conductivity zones. Figure 3.63b and 3.64b show the standard deviations in the hydraulic head are much greater in the center of the pile where the gradients are much larger due to the lower conductivity media in the center of the impoundment. The standard deviation is zero at the base of the impoundment due to the prescribed pressure head boundary and it is greatest at the surface of the impoundment (in the low conductivity zones) because the pressure head in that region is very dependent on the random hydraulic conductivity. Since the boundary condition at the surface of the impoundment is one of prescribed flux, the pressure head is apt to be quite variable due to the random nature of the hydraulic conductivity. As with the standard deviation of the seepage rates, the standard deviation of the pressure and hydraulic head fields for MC1 shown in Figures 3.63b, 3.65b, are greater in portions of the pile exhibiting relatively small hydraulic gradients than for MC2 shown in 3.64b, and 3.66b, even though the conductivity fields exhibit a smaller variance. However, examination of the inner portion of the impoundment reveals that the standard deviation of the pressure field is greater in MC2 then for MC1. This would be expected since the hydraulic gradients are much greater in this region and fluid is forced around areas of low conductivity by high gradients rather than flowing through low conductivity areas because small gradients do not mandate rapid

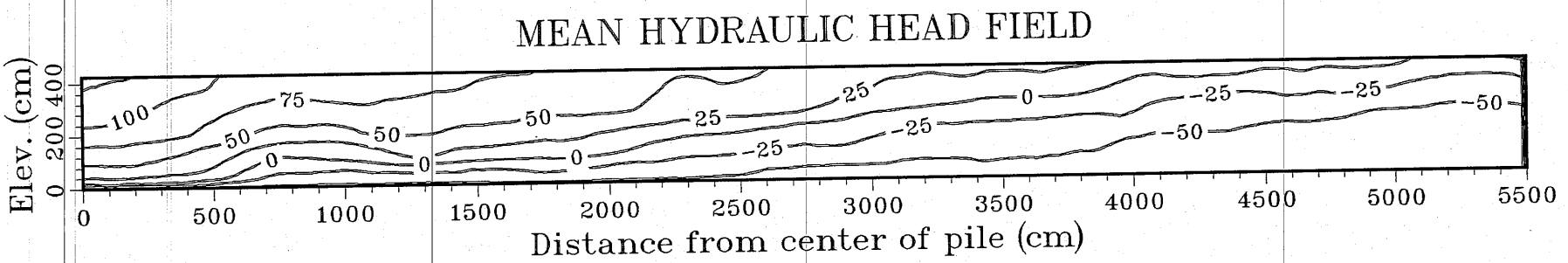

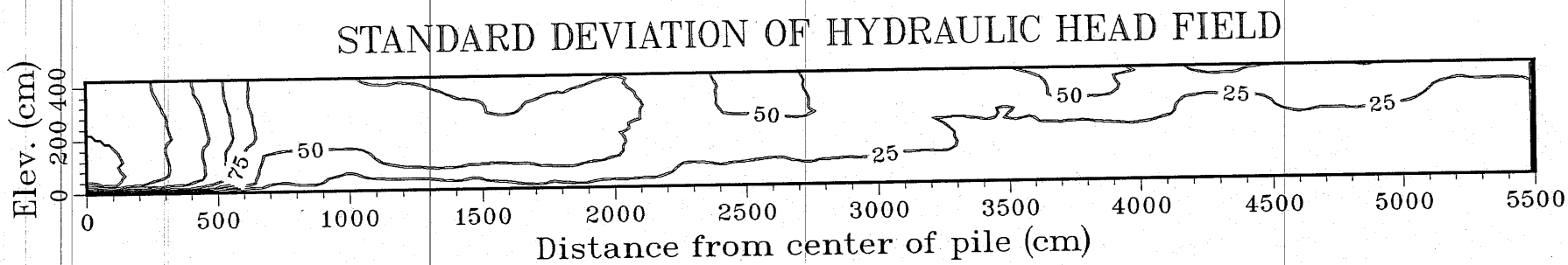

Figure 3.63(a,b). Mean and standard deviation of hydraulic head fields respectively from MC1.

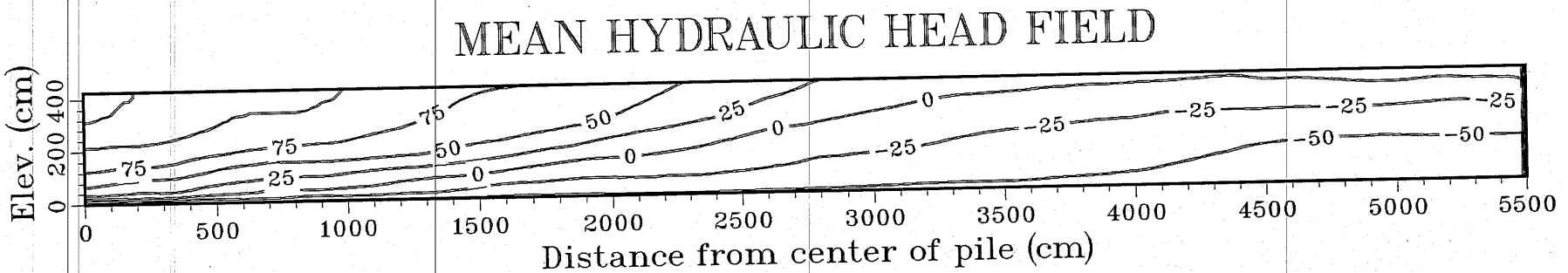

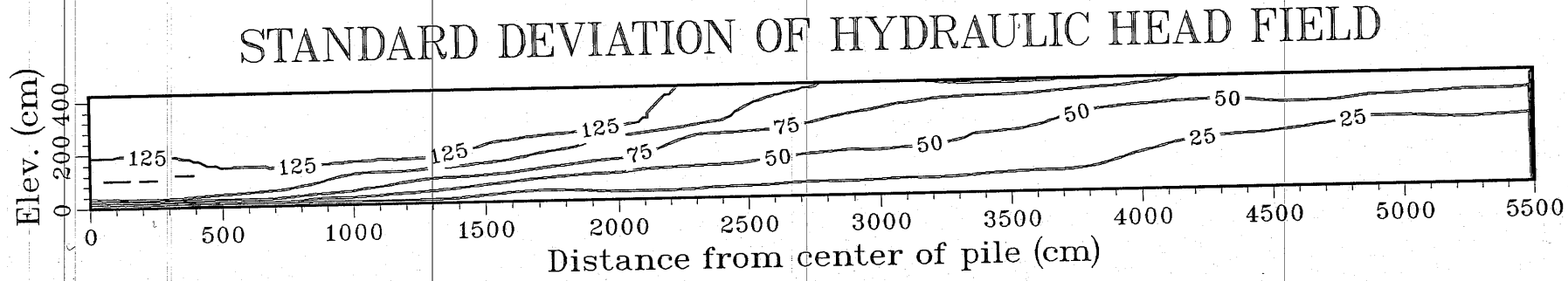

Figure 3.64(a,b). Mean and standard deviation of hydraulic head fields respectively from MC2.

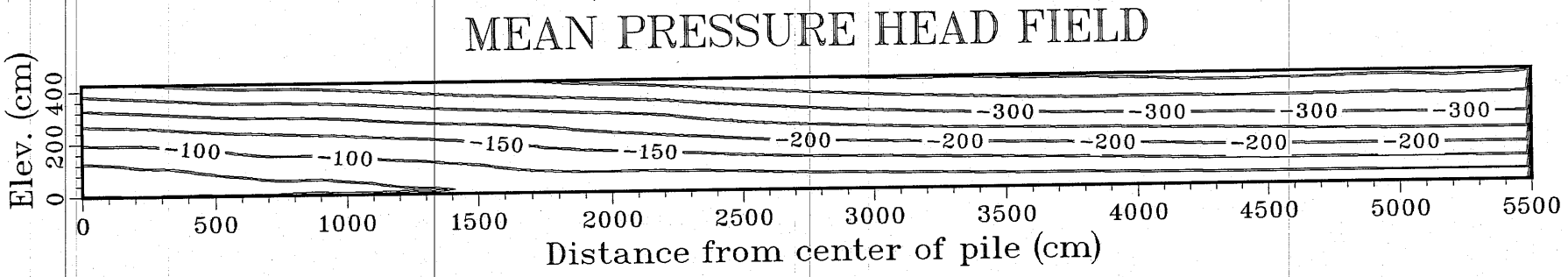

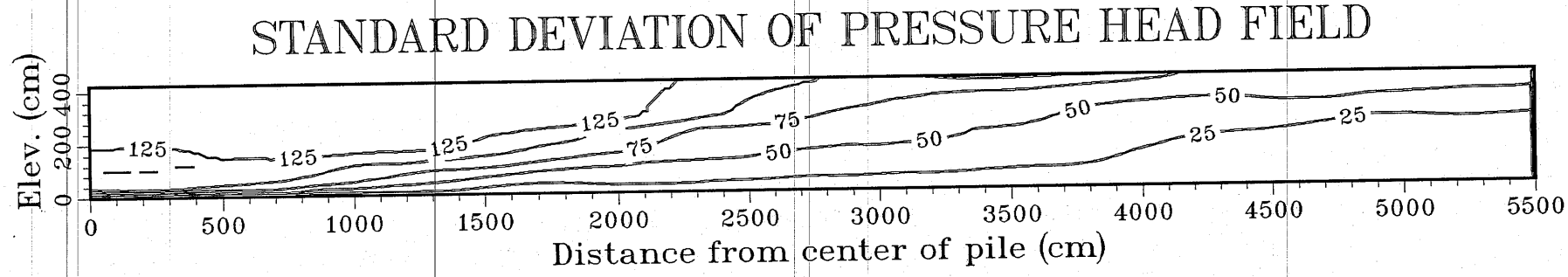

Figure 3.65(a,b). Mean and standard deviation of pressure head fields respectively from MC1.

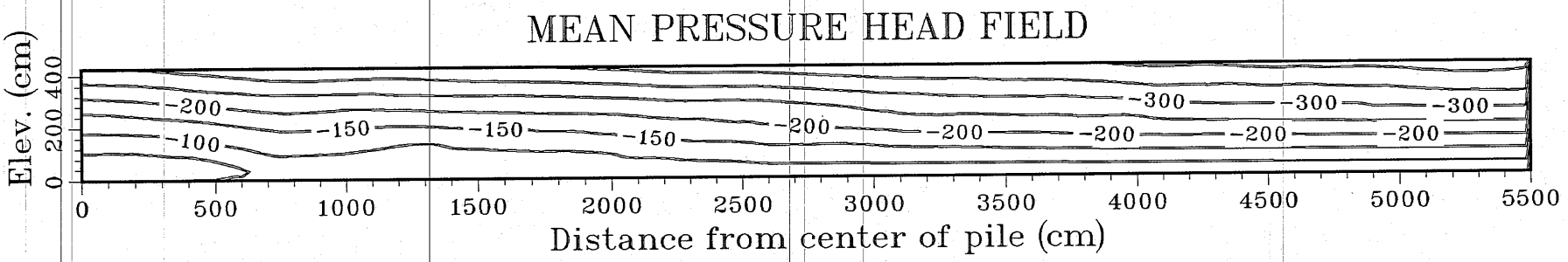

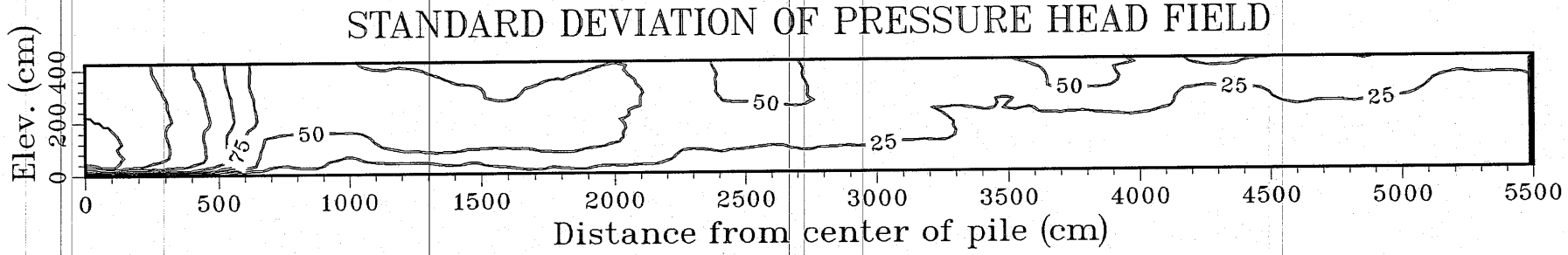

Figure 3.66(a,b). Mean and standard deviation of pressure head fields respectively from MC2.

movement. As shown in Figures 3.67b and 3.68b, the variation in saturation is very low in the outer portions of the impoundment and greater in the center of the impoundment due to the increased variability in the pressure head. Also note that the saturation deviations are greater for MC1 than for MC2.

Under unsteady flow conditions, uncertainty in moisture movement and distribution is expected to be greater than that depicted in the steady-state simulations performed here. Redistribution processes will be greatly affected by the heterogeneous anisotropic media, imparting larger uncertainty in contaminant travel times.

One important point to recall when reviewing these results that the downward flux rate in the MC1 and MC2 is constant across the top of the impoundment. This boundary condition imparts mainly vertical hydraulic gradients which decrease the propensity of lateral flow components in the impoundment. If the source of fluid in the impoundment is instead limited to more of a point source, lateral hydraulic gradients may cause significant lateral flow components. This point is illustrated in Figure 3.69a,b,c,d. The hydraulic conductivity field used in this simulation is a realization similar to those shown in Figure 3.58. The boundary conditions for the simulation are as follows: 15cm ponding from center of pile to 22m outward, prescribed pressure head of -400cm at surface of impoundment from 22m to the edge of the pile, and prescribed pressure head of -55cm at the base of the impoundment. Figure 3.69b shows magnitude of the lateral hydraulic gradients to be much greater then in MC1 and MC2 since the fluid in the pond is pulled from the ponded region to the outer portion of the impoundment. This variation in boundary conditions leads to significant lateral flow components since the influx of fluid is concentrated in the center of the impoundment. This finding is consistent with field and lab results of *Stephens and Heerman [1988]* and *Stephens et.al [1988]*. In this simulation, the

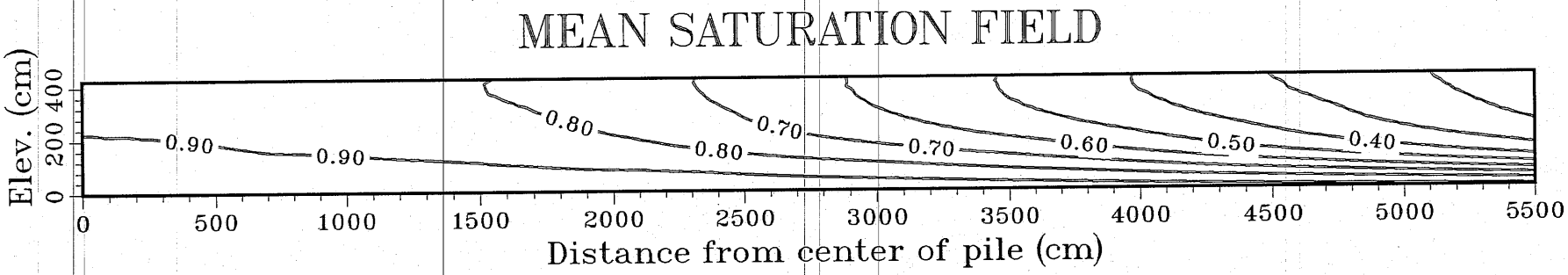

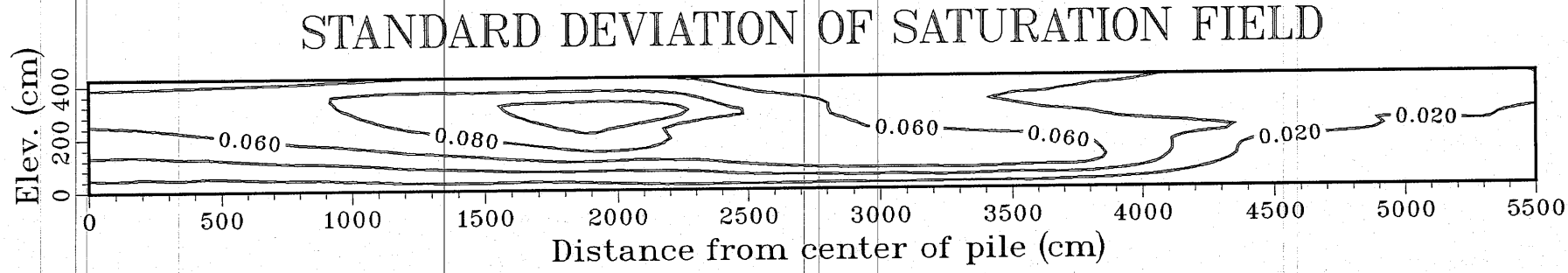

Figure 3.67(a,b). Mean and standard deviation of saturation fields respectively from MC1.

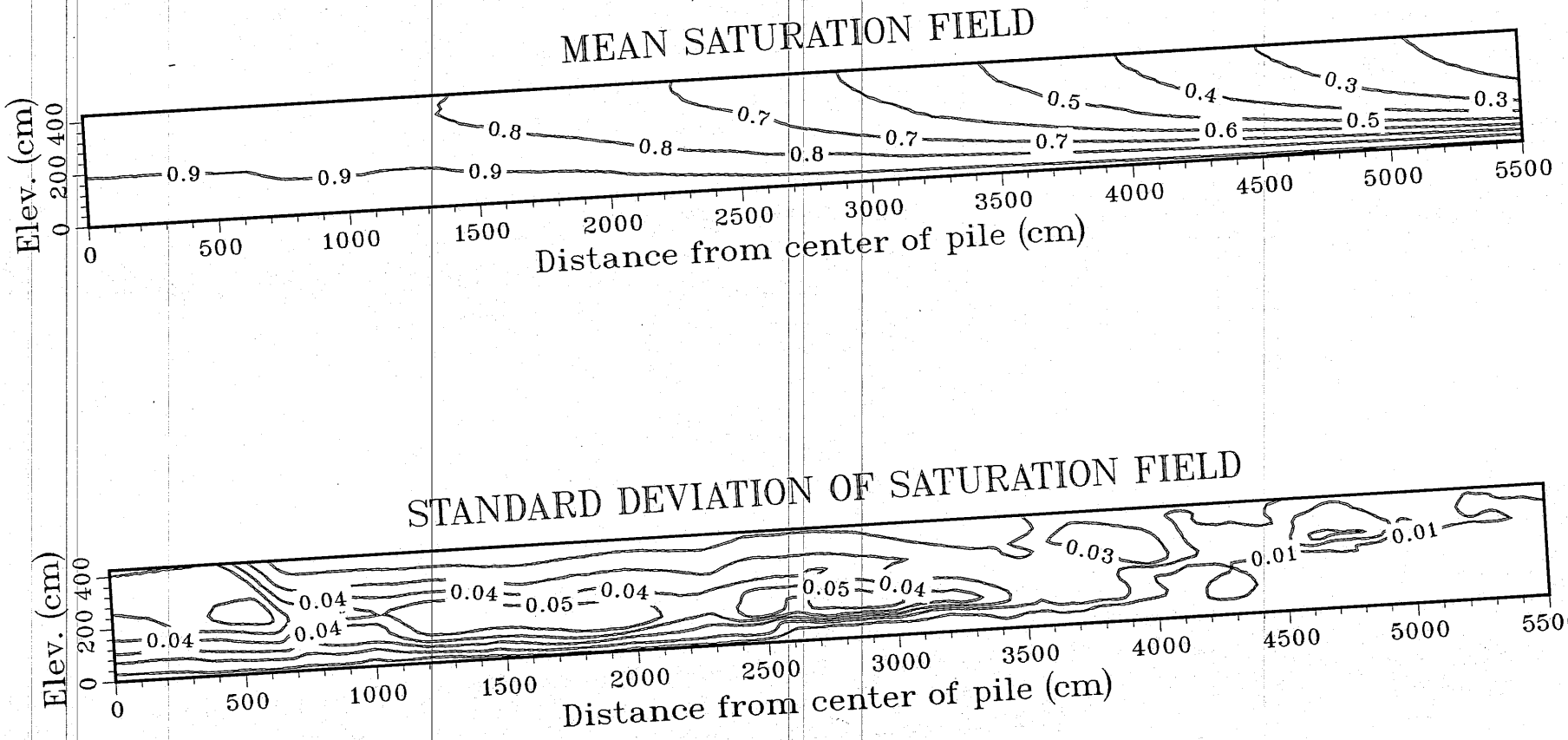

Figure 3.68(a,b). Mean and standard deviation of saturation fields respectively from MC2.

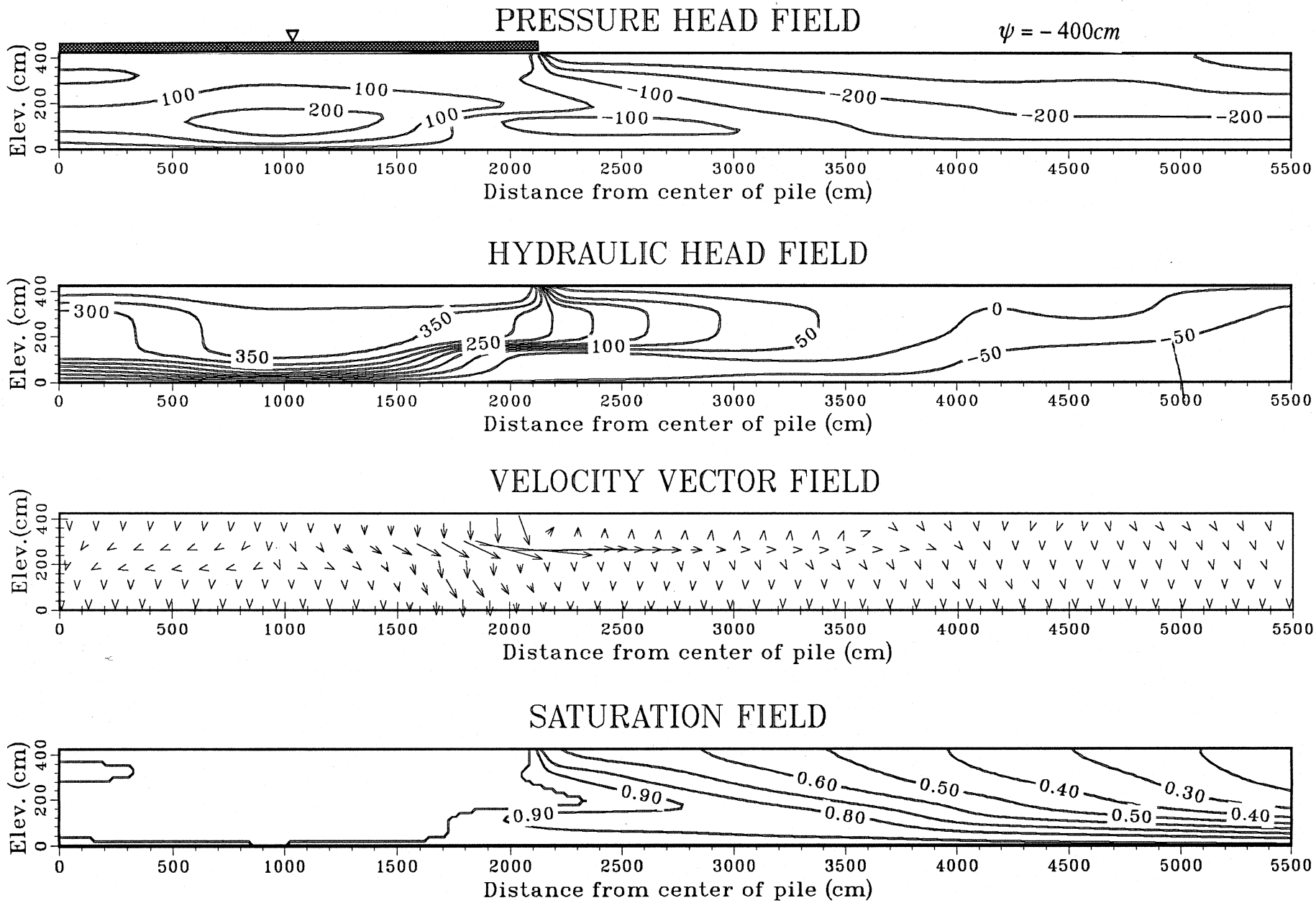

Figure 3.69(a,b,c,d). Steady-state results from one stochastic realization of saturated hydraulic conductivity. Conductivity field is similar to the realizations shown in Figure 3.58.

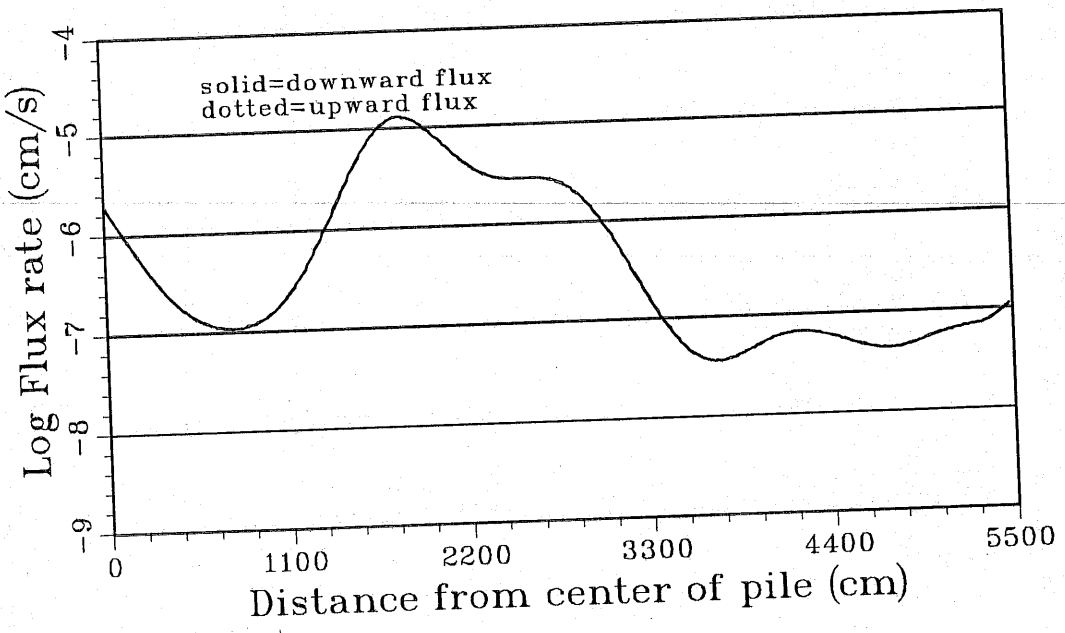

Figure 3.70. Flux distribution at the base of the impoundment from one realization incorporating a stochastic conductivity field similar to those shown in Figure 3.58.

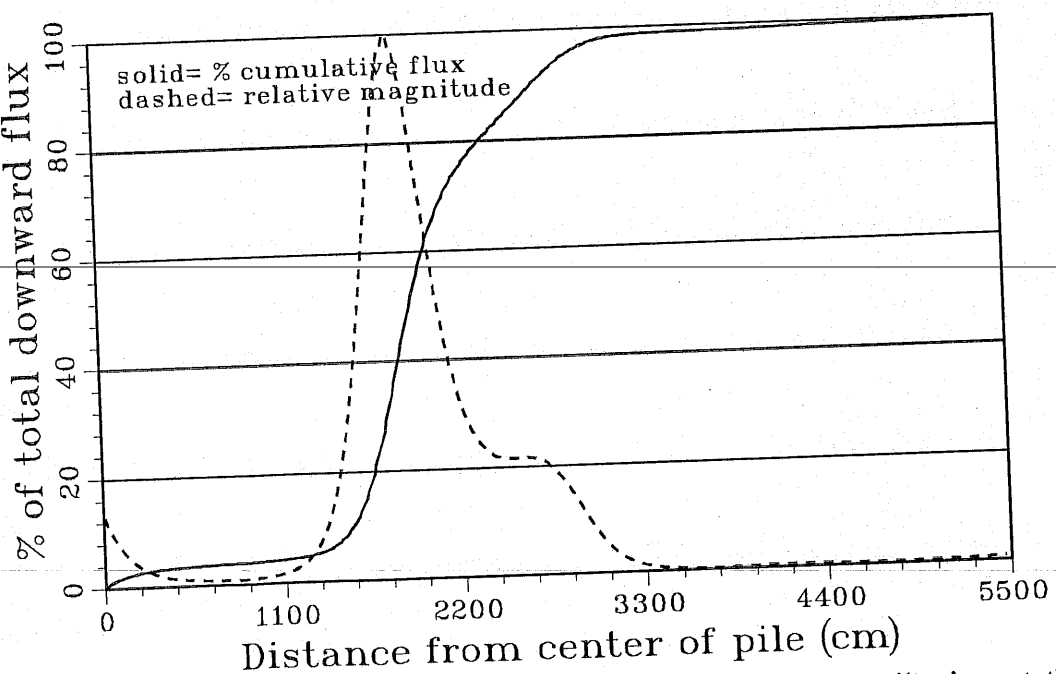

Figure 3.71. Cumulative flux curve and and relative flux distribution at the base of the impoundment from one realization incorporating a stochastic conductivity field similar to those shown in Figure 3.58.

porous media was considered isotropic in each element, if anisotropy had been incorporated, the lateral flow components would have been more significant. Figure 3.70 displays the immense variation in seepage rates due to the incorporated heterogeneity and ponding. Figure 3.71 demonstrates that 80–90% of the seepage from the impoundment exits in the distance from about 15–25m from the center of the impoundment. Also, 20% of the seepage from the base of the impoundment occurs from the outside the ponded area. These result is quite relevant when considering contaminant movement from point sources in layered and heterogeneous media. Obviously, conceptual models concerned with accurately predicting contaminant transport should properly incorporate heterogeneity of the flow system if possible.

In the next set of Monte Carlo simulations, we attempt to ascertain the level of uncertainty involved in predictions for a more "active" flow regime. MC3 used the same conductivity fields as MC2. The only difference in the simulations were the boundary conditions on the flow system. The boundary conditions for MC3 are as follows: 15cm ponding from center of pile to 22m outward, prescribed pressure head of -100cm at surface of impoundment from 22m to the edge of the pile, and prescribed pressure head of -55cm at the base of the impoundment. Figure 3.72 shows the seepage statistics for MC3. Much more uncertainty is imparted to the seepage distribution under these boundary conditions than in MC2. The variation of seepage about the mean as defined by plus or minus one standard deviation is about 1 order of magnitude throughout most of the impoundment. For comparison to MC2, Figure 3.73 shows the mean and standard deviations of the pressure head field. Although the type of boundary conditions used in each set of simulations is different, it is still evident that the standard deviations in the pressure head field are greater in MC3 than MC2 because the hydraulic gradients are much greater and the flow regime is

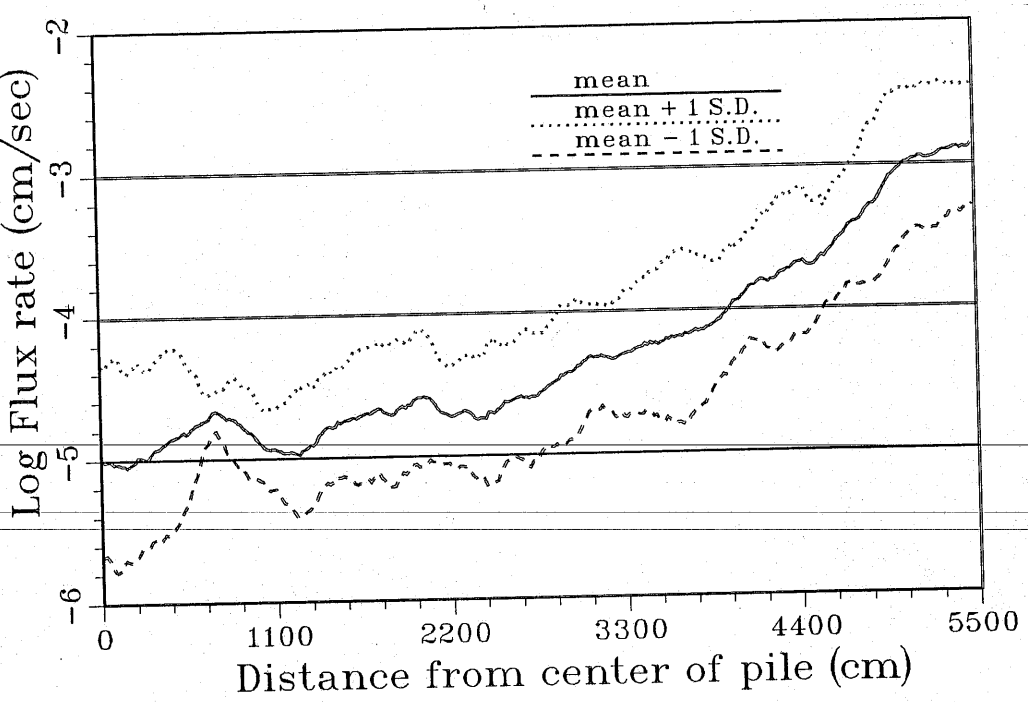

Figure 3.72. Seepage statistics from Monte Carlo simulation 3 (MC3).

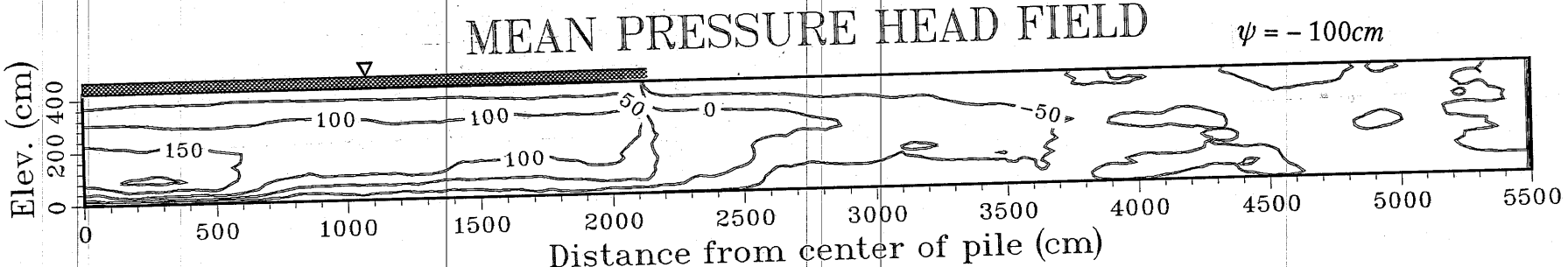

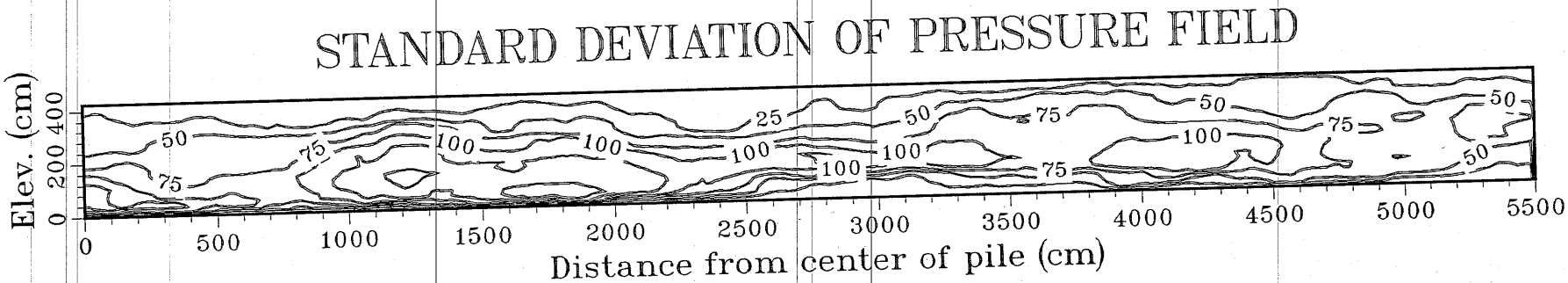

Figure 3.73(a,b). Mean and standard deviation of pressure head fields respectively from MC3.

more active, i.e. more fluid is being transmitted through the impoundment. This comparison exhibits how the activity of the flow regime can affect the uncertainty in model predictions. If hydraulic gradients are relatively large, uncertainty in the model prediction is greater then if the flow regime is "relaxed", i.e. when the hydraulic gradients are relatively low. This is intuitive if we consider the movement of a single fluid particle in a heterogeneous media. The fluid particle will always take the path of least resistance. However, given the same heterogeneous, multidimensional field, the fluid particle will show a much more random or uncertain behavior under higher hydraulic gradients than when exposed to lower hydraulic gradients. The more random movement of the fluid particles in heterogeneous fields leads to a higher uncertainty in the location of the particle at any time, given the uncertainty in the hydraulic property field.

MC4 was completed in order to compare the variation in seepage statistics from conductivity fields given "similar" correlation scales but different covariance structures. So that some comparison could be made between the seepage statistics from Monte Carlo simulations incorporating conductivity fields from different covariance structure, a "similar" correlation scale was calculated for the covariance structures shown in equations 3.15 and 3.16 using a conceptual scale known as the integral scale. The integral scale is defined as:

$$\lambda_i = \int_0^\infty \frac{C(\xi)}{C(0)} d\xi \qquad (3.17)$$

where $C(\xi)$ = covariance function as a function of ξ
$C(0)$ = variance of process
ξ = separation distance

The integral scale essentially defines the total area under the covariance structure from zero separation to infinite separation distance. It is simply one attempt to define the total "correlation" in the stochastic process over

the entire space where the process exhibits correlation. For an exponential covariance structure as shown in equation 3.15, the integral scale is simply given by the "correlation" scale β_x and β_z. For the double exponential structure in equation 3.16, the integral scale is $\frac{\beta\sqrt{\pi}}{2}$. The calculated integral scale for the exponential covariance is simply equal to the assumed "correlation scale" of 850 cm in the horizontal direction and 85cm in the vertical, while the integral scale for the double exponential covariance structure was 753cm and 75cm in the horizontal and vertical directions respectively. The variance of the conductivity fields was 0.50 as in MC3 and hydraulic anisotropy was 20.

Seepage statistics from MC4 are shown in Figure 3.74. One noticeable difference in the seepage statistics from MC4 and MC3 is the smoother distribution in the flux across the impoundment. This is a result of the smoother conductivity fields as depicted by the double exponential fields in Figure 3.58. Comparison of Figure 3.74 to 3.72 demonstrates the similarity in the seepage statistics from simulations incorporating different types of covariance structure but equivalent integral scales. Although the values are not presented here, the total seepage from the impoundment as depicted by the mean seepage rate is approximately 2 times greater for MC4 than in MC3. The standard deviation of the hydraulic head field shown in Figure 3.75b exhibits relatively the same spatial variation as does the standard deviation in the pressure head field from MC3 shown in Figure 3.73b. The standard deviations of the saturation field shown in Figure 3.76b are larger than those of MC1 and MC2 shown in Figures 3.67b and 3.68b respectively due to the higher hydraulic gradients. Figure 3.77 displays four realizations of velocity vector fields from MC4 showing the variation in velocity vectors throughout the impoundment for different realizations of hydraulic conductivity fields.

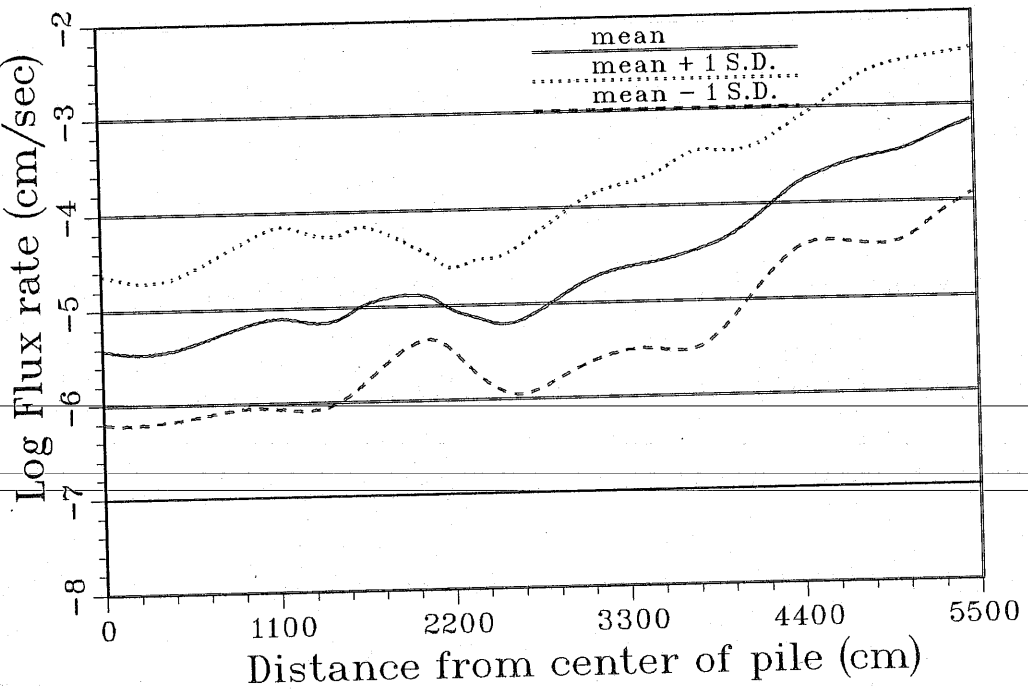

Figure 3.74. Seepage statistics from Monte Carlo simulation 4 (MC4).

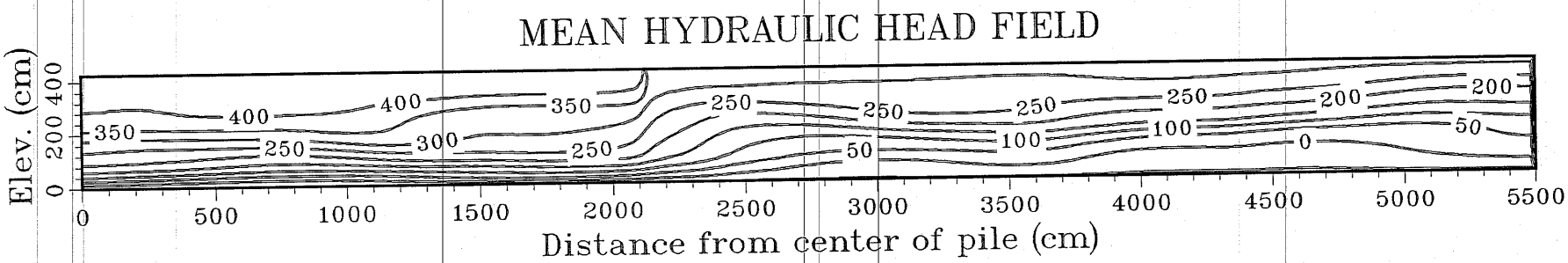

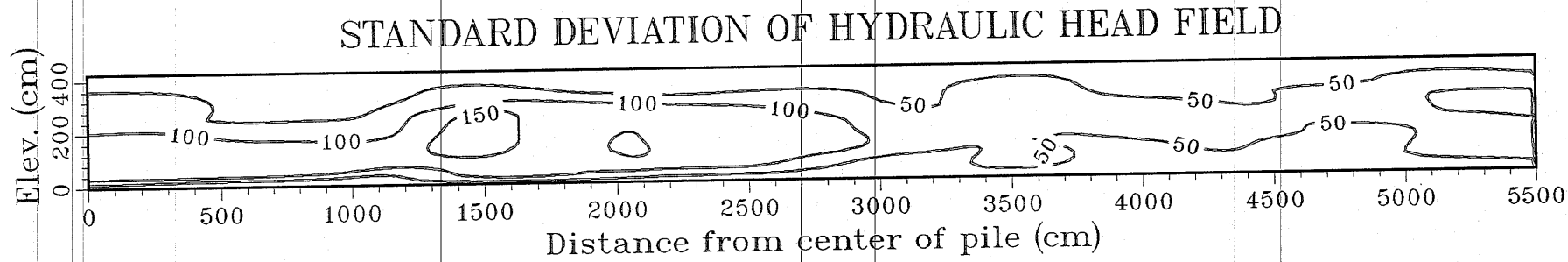

Figure 3.75(a,b). Mean and standard deviation of hydraulic head fields respectively from MC4.

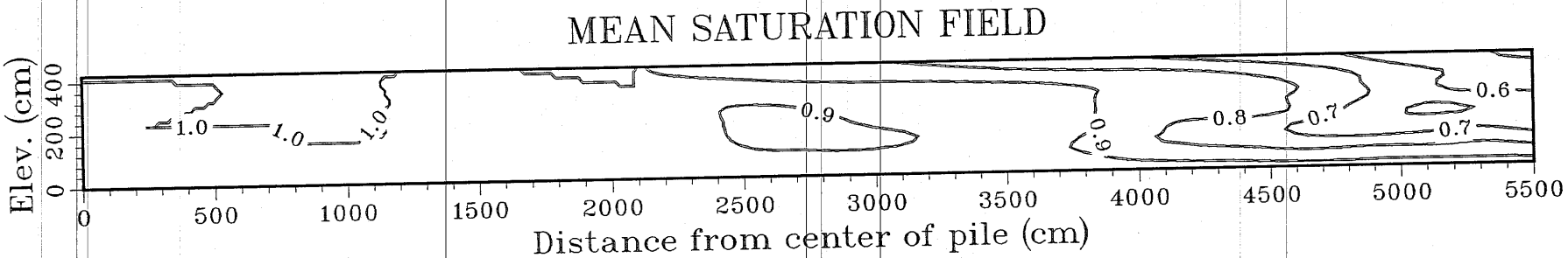

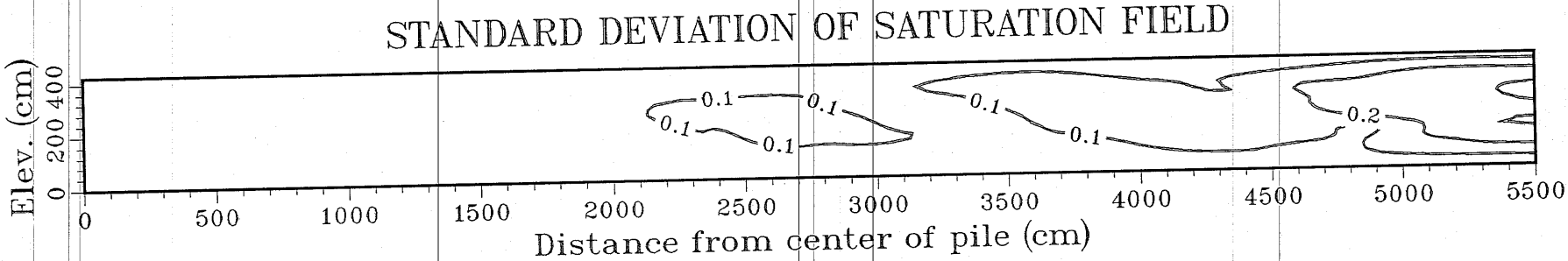

Figure 3.76(a,b). Mean and standard deviation of saturation fields respectively from MC4.

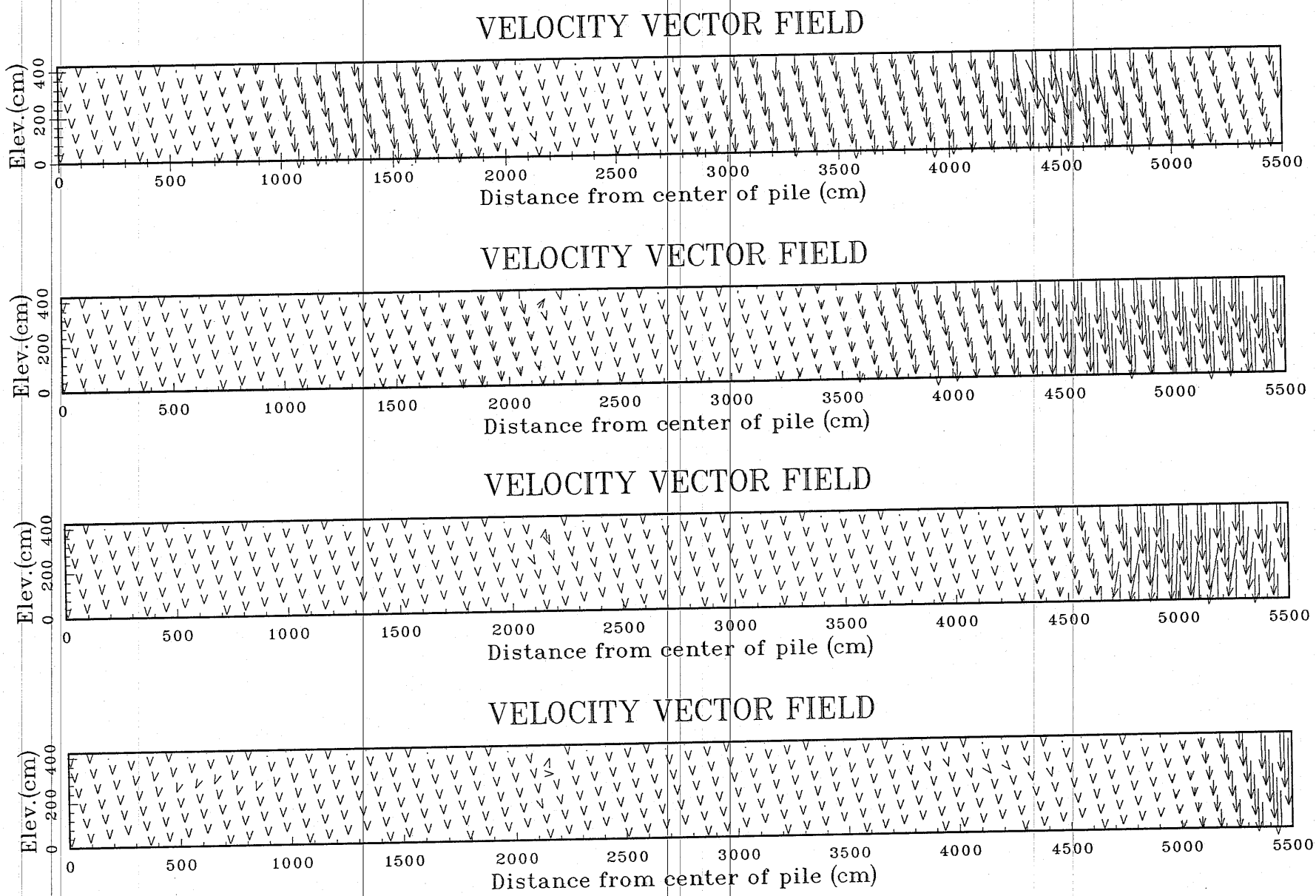

Figure 3.77(a,b,c,d). Four realizations of velocity vector fields generated in MC4.

The final Monte Carlo simulation (MC5) was performed in order to compare the results of the unconditional simulation approach used here to those from the conditional simulation approach to be discussed in the next section. In order to determine the ability of conditioning to decrease the variance in the model output, a comparison will be made between MC5 and conditional simulation #1 (CS1) in the next section of this paper. The same boundary conditions were used for MC5 as was used for MC4. The variance of the conductivity fields is 0.50, and correlation scale in horizontal and vertical directions are 1700cm and 170cm respectively. Three realizations of the log conductivity fields used in MC5 are shown in Figure 3.78. A more extensive "layering effect" is evident in these conductivity fields due to the larger correlation distances in the horizontal direction. A hydraulic anisotropy of 20, ($K_x/K_z = 20$, for each finite element) was also incorporated in MC5.

Seepage statistics from MC5 are shown in Figure 3.79. Comparison of Figures 3.72 (MC3) and 3.79 shows the large difference in mean seepage rates produced from conductivity fields which exhibit the same variance but different correlation scales. As shown in Table 3.5, the horizontal and vertical correlation scales for MC3 were 850cm and 85cm respectively. The increase in horizontal correlation scale for MC5 significantly decreases the total seepage from the impoundment due to the increased layering imparted by the larger correlation scales. The larger correlation scales increase the probability that fluid particles will encounter low conductivity while traveling downward under essentially vertical hydraulic gradients. Since the "layers" exhibit substantial lateral extent, it is more likely that relatively low conductivity zones are present at different depths throughout the entire impoundment. Therefore, the harmonic mean of the conductivity in the vertical direction is significantly decreased, leading to significant lateral flow components within the impoundment as shown in the four

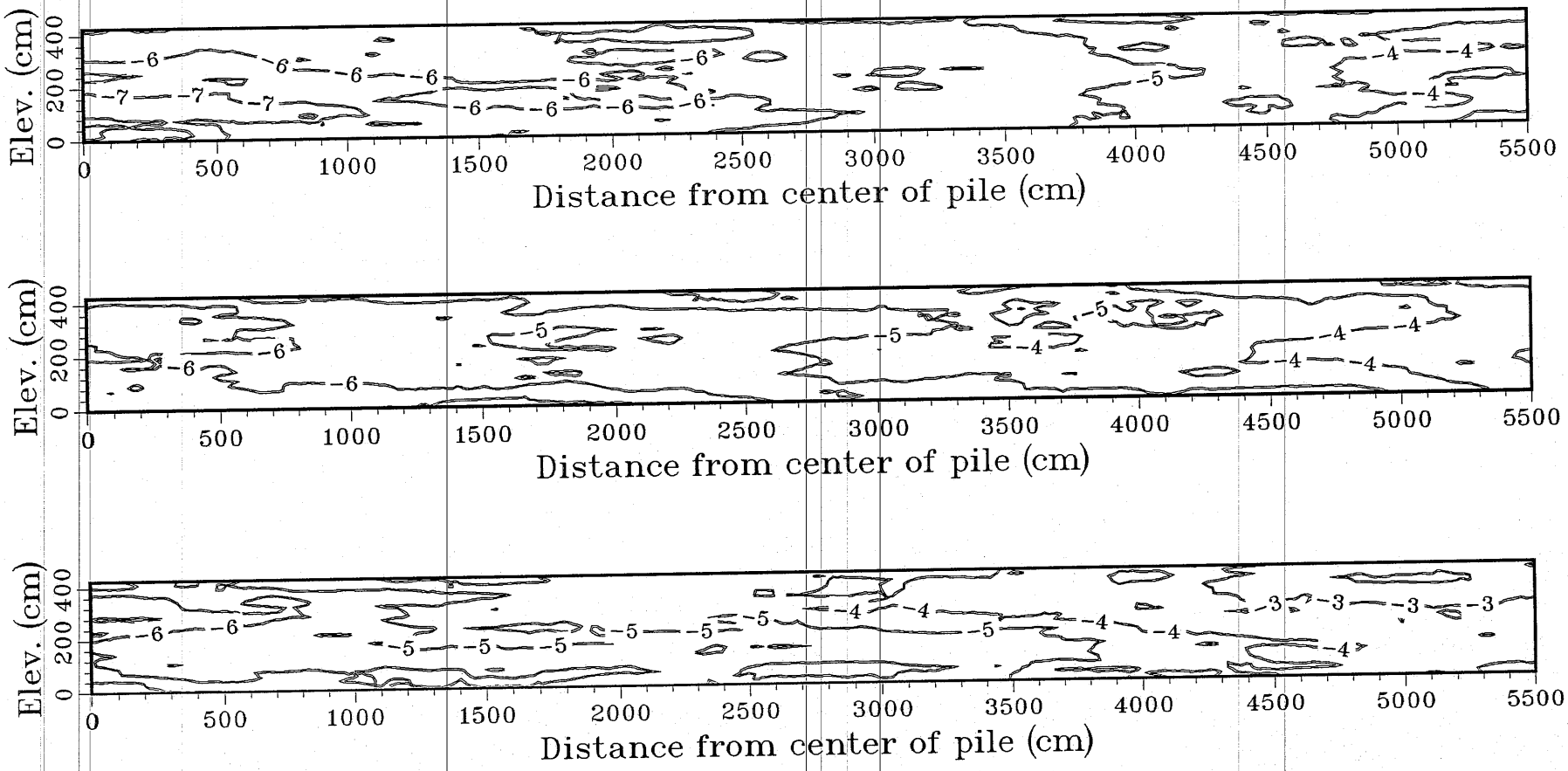

Figure 3.78(a,b,c). Three replicates of log saturated hydraulic conductivity used in MC5.

realizations of velocity vector fields shown in Figure 3.80. Note the horizontal variation in velocity vectors from the exponential fields as shown in Figure 3.80 is much larger than that produced from the double exponential fields shown in Figure 3.77. Although the correlation scale is greater in MC5, the cause of the lateral variability lies mainly in the type of covariance structure implemented. The exponential fields show much greater conductivity variation over small distances, leading to significant horizontal fluid movement. These results suggest the importance of properly defining the type of structure present in the conductivity fields when predicting transport of contaminants in heterogeneous media. It may be misleading to compare the seepage statistics and assume that both correlation structures would give equivalent results for transport statistics, ie. travel times or contaminant concentrations in pumping wells. Figure 3.80 also displays the large variation in velocity fields from the unconditional simulations. This is further exemplified in Figure 3.81a and 3.81b which show the mean and standard deviation of the velocity vector fields respectively. Figure 3.81b show the magnitude and direction of the standard deviation of the vector components in the horizontal and vertical directions. Figure 3.82 graphically describes this representation. The representation is analogous to plotting the velocity vector components, except of course that the standard deviation always show a positive orientation in both directions. The vectors in each plot are normalized to the largest vector in the domain. The variance of the velocity vectors is much greater in the outer portion of the impoundment since the magnitude of the vector components is much greater. The directional components of the velocity vectors show substantially more variance in the lateral direction than in the vertical direction throughout most of the impoundment.

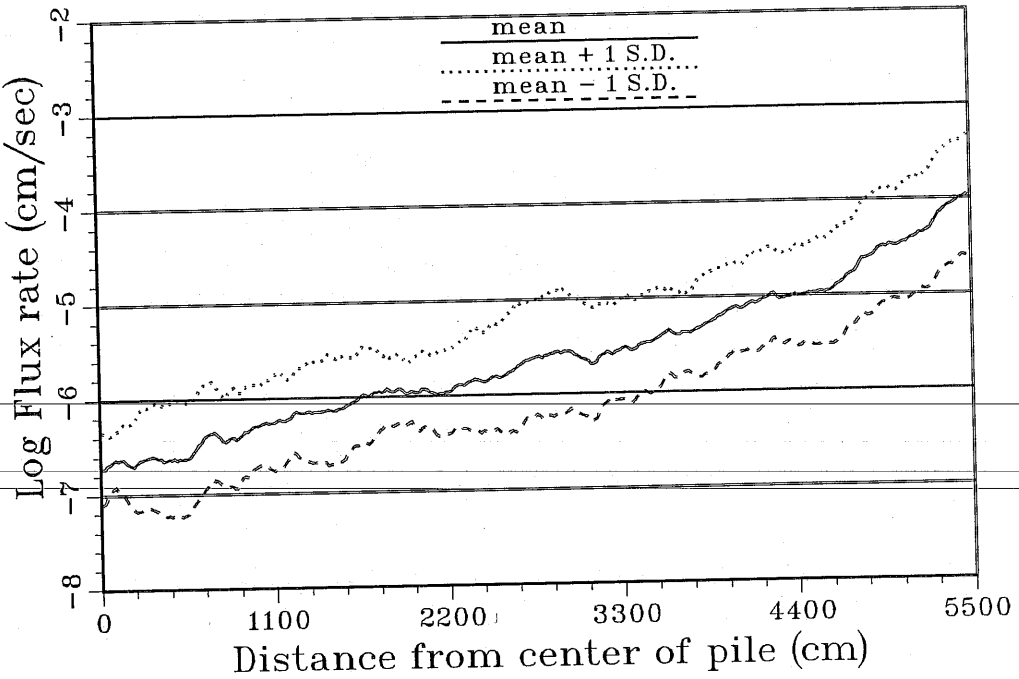

Figure 3.79. Seepage statistics from Monte Carlo simulation 5 (MC5).

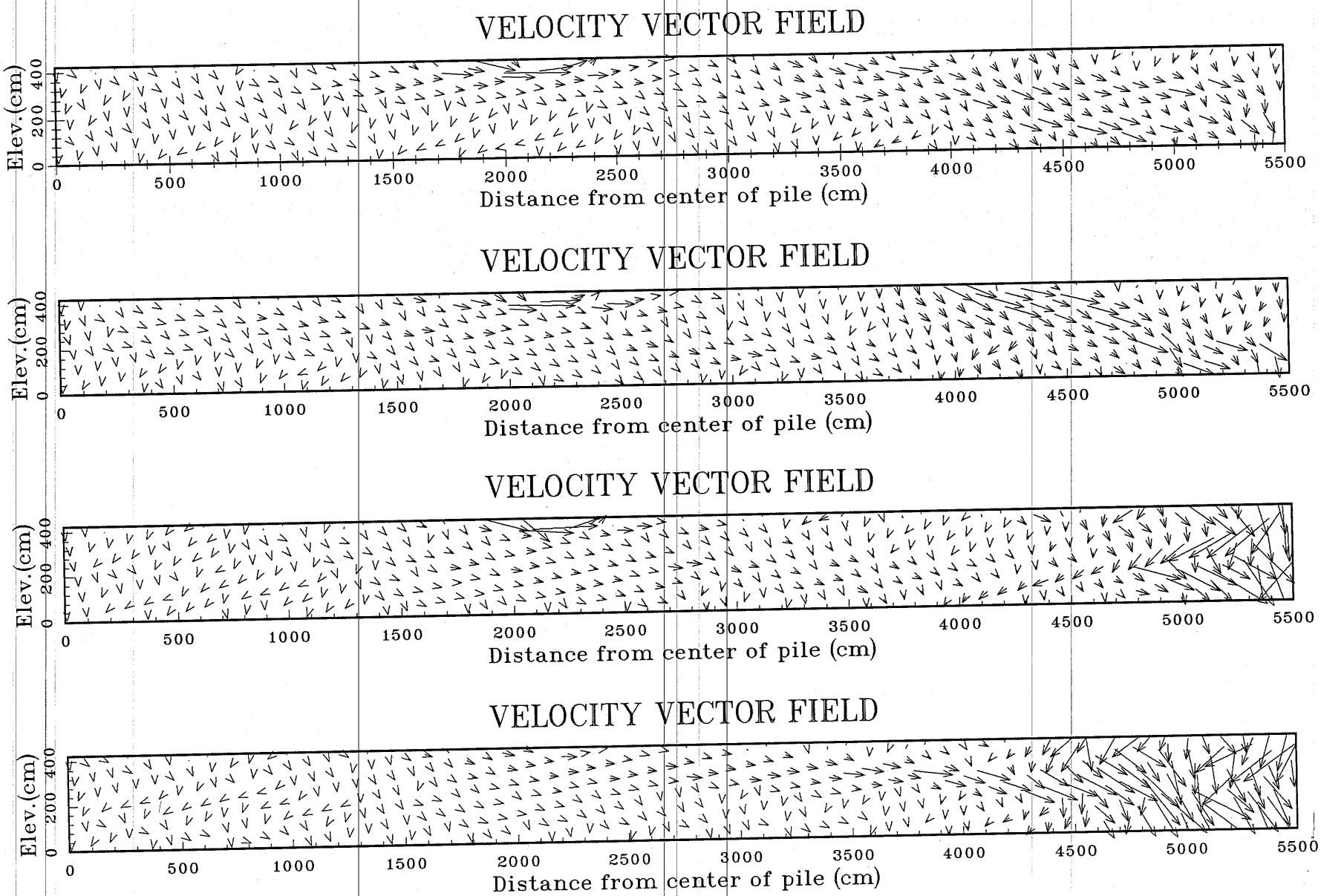

Figure 3.80(a,b,c,d). Four realizations of velocity vector fields generated in MC5.

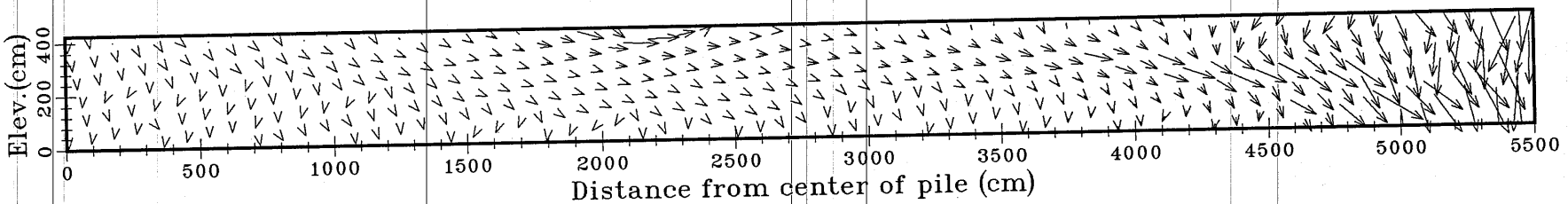

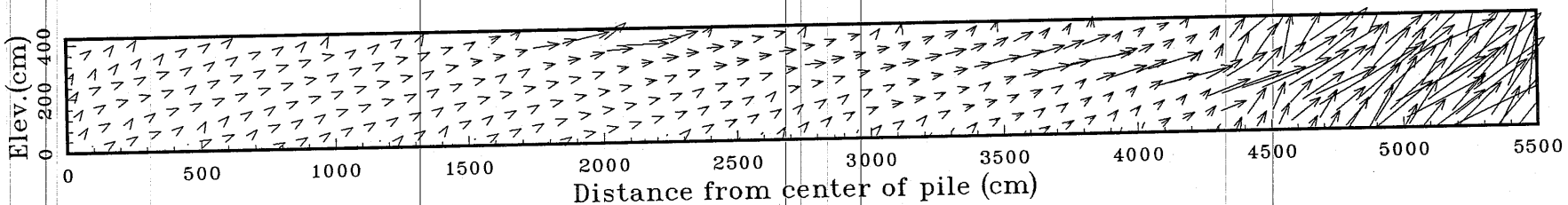

Figure 3.81(a,b). Mean and standard deviation of velocity vector fields respectively from MC5.

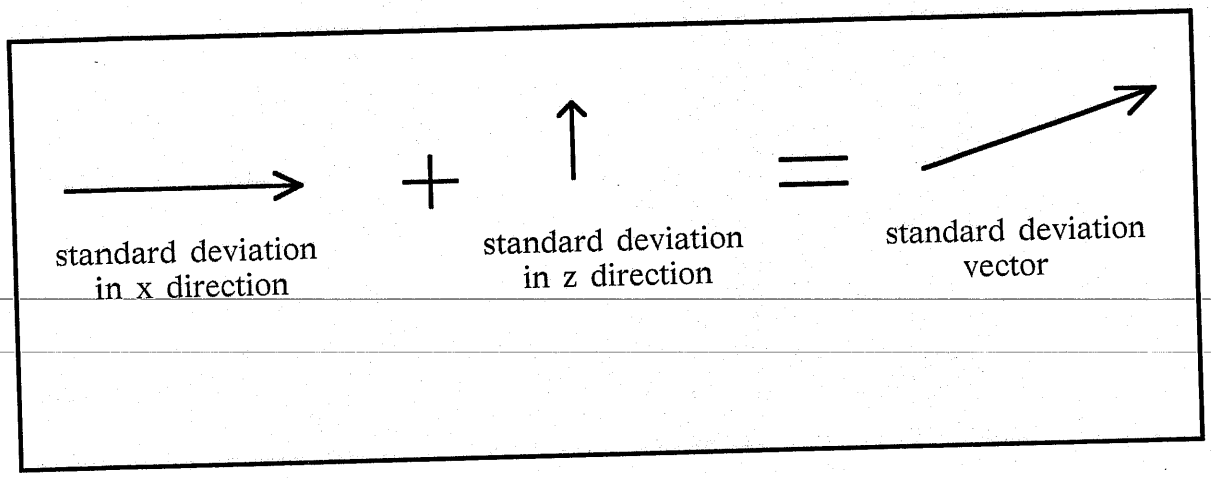

Figure 3.82. Graphical explanation of velocity vector standard deviation plot.

The variance in lateral flow components is an issue of utmost importance when modeling uncertainty of contaminant transport in the variably saturated flow systems. The mean vector field shown in Figure 3.81a displays the extensive lateral flow components present in the impoundment under the proposed scenario of hydraulic property heterogeneity.

The mean hydraulic head field (Figure 3.83a) is very similar to the hydraulic head field produced in the deterministic simulation performed previously (Figure 3.24b), generated under the same boundary conditions. The same is true of the pressure head and saturation fields (Figure 3.84a and 3.85a) when compared to Figures 3.24a and 3.24d. This similarity is partially due to the prescribed pressure head boundary conditions imparted on the domain. However, the standard deviations of the head fields shown in Figures 3.83b and 3.84b show the variability which can occur for different realizations of the conductivity field. The standard deviations of the saturation field shown in Figure 3.85b displays very substantial deviations if we consider the importance of the predicted saturation field in correctly modeling transport of contaminants in

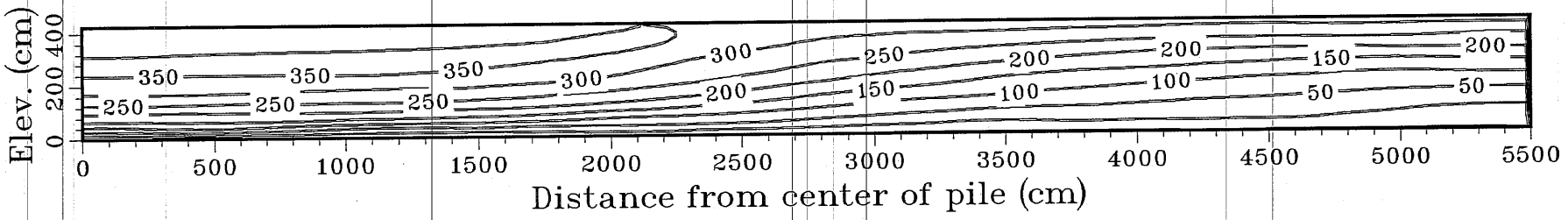

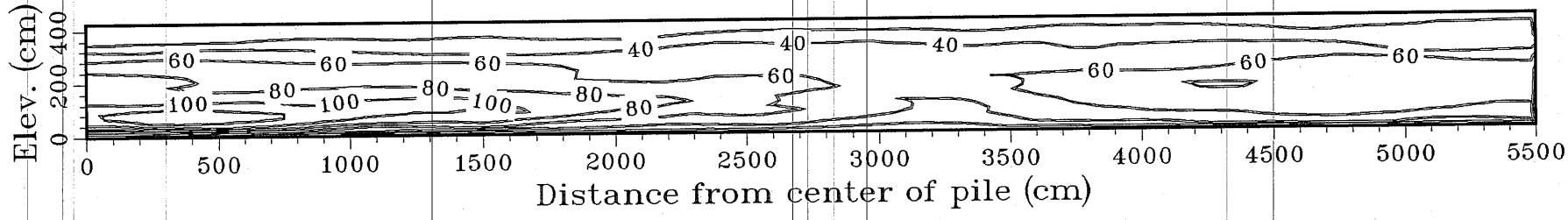

Figure 3.83(a,b). Mean and standard deviation of hydraulic head fields respectively from MC5.

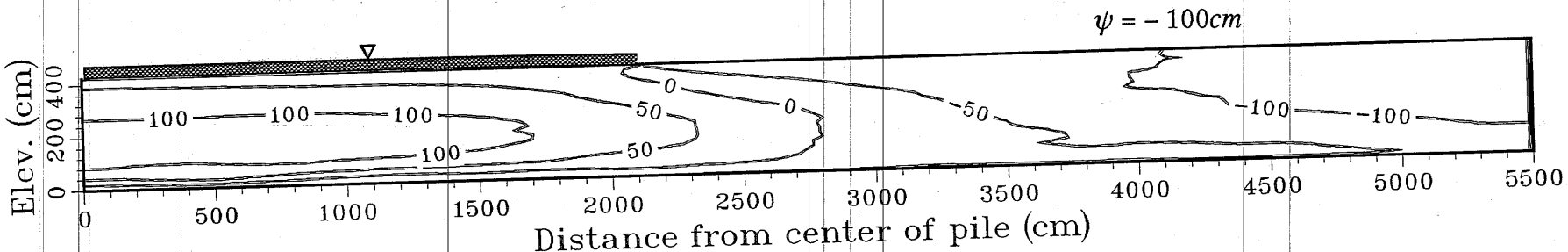

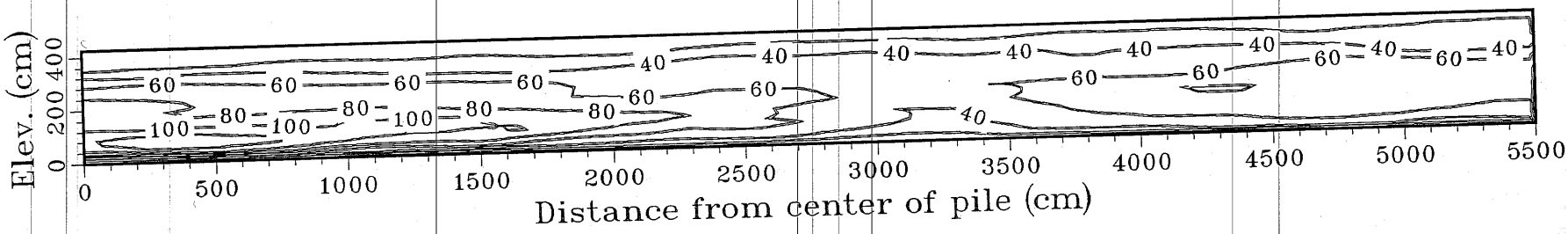

Figure 3.84(a,b). Mean and standard deviation of pressure head fields respectively from MC5.

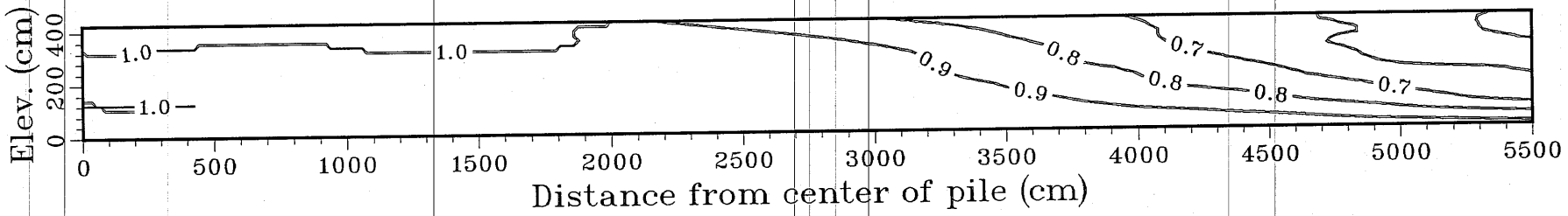

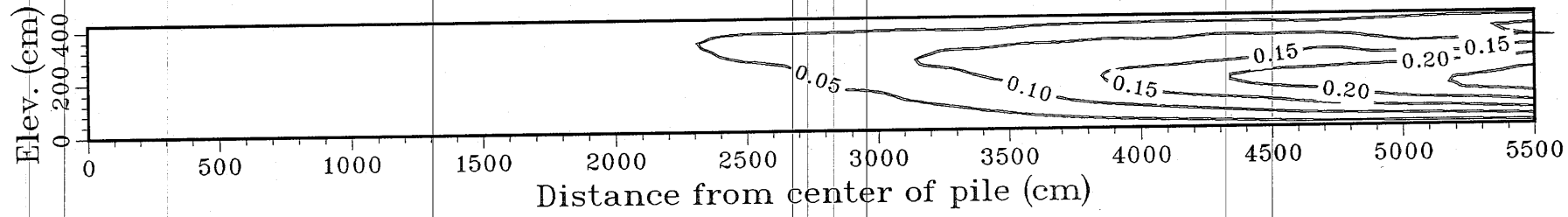

Figure 3.85(a,b). Mean and standard deviation of saturation fields respectively from MC5.

the vadose zone using an equation such as,

$$\frac{\partial}{\partial x_i}\left(D_{ij}\frac{\partial c}{\partial x_j}\right) - \frac{\partial}{\partial x_i}(v_i c) = \frac{\partial}{\partial t}[\phi S_w c + \varrho_s(1-\phi)c_s] - qc^* + \lambda[\phi S_w c + \varrho_s(1-\phi)c_s] \qquad (3.18)$$

where
D_{ij} = the hydrodynamic dispersion tensor, $[L^2/T]$
c = solute concentration in solution, $[M/L^3]$
c^* = solute concentration of input fluid, $[M/L^3]$
c_s = adsorbed concentration, $[M/L^3]$
v_i = darcy velocity, $[L/T]$
S_w = water phase saturation, $[L^3/L^3]$
ϱ_s = density of solid particles, $[M/L^3]$
ϕ = porosity, $[L^3/L^3]$
q = volumetric flow rate via source and sinks per unit volume porous media, $[L^3/L^3T]$

Nielsen and Biggar [1961] show evidence that dispersion may be related to the degree of saturation in a porous media. The retardation of contaminants is also greatly affected by the degree of saturation. These facts reemphasize the importance of properly determining the saturation and velocity fields when predicting transport and fate of contaminants in the vadose zone.

The results of one realization from MC5 are shown in Figure 3.86a,b,c,d. The velocity vector field shows the variability that can occur in the field and the significant lateral flow which can occur even if the hydraulic head field is oriented essentially vertically downward.

The unconditional stochastic–deterministic simulations have shown that considering uncertainty in hydraulic properties may be important in properly identifying fluid movement and thus contaminant transport in variably saturated media if some quantitative confidence intervals are to be placed on the prediction. Under some boundary conditions present in the field, such as moisture movement in the deep vadose zone, it was shown that uncertainty in the

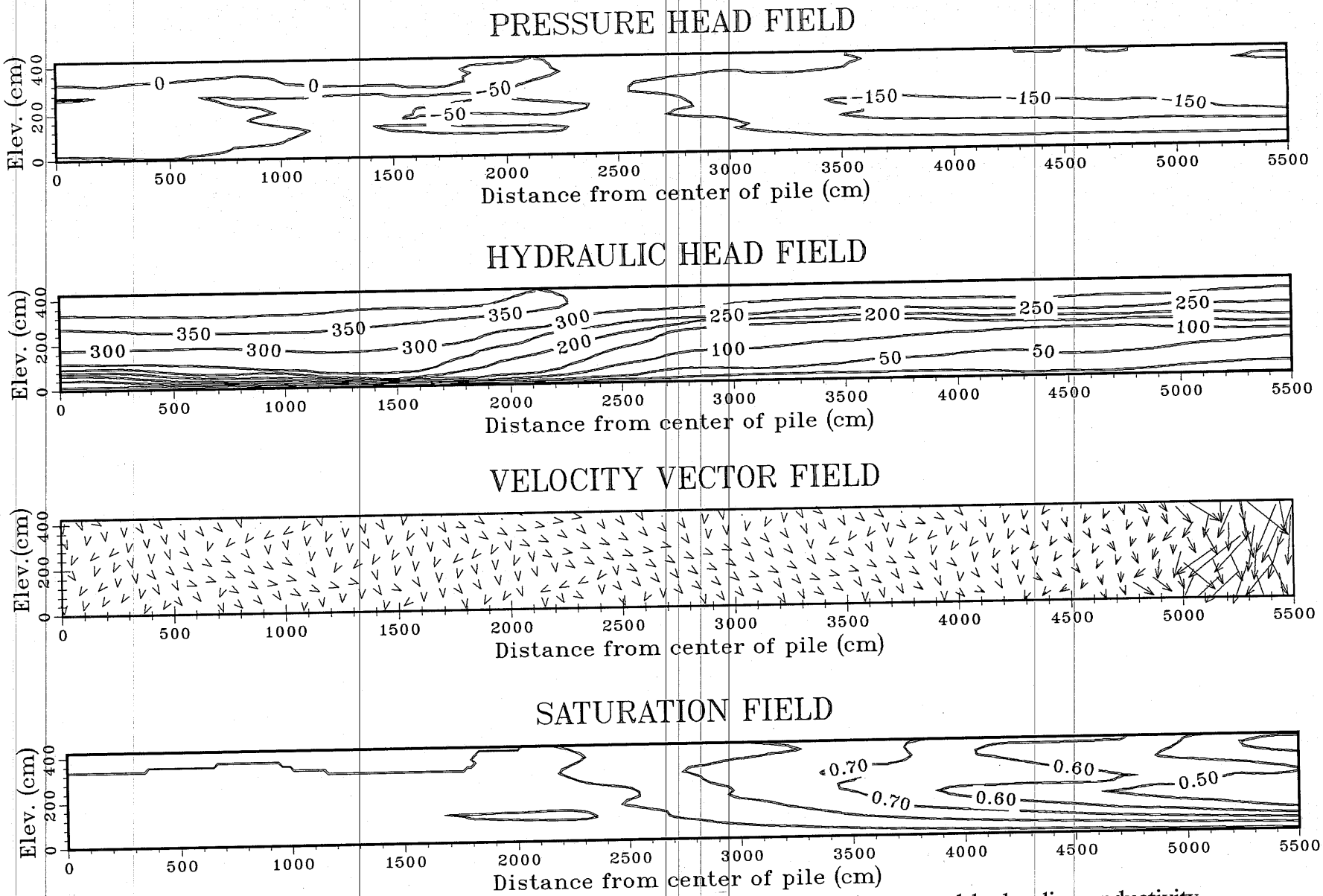

Figure 3.86(a,b,c,d). Steady-state results from one stochastic realization of saturated hydraulic conductivity from MC5.

hydraulic properties may not be the most important variable to characterize. It was also shown that fluid particle direction is strongly dependent upon the correlation scale of the heterogeneous media under ponding conditions. Incorporation of anisotropy into the conductivity tensor for each finite element did not increase horizontal flow in the same manner as it did in the smoother fields used in the deterministic simulations. The location of extreme conductivity zones in the horizontal direction seemed to be the dominant factor in determining fluid movement in the heterogeneous media. In the next section, a geostatistical technique is used in an effort to reduce the model output variance by incorporating conductivity measurements observed in the field.

CONDITIONAL SIMULATION APPROACH

The stochastic–deterministic approach taken in the previous section allows examination of the variability in model output based given uncertainty in the input parameters. However, unconditional stochastic fields generated by the FFT method retain only the proper statistics and covariance structure in a given field but do not account for "measured" or known data in the field. It is more realistic to incorporate our knowledge of the hydraulic properties at the locations where they have been measured. In conditional simulations, as with stochastic–deterministic simulations, the correct statistical properties and covariance structure are retained in the predicted hydraulic property fields. As the name implies however, one added feature of the technique is the "conditioning" of the predicted fields on the "known" data in the domain. If the value of the prescribed variable is known at a certain point in the domain, the conditioned field will maintain the value of the variable at that location while predicting the values of the variable at other locations according to the covariance structure of the statistical model. This procedure ultimately decreases the variance in the input parameters and consequently the model output variance. The next section contains a more complete description of the techniques used to condition the hydraulic property data.

Introduction to Conditional Simulations

One of the most common techniques used for conditioning a field of predictions on a particular data set incorporates a geostatistical approach known as kriging. *Journel [1974]* used this technique and applied it to various fields including mining, meteorology, and hydrogeology. He pointed out that conditional simulations require: (1) each conditional path should meet a

particular spatial autocorrelation function which characterizes the reality observed in the experimental values; and (2) the simulated values at data locations equal the experimental values. *Delhomme [1979]* further employs this method of conditioning in order to characterize the uncertainty of head measurements based on uncertainty of groundwater flow parameters such as transmissivity. He used the geostatistical conditioning technique in conjunction with flow modeling to characterize uncertainty in the output from the flow model. *Smith and Schwartz [1981c]* use conditioned hydraulic property fields in an effort to cut the variation in travel times of particles. *Dagan [1982]* outlines the application of this conditioning method to field problems. This method relies on the incorporation of statistical information of the known data set such as mean, variance, covariance structure, and the known data values at certain locations in the domain. This geostatistical approach to conditioning can be used to produce numerous "conditioned" paths or fields which can be used in Monte Carlo studies to incorporate the uncertainty in the predicted fields but still honor the data values at measurement locations.

Description of method used to produce conditioned hydraulic property fields

Assume that experimental data has been gathered in a field setting. Even though this conditional simulation approach can be easily applied to three-dimensional space, assume for simplicity the data is gathered in a vertical two-dimensional plane. Let $\overline{V}(\vec{x})$ represent the measured or experimental values in the domain at a given location x and z. If variogram analysis provides information about the correlation scale and covariance structure of the physical system, it is possible to use kriging as a best linear unbiased estimator (BLUE) to make predictions in the neighborhood of the measurement values based on the estimated covariance structure described by the statistics of the physical system.

[see *Journel and Huijbregts (1978)*, *Delhomme (1978)*, *Gutjahr (1985)*, and *de Marsily (1986)*] The following steps could then be taken in order to produce fields conditioned on the experimental data.

1. Krige the experimental field according to the covariance structure and statistics determined from the experimental data. Kriging predictions are made at any location where a conditioned prediction is needed. This field will be referred to as $V^*(\vec{x})$.

2. Generate stochastic nonconditional simulations or fields $W(\vec{x})$ which maintain the proper statistics and covariance structure that has been inferred from the original experimental data. For this study, a Fast Fourier Transform (FFT) method was used because an algorithm (FFT2D) was readily available to generate stochastic fields. The FFT method also insures statistical consistency between the unconditioned stochastic fields and the conditioned fields.

3. Sample the stochastic nonconditional field $\overline{W}(\vec{x})$ at the same locations as the experimental field. These values are also kriged according to the same covariance structure and statistics determined from the experimental data to produce a field $W^*(\vec{x})$. Once again, kriging predictions are made at every location in the domain where a "conditioned" value is needed.

The conditioned path or field $V_{cs}(\vec{x})$ is then given by

$$V_{cs}(\vec{x}) = V^*(\vec{x}) + [W(\vec{x}) - W^*(\vec{x})] \tag{3.19}$$

It can be shown that the $V_{cs}(\vec{x})$ does retain the value of the original experimental value since kriging is an exact interpolator. Also, the average of numerous conditional simulations at a certain location is equal to the kriging estimate at that location and the variance of the values are equal to the kriging variance

[Delhomme, 1979]. The variance of the values at any location thus represents the uncertainty in the prediction at those points. Thus, the prediction variance at the measurement points is zero, but increases with distance from the point of measurement. The hydraulic conductivity fields which result from the conditioning process are also smoothed due to the smoothing nature of the kriging equations. Once again, this is an added advantage when solving the nonlinear systems of equations which result from implementation of the finite element scheme in unsaturated media.

I developed a FORTRAN program called CONDITION.FOR to carry out this conditioning procedure. A listing of the code is given in Appendix B. The code performs kriging and other automated tasks to make the conditioning process as easy as possible for the user.

Description of Simulations Performed Using Conditioned Fields

We have discussed the validity of incorporating a stochastic conceptualization to quantify the spatial variability in mill tailings hydraulic properties. If we assume the stochastic conceptualization is correct, the process of conditioning the data fields only requires that we assume we can correctly determine the values of the hydraulic properties at certain points in the domain. Any mindful scientist knows that there is some measurement error associated with the field data, but we generally make the assumption that these data values are "exact", even though it is possible to incorporate the measurement error and source of uncertainty in the stochastic model. In this study, the distribution of saturated hydraulic conductivity is considered a stochastic process of given covariance structure, therefore conditioning was performed using the saturated hydraulic conductivity measurements taken from *Johnson [1987]*.

Johnson [1987] gives numerous measurements of saturated hydraulic conductivity but concludes that no spatial correlation is evident in the data. In order to access the ability of conditioning to reduce the variance in model output, for instance, seepage at the base of the impoundment, hypothetical fields of a given covariance structure and statistics were synthetically produced. The sample locations used for the "conditioning" points were obtained from the actual data gathered in the field by Johnson. The samples used in the conditioning procedure were picked so that a minimum number of observations would maximize uncertainty reduction in the output. This was accomplished by spacing the "conditioning" points at locations where the assumed covariance structure would have a significant effect on the synthetically produced measurements at locations between the "measured" values. Figure 3.87 shows the locations of the 56 samples that were taken as "conditioning" points. I should note at this time that the actual data (taken from *Johnson [1987]*) used as the "conditioning" points did not neccesarily exhibit the same covariance structure as that assumed for the synthetically produced random fields. However, this fact does not invalidate the conditioning approach, since the sampled data could have just as easily been sampled from one of many random fields produced with the assumed covariance structure.

An anisotropy ratio of 10 was chosen for the horizontal to vertical "correlation scales". The "correlation" in the horizontal and vertical directions is 1700cm and 170cm respectively. Of course, these values are only parameters in the covariance structure, but the term correlation scale is used for lack of a better expression. These correlation scales may be too large for many systems, including mill tailings impoundments. However, the main purpose of this exercise is to determine the usefulness of conditioning hydraulic property fields for Monte Carlo studies where the hydraulic properties are correlated over

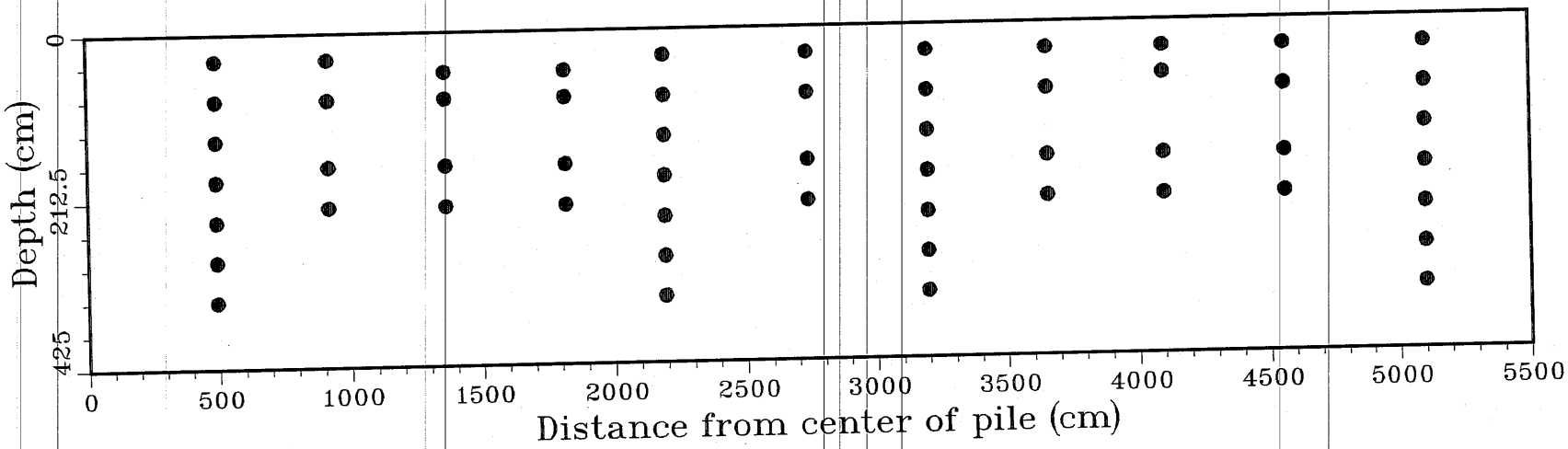

Vertical Exaggeration = 3x

Figure 3.87. Cross-section of impoundment showing locations of "conditioning" sample locations used in conditional simulation 1 (CS1).

significant distances, therefore, these relatively large correlation scales are used in the conditional simulations.

Discussion of Model Output Statistics from Conditional Simulations

In order to compare the effectiveness of conditioning in reducing uncertainty in model output, conditional simulations were performed which incorporated the same boundary conditions as did previous unconditional simulations. The set of boundary conditions chosen were those used in DS1 because they imparted significant uncertainty in the unconditional simulations. Even though these boundary conditions may not be the most realistic used in the previous simulations, they were chosen because a reduction in model output variance would be most noticeable under the prescribed boundary conditions. The hydraulic properties used in the conditional simulations were identical to those used in Monte Carlo simulation #5 (MC5) with the exception that the saturated hydraulic conductivities were conditioned through the procedure discussed in the previous section. As stated earlier, a full Monte Carlo approach was not feasible for this study due to the computer intensive nature of the unsaturated flow scenario. Therefore, as with the stochastic–deterministic simulations, only 10 conditional simulations were performed in order to gain insight into the model output statistics.

Figure 3.88 shows the seepage statistics at the base of the impoundment for the conditional simulations. The graph shows the distribution of the mean seepage rate from the simulations and the variation about the mean described by plus or minus one standard deviation. Comparison of Figure 3.88 with Figure 3.79 shows the considerable decrease in variance about the mean seepage rate in the conditional simulations as compared to the unconditional simulations from MC5. The reduction in the variance of the seepage rates is

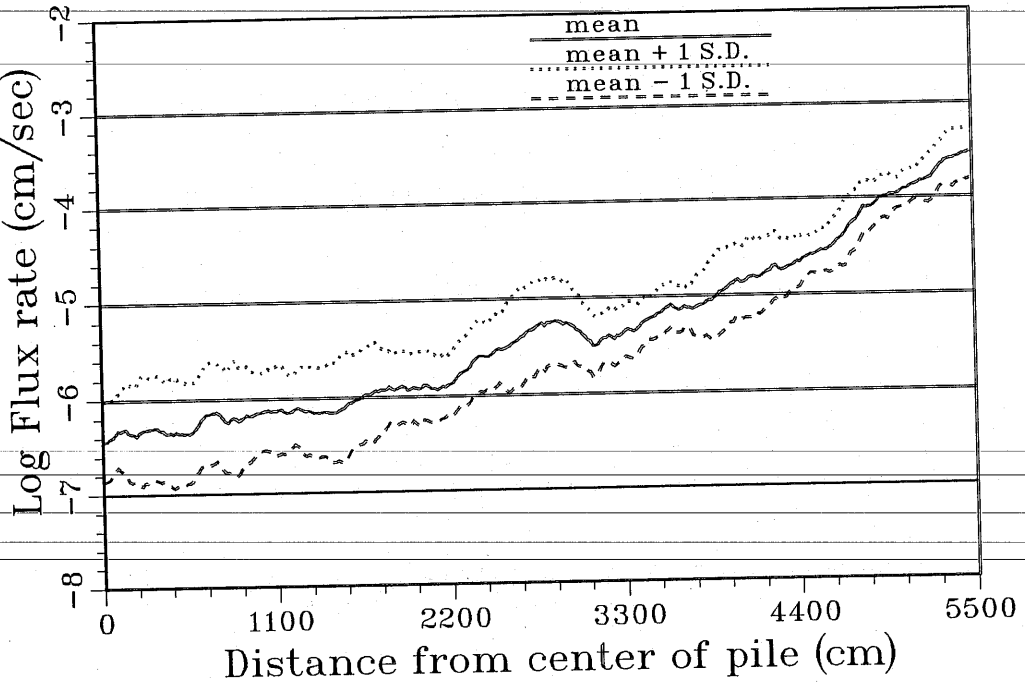

Figure 3.88. Seepage statistics from conditional simulation 1 (CS1).

clearly the result of decreasing the variance in the saturated hydraulic conductivity field. Figure 3.89a,b,c,d shows four realizations of the conditional simulation velocity fields. The large variation in the velocity vectors throughout the impoundment is still evident. Figure 3.90a shows the that the mean velocity vector field is similar to mean velocity vector field from the unconditional simulations. However, comparison of Figure 3.90b and Figure 3.81b demonstrates that the conditioned fields from CS1 show a smaller overall variance in the velocity magnitudes than those of MC5 as depicted by the shorter "variance" vectors. This reduction in variation is more notable for the vertical component of seepage. The reduction in the vertical velocity uncertainty is a function of the locations of the conditioning points in the domain. Since the conditioning points are spaced relatively close in the vertical, the conditioning procedure reduces the uncertainty in the conductivity prediction more effectively in the vertical then in the horizontal. The "harmonic mean" of the conductivity in the vertical direction is very similar in all of the replicates of the conductivity fields used in the conditional simulations, therefore the variation in vertical seepage components is reduced. Figure 3.91 displays the mean and standard deviations of the hydraulic head from the conditional simulations. Once again, on comparison to Figure 3.83, the mean fields of the unconditional and conditional simulations appear much the same but the variation in hydraulic head described by the standard deviation field is lower for the conditional simulation results. The mean pressure head field shown in Figure 3.92a is also much the same as for the unconditional simulation results shown in Figure 3.84a. One very important implication of the conditioning procedure is exhibited in Figure 3.93a,b. The figure displays the mean and standard deviation fields for saturation from the conditional simulations. Comparison to Figure 3.85b shows a significant decrease in the saturation variance when the saturated conductivity

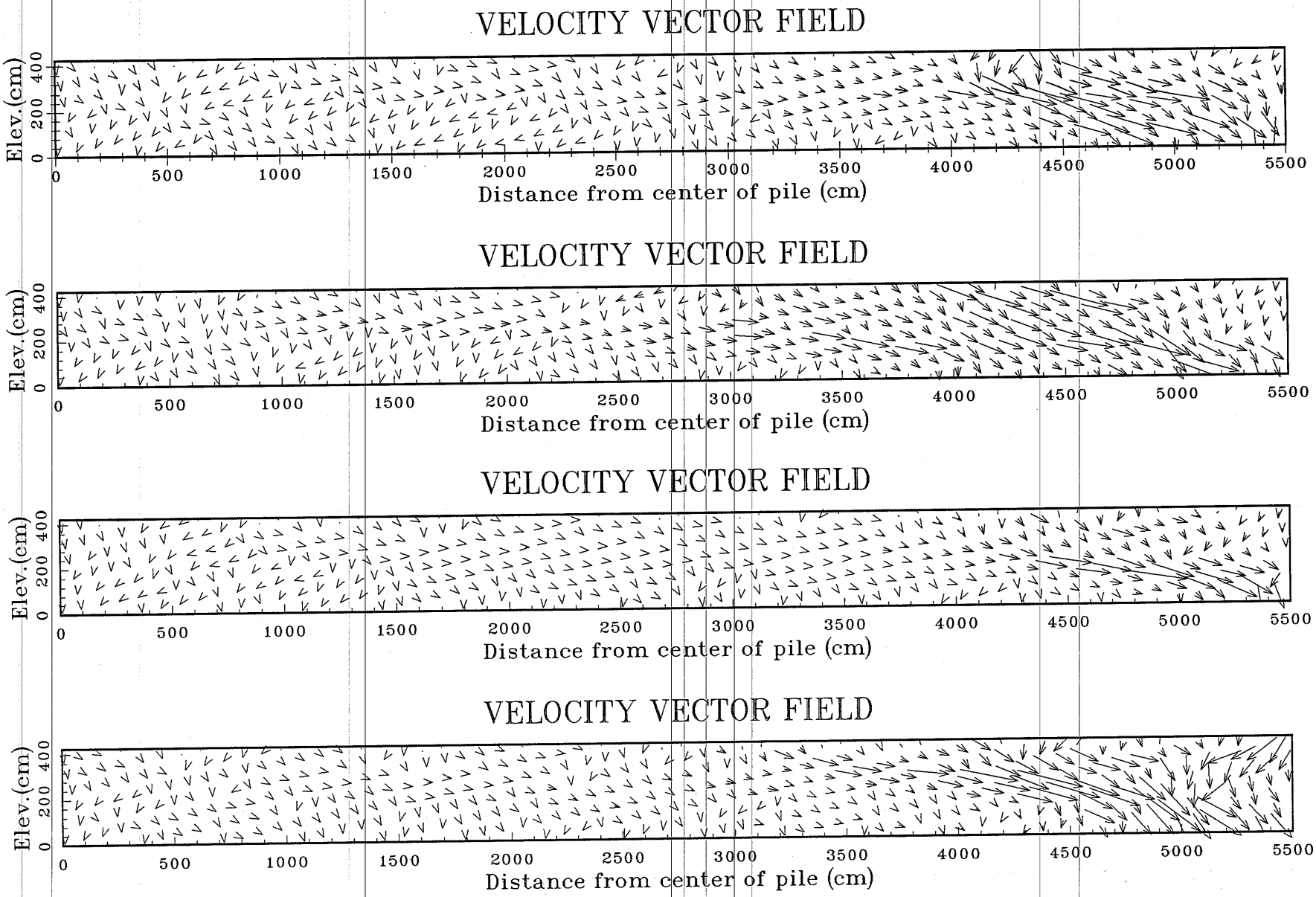

Figure 3.89(a,b,c,d). Four realizations of velocity vector fields generated in CS1.

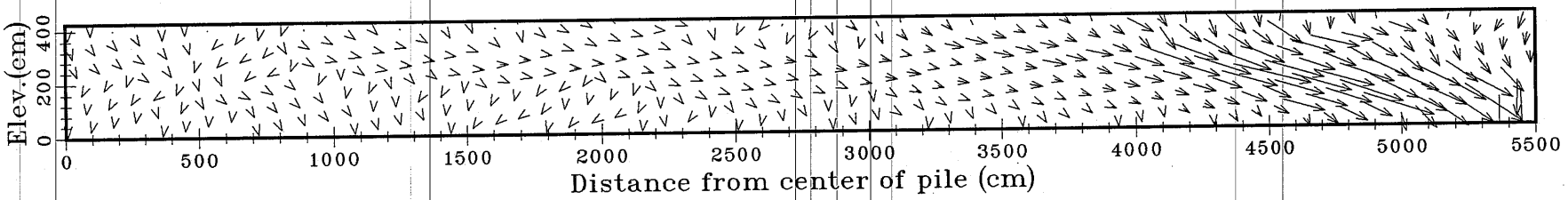

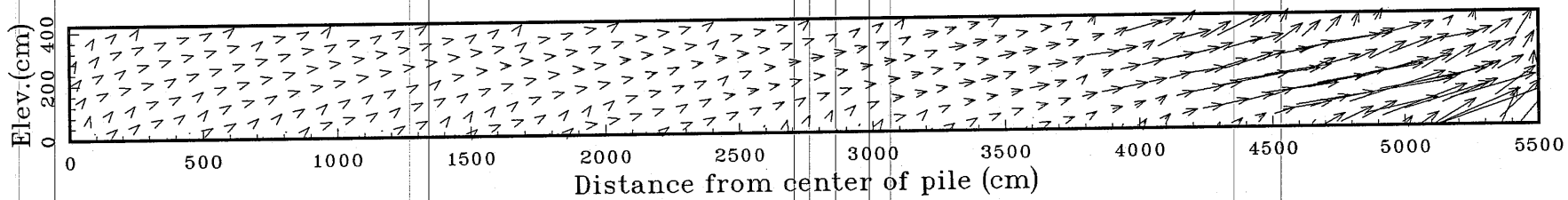

Figure 3.90(a,b). Mean and standard deviation of velocity vector fields respectively from CS1.

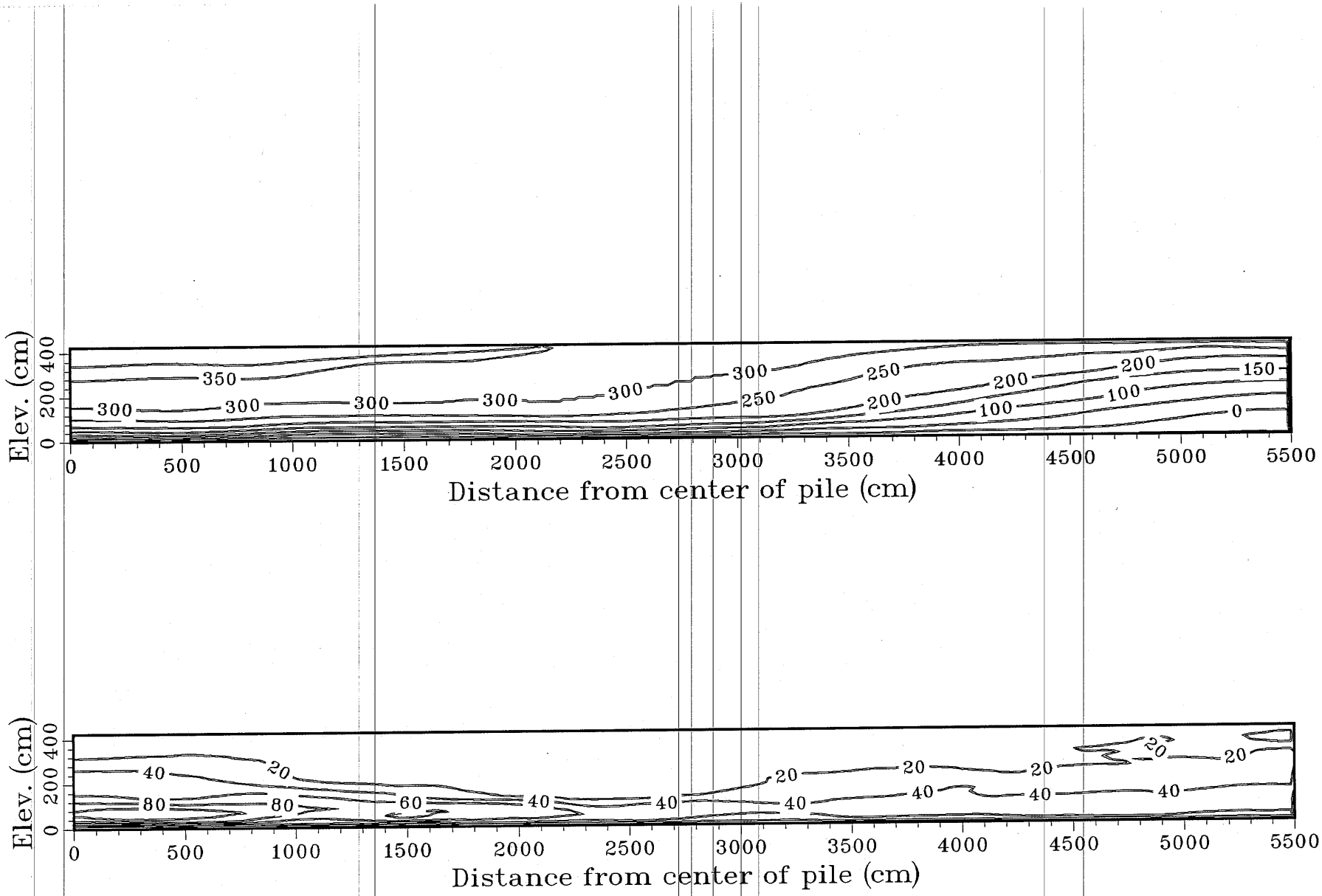

Figure 3.91(a,b). Mean and standard deviation of hydraulic head fields respectively from CS1.

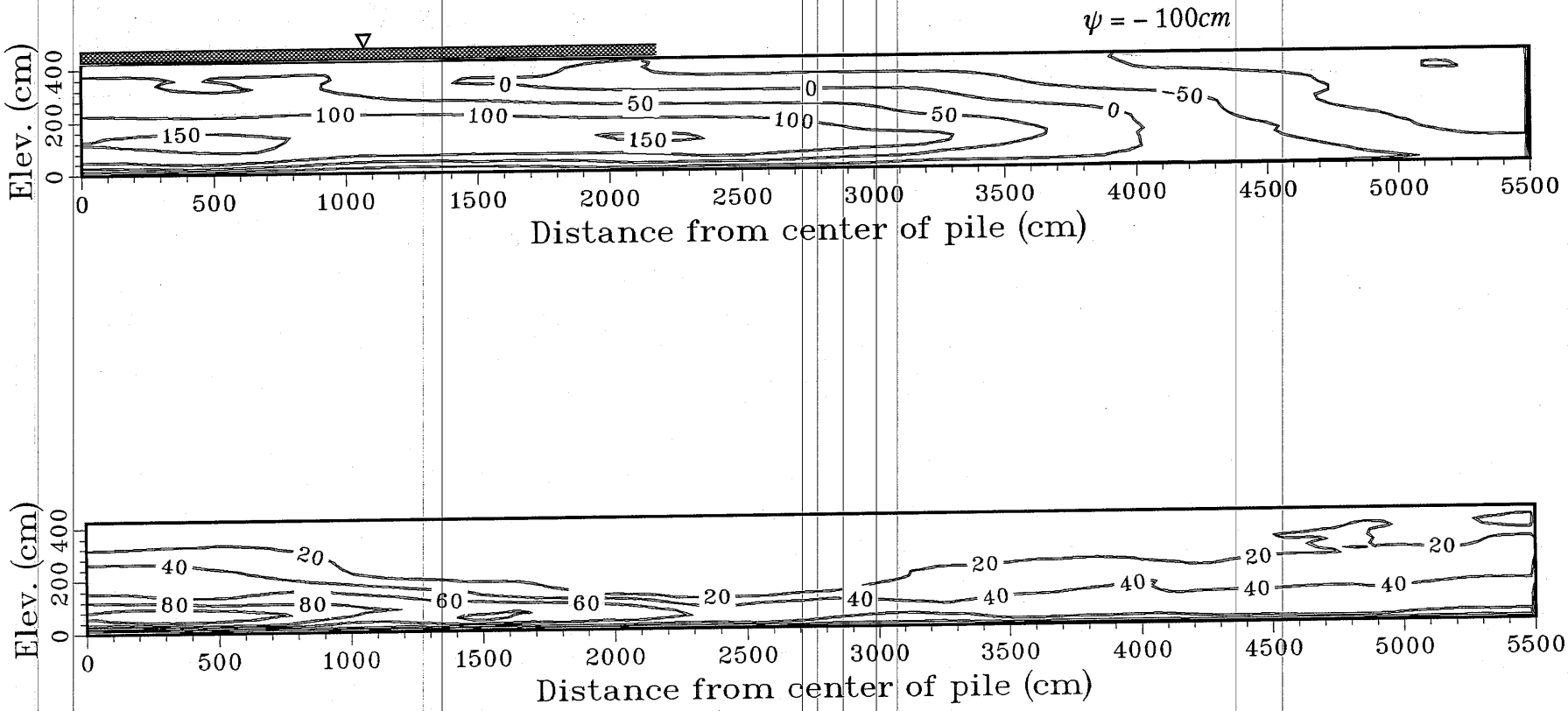

Figure 3.92(a,b). Mean and standard deviation of pressure head fields respectively from CS1.

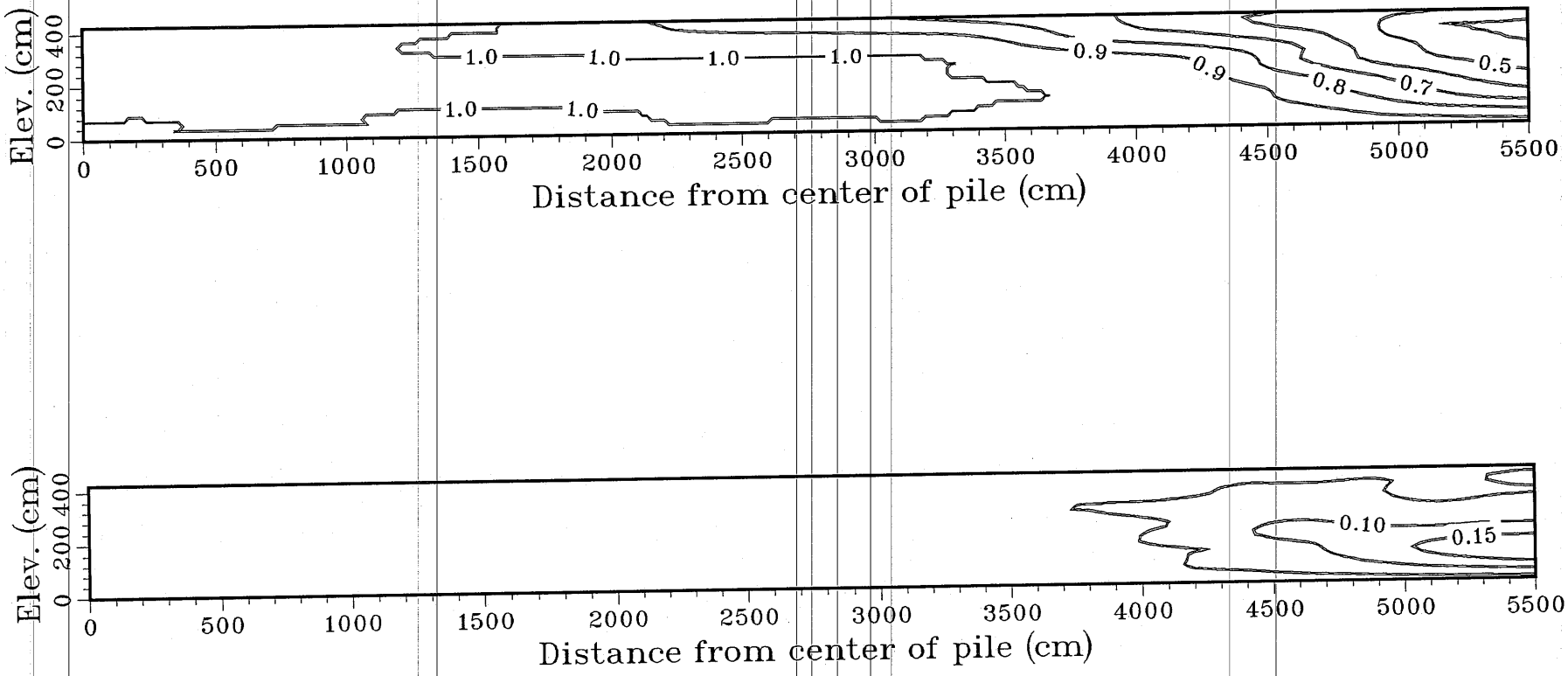

Figure 3.93(a,b). Mean and standard deviation of saturation fields respectively from CS1.

fields are conditioned on known data. This result is very important when considering transport processes in unsaturated media. The large variation in saturation profiles resulting from the unconditional simulations will tend to increase the variance in particle travel times, concentration profiles, and plume movement since the saturation profile is very important in the transport modeling as depicted in equation 3.18.

Only a single set of conditional simulations was completed. However, it is apparent that the geostatistical conditioning approach may be very helpful in reducing uncertainty in model output if hydraulic properties exhibit significant correlation scales. Reduction in model output variance through incorporation of known data is an important step in properly understanding flow and transport processes and in delineating long term fate of contaminants and radionuclides in variably saturated media.

Results of Simulations Incorporating Kriged Conductivity Fields

Geostatistical kriging is often used as an interpolator for predicting hydraulic property fields based on some assumed covariance structure. In this short section, we investigate the variation in conductivity fields and model output from various kriged fields which were produced assuming different covariance structures. Covariance models used to krige conductivity fields are summarized in Table 3.6. The sampling scheme used to predict the kriged fields is identical to that shown in Figure 3.87. The exponential covariance structure shown in Equation 3.15 was used to krige all of the conductivity fields in this analysis. Figure 3.94a,b,c shows the contoured plot of the log conductivity generated for simulations KS1, KS2, and KS3 respectively. Boundary conditions for the simulations are identical to those used in DS1. The fields are very similar considering the significant variation in covariance models. A comparison of the

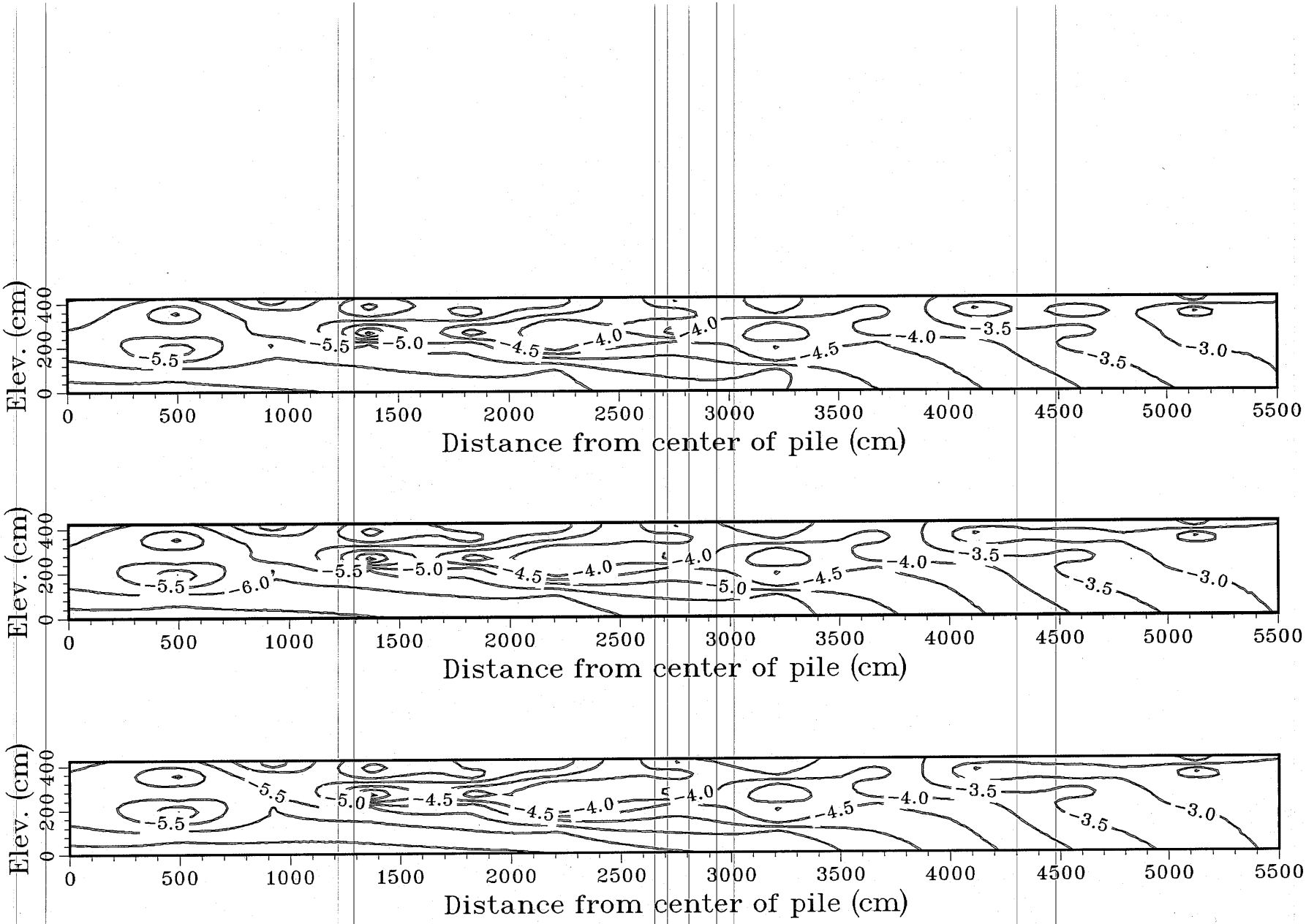

Figure 3.94(a,b,c). Three contour plots of kriged log saturated conductivity based on covariance models used in KS1, KS2, and KS3 respectively.

seepage distributions from the five models is shown in Figure 3.95. The seepage distribution and the total seepage from the impoundment are quite similar. There is an increase in total seepage per unit width with increasing correlation scales. As the continuity of the horizontal conductivity increases, there is an increase in the horizontal flow component which effectively increases the anisotropy and thus the seepage is increased. The same result was obtained in the deterministic simulations when the anisotropy was increased. Variance of the conductivity in the kriging model is shown to have no effect on the seepage distribution.

simulation	$\sigma_{K_{sat}}^2$	λ_x	λ_z	Seepage (cm^2/s)
KS1	1.0	850cm	85cm	.164
KS2	1.0	1500cm	150cm	.175
KS3	1.0	3000cm	300cm	.177
KS4	.50	850cm	85cm	.164
KS5	.50	1500cm	150cm	.175

Table 3.6. Summary of covariance models and seepage predictions from simulations incorporating kriged fields.

Figure 3.96a,b,c,d shows the steady-state results of KS2. The velocity vector field shows significant lateral flow components, as did the Monte Carlo and conditional simulations. It appears that assumed covariance structure has a minimum effect on the interpolated conductivity field if the correlation scales of the hydraulic properties are of the same order as the distance between sampling locations. Assumed covariance structure will have a greater effect if the

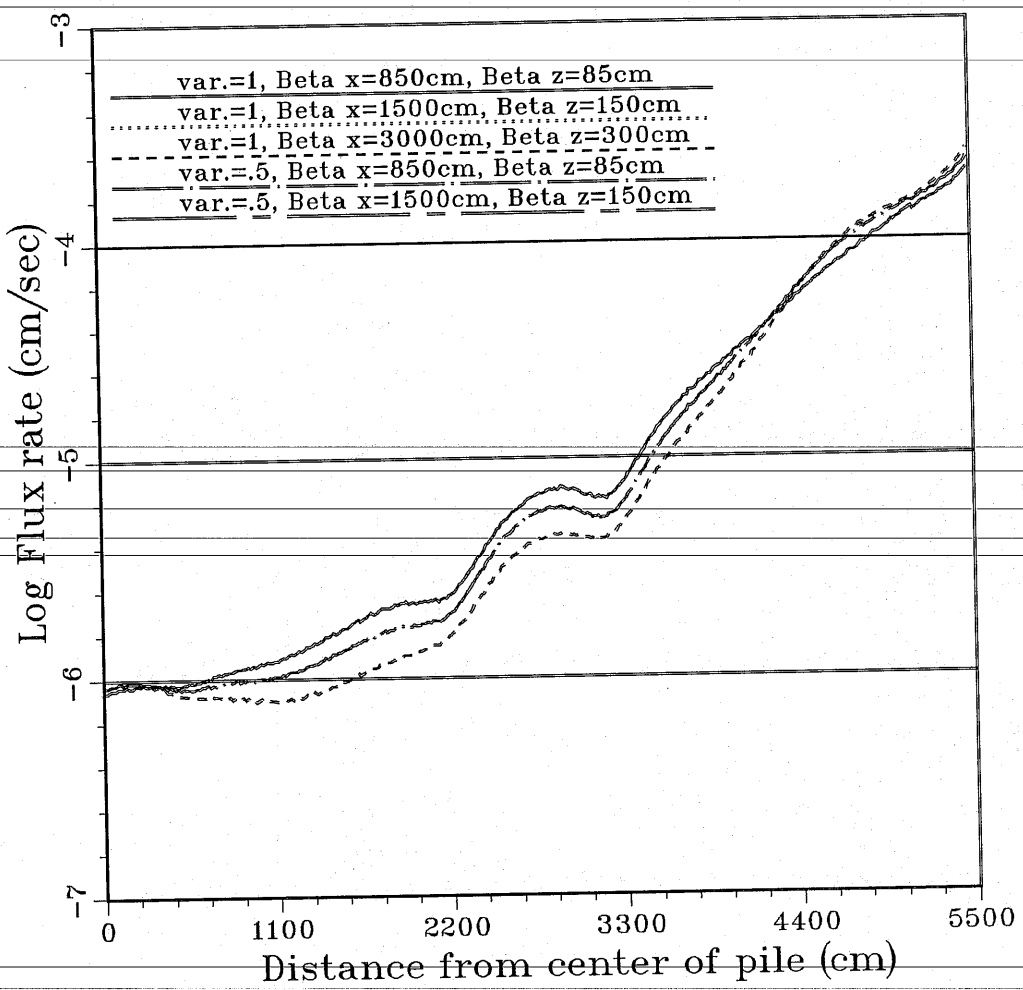

Figure 3.95. Seepage distribution from the five kriged conductivity fields generated using covariance structures shown in Table 3.6.

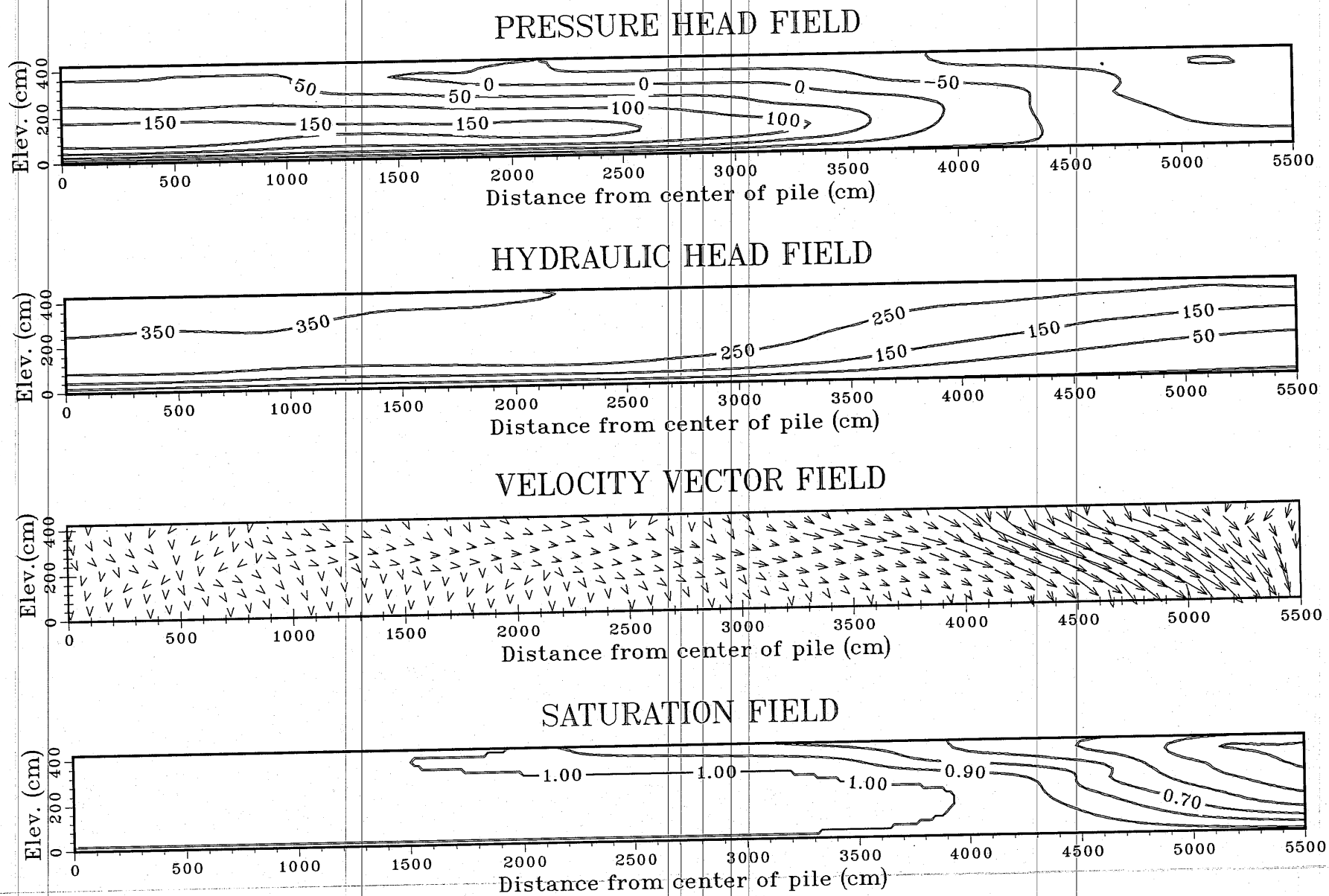

Figure 3.96(a,b,c,d). Steady–state results from KS2. Summary of covariance model used to generate conductivity field is shown in Table 3.6.

correlation scales are significantly smaller than the mean distance between sampling locations.

Discussion of Methods used to Incorporate Spatial Variability into Numerical Models

Several conceptual models have been incorporated to delineate flow phenomena in variably saturated media. Deterministic models were used to investigate effects of anisotropy and various boundary conditions. The uncertainty involved in the model output have been characterized using "quasi" Monte Carlo techniques incorporating both unconditional and conditional stochastic fields. Each conceptualization used in this study is useful but also has disadvantages. It is important to consider the advantages and disadvantages of each method when considering a conceptual model to analyze flow and transport phenomena, therefore a brief discussion of this issue is given here.

Advantages and Disadvantages of Each Method

The deterministic modeling approach of course requires less computer time because a limited number of simulations are completed. This type of modeling approach is most often used in "real world" applications due to budget and time restraints as well as computer resource limitations. Unless multiple deterministic simulations are performed, insight into the uncertainty in model predictions cannot be gained. In deterministic studies, multiple simulations are generally completed during model calibration. However, beyond this point in the modeling process, the flow and transport processes are often treated in a deterministic framework due to the restrictions mentioned above. In many cases, this approach is adequate to address the problem at hand, but uncertainty in

model input may cause significant deviations in model predictions and field conditions. If there is a specific need to determine the uncertainty in model predictions, for instance, transport of contaminants over large times scales when conditions determining flow and transport processes are highly uncertain, it may be nessecary to consider an approach which will produce some quantitative description of the uncertainty involved in model output.

In this case, a Monte Carlo approach often taken is to investigate the uncertainty in model output. This method is generally very time consuming and can lead to extensive costs in computer resources, especially for complex, large scale problems. More often than not, the data needed to properly define the range of uncertainties in model input are not available, and thus uncertainty in the uncertainty can lead to extremely large and and possibly incorrect model output variance. As an example, hydraulic properties which are generally highly correlated are often treated as independent random variables in conceptual models used to determine the uncertainty in flow and transport phenomena. In Monte Carlo simulations employing unconditional realizations of input parameters, misleading output variances may result as a consequence of not incorporating all the known data in the model input. It is very important to retain reasonable estimates of model input uncertainty if model statistics from Monte Carlo simulations are to serve as a meaningful guide for regulatory actions concerning water resource management, remediation schemes, aquifer protection measures, and protection of human resources.

In an effort to address one of the problems of unconditional Monte Carlo simulations, conditional simulations may be completed in an effort to incorporate the "observed" data so that model output variance can be reduced to within some meaningful bounds. As discussed and implemented in the previous section, one technique available to perform this task is the use of a geostatistical

approach to "condition" spatial or temporal data for model input. The disadvantage of this approach is its reliance on classical theories of geostatistics which may not be valid in some cases. An extensive data base and much characterization work is also needed to properly determine the parameters needed for this method of conditioning. If the process defining the distribution of the random variables cannot be described using the classical geostatistical concepts, the method is of limited use. If the correlation scales of the random variables are relatively small, the ability of this method to reduce model input variance and thus model output variance is limited. If assumptions are made concerning the geostatistical models used in the model, there is some uncertainty incorporated in the analysis.

Therefore, as stated in the beginning of this analysis, it is of utmost importance to realize the weaknesses of conceptual mathematical models chosen to represent actual field conditions. It is obvious that we can never accurately model field events via mathematical models without imparting uncertainty either knowingly or inadvertently, but it is always important to view the results of any "model" with a healthy dose of skepticism since we should realize the limiting assumptions and uncertainty involved in their fabrication.

TRANSIENT SIMULATIONS

Steady-state simulations have been performed to study the effects of various methods of data incorporation on numerical model output variance. However, steady-state simulations do not provide insight into the transient nature of the flow phenomena in the tailing impoundment. In steady-state simulations for example, information can not be gained concerning the amount of time needed for drainage and redistribution to occur in the mill tailings. In this

section, we investigate the transient nature of drainage processes in mill tailings impoundments. One-dimensional simulations will be performed in order to assess drainage phenomena in various locations of an impoundment. Two-dimensional simulations are avoided since the computer time needed for such simulations would be restrictive for this study.

Purpose of Transient Simulations

Mill tailings impoundments are often conceptualized as homogeneous and isotropic. It has become apparent in this study that this conceptualization is not always sufficient in modeling flow an transport from tailings impoundments. Thus far, we have shown this through steady-state simulations. Many times however, flow processes in tailings impoundments cannot be assumed to be in a quasi steady-state. In some cases, it may very important to analyze transient flow processes in tailings impoundments. One such example is the drainage process that occurs when mill tailing impoundments become inactive or the when remediation schemes are implemented to reduce the infiltration through the surface of the impoundment. How long does it take for seepage from an impoundment to decrease to regulatory limits if the pile is remediated? In order to shed light on this issue, transient simulations were performed in a one-dimensional framework.

One-dimensional Model Approach

In the one-dimensional simulations, the media is considered homogeneous and isotropic. In this approach, three homogeneous zones are defined; sand, transition, and slime as shown in Figure 1.1. Hydraulic properties are incorporated into the models which represent some "average" of the property values for the portion of the pile that is being modeled. Parameters used in the

model are shown in Table 3.7. The initial conditions for each simulation were a condition of full saturation, or pressure head equal to zero. A boundary condition of zero pressure head was implemented at the base of each one-dimensional column corresponding to a water table condition. It is important to note that the prescribed boundary conditions only allow fluid exit at the bottom of the column; no evaporation or infiltration is allowed. Drainage in each column was then simulated until most of the fluid had drained from storage.

	zone		
Hydraulic property	slime	transition	sand
K_{sat} *(saturated conductivity)*	9.85E-3 cm/d	0.864 cm/d	86.4 cm/d
n (*Brooks/Corey*)	7.5	5.5	4.5
S_s *(specific storage)*	1.0E-4	5.0E-5	1.0E-5
ϕ *(porosity)*	0.50	0.40	0.30
S_{rw} *(residual saturation)*	0.45	0.25	0.10
n *(van Genuchten)*	1.2	1.8	2.2
α *(van Genuchten)*	0.010	0.013	0.016
m *(van Genuchten)*	0.167	0.444	0.545

Table 3.7. Hydraulic properties incorporated into one-dimensional models for transient simulations.

Results of One-dimensional Transient Simulations

One important step in many remediation schemes is dewatering of the mill tailings prior to implacing covers designed to prevent infiltration. Another approach which may be taken is to cover the tailings and allow the fluid which is present in the tailings to drain under gravity forces. How long does this

"dewatering" occur under natural gravity drainage? Obviously, it will depend on the hydraulic properties of the porous media and the type of conditions which are present at the impoundment (i.e. liners, covers, presence of ponding). In this set of one-dimensional transient simulations, an attempt is made to simulate the transient flow processes which would occur if a tailings impoundment was covered immediately after the impoundment becomes inactive (tailings are assumed completely saturated) and covered so efficiently as to allow no downward infiltration from natural recharge. This is a somewhat physically implausible model but is a useful scenario for illustrative purposes. Results of the simulations are shown in Figures 3.97 and 3.98. Figure 3.97 shows the time dependent Darcy seepage velocities at the base of each one-dimensional column. Clearly, the hydraulic properties of the media play a very important role in the transient drainage process. The sandy portions of the impoundment will exhibit relatively high seepage rates for less than a day before seepage rates diminish very rapidly. The slime zone of the impoundment will exhibit relatively small seepage rates for very long periods, (possibly years) before seepage rates begin to decrease. Seepage rates from the transition zone begin to decrease in less than 100 days. Figure 3.98 shows the cumulative seepage volume in time from each column of media modeled. The graph depicts a very important aspect of transient flow and fluid storage in unsaturated media. Table 3.8 shows the percentages of original fluid present in each column after drainage to quasi steady-state conditions. For the case of a water table boundary condition at the base of the impoundment, the sand zone releases more fluid from storage than the slime or transition zones, even though it contained less fluid in storage at full saturation. Of course, if the boundary condition at the base of the impoundment becomes "drier", the slimes and transition zones will release more water until total volume drained surpasses that of the sand zone.

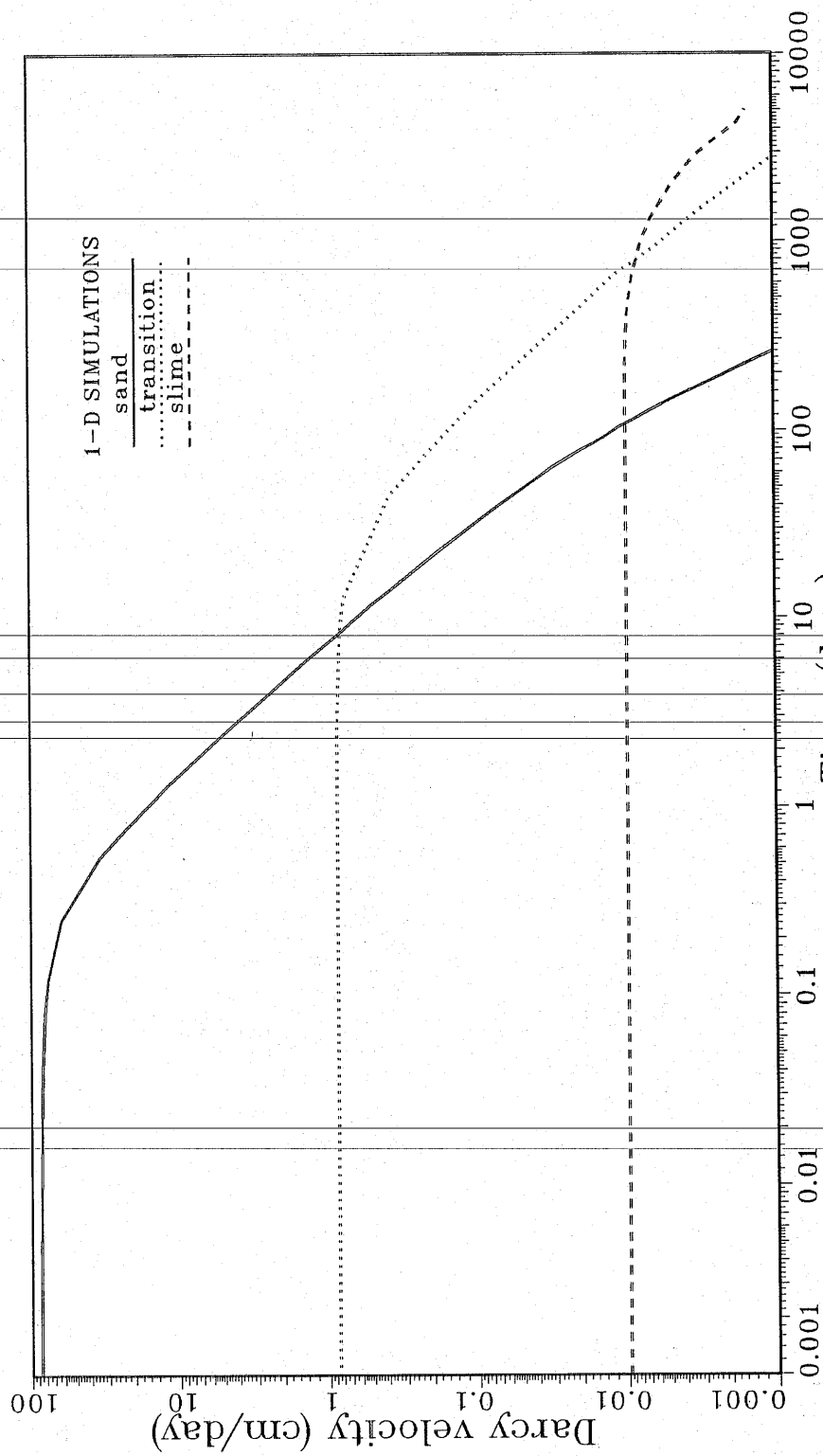

Figure 3.97. Results of one-dimensional transient simulations showing darcy velocity at the base of the column versus time for the various media simulated.

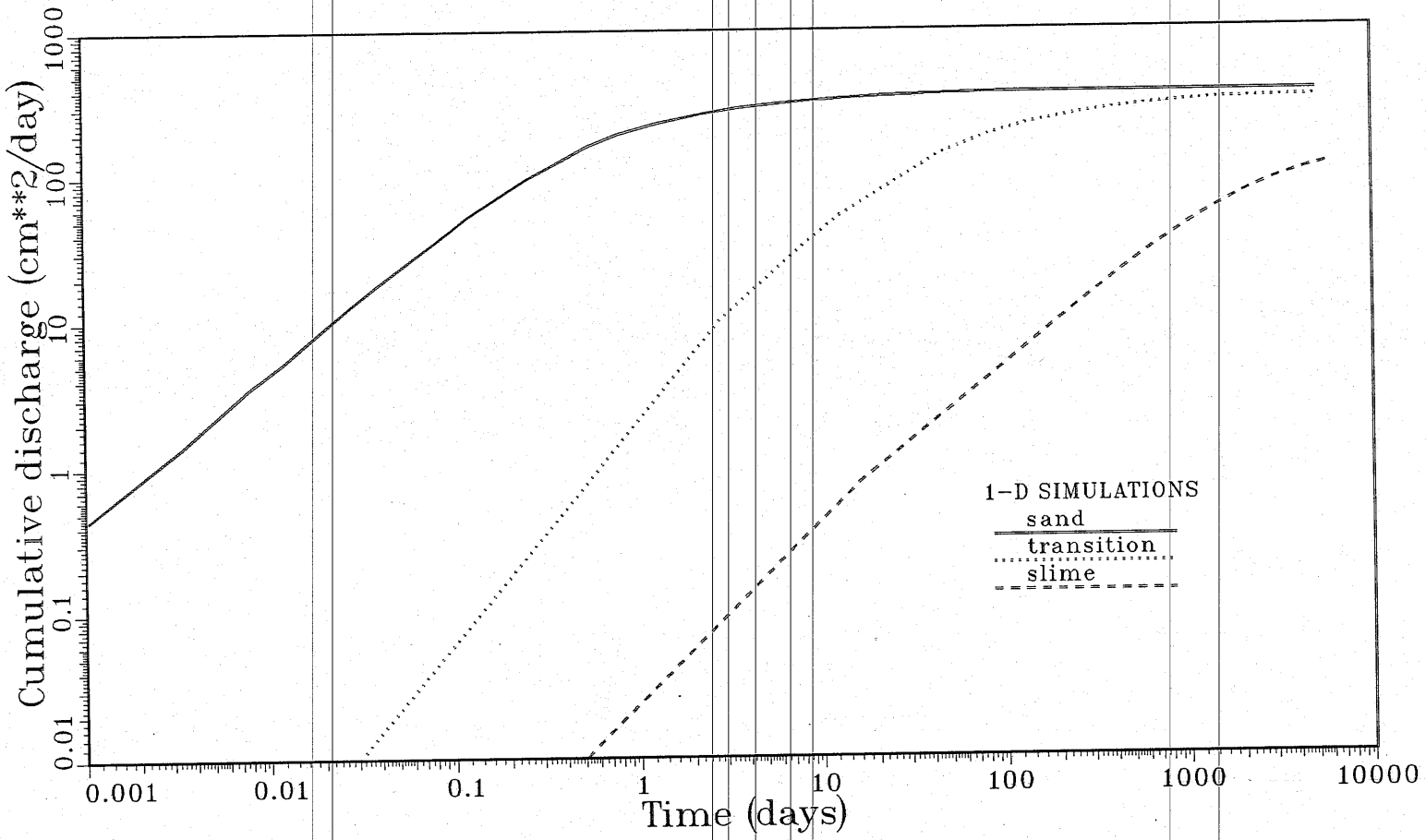

Figure 3.98. Results of one-dimensional transient simulations showing cumulative discharge at the base of the column versus time for the various media simulated.

		drainage per unit column width	
zone	original fluid vol.	cumulative drainage	% drained
slime	1062 cc	120 cc	11.3
transition	850 cc	320 cc	26.6
sand	638 cc	350 cc	54.8

Table 3.8. Amount and percentage of fluid drained from each zone according to one-dimensional transient simulations. Values are calculated at "quasi steady-state".

Drainage from a truly three-dimensional impoundment will show deviations from what is seen for the one-dimensional scenarios described above. As seen in the steady-state simulations, the lateral flow components within the impoundment will be greatly increased as the anisotropy and layered heterogeneity are increased. These lateral flow components will have a profound impact on transient drainage processes. Lateral hydraulic gradients produced by the variation in drainage times within the impoundment will induce horizontal flow toward the outer portions of the impoundment and thus the drainage process will be hastened.

CHAPTER 4

RECOMMENDATIONS FOR REMEDIAL SCHEMES AND MODEL APPROACH

Practical implications of the results of the modeling study discussed in chapter 3 should be reemphasized since these issues are often very important in determining effective schemes to combat future groundwater contamination through prevention or remediation. In this chapter, we review a few of the many papers concerning shallow waste burial and mill tailings remedial action programs. A qualitative discussion of results from this study is also presented with emphasis on implications for groundwater protection and practical approaches to modeling studies for waste impoundments. The results of numerical simulations discussed in chapter 3 can offer insight into proper design and remedial action of waste impoundments for groundwater protection. Though many simulations were "academic" in nature, the results contain practical implications for the many concerns surrounding design and remediation of waste impoundments.

Review of Pertinent Literature

Concern for transport and fate of contaminants escaping from shallow waste burial sites and mill tailings impoundments have produced a large number of research efforts aimed at better understanding of the physical processes responsible for contaminant transport. Many papers have also been published concerning practical issues of land burial of wastes and improvements to contamination prevention and remedial schemes for mill tailings impoundments. It is therefore worthwhile to briefly review a few of these publications at this time.

Kealy and Busch *[1979]* point out "state of the art" in mine tailings disposal. These authors point out that mill tailings waste can no longer be disposed of in the cheapest and easiest method without concern environmental resources. Shields *[1975]* shows that traditional methods for tailings disposal may unneccesarily compromise public safety and environmental protection and defines two simple engineering designs which will decrease acid water seepage from abandoned impoundments. The designs involve placing the slurry in a cone shaped pile and allowing fluid to drain off. This would prevent dam failure and decrease seepage from abandoned piles. Robinsky *[1975]* discusses a tailings design very similar to that of Shields and suggests that this type of design is less expensive to operate and close down while causing less environmental damage due to seepage of waste water. Frano et.al *[1985]* discuss aspects of planning, engineering, contracting, permitting, and monitoring design for a new waste disposal facility. Moldt et.al *[1985]* present a systematical approach to investigation and design of mill tailings impoundment for a precious metal mine. Kennedy and Hoffman *[1985]* define site specific remedial action measures for a uranium mill tailings impoundment which incorporate pumping and injection schemes to intercept tailings seepage. Other aspects of hydrogeologic problems concerning waste disposal in the subsurface are discussed by *Cartwright [1986], Siefken et.al [1982], Lane and Nyhan [1981], Robertson [1986], Bonano and Cranwell [1988]* and *Haimes [1986]*.

Monitoring programs needed for flow and transport delineation

Monitoring programs aimed at determining quantity and quality of seepage from waste impoundments often concentrate on sampling only the saturated zone in order to determine if contamination of groundwater supplies has occurred. However, this procedure can lead to a significant time lag between

release of contaminants and actual detection at the water table surface. This time lag may be even more pronounced if the flow system is heterogeneous and layered because significant lateral spreading can occur before the contaminant actually reaches the saturated zone and is detected. In certain cases, it may be advisable to sample fluids in the vadose zone in order to shorten the time lag between release of contaminants and detection.

Several factors play a role in determining the type of monitoring scheme needed to detect release of the contaminants into underlying geologic formations. The nature of the contaminant(s), depth to the saturated zone, waste impoundment design, and the nature of underlying porous media are important considerations in monitoring program design.

Contaminants exhibit a wide variety of transitory characteristics, some are strongly adsorbed to the porous media, others undergo ion exclusion and move faster then the mean flow of groundwater. Biological and chemical degradation of pollutants and radioactive decay of radionuclides are an important determinant in contaminant transport and fate. It is important to understand the behavior of contaminants in the subsurface in order to properly design monitoring schemes needed to properly characterize their fate. Some radionuclides can remain a source of potential contamination for many decades or even centuries, therefore it is especially important to detect their release from waste impoundments as quickly as possible in order to minimize environmental risks and remediate the problem as quickly as possible. Early detection of pollutant release is obviously a great advantage in remediation attempts since the contaminant can be retained in a smaller area.

If there is an extensive unsaturated zone below waste impoundments, it becomes increasingly important to monitor unsaturated seepage. If monitoring devices are placed only at the phreatic surface, there is a great propensity for

extensive contaminant buildup in the vadose zone before the contaminant is detected. This hinders remedial schemes by increasing total effort needed to abate the problem.

If analysis of well water discloses that contamination has occurred, the next step is often determination of contaminant origin. In some cases, this may be relatively simple. However, if there is more then one party suspected of contaminant release, it may be very difficult and expensive to determine and prove the origin of the pollutant(s), especially if complex flow and transport processes and shrewd lawyers are involved. In such cases, it would be very beneficial to have monitoring systems capable of determining the origin of pollutants before they appear in household taps. One possible alternative is implementation of vadose zone monitoring schemes for sites exhibiting a high propensity for pollutant release prior to release so that early detection is possible. This approach would also be helpful in determining the origin of specific contaminants and the parties responsible for releases. Of course, this alternative would be expensive to implement but would probably be less costly then the lawyers and remediation schemes needed to address the alternative problem.

Proposed Conceptual Models to Minimize Seepage from Tailings Impoundments

In this section, possible conceptual models to minimize seepage from impoundments are proposed based on the results of simulations previously performed and discussed in the chapter 3. Seepage prevention and remedial schemes are always site specific and it is never possible to make broad recommendations based on limited knowledge, but it may be helpful to present simple conceptual models which may be appropriate for consideration in some cases.

It is obvious from the results of the evaporation simulations that significant seepage may occur from ponded impoundments. Unlined impoundments may serve more effectively as infiltration ponds than as "evaporation" ponds. If the impoundment is abandoned and the surface is not reshaped in order to shed water to the outside edges, runoff water may pond in the center of the impoundment. In many cases, ponded water in the center of abandoned impoundments may be the major source of water for seepage. As the steady-state simulations have shown, seepage from unlined impoundments may be much greater than evaporation. Therefore, one way to limit the amount of seepage from the impoundment is to simply remove the ponded water from the surface of the impoundment. Figure 4.1 and 4.2 show two possible conceptual models which may serve as effective and simple methods to remove water from abandoned impoundments. Figure 4.1 depicts a simple engineering approach to rid the surface of residual ponding. A conduit is placed in the center of the impoundment so that the ponded water can be drained off of the impoundment before significant infiltration occurs. This method may be implemented very easily in many cases since most impoundments contain a decant tower designed for this very purpose during the active lifetime of the impoundment. If water from precipitation events is drained quickly from the surface of the impoundment, chemical treatment may not be required.

Reshaping the surface of the pile may also be a relatively simple and inexpensive method to produce effective runoff characteristics and avoid ponding in the center of the impoundment. Figure 4.2 displays one reshaping strategy to rid abandoned impoundments of residual ponded water. In this scenario, the impoundment is mounded with natural materials in the inner regions so that runoff will move to the outer portions of the impoundment and off the impoundment. If erosion of the surface is a major concern, riprap may be added

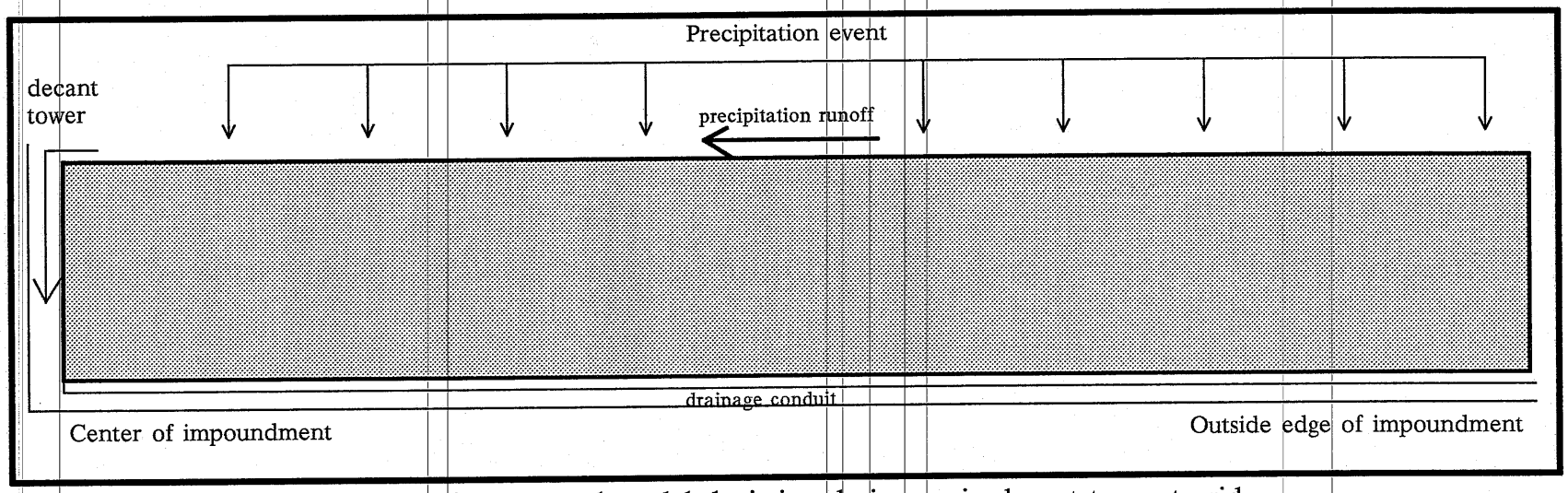

Figure 4.1. Cross-section of conceptual model depicting drainage via decant tower to rid impoundment of surface ponding and decrease infiltration potential.

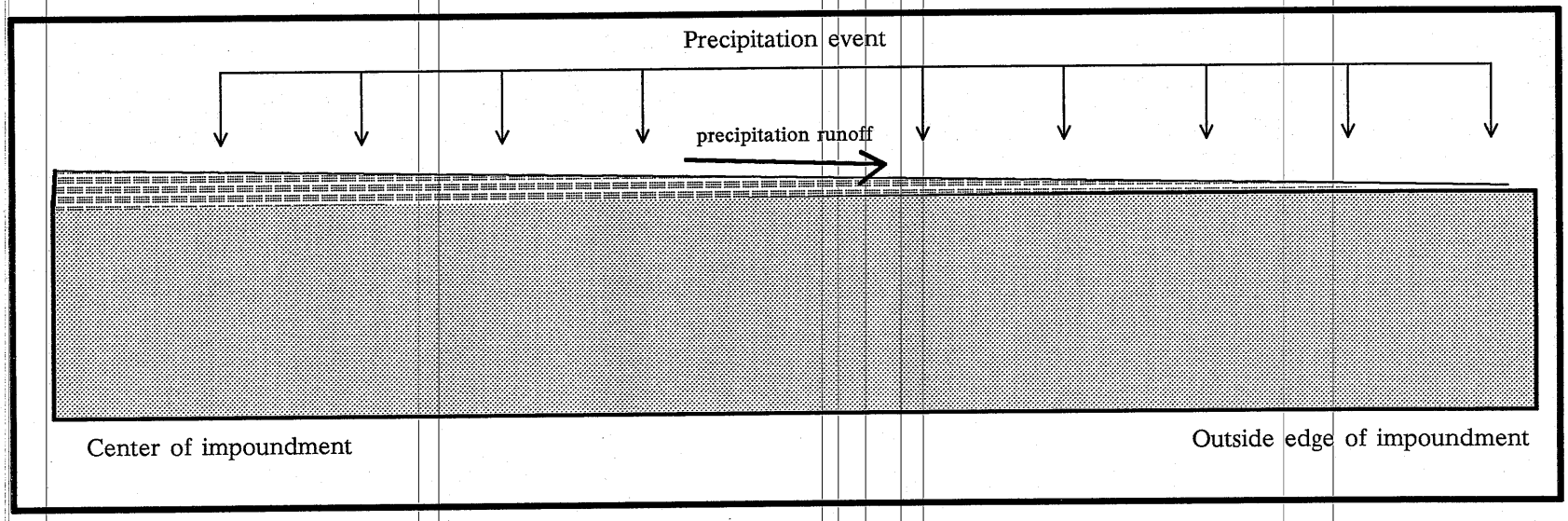

Figure 4.2. Cross-section of conceptual model depicting drainage from surface to outer edge of impoundment after reshaping surface.

to the surface to combat the problem. This design limits infiltration and requires relatively small construction and maintenance costs.

One result apparent from all the simulations performed is the importance of lateral flow components in heterogeneous, anisotropic tailings impoundments. Lateral flow components can lead to significant horizontal spreading of fluid and contaminants from tailings impoundments which can lead to a significant increase in seepage from unlined tailings impoundments. Slurry walls are one relatively simple technique which could be used to combat lateral flow. Figure 4.3 shows a conceptual model of flow in an anisotropic impoundment based on results of previous simulations. Figure 4.4 shows the proposed conceptual model implementing a slurry wall to decrease lateral flow components and thus decreasing total flow from the impoundment. The slurry wall should be constructed of a material of extremely low hydraulic conductivity at high saturation so that lateral flow components are significantly inhibited. This design could be easily adaptable to impoundments which are being constructed since the slurry wall could be maintained and extended upward as needed. The effectiveness of this design depends on the size of the impoundment and the relative distributions of the sand, transition, and slime zones.

IMPLICATIONS FOR APPROACHES TO MODELING WASTE IMPOUNDMENTS

Several approaches have been taken in this study to examine seepage characteristics of a variably saturated impoundment. Data needs for each method and the assumptions inherent in the analysis vary widely for each approach. It is important to consider these points when undertaking numerical modeling studies to delineate of flow and transport in heterogeneous systems. Model approach and conceptualization is generally an iterative process in the

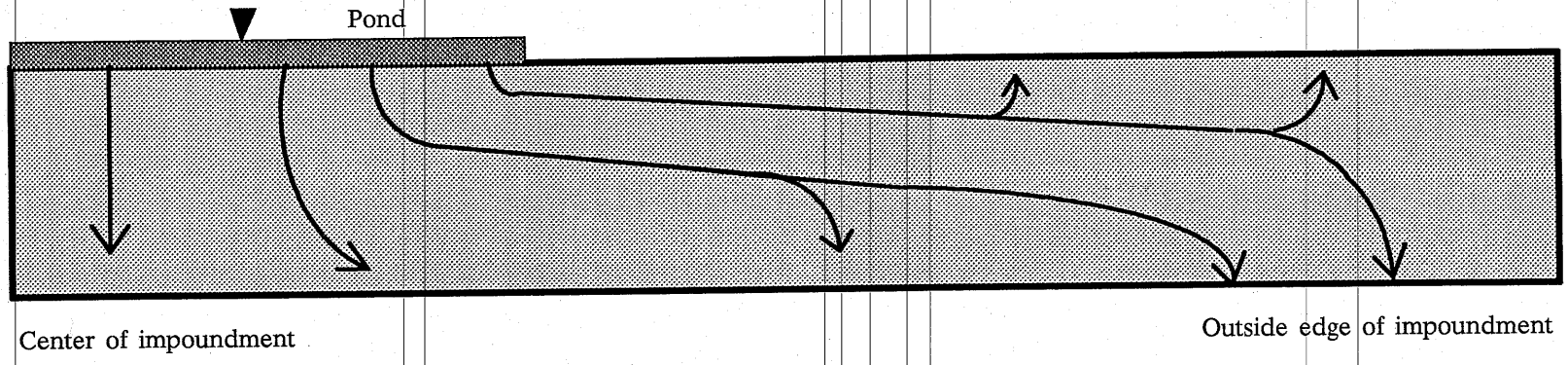

Figure 4.3. Cross-section of conceptual model for flow from anisotropic tailings impoundment revealing lateral flow components.

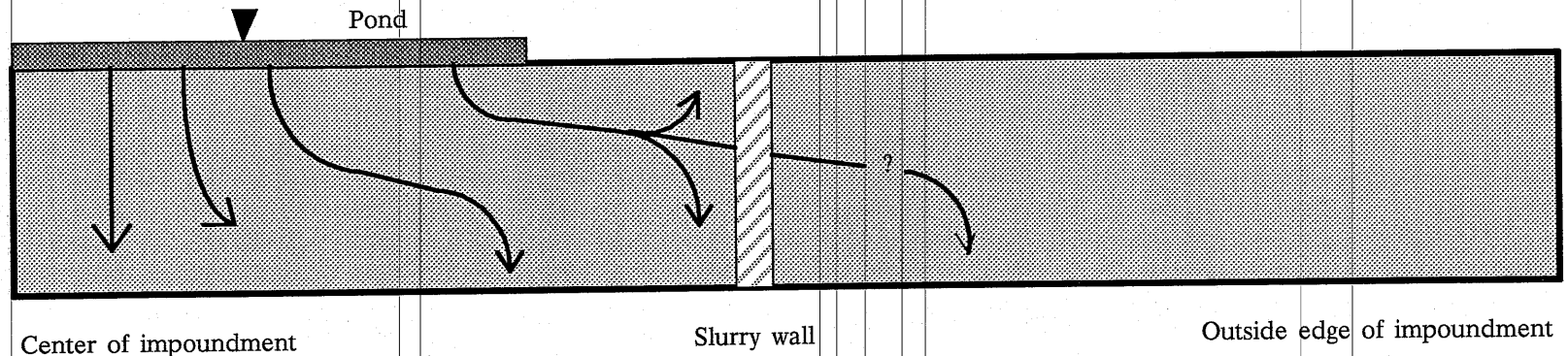

Figure 4.4. Cross-section of conceptual model for flow from anisotropic impoundment after emplacement of slurry wall.

beginning stages of analysis since ever increasing knowledge of the system necessitates improvement of the working model. The type of conceptual model used to analyze a flow system is of course highly dependent on the objectives of the analysis. In this section, we discuss data needs for incorporation of various models.

Data Needs for Various Model Approaches

If the hydraulic properties of a system are relatively easy to define and are somewhat constant throughout the domain of interest, a deterministic approach may be adequate to define the mean flow and transport characteristics. In this case, definition of proper boundary conditions for use in the mathematical model is often the most important variable to correctly determine if accurate predictions are to be constructed via the model. For the deterministic analysis performed herein, regression analysis proved to be a valuable tool in defining major spatial trends in hydraulic properties. If the heterogeneity can be defined by this type of averaging model, relatively few measurements of hydraulic properties are needed.

Relatively large amounts of data are required to validate a unconditional stochastic–deterministic conceptual model for use in modeling uncertainty in actual field conditions. Assuming all intrinsic assumptions are satisfied, the stochastic–deterministic model approach requires knowledge of statistical parameters for the hydraulic properties, which inherently mandates a large number of samples. This is not always feasible in real world problems due to budget and time restrictions. Of course, statistical parameters of the hydraulic properties can be assumed in order to gain insight into relative sensitivity of model output based on a given model for model input uncertainty. However, as stated in chapter 3, we must be careful to insure that reasonable models of input

uncertainty are incorporated in the analysis to insure credible output statistics. The method of performing conditional simulations used herein requires basically the same assumptions as does the unconditional stochastic–deterministic simulation approach. However, it is the author's opinion that this approach is intuitively less sensitive to the incorporated covariance structure, since the realizations of the stochastic process are always conditioned on observed data. In other words, since the observed data are always "honored", the correlation structure effectively plays a less significant role in determining the resulting "conditioned" stochastic process.

Kriging can be a very useful tool to interpolate scattered data. The results of various kriging realizations due to the incorporated assumptions can be compared to the results of hand contours produced by different people for a particular set of data. Hand contouring involves the same type of assumptions on the "connectivity" of data as does assuming or calculating a covariance structure. Because kriging is an exact interpolator, it can be useful in producing fields which honor the observed data.

Sampling and Characterization Procedures Needed for Stochastic Modeling Approaches

In this study, covariance structures for hydraulic properties were assumed because this data was lacking for the study. Analysis was performed incorporating various covariance models in order to compare statistics from Monte Carlo simulations. How would one approximate the conductivity correlation structure in a flow regime? As stated earlier, it would probably take an immense commitment of time and effort to complete the sampling and characterization needed to determine the correlation structure of the hydraulic properties. Designing a sampling system to properly characterize heterogeneity

will depend on several factors. Modeling objectives, available time and finances, methods of sampling and hydraulic characterization, size and dimensionality of modeled region, and nature of the porous media are factors which must be considered in design.

Modeling objectives are those which will lead to the final product of the analysis. Sampling strategies will differ as the modeling objective change. Sampling and characterization strategies employed for production of hydraulic head contours in a vertically integrated saturated flow model will (or should) differ from that needed for prediction of travel paths for radionuclides in a heterogeneous, anisotropic unsaturated flow system. Russo *[1984]* presents schemes for optimal design of sampling strategies for variogram characterization. Methods of sampling and hydraulic characterization may play an important role in determining the strategy used to determine spatial correlation of hydraulic properties. The scale of the measurement for hydraulic properties may vary greatly. Hydraulic conductivity may be measured by taking a small core sample or by performing a large scale aquifer test. Thus, the type of characterization methods will have an impact on the type of conceptual model implemented. The nature of the variability in the hydraulic properties is perhaps one of the most important factors determining the type of sampling strategy needed to properly characterize the statistical parameters of the hydraulic properties. If correlation scales are very small, the sampling program should reflect this with smaller sample separation distances if the correlation is to be identified.

CHAPTER 5

SUMMARY AND CONCLUSIONS

A numerical model has been implemented to investigate effects of spatial variability in hydraulic properties on steady-state seepage characteristics from a variably saturated mill tailings impoundment. Deterministic simulations were performed to investigate the influence of boundary conditions and anisotropy. One-dimensional transient simulations were performed in order to observe temporal variations in seepage in different regions of the impoundment. One-dimensional steady-state seepage simulations were performed to investigate differences in one and two-dimensional model predictions under the same boundary conditions. Unconditional "quasi" Monte Carlo simulations were performed to examine seepage uncertainty given various models describing uncertainty in hydraulic properties. In order to investigate the ability of data conditioning to reduce model output variance, a geostatistical approach was taken to complete conditional simulations which incorporated observed data from the tailings impoundment.

Results from deterministic simulations clearly show the importance of incorporating major trends in saturated and unsaturated hydraulic properties into numerical models. The sandy unsaturated portion of the impoundment exhibited greater seepage than the ponded regions where the tailings material is much finer. Anisotropy was shown to have a significant effect on seepage distribution at the base of the impoundment, especially under drier conditions. Lateral flow components induced by anisotropy is expected to greatly influence the movement of contaminants within variable saturated flow regimes. Two-dimensional

simulations show that fluid from the ponded area of an impoundment can travel significant distances in the lateral direction. This result shows the importance of multi-dimensional flow phenomena in heterogeneous, anisotropic flow systems. Multi-dimensional flow effects should always be considered in determining the conceptual model used to analyze flow and transport processes in the unsaturated zone. One-dimensional transient simulations demonstrate the large variation in drainage characteristics from different regions of unlined tailings impoundments. Variation in drainage times in different zones of impoundments is expected to increase the lateral flow components and thus hasten the drainage process. One-dimensional steady-state seepage results differ greatly from two-dimensional results, especially in the areas exhibiting significant lateral flow components due to hydraulic gradients and anisotropy.

Unconditional "quasi" Monte Carlo simulations showed that uncertainty in seepage predictions from the impoundment is significantly increased under high hydraulic gradients. This result suggests that the boundary conditions placed on the flow domain are an important consideration in determining the importance of quantifying uncertainty in flow and transport in the vadose zone. Under steady-state conditions, the uncertainty in seepage predictions was relatively inconsequential when the flow regime exhibited small hydraulic gradients. Flow regimes under higher hydraulic gradients displayed a much greater variance in seepage at the base of the impoundment and greater variations in saturation throughout the impoundment. As the horizontal correlation scale of the stochastic conductivity fields was increased, seepage from a partially ponded impoundment was significantly decreased due to the layering effect present in the media. One simulation (Figure 3.69) considering fluid flow from a "semi" point source shows the importance of lateral flow components in small scale contaminant movement. Comparison of seepage statistics from

Monte Carlo simulations incorporating two different covariance structures in the conductivity fields assuming equivalent integral scales show relatively small variations. However, the variability in the velocity vectors is much greater when an exponential covariance structure is incorporated as compared to a "double exponential" covariance structure. This result suggests that the type of covariance structure chosen for conceptual models may have profound effects on the results of flow and transport analysis, even if equivalent "correlation scales" are incorporated.

Geostatistical conditioning of conductivity fields on observed data is shown to reduce the variance in model output statistics. If nessecary statistics can be established for the hydraulic properties in a flow regime, this method of conditioning can significantly reduce uncertainty in probabilistic flow and transport predictions.

REFERENCES

Andersson, J. and Allen M. Shapiro, 1983. Stochastic Analysis of One-Dimensional Steady State Unsaturated Flow: A Comparison of Monte Carlo and Perturbation Methods. Water Resources Research, 19(1), pp. 121-133.

Bakr A.A., L.W. Gelhar, A.L. Gutjahr, and J.R. Macmillan, 1978. Stochastic Analysis of Spatial Variability in Subsurface Flows. 1. Comparison of One- and Three-Dimensional Flows. Water Resources Research, 14(2), pp. 263-271.

Bear, J., 1979. Hydraulics of Groundwater, McGraw-Hill, New York.

Bonano, E.J., R.M. Cranwell, 1987. Treatment of Uncertainties in the Perfomance Assessment of Geologic High-Level Radioactive Waste Repositories. Journal of Mathematical Geology.

Brooks, R. H. and A.T. Corey, 1966. Properties of Porous Media Affecting Fluid Flow, ASCE J. of Irrigation Drainage Division., 92(IR2): pp. 61-88.

Byer E., and D.B. Stephens. 1983. Statistical and Stochastic Analysis of Hydraulic Conductivity and Particle Size in a Fluvial Sand. Soil Science Society of America Journal. vol 47, pp. 1072-1081

Cartwright, K. 1986. Shallow Land Burial of Municipal Wastes. EPA Document, Studies in Geophysics, pp. 67-77.

Chandler, B.L., T.A. Shepherd., and D.R. Stewart. 1985. Field Evaporation Test of Uranium Tailings Solution. Proceedings of the Seventh Symposium on Management of Uranium Mill Tailings, Colorado State University, Ft. Collins, Colorado.

Dagan, G. 1982. Stochastic Modeling of Groundwater Flow by Unconditional and Conditional Probabilities. 1. Conditional Simulation and the Direct Problem. Water Resources Research, 18(4), pp. 813-833.

Davidoff, B., J.W. Lewis, and H.M. Selim, 1986. A Method to Verify the Presence of a Trend in Studying Spatial Variability of Soil Temperature. Soil Sci. Soc. Am. J. 50:1122-1127.

de Marsily, G. 1986. Quantitative Hydrogeology Academic Press, Inc. San Diego, California

Delhomme J.P., 1979. Spatial Variability and Uncertainty in Groundwater Flow Parameters: A Geostatistical Approach. Water Resources Research, 15(2), pp. 269–280.

Frano, A.J., G.S. Numes, R. Edwards, and W.G. Schwartz, 1985. Design and Construction of Hazardous Waste Landfill Components. Proceedings of the Seventh Symposium on Management of Uranium Mill Tailings, Colorado State University, Ft. Collins, Colorado.

Freeze. R.A., 1975. A Stochastic–Conceptual Analysis of One–Dimensional Groundwater Flow in Nonuniform Homogeneous Media. Water Resources Research, 11(5), 725–741.

Gardner, W.R., 1958. Solutions of the Flow Equation for the Drying of Soils and Other Porous Media. Soil Science Society of America Proceeding.

Gardner, W.R. and D.I. Hillel, 1962. The Relation of External Evaporative Conditions to the Drying of Soils. Journal of Geophysical Research, v. 67, no. 11., pp. 4319–4325.

Gelhar L. W. 1974. Stochastic Analysis in Phreatic Aquifers. Water Resources Research, 10(3), pp. 539–545.

Gelhar L. W. and C.L. Axness 1983. Three–Dimensional Stochastic Analysis of Macrodispersion in Aquifers. Water Resources Research, 19(1), pp. 161–180.

Gutjahr, A.L. 1985. Spatial Variability: Geostatistical Methods. Soil Spatial Variability (proceedings of a workshop of the ISSS and SSSA, Las Vegas, USA, 11/30/84 – 12/1/84) Pudoc Wageningen Publishers, pp. 9–34.

Gutjahr A.L., L.W. Gelhar, A.A. Bakr, and J.R. Macmillan, 1978. Stochastic Analysis of Spatial Variability in Subsurface Flows. 2. Evaluation and Application. Water Resources Research, 14(5), pp. 953–959.

Haimes. Y.Y. 1986. Risk Assessment for the Prevention of Groundwater Contamination. EPA Document, Studies in Geophysics, pp. 166–178.

Harris, K.A., 1987. Incorporation of Spatial Variability of Mill Tailings Hydraulic Properties into a Numerical Model: Implications for Movement and Retention of Moisture. Master's thesis, Department of Geoscience, New Mexico Institute of Mining and Technology, Socorro, New Mexico.

Hillel, D. 1980. Fundamentals of Soil Physics, Academic Press, New York.

Hopmans, J. W., J. Schukking, and P.J.J.F. Torfs, 1988. Two Dimensional Steady State Unsaturated Water Flow in Heterogeneous Soil With Autocorrelated Soil Hydraulic Properties. Water Resources Research, 24(12), 2005–2017.

Huyakorn, P.S., and G.I. Pinder, 1983. Computational Methods in Subsurface Flow, Academic Press, New York

Huyakorn, P.S., S.D. Thomas, and B.M. Thompson, 1984. Techniques for making finite elements competitive in modeling flow in variably saturated porous media. Water Resources Research., v. 20, no. 8, pp. 1099–1115.

Johnson, G.D., 1987. Characterization of the Spatial Variability of Mill Tailings Hydraulic Properties: A Statistical and Geostatistical Analysis. Independent Study Paper, Department of Geoscience, New Mexico Institute of Mining and Technology, Socorro, New Mexico.

Journel, A.G. 1974. Geostatistics for Conditional Simulation of Ore Bodies. Economic Geology, vol 69, pp. 673–687.

Journel, A.G., and Ch.J. Huijbregts, 1978. Mining Geostatistics. Academic Press, New York.

Kealy, C.D., and Busch, R. 1979. Evaluation of Mine Tailings Disposal. "Current Geotechnical Practice in Mine Waste Disposal", ASCE.

Kennedy, E.E., and G.L. Hoffman, 1985. Remedial Measures to Contain Seepage From Homestakes's Uranium Tailings at Milan, New Mexico. Proceedings of the Seventh Symposium on Management of Uranium Mill Tailings, Ft. Collins, Colorado, 2/6–8/85, pp. 513–522.

Lam L. and S. L. Barbour, 1985. Saturated–Unsaturated Mass Transport Modeling by Finite Element Method. Proceedings of the Seventh

Symposium on Management of Uranium Mill Tailings, Colorado State University, Ft. Collins, Colorado.

Lane, L.J. and J.W. Nyhan. 1981. Water and Contaminant Movement: Migration Barriers. Los Alamos National Laboratory Document 10242–MS.

Larson, B.M., and D.B. Stephens, 1985. A Comparison of Methods to Characterize Unsaturated Hydraulic Properties of Mill Tailings. Proceedings of the Seventh Symposium on Management of Uranium Mill Tailings, Colorado State University, Ft. Collins, Colorado.

Lewis, G.J., D.B. Stephens, 1985. Analysis of Infiltration Through Mill Tailings Using a Bromide Tracer. Proceedings of the Seventh Symposium on Management of Uranium Mill Tailings, Ft. Collins, Colorado, 2/6–8/85, pp. 347–359.

Mantoglou, A. and L.W. Gelhar, 1987. Stochastic Modeling of Large–Scale Transient Unsaturated Flow Systems. Water Resources Research, 23(1), 37–46.

Mantoglou, A. and L.W. Gelhar, 1987. Capillary Tension Head Variance, Mean Soil Moisture Content, and Effective Specific Moisture Capacity of Transient Unsaturated Flow in Stratified Soils. Water Resources Research, 23(1), 47–56.

Mantoglou, A. and L.W. Gelhar, 1987. Effective Hydraulic Conductivities of Transient Unsaturated Flow in Stratified Soils. Water Resources Research, 23(1), 57–67.

Mantoglou, A. and J.L. Wilson, 1981. Simulation of Random Fields Using the Turning Bands Method, Report no. 26. Dept. of Civil Engineering, Mass. Institute of Technology, 199p.

McCord, J.T. 1988. Phd. Dissertation, New Mexico Institute of Mining and Technology, Socorro, New Mexico.

McCord, J.T., D.B. Stephens, 1988. Comment of 'Effective and Relative Permeabilities of Anisotropic Porous Media' by Bear, Braester, and Menier. Transport in Porous Media, (3), 207–210.

McIntosh, B.J. and D. van Zyl, 1985. Probabilistic Approach to Unsaturated Seepage Analysis. Proceedings of the Seventh Symposium on Management of Uranium Mill Tailings, Colorado State University, Ft. Collins, Colorado.

Mckay, D.H., 1988. A Fast Fourier Transform Method for Generation of Random Fields. M.S. Thesis, N.M. Institute of Mining and Technology, Socorro, N.M.

McLauglin, D., 1988. Developing a Systematic Approach to Model Validation. (Proceedings of an International Conference and Workshop on the Validation of Flow and Transport Models for the Unsaturated Zone) Ruidoso N.M., 5/22/88

McWhorter, D.B., J.D. Nelson, 1979. Unsaturated Flow Beneath Tailings Impoundments. Journal of the Geotechnical Engineering Division, 1317–1334.

Mizell, S.A., A.L. Gutjahr, L.W. Gelhar, 1982. Stochastic Analysis of Spatial Variability in Two-Dimensional Steady Groundwater Flow Assuming Stationary and Nonstationary Heads. Water Resources Research, 18(4), pp. 1053–1067.

Moldt, S.F, R.G. Miller, K. Johnson, 1985. Design and Construction of an Impoundment for Precious Metal Mill Tailings. Proceedings of the Seventh Symposium on Management of Uranium Mill Tailings, Ft. Collins, Colorado, 2/6–8/85, pp. 533–542.

Mualem Y., 1976. A New Model for Predicting the Hydraulic Conductivity of Unsaturated Porous Media. Water Resources Research, 12(3), 513–522.

Narasimhan, T.N., A.F. White, T. Tokunago, 1986. Groundwater Contamination from an Inactive Uranium Mill Tailings Pile, 2. Applications of a Dynamic Mixing Model. Water Resources Research, 22(13), 1820–1834.

Neuman, S.P., R.A. Feddes, and E. Bresler, 1974. Finite element simulation of flow in saturated and unsaturated soils considering water uptake by plants, Hydrodynamics and Hydraulic Engineering Laboratory Report for Project No. ALO–SWC–77, Haifa, Israel.

Neuman. S.P., 1982. Statistical Characterization of Aquifer Heterogeneities: An Overview. Geological Society of America, Special Paper 189.

Nielsen, D.R., and J.W. Biggar, 1961. Miscible Displacement in Soils: I. Experimental Information. Soil Science Society of America Proceedings, vol. 25, no. 1, pp. 1–5.

Parsons, A.M. 1988. Independent Study Paper, Department of Geoscience, New Mexico Institute of Mining and Technology, Socorro, New Mexico.

Pinder, G.F. and W.G. Gray 1977. Finite Element Simulation in Surface and Subsurface Hydrology. New York: Academic Press. 295 pp.

Poulovassilis A. and M. Psychoyou, 1985. Steady State Evaporation from Layered Soils. Soil Science, v. 140, pp. 399–405.

Robertson, J.B. 1986. Geologic Problems at Low–Level Radioactive Waste–Disposal Sites. EPA Document, Studies in Geophysics, pp. 104–108.

Robinsky, E.I., 1975. Thickened Discharge – A New Approach to Tailings Disposal. CIM Bulletin, December, pp. 47–54.

Russo, D. 1984. Design of an Optimal Sampling Network for Estimating the Variogram. Soil Sci. Soc. Am. J. 48: 798–716.

Russo, D., and E. Bresler, 1982. Soil Hydraulic Properties as Stochastic Processes: II. Errors of Estimates in a Heterogeneous Field. Soil Sci. Soc. Am. J. 46:20–26.

Shields, D.H., 1975. Innovations in Tailings Disposal. Canadian Geotechnical Journal, (12), pp. 320–336.

Siefken, D., G. Pangburn, R. Pennifill, R. J. Starmer. 1982. Site Suitability, Selection and Characterization. NUREG Report–0902.

Siegel, J., D.B. Stephens, 1980. Numerical Simulation of Seepage Beneath Lined Ponds. (Proceedings of a Symposium on Uranium Mill Tailings Management, Fort Collins, Colorado, November 24–25)

Smith, L., R.A. Freeze, 1979. Stochastic Analysis of Steady State Groundwater Flow in a Bounded Domain, 1. One-Dimensional Simulations. Water Resources Research, 15(3), pp. 521-528.

Smith, L., R.A. Freeze, 1979. Stochastic Analysis of Steady State Groundwater Flow in a Bounded Domain, 2. Two-Dimensional Simulations. Water Resources Research, 15(6), pp. 1543-1559.

Smith, L., F.W. Schwartz, 1981. Mass Transport, 3. Role of Hydraulic Conductivity Data in Prediction. Water Resources Research, 17(5), pp. 1463-1479.

Staple, W. J., 1974. Modified Penman Equation to Provide the Upper Boundary Condition in Computing Evaporation from Soil. Soil Science Society of America Proceedings. vol. 38, pp. 837-839.

Stephens, D.B., R. Knowlton, 1986. Soil Water Movement and Recharge Through Sand at a Semiarid Site in New Mexico. Water Resources Research, 22(6), 881-889.

Stephens, D.B., 1985. Significance of Natural Ground-water Recharge in Site Selection for Mill Tailings Disposal. Society of Mining Engineers of AIME. SME Preprint 85-323 SME Fall Meeting, Albuquerque, N.M.

Stephens, D.B., A.M. Parsons, E.D. Mattson, K. Black, K. Flanigan, R.S. Bowman, W.B. Cox, 1988. A Field Experiment of Three-Dimensional Flow and Transport in a Stratified Soil. (Proceedings of an International Conference and Workshop on the Validation of Flow and Transport Models for the Unsaturated Zone.)

Stephens, D.B., S. Heermann, 1988. Dependence of Anisotropy on Saturation in a Stratified Sand. Water Resources Research, 24(5), 770-778.

van Genuchten, R., 1978. Calculating the Unsaturated Hydraulic Conductivity with a New Closed-Form Analytical Model. Research Report No. 78-WR-08. Water Resources Program, Dept. of Civil Engineering, Princeton University, Princeton, N.J. 08540.

Wang, H.F., M.P. Anderson, 1982. Introduction to Groundwater Modeling W.H. Freeman and Company, pp.237.

Wilson, J.L., and A.L. Gutjahr, 1989. Synthetic Generation of Random Permeability Fields for Heterogeneous Reservoir Simulation. *SPE* Paper 18435.

Yeh, T.C. Jim, L.W. Gelhar, 1982. Unsaturated Flow in Heterogeneous Soils, in The Role of the Unsaturated Zone in Radioactive and Hazardous Waste Disposal, J.W.Mercer et.al, eds, Ann Arbor Science, Ann Arbor, MI.

Yeh, T.C. Jim, Lynn W. Gelhar, and Allan L. Gutjahr, 1985. Stochastic Analysis of Unsaturated Flow in Heterogeneous Soils 1. Statistically Isotropic Media. Water Resources Research, 21(4), 447–456.

Yeh, T.C. Jim, Lynn W. Gelhar, and Allan L. Gutjahr, 1985. Stochastic Analysis of Unsaturated Flow in Heterogeneous Soils 2. Statistically Anisotropic Media with Variable α .Water Resources Research, 21(4), 457–464.

Yeh, T.C. Jim, Lynn W. Gelhar, and Allan L. Gutjahr, 1985. Stochastic Analysis of Unsaturated Flow in Heterogeneous Soils 3. Observations and Applications. Water Resources Research, 21(4), 465–471.

APPENDIX A

Contents:

As discussed in chapter 3, multiple regression analysis was used to define the major trends in the hydraulic properties of the mill tailings impoundment. For future reference, the regression equations defining the trends are given below as well as a discussion of their derivation.

The independent variables used in the multiple regression analysis were the spatial location of the unknown parameter within the impoundment. In order to fit the trends in some of the data, it was discovered that a quadratic equation in X^2 gave favorable results. For the purpose of x and y locations, the origin (0,0) of the vertical cross-section was taken at the lower left corner. Thus, the upper right hand corner had coordinates of (5491,425) cm. With this information, the property fields can be easily reproduced incorporating the following equation and using the regression coefficients listed in Table A1.

$$Z_i = \beta_0 + \beta_1 X + \beta_2 Y + \beta_3 X^2 \qquad (A1)$$

where: Z_i = dependent variable

β_i = regression coefficients

X, Y = independent variables

The multiple correlation coefficient R^2 is relatively small for the the van Genuchten parameters as compared to the saturated hydraulic conductivity coefficient, but the equations derived from the multiple regression analysis do define the major trends in these parameters.

The symbol (na) in Table A1 means not applicable. This means that the data needed for multiple regression analysis was not available. In these cases, the field of hydraulic properties was produced by estimating values for the

variable at a several locations in the domain and producing a smooth field via multiple regression analysis for input into the numerical model.

The value β_0 is the constant for the multiple regression equations. The coefficients for the independent variables are listed in the respective columns.

		regression coefficients				
dependent variable	R^2	β_0	β_1	β_2	β_3	NP^*
$\log K_{sat}$	.725	−2.969	.0693	.634	.00066	366
van Genuchten α	.454	.02034	−.00044	−.00086	.42 E−7	42
van Genuchten n	.603	2.707	.00203	.00022	.53 E−10	42
S_{rw}	na	na	na	na	na	na
Brooks/Corey n	na	na	na	na	na	na

* NP = number of observations

na = not applicable

Table A1. Coefficients for multiple regression equations and correlation coefficients from analysis.

APPENDIX B

Contents:

1. Program listing of MULTREG.FOR . Program to perform multiple regression.

2. Discussion concerning incorporation of anisotropic covariance behavior into kriging and conditioning algorithm.

3. Program listing of CONDITION.FOR. Program to perform kriging and geostatistical conditioning of random fields.

4. Sample input file for program CONDITION.FOR.

5. Program listing of FFT2D.FOR. Program to generate two-dimensional stochastic random fields.

```
      PROGRAM MULTREG
C=====================================================================
C     PROGRAM TO PEFORM MULTIPLE REGRESSION WITH INCREASED ACCURACY
C     THE DATA IS READ FROM A FILE (N X M)
C     STANDARDIZED PARTIAL REGRESSION COEFFICIENTS ARE PRINTED
C     AND THE PARTIAL REGRESSION COEFFICIENTS FOUND FROM THESE
C     STATISTICS, DEVIATIONS, AND A MATRIX FOR CONTOURING ARE PRINTED
C     APPROPRIATE SUBRROUTINES ARE ALSO INCLUDED
C     INPUT IS INTERACTIVE
C
C=====================================================================
C
        COMMON/PAR/IPFOD,NUNIT,IOWN
        COMMON/BASIC/ X(500,20),XM(500,20),D(500,3),ZCONT(8075),ZZ(8075)
        COMMON/ARRAY/ A(50,50),B(50),C(50),IEXPX(20),IEXPY(20)
        CHARACTER*80 FILIN,FILOUT,FILC,HEADING
        PARAMETER (ND=500,MD=50,MM=50)
C
C     READ THE DATA AND PRINT
C
          WRITE(6,*)' ENTER THE INPUT DATA FILE NAME'
          READ(5,'(A)') FILIN
          OPEN(UNIT=90,FILE=FILIN,STATUS='OLD')
          WRITE(6,*)' ENTER THE OUTPUT FILE NAME'
          READ(5,'(A)') FILOUT
        OPEN(UNIT=91,FILE=FILOUT,STATUS='UNKNOWN',CARRIAGECONTROL='LIST')
           WRITE(6,*)' INPUT FROM SCREEN OR FILE '
           WRITE(6,*)'   1=SCREEN    2=FILE'
           READ(5,*)ISCREN
           IF(ISCREN.EQ.1)THEN
             NUNIT=5
           ELSEIF(ISCREN.EQ.2)THEN
             NUNIT=90
           ENDIF
C
           WRITE(6,*)' NEED FIELD FROM YOUR OWN REGRESSION COEFFICIENTS'
           WRITE(6,*)'       1 = YES'
           READ(NUNIT,*)IOWN
           IF(IOWN.EQ.1)THEN
              CALL MAKMAP
              GOTO 9999
           ENDIF
C
           WRITE(6,*)' ENTER THE HEADING TO GO IN THE OUTPUT FILE'
           READ(NUNIT,'(A)')HEADING
           WRITE(91,'(A)')HEADING
           WRITE(6,*)' WHAT FORM IS NEEDED FOR THE OUTPUT'
           WRITE(6,*)'    1 = EXPONENTIAL'
           WRITE(6,*)'    2 = REAL '
           READ(NUNIT,*)IPFOD
           CALL READD(X,N,M,ND,MD)
           WRITE(6,*)' PRINT THE INPUT DATA MATRIX  1=YES'
           READ(NUNIT,*)IANS
           IF(IANS.EQ.1)THEN
               WRITE(91,1005)
               CALL WRITED(X,N,M,ND,MD)
           ENDIF
C
C     STANDARDIZE AND PRINT IF NEEDED
C
          DO 100 I=1,N
          DO 100 J=1,M
             XM(I,J)=X(I,J)
100       CONTINUE
          CALL STAND(XM,N,M,ND,MD)
           WRITE(6,*)' PRINT THE STANDARDIZED MATRIX 1=YES'
           READ(NUNIT,*)IANS
           IF(IANS.EQ.1)THEN
               WRITE(91,1006)
               CALL WRITED(XM,N,M,ND,MD)
           ENDIF
C
C    COMPUTE CORRELATION BETWEEN COLUMNS AND PRINT IF NEEDED
C
          CALL RCOEF(XM,N,M,ND,MD,A,MM)
          WRITE(6,*)' PRINT THE CORRELATION BETWEEN COLUMNS 1=YES'
```

```
      READ(NUNIT,*)IANS
      IF(IANS.EQ.1)THEN
          WRITE(91,1007)
          CALL WRITED(A,M,M,MM,MM)
      ENDIF
C
C     SOLVE SIMULTANEOUS EQUATIONS
C
      DO 200 I=2,M
         C(I-1)=A(I,1)
           DO 200 J=2,M
             A(I-1,J-1)=A(I,J)
200   CONTINUE
      CALL SLE(A,C,M-1,MM,1.0E-08)
C
C     CALCULATE PARTIAL REGRESSION COEFFICIENTS
C
      DO 300 I=1,M
         A(1,I)=0.0
         A(2,I)=0.0
           DO 300 J=1,N
             A(1,I)=A(1,I)+X(J,I)
             A(2,I)=A(2,I)+X(J,I)**2
300   CONTINUE
        AA=N
        AB=N-1
        SEC=A(1,1)**2/AA
        FIR=A(2,1)
        AC=SQRT((FIR-SEC)/AB)
        B(1)=A(1,1)/AA
           DO 400 I=2,M
             B(I)=C(I-1)*AC/SQRT((A(2,I)-A(1,I)*A(1,I)/AA)/AB)
             B(1)=B(1)-B(I)*A(1,I)/AA
400        CONTINUE
C
C     COMPUTE ESTIMATED VALUE AND DEVIATION FROM EACH OBSERVATION
C
        DO 500 I=1,N
          D(I,1)=X(I,1)
          D(I,2)=B(1)
           DO 501 J=2,M
             D(I,2)=D(I,2)+B(J)*X(I,J)
501        CONTINUE
             D(I,3)=D(I,1)-D(I,2)
500     CONTINUE
C
C     PRINT DEVIATIONS IF NEEDED
C
       WRITE(6,*)' PRINT THE DEVIATIONS AND OBSERVATIONS 1=YES'
        READ(NUNIT,*)IANS
        IF(IANS.EQ.1)THEN
            WRITE(91,1008)
            CALL WRITED(D,N,3,ND,3)
        ENDIF
C
C     PRINT PARTIAL REGRESION COEFFICIENTS AND STANDARDIZED COEFF.
C
        WRITE(91,1009)
        CALL WRITED(B,M,1,MM,1)
        WRITE(91,1010)
        CALL WRITED(C,M-1,1,MM,1)
C
C     CHECK IF A MATRIX FOR CONTOURING IS NEEDED
C
      WRITE(6,*)'    NEED A MATRIX OF VALUES FOR CONTOURING '
      WRITE(6,*)'    THIS OPTION IS GENERALLY USED IF '
      WRITE(6,*)'    SPATIAL DATA ARE THE INDEPENDENT '
      WRITE(6,*)'    VARIABLE. MAX # OF INDEPENDENT VARIABLES=9.'
      WRITE(6,*)'               1=YES  '
      WRITE(6,*)'     '
      READ(NUNIT,*)ICON
      IF(ICON.EQ.1)CALL CONTOUR(M)
C
C     COMPUTE ERROR MEASUREMENTS
C
        SY=0.0
```

```
      SYY=0.0
      SYC=0.0
      SYYC=0.0
      DO 600 I=1,N
        SY=SY+D(I,1)
        SYY=SYY+D(I,1)**2
        SYC=SYC+D(I,2)
        SYYC=SYYC+D(I,2)**2
600   CONTINUE
      SST=SYY-SY*SY/FLOAT(N)
      SSR=SYYC-SYC*SYC/FLOAT(N)
      SSD=SST-SSR
      NDF1=M-1
      AMSR=SSR/FLOAT(NDF1)
      NDF2=N-M
      AMSD=SSD/FLOAT(NDF2)
      R2=SSR/SST
      R=SQRT(R2)
      F=AMSR/AMSD
      NDF3=N-1
C
C     PRINT ERROR STUFF
C
      WRITE(91,1000)
      WRITE(91,1001)SSR,NDF1,AMSR,F
      WRITE(91,1002)SSD,NDF2,AMSD
      WRITE(91,1003)SST,NDF3
      WRITE(91,1004)R2,R
9999  STOP
C
1000  FORMAT(/,T2,20('*'),' ERROR MEASURES ',20('*'),//,T2,'SOURCE OF',
     &   13X,'SUM OF',
     1'  DEGREES OF   MEAN',/,T2,'VARIATION',13X,'SQUARES   FREEDOM',
     2'   SQUARES    F-TEST',/,T2,60('-'))
1001  FORMAT(T2,'REGRESSION',10X,E10.3,I8,2X,E10.3,/,51X,E10.3)
1002  FORMAT(T2,'DEVIATION',11X,E10.3,I8,2X,E10.3)
1003  FORMAT(T2,'TOTAL VARIATION',5X,E10.3,I8,/,T2,60('-'))
1004  FORMAT(//T2,'GOODNESS OF FIT = ',F10.4,/,
     1T2,'CORRELATION COEFFICIENT = ',F10.4)
1005  FORMAT(//,T12,'INPUT DATA MATRIX ',//,T2,' DATA #  OBSERVED',
     1'    VARIABLES (1...M)------>',/,T13,'VALUES')
1006  FORMAT(/,T12,'STANDARDIZED DATA MATRIX',//)
1007  FORMAT(/,5X,'CORRELATION MATRIX   VARIABLE 1 IS Y',//)
1008  FORMAT(/,T9,'  OBSERVED   ESTIMATED  DEVIATION',//)
1009  FORMAT(/,T2,'  REGRESSION COEFFICIENTS -- #1 IS THE CONSTANT',//)
1010  FORMAT(/,T2,'STANDARDIZED PARTIAL REGRESSION COEFFICIENTS',//)
1020  FORMAT(8E10.3)

      END
C
C
      SUBROUTINE RCOEF(X,N,M,N1,M1,A,M2)
C=============================================================================
C
C    CALCULATES THE CORRELATION BETWEEN COLUMNS OF DATA MATRIX
C=============================================================================
C
      REAL X(N1,M1),A(M2,M2)
      AN=N
C
      DO 100 I=1,M
      DO 100 J=1,M
         SX1=0.0
         SX1X1=0.0
         SX2X2=0.0
         SX1X2=0.0
C
C    CALCULATE SUMS, SUM OF SQUARES AND SUM OF CROSSPRODUCT OF COLUMNS I AND J
C
            DO 200 K=1,N
               SX1=SX1+X(K,I)
               SX2=SX2+X(K,J)
               SX1X1=SX1X1+X(K,I)**2
               SX2X2=SX2X2+X(K,J)**2
               SX1X2=SX1X2+X(K,I)*X(K,J)
200         CONTINUE
```

```
C
C     CALCULATE CORRELATION COEEFICIENT AND PUT IN A
C
       R=(SX1X2-SX1*SX2/AN)/SQRT((SX1X1-SX1*SX1/AN)*(SX2X2-SX2*SX2/AN))
       A(I,J)=R
       A(J,I)=R
 100   CONTINUE
       RETURN
       END

       SUBROUTINE STAND(X,N,M,N1,M1)
C=======================================================================================
C
C     STANDARDIZES THE COLUMNS OF A MATRIX
C=======================================================================================
C
       REAL X(N1,M1)
C
         DO 100 I=1,M
            SX=0.0
            SXX=0.0
              DO 200 J=1,N
                SX=SX+X(J,I)
                SXX=SXX+X(J,I)**2
 200          CONTINUE
                XM=SX/FLOAT(N)
                SD=SQRT((SXX-SX*SX/FLOAT(N))/FLOAT(N-1))
                WRITE(6,*)' STANDARD DEVIATION OF COLUMN #',J,' = ',SD
C
C     SUBTRACT THE MEAN FROM EACH ELEMENT OF THE COLUMN
C
              DO 300 J=1,N
                 X(J,I)=(X(J,I)-XM)/SD
 300          CONTINUE
 100     CONTINUE
       RETURN
       END

       SUBROUTINE READD(A,N,M,N1,M1)
C=======================================================================================
C
C     READS MATRIX OF N ROWS AND M COLUMNS
C=======================================================================================
C
      REAL A(N1,M1)
      COMMON/PAR/IPFOD,NUNIT,IOWN
      WRITE(6,*)' DATA CAN BE FREE-FORMATTED '
      WRITE(6,*)'   Y    X1    X2     X3    X4   XM'
      WRITE(6,*)'   '
      WRITE(6,*)' ENTER # OF VARIABLES (NUMBER OF X VALUES FOR EACH Y)'
      READ(NUNIT,*)INNU
      M=INNU+1
      DO 100 I=1,1000
         READ(90,*,END=99) (A(I,J),J=1,M)
100   CONTINUE
99    N = I-1
      MORIGIN=M
      WRITE(6,*)' NEED TO EXCLUDE ANY COLUMNS OF INDEPENDENT VARIABLES'
      WRITE(6,*)'  IF SO, ENTER HOW MANY COLUMNS SHOULD BE  EXCLUDED'
      READ(NUNIT,*)ICOLE
         DO 70 MM=1,ICOLE
            WRITE(6,*)' ENTER THE COLUMN # TO EXCLUDE'
            WRITE(6,*)' BEGIN WITH THE LOWEST COLUMN #'
            WRITE(6,*)' COLUMN # 1 IS THE FIRST INDEPENDENT VARIABLE '
            IF(MM.GT.1)THEN
              WRITE(6,*)'   '
              WRITE(6,*)' REMEMBER, THE COLUMNS HAVE BEEN RENUMBERED'
              WRITE(6,*)'   '
            ENDIF
            READ(NUNIT,*)ICN
               DO 80 J=ICN+1,MORIGIN-1
                 DO 90 I=1,N
                    A(I,J)=A(I,J+1)
 90              CONTINUE
 80            CONTINUE
                 M=M-1
```

```
                WRITE(6,*)' COLUMN # ',ICN,' HAS BEEN EXCLUDED'
70      CONTINUE
      WRITE(6,*)' NEED TO TAKE THE LOG OF THE Y VALUES 1=YES'
      READ(NUNIT,*)ILO
      IF(ILO.EQ.1)THEN
         DO 60 I=1,N
           A(I,1)=LOG10(A(I,1))
60       CONTINUE
      END IF
      WRITE(6,*)' NEED A COMBINATION OF THE INDEPENDENT VARIABLES'
      WRITE(6,*)' FOR INSTANCE, X*Y**2,  1=YES'
      READ(NUNIT,*)ICOMTR
      IF(ICOMTR.EQ.1)THEN
         WRITE(6,*)' HOW MANY EXTRA DEPENDENT VARIABLES ARE NEEDED'
         READ(NUNIT,*)NMCN
       DO 200 III=1,NMCN
         WRITE(6,*)' ENTER 2 COLUMN #S THAT ARE TO BE MULTIPLIED'
         WRITE(6,*)' THESE ARE FROM ANY COLUMNS THAT EXIST'
         WRITE(6,*)' COLUMN # 1 IS THE FIRST DEPENDENT VARIABLE'
         READ(NUNIT,*)IMC1,IMC2
         IMC1=IMC1+1
         IMC2=IMC2+1
         WRITE(6,*)' ENTER THE EXPONENT FOR COLUMN 1 AND 2 '
         READ(NUNIT,*)IXPN1,IXPN2
              M=M+1
              DO 300 NN=1,N
                   A(NN,M)=(A(NN,IMC1)**IXPN1)*(A(NN,IMC2)**IXPN2)
300           CONTINUE
200    CONTINUE
      END IF
      WRITE(6,*)' THE NUMBER OF OBSERVATIONS =',N
      RETURN
      END

      SUBROUTINE WRITED(A,N,M,N1,M1)
C=======================================================================
C
C     PRINTS OUT THE MATRIX OF N ROWS AND M COLUMNS
C=======================================================================
C
      COMMON/PAR/IPFOD,NUNIT,IOWN
      REAL A(N1,M1)
      DO 100 IB=1,M,10
        IE = IB + 9
         IF(IE-M) 2,2,1
1          IE = M
C       PRINT THE HEADING
2          WRITE(91,2000) (I,I=IB,IE)
           IF(IPFOD.EQ.1)GOTO 250
             DO 101 J=1,N
               WRITE(91,2001) J,(A(J,K),K=IB,IE)
101          CONTINUE
           GOTO 251
250         DO 201 J=1,N
               WRITE(91,2002) J,(A(J,K),K=IB,IE)
201         CONTINUE
251       CONTINUE
100   CONTINUE
2000  FORMAT(T2,10I12)
2001  FORMAT(T2,I5,10F12.4)
2002  FORMAT(T2,I5,10E12.4)
      RETURN
      END

      SUBROUTINE SLE(A,B,N,N1,ZERO)
C=======================================================================
C
C    SOLVES A SYSTEM OF N SIMULTANEOUS EQUATIONS
C=======================================================================
C
       REAL  A(N1,N1),B(N1)
       DO 100 I=1,N
         DIV= A(I,I)
           IF(ABS(DIV)-ZERO) 99,99,1
1        DO 101 J=1,N
           A(I,J)= A(I,J)/DIV
```

```
101      CONTINUE
         B(I)= B(I)/DIV
         DO 102 J=1,N
           IF (I-J) 2,102,2
2          RATIO = A(J,I)
             DO 103 K=1,N
               A(J,K)= A(J,K) - RATIO*A(I,K)
103          CONTINUE
             B(J)= B(J)- RATIO*B(I)
102     CONTINUE
100    CONTINUE
99    CONTINUE
      RETURN
      END

      SUBROUTINE CONTOUR(M)
C=====================================================================
C    SUBROUTINE TO PRODUCE A CONTOUR FILE IN THE CORRECT FORM FOR THE
C    DISSPLA ROUTINES
C=====================================================================
C
        CHARACTER *80 FILC,FILDAT,LAMFIL
        COMMON/BASIC/ X(500,20),XM(500,20),D(500,3),ZCONT(8075),ZZ(8075)
        COMMON/ARRAY/ A(50,50),B(50),C(50),IEXPX(20),IEXPY(20)
        COMMON/PAR/IPFOD,NUNIT,IOWN
        COMMON/REGRES/ COEFF(10)
        REAL ZATA(8075)

        IF(IOWN.EQ.1)THEN
            DO 50 I=1,10
               B(I)=COEFF(I)
               WRITE(6,*)' B',I,'  =',B(I)
 50         CONTINUE
        ELSEIF(IOWN.EQ.0)THEN
            CONTINUE
        ENDIF

           WRITE(6,*)'  ENTER THE FILENAME FOR THE CONTOUR DATA'
           READ(NUNIT,'(A)')FILC
      OPEN(UNIT=95,FILE=FILC,STATUS='UNKNOWN',CARRIAGECONTROL='LIST')
           WRITE(6,*)'    ENTER THE MINIMUM DISTANCE, SPACING,'
           WRITE(6,*)' & HOW MANY GRID LINES IN THE X-DIRECTION '
           WRITE(6,*)'     NO ZEROES ALLOWED '
           READ(6,*)XMIN,DELX,NGRIDX
           WRITE(6,*)'     '
           WRITE(6,*)'    ENTER THE MINIMUM DISTANCE, SPACING,'
           WRITE(6,*)' & HOW MANY GRID LINES IN THE Y-DIRECTION '
           WRITE(6,*)'     NO ZEROES ALLOWED '
           READ(6,*)YMIN,DELY,NGRIDY
           WRITE(6,*)'     '
C
           DO 449 I=1,9
               IEXPX(I)=0.0
               IEXPY(I)=0.0
 449       CONTINUE
           DO 450 I=1,M-1
           WRITE(6,*)' ENTER EXPONENT OF X AND Y IN INDEPENDENT VAR.#',I
           READ(NUNIT,*)IEXPX(I),IEXPY(I)
 450       CONTINUE
C
            NUMPTS=NGRIDX*NGRIDY
            YMAX=NGRIDY*DELY+YMIN-DELY
            XMAX=NGRIDX*DELX+XMIN-DELX
            I=0
             DO 550 YP=YMIN,YMAX,DELY
               DO 560 XP=XMIN,XMAX,DELX
                  I=I+1
           ZCONT(I)=B(1)+(B(2)*XP**IEXPX(1)*YP**(IEXPY(1)))+
     1                   (B(3)*XP**IEXPX(2)*YP**(IEXPY(2)))+
     2                   (B(4)*XP**IEXPX(3)*YP**(IEXPY(3)))+
     3                   (B(5)*XP**IEXPX(4)*YP**(IEXPY(4)))+
     4                   (B(6)*XP**IEXPX(5)*YP**(IEXPY(5)))+
     5                   (B(7)*XP**IEXPX(6)*YP**(IEXPY(6)))+
     6                   (B(8)*XP**IEXPX(7)*YP**(IEXPY(7)))+
     7                   (B(9)*XP**IEXPX(8)*YP**(IEXPY(8)))+
     8                   (B(10)*XP**IEXPX(9)*YP**(IEXPY(9)))
```

```
560           CONTINUE
550         CONTINUE
          WRITE(6,*)' INVERT THE CONTOUR MATRIX'
          READ(NUNIT,*)INVERT
          IF (INVERT.EQ.1)THEN
             II=0
             DO 650 I=1,NGRIDY
               DO 660 J=1,NGRIDX
                  II=II+1
                  KKK=NUMPTS-(I*NGRIDX)+J
                  ZATA(II)=ZCONT(KKK)
660           CONTINUE
650         CONTINUE
                  WRITE(95,1020)(ZATA(I),I=1,NUMPTS)
          ELSE
                  WRITE(95,1020)(ZCONT(I),I=1,NUMPTS)
          ENDIF

          WRITE(6,*)' THE DATA HAS BEEN WRITTEN TO FILE ',FILC
          WRITE(6,*)'  ENTER THE FILENAME FOR THE INPUT DATA'
          READ(NUNIT,'(A)')FILDAT
       OPEN(UNIT=94,FILE=FILDAT,STATUS='UNKNOWN',CARRIAGECONTROL='LIST')
C
C      REARRANGE THE MATRIX FROM CONTOURING FORMAT TO THE INPUT DATA FORMAT
C
          WRITE(6,*)' TAKE THE ANTI-LOG OF THE NUMBERS 1=YES'
          READ(5,*)ITAKLOG
          IF(INVERT.EQ.1)THEN
          DO 790 I=1,NUMPTS
             ZZ(I)=ZATA(I)
 790      CONTINUE
          DO 791 I=1,NUMPTS
             ZCONT(I)=ZZ(I)
 791      CONTINUE
          ENDIF

          JJ=0
          KK=1
          NUMPT=NUMPTS
              DO 701 J=1,NUMPTS
                   KKK=JJ*NGRIDX+KK
                   IF(ITAKLOG.EQ.1)THEN
                     CONST1=ABS(ZCONT(KKK))
                     ZATA(J)=1.0/10**CONST1
                   ELSEIF(ITAKLOG.EQ.0)THEN
                     ZATA(J)=ZCONT(KKK)
                   ENDIF
                   IF(ZATA(J).EQ.0.0)WRITE(6,*)' ZERO AT #',J,KKK
                   JJ=JJ+1
                      IF(JJ.EQ.NGRIDY)THEN
                        JJ=0
                        KK=KK+1
                      ENDIF
 701         CONTINUE
       WRITE(94,1020)(ZATA(I),I=1,NUMPTS)
       WRITE(6,*)'     NEED A FILE OF LAMBDA VALUES   '
       WRITE(6,*)'      WHERE   (LAMBDA = 1 - 1/N)  '
       WRITE(6,*)'            1 = YES'
       READ(NUNIT,*)ILAMFI
       IF(ILAMFI.EQ.1)THEN
        WRITE(6,*)' ENTER THE FILE NAME FOR THE LAMBDA DATA'
        READ(NUNIT,'(A)')LAMFIL
       OPEN(UNIT=80,FILE=LAMFIL,STATUS='UNKNOWN',CARRIAGECONTROL='LIST')
          JJ=0
          KK=1
          NUMPT=NUMPTS
             DO 750 J=1,NUMPTS
                   KKK=JJ*NGRIDX+KK
                   ZATA(J)= 1.0 - 1.0/ZCONT(KKK)
                   IF(ZATA(J).EQ.0.0)WRITE(6,*)' ZERO AT #',J,KKK
                   JJ=JJ+1
                      IF(JJ.EQ.NGRIDY)THEN
                        JJ=0
                        KK=KK+1
                      ENDIF
 750                  CONTINUE
```

```
      ENDIF
      WRITE(80,1020)(ZATA(I),I=1,NUMPTS)
1020  FORMAT(8E10.3)
      RETURN
      END

      SUBROUTINE MAKMAP
C=====================================================================
C
C     SUBROUTINE TO PRODUCE A FIELD OF VALUES FROM SUPPLIED REGRESSION
C     COEFFICIENTS.  CALLS CONTOUR SUBROUTINE TO PROVIDE A CONTOUR
C     MAP.
C=====================================================================
C
      COMMON/PAR/IPFOD,NUNIT,IOWN
      COMMON/REGRES/ COEFF(10)
      WRITE(6,*)' ENTER THE NUMBER OF REGRESSION COEFFICIENTS'
      WRITE(6,*)' INCLUDING THE CONSTANT, WHICH IS COEFF. #1'
      READ(NUNIT,*)NREGCO
      DO 100 I=1,NREGCO
            WRITE(6,*)' ENTER REGRESSION COEFFICIENT # ',I
            READ(5,*)COEFF(I)
 100  CONTINUE
      CALL CONTOUR(NREGCO)
      RETURN
      END
```

Discussion of method used to incorporate anisotropic covariance structure in kriging algorithm.

In order to consider anisotropic covariance structure in the conditioned hydraulic property fields, incorporation of anisotropic covariance structure in the kriging equations was performed. If the anisotropy is at right angles and is aligned with the principle axes, it can be handled by a simple coordinate transformation. Assume the correlation scales for the properties are given by λ_x and λ_z in the horizontal and vertical directions respectively. If λ_x is not equal to λ_z, a new coordinate system x' and z' can be defined to account for the anisotropic nature of the covariance structure. Let λ' equal some arbitrary correlation length, usually taken as either λ_x or λ_z for convenience. Then the effective isotropic coordinates can be defined as follows:

$$x' = \sqrt{\lambda'/\lambda_x}$$

$$z' = \sqrt{\lambda'/\lambda_z}$$

This simple transformation is analogous to the transformation of a coordinate system in which anisotropy exists in the hydraulic conductivity. With the transformed coordinate system, kriging and conditioning can be performed as if an isotropic covariance structure existed and the prediction locations can be transformed back to the original coordinate system to obtain the true anisotropic structure of the data. This simple procedure is performed in the subroutine SCALFAC of program CONDITION.FOR.

```
      PROGRAM CONDITION
C=======================================================================
C
C     ROUTINE TO PERFORM KRIGING OR FIELD CONDITIONING ON A
C     GIVEN SET OF DATA.  THE MAIN PURPOSE
C     BEING TO CALCULATE CONDITIONAL SIMULATION FIELDS GIVEN A
C     CERTAIN COVARIANCE STRUCTURE AND KNOWN DATA VALUES AT GIVEN
C     LOCATIONS IN THE DOMAIN.
C
C=======================================================================
C
C                ******     VARIABLES     *******
C
C       NPTS      = NUMBER OF ORIGINAL DATA POINTS IN THE FIELD
C       A         = COVARIANCE MATRIX
C       BB        = 1-D ARRAY OF THE COVARIANCE STRUCTURE OF GIVEN POINTS
C                   AND THE POINT OF CONSIDERATION FOR PRECDICTION
C       DLOCX     = ARRAY OF ORIGINAL DATA LOCATIONS IN X DIRECTION
C       DLOCY     = ARRAY OF ORIGINAL DATA LOCATIONS IN Y DIRECTION
C       EST       = ARRAY OF KRIGED VALUES FROM THE ORIGINAL DATA FIELD
C       IC        = COUNTER ON LOOP TO CONTROL THE CONDITIONING
C                     IC=1   =======> KRIGE THE ACTUAL DATA
C                     IC=2   =======> KRIGE THE UNCONDITIONED FIELD
C       ICOV      = FLAG TO DETERMINE THE COVARIANCE STRUCTURE
C                     ICOV = 1 =====> BELL SHAPED, NORMAL, OR "GAUSSIAN"
C                     ICOV = 2 =====> EXPONENTIAL
C                     ICOV = 3 =====> LINEAR
C       IFLAGC    = FLAG TO CHECK IF CONDITIONAL SIMULATION IS TO BE PERFORMED
C                     IFLAGC = 1   TO KRIG DATA ONLY
C                     IFLAGC = 2   TO GET CONDITIONAL FIELD
C       ILOGV     = FLAG TO TAKE THE LOG BASE 10 OF THE DATA FIELD
C                     ILOGV =1  =====>  YES
C                     ILOGV =0  =====>  NO
C       IMEAN     = FLAG TO CHECK IF MEAN FIELD SHOULD BE SUBTRACTED
C                     IMEAN =1  =====>  YES
C                     IMEAN =0  =====>  NO
C                     !!!!!!   NOTE   !!!!!!!
C                     (IF IMEAN EQUALS 1, THE MEAN FIELD WILL BE SUBTRACTED
C                     FROM THE UNCONDITIONED FIELD AND THE ORIGINAL DATA. )
C       INDEX     = ARRAY CONTAINING THE PREDICTION IDENTIFICATION # OF
C                   THE "OBSERVED" DATA
C       IPIN      = FLAG TO PRINT INPUT
C                     IPIN =1  =====>  YES
C                     IPIN =0  =====>  NO
C       IPM       = FLAG TO PRINT MEAN FIELD
C                     IPM =1  =====>  YES
C                     IPM =0  =====>  NO
C       IPMO      = FLAG TO PRINT "MEAN ZERO" FIELD
C                     FIELD OF TRUE VALUES MINUS THE MEAN
C                     IPM =1  =====>  YES
C                     IPM =0  =====>  NO
C       IPPL      = FLAG TO PRINT PREDICTION LOCATIONS
C                     IPPL =1  =====>  YES
C                     IPPL =0  =====>  NO
C       IPTRAN    = FLAG TO PRINT TRANSFORMED ANISOTROPIC LOCATIONS
C                     IPTRAN =1  =====>  YES
C                     IPTRAN =0  =====>  NO
C       IPUN      = FLAG TO PRINT UNCONDITIONAL FIELD
C                     IPUN =1  =====>  YES
C                     IPUN =0  =====>  NO
C       IPPUNC    = FLAG TO PRINT PICKED LOCATIONS OF UNCONDITIONAL FIELD
C                     IPPUNC =1  =====>  YES
C                     IPPUNC =0  =====>  NO
C       KFLAG     = FLAG TO CHECK IF PREDICTION LOCATIONS COME FROM FILE
C                     KFLAG = 1  =====> YES
C                     KFLAG = 2  =====> NO
C       NP        = PARAMETER TO INDICATE THE MAXIMUM SIZE OF THE ARRAYS
C                 = >= THE MAXIMUM NUMBER OF OBSERVED VALUES
C       NPR       = PARAMETER TO INDICATE SIZE OF PREDICTION ARRAYS
C                 = >= THE MAXIMUM NUMBER OF PREDICTIONS
C       NPRED     = NUMBER OF PREDICTION LOCATIONS
C       NUNF      = NUMBER OF UNCONDITIONAL FILES TO BE READ AND CONDITIONED
C       PLOCX     = ARRAY OF PREDICTION LOCATIONS IN X DIRECTION
C       PLOCY     = ARRAY OF PREDICTION LOCATIONS IN Y DIRECTION
C       S         = [Y*V]
C       SCALEX    = CORRELATION LENGTH IN X DIRECTION
```

```
C       SCALEY    = CORRELATION LENGTH IN Y DIRECTION
C       SCALET    = PRESCRIBED CORRELATION LENGTH IN TRANSFORMED COORDINATES
C       PUNCON    = ARRAY DATA FROM UNCONDITIONED FIELD WHICH ARE PICKED AT THE
C                   SAME LOCATIONS AS THE "OBSERVED" FIELD
C       UNCOND    = ARRAY OF THE UNCONDITIONED DATA
C       V         = ARRAY OF GIVEN OR "OBSERVED" DATA
C       VAR       = VARIANCE OF THE COVARIANCE MODEL
C       VCS       = ARRAY CONTAINING THE CONDITIONED FIELD
C       VH        = KRIGED ESTIMATE OF THE "OBSERVED" DATA AT A LOCATION
C       WH        = ARRAY OF KRIGED VALUES FROM THE UNCONDITIONAL DATA FIELD
C       XMIN      = MINIMUM X DISTANCE IN GRID OF PREDICTION LOCATIONS
C       XSKIP     = DELTA X DISTANCE IN GRID OF PREDICTION LOCATIONS
C       XSTART    = LOCATION OF STARTING POINT IN GRID OF PREDICTION LOCATIONS
C       XMAX      = MAXIMUM X DISTANCE IN GRID OF PREDICTION LOCATIONS
C       YMIN      = MINIMUM Y DISTANCE IN GRID OF PREDICTION LOCATIONS
C       YSKIP     = DELTA Y DISTANCE IN GRID OF PREDICTION LOCATIONS
C       YSTART    = LOCATION OF STARTING POINT IN GRID OF PREDICTION LOCATIONS
C       YMAX      = MAXIMUM Y DISTANCE IN GRID OF PREDICTION LOCATIONS
C       Y         = INVERTED MATRIX (REAL*16 FOR PRECISION)
C       Z         = INVERTED MATRIX (REDUCED TO REAL*8 FOR EFFICIENCY IN
C                   CALCULATION OF KRIGED AND CONDITIONED PATH)
C
C=======================================================================
C
        IMPLICIT REAL*8 (A-H,O-Z)
        PARAMETER(NP=100,NPR=8424)
        REAL*16 A(NP,NP),Y(NP,NP)
        REAL*8 VH(NP,1),S(NP,NP),EST(NPR),Z(NP,NP),
     *       PLOCX(NPR),PLOCY(NPR),DLOCX(NP),DLOCY(NP),BB(NP,1),
     *       VCS(NPR),WH(NPR),UNCOND(NPR,1),V(NP,1),PUNCON(NP,1)
        COMMON/DATA/ SCALEX,SCALEY,SCALET,VAR,NPTS,NPRED,IPMO,IMEAN,IPM
        COMMON/FLAGS/IFLAGC,IPIN,KFLAG,IPPL,IPTRAN,IPUNC,NUNF,IPPUNC
        COMMON/MATRX/NPX,NPY,IDIREC,XMIN,XMAX,XSKIP,YMIN,
     *              YSKIP,YMAX,XSTART,YSTART
        COMMON/FILES/FILUNC(20),NCF(20),FILPD(20),NCFP(20)
        CHARACTER *80 FILDAT,FILOUT,FILPRD,FILUNC,FILPD,FILUN,FILP
        INTEGER INDEX(NP)
C
C=====  READ THE DATA ON WHICH KRIGING WILL BE CONDUCTED
C
        CALL READD(V,PLOCX,PLOCY,DLOCX,DLOCY,UNCOND,PUNCON,INDEX)
C
C=====  LOAD COVARIANCE MATRIX
C
        CALL LOADC(A,DLOCX,DLOCY)
C
C=====  INVERT THE COVARIANCE MATRIX
C
        CALL INVERT(A,Y,NPTS)
         DO 80 I=1,NPTS
           DO 81 J=1,NPTS
            Z(I,J)=Y(I,J)
 81        CONTINUE
 80       CONTINUE

C
C=====  START A LOOP FOR EACH OF THE RUNS TO CONDITION A FIELD FROM AN
C       UNCONDITIONED FIELD
C
      DO 500 NU=1,NUNF
        IF(IFLAGC.EQ.2)THEN
          FILUN=FILUNC(NU)(:NCF(NU))
          OPEN(60,FILE=FILUN,STATUS='OLD')
          FILP=FILPD(NU)(:NCFP(NU))
          WRITE(6,*)' WORKING OF FILE ',FILP
          OPEN(75,FILE=FILP,STATUS='UNKNOWN',CARRIAGECONTROL='LIST')
          NUN=75
C
          READ(60,1000)(UNCOND(I,1),I=1,NPRED)
          IF(IMEAN.EQ.1)CALL MEAN(UNCOND,V,INDEX,2,DLOCX,DLOCY)
          CALL PICK(UNCOND,PUNCON,PLOCX,PLOCY,INDEX)
C
            IF(IPUNC.EQ.1)THEN
              WRITE(90,1010)
              WRITE(90,*)(UNCOND(I,1),I=1,NPRED)
            ENDIF
```

```
        ELSEIF(IFLAGC.EQ.1)THEN
          NUN=90
        ENDIF

C
C=====  GO THROUGH THE CONDITIONAL SIMULATION PROCEDURE FOR EACH LOCATION
C       A PREDICTION IS NEEDED
C
         ITOTP=IFLAGC*NPRED
         JT=0
         DO 200 IC=1,IFLAGC
C
C=====  FIND [Y*V] FOR ALL OF THE CONDITIONS
C
          IF(IC.EQ.1.AND.NU.EQ.1)THEN
             CALL MULTIP(Z,V,S,NPTS,NPTS,1)
          ELSEIF(IC.EQ.2)THEN
             CALL MULTIP(Z,PUNCON,S,NPTS,NPTS,1)
          ENDIF
C
C=====TRANSPOSE MATRIX
C
         DO 100 I=1,NPTS
             S(1,I)=S(I,1)
 100     CONTINUE
C
C=====   PREDICT THE FIELD
C
          JCONT=0
          IF(IC.EQ.1.AND.NU.EQ.1)THEN
            WRITE(*,*)' KRIGING FIELD #',NU,'  OF',NUNF
          ELSEIF(IC.EQ.2)THEN
            WRITE(*,*)' CONDITIONING FIELD #',NU,'  OF',NUNF
          ENDIF
            DO 300 J=1,NPRED
                JT=JT+1
                JCONT=JCONT+1
                IF(JCONT.EQ.1000)THEN
                  JCONT=0
                  WRITE(*,*)' COMPLETED',JT,' OF',ITOTP,' POINTS'
                ENDIF
                IF(IC.EQ.1.AND.NU.EQ.1)THEN
                   CALL LOADB(BB,PLOCX(J),PLOCY(J),DLOCX,DLOCY)
                   CALL MULTIP(S,BB,VH,1,NPTS,1)
                   EST(J)=VH(1,1)
                ELSEIF(IC.EQ.2)THEN
                   CALL LOADB(BB,PLOCX(J),PLOCY(J),DLOCX,DLOCY)
                   CALL MULTIP(S,BB,VH,1,NPTS,1)
                   WH(J)=VH(1,1)
                ENDIF
 300         CONTINUE
 200     CONTINUE
C
C===== COMPUTE THE CONDITIONAL FIELD IF NEEDED AND PRINT
C
       IF(IFLAGC.EQ.1)THEN
         IF(IMEAN.EQ.1)CALL MEAN(EST,V,INDEX,1,DLOCX,DLOCY)
          WRITE(NUN,1002)
          WRITE(NUN,1000)(EST(I),I=1,NPRED)
       ELSEIF(IFLAGC.EQ.2)THEN
          DO 400 I=1,NPRED
               VCS(I)=EST(I)+(UNCOND(I,1)-WH(I))
 400     CONTINUE
         IF(IMEAN.EQ.1)CALL MEAN(VCS,V,INDEX,1,DLOCX,DLOCY)
c         WRITE(NUN,1003)
         WRITE(NUN,1000)(VCS(I),I=1,NPRED)
       ENDIF
       CLOSE(60)
       CLOSE(75)
 500  CONTINUE
C
C=====
C
 1000  FORMAT(8E10.3)
 1001  FORMAT(8G10.3)
 1002  FORMAT(79('*'),///,20X,'KRIGED FIELD',/79('*'))
```

```
 1003  FORMAT(79('*'),///,20X,'CONDITIONED FIELD',/,79('*'))
 1005  FORMAT(8E10.3)
 1007  FORMAT(I8,T10,G13.4,T25,G13.4,T45,G13.4)
 1010   FORMAT(//,10X,' INPUT DATA FROM THE UNCONDITIONAL FIELD',/)


C
C=====  FINISHED !!!
C
         STOP
         END
C
C
C
        SUBROUTINE GETPRED(DLOCX,DLOCY,PLOCX,PLOCY,INDEX)
C============================================================ SUBROUTINE GETPRED
C
C     SUBROUTINE TO GET A REGULAR GRID OF PREDICTION LOCATIONS FOR THE
C     CONDITIONAL SIMULATION ALGORITHM.
C
C=========================================================================
C
C
         IMPLICIT REAL*8 (A-H,O-Z)
         PARAMETER(NP=100,NPR=8424)
         REAL*8 PLOCX(NPR),PLOCY(NPR),DLOCX(NP),DLOCY(NP)
         INTEGER INDEX(NP)
         COMMON/MATRX/NPX,NPY,IDIREC,XMIN,XMAX,XSKIP,YMIN,
     *               YSKIP,YMAX,XSTART,YSTART
         COMMON/DATA/ SCALEX,SCALEY,SCALET,VAR,NPTS,NPRED,IPM0,IMEAN,IPM
         COMMON/FLAGS/IFLAGC,IPIN,KFLAG,IPPL,IPTRAN,IPUNC,NUNF,IPPUNC
C
C=====   CALCULATE THE SIZE OF GRID AND CHECK WHERE TO START
C
          NPX=(AINT(XMAX-XMIN)/XSKIP)+1
          NPY=(AINT(YMAX-YMIN)/YSKIP)+1
          NPRED=NPX*NPY
          IF(YSTART.EQ.YMAX)THEN
               YMULT=-1.0
               YS=YMAX
          ELSEIF(YSTART.EQ.YMIN)THEN
               YMULT=1.0
               YS=YMIN
          ENDIF
          IF(XSTART.EQ.XMAX)THEN
               XMULT=-1.0
               XS=XMAX
          ELSEIF(XSTART.EQ.XMIN)THEN
               XMULT=1.0
               XS=XMIN
          ENDIF
C
C===== BUILD MATRIX OF PREDICTION LOCATIONS
C
       ICONT=0
       IF(IDIREC.EQ.1)THEN
          DO 200 I=1,NPY
            DO 300 J=1,NPX
               ICONT=ICONT+1
                PLOCX(ICONT)=XS+XMULT*(J-1)*XSKIP
                PLOCY(ICONT)=YS+YMULT*(I-1)*YSKIP
                 IF(IMEAN.EQ.1.OR.IFLAGC.EQ.2)THEN
                   DO 400 JJ=1,NPTS
                     IF(INDEX(JJ).GT.0)GOTO 400
                     IF(PLOCX(ICONT).EQ.DLOCX(JJ)) THEN
                       IF(PLOCY(ICONT).EQ.DLOCY(JJ)) THEN
                          INDEX(JJ)=ICONT
                       ENDIF
                     ENDIF
 400               CONTINUE
                ENDIF
 300         CONTINUE
 200       CONTINUE

       ELSEIF(IDIREC.EQ.2)THEN
          DO 201 J=1,NPX
```

```
            DO 301 I=1,NPY
               ICONT=ICONT+1
                PLOCX(ICONT)=XS+XMULT*(J-1)*XSKIP
                PLOCY(ICONT)=YS+YMULT*(I-1)*YSKIP
                 IF(IMEAN.EQ.1.OR.IFLAGC.EQ.2)THEN
                  DO 500 JJ=1,NPTS
                     IF(INDEX(JJ).GT.0)GOTO 500
                     IF(PLOCX(ICONT).EQ.DLOCX(JJ)) THEN
                       IF(PLOCY(ICONT).EQ.DLOCY(JJ)) THEN
                          INDEX(JJ)=ICONT
                       ENDIF
                     ENDIF
500               CONTINUE
                 ENDIF
301           CONTINUE
201        CONTINUE
         ENDIF
          IF(IFLAGC.EQ.2)THEN
            DO 700 I=1,NPTS
             IF(INDEX(I).EQ.0)THEN
                 WRITE(*,*)'       !!!!!!!!!!  WARNING  !!!!!!!!!!!'
                 WRITE(*,*)' INDEX(',I,')',' = ',INDEX(I)
                 WRITE(90,*)'       !!!!!!!!!!  WARNING  !!!!!!!!!!!'
                 WRITE(90,*)' INDEX(',I,')',' = ',INDEX(I)
             ENDIF
700        CONTINUE
          ENDIF
         RETURN
         END
C
C
          SUBROUTINE INVERT(A,Y,N)
C=============================================================== SUBROUTINE INVERT
C
C       SUBROUTINE TO INVERT A MATRIX BY CALLING OTHER SUBROUTINES WHICH
C       PERFORM LU DECOMPOSTION AND BACKWARD SUBSTITUTION.
C
C=============================================================================
C
          IMPLICIT REAL*8 (A-H,O-Z)
          PARAMETER(NP=100,NPR=8424)
          REAL*16 INDX(NP),A(NP,NP),Y(NP,NP)
C
             DO 100 I=1,N
                DO 110 J=1,N
                    Y(I,J)=0.0
110             CONTINUE
                Y(I,I)=1.
100          CONTINUE
                   CALL LUDCMP(A,N,INDX,D)
             DO 120 J=1,N
                   FRAC=(FLOAT(J)/FLOAT(N))*100.
                   WRITE(*,1000)FRAC
                   CALL LUBKSB(A,N,INDX,Y(1,J))
120          CONTINUE
1000       FORMAT(G12.3,' % COMPLETED WITH LU BACK SUBSTITUTION')
           RETURN
           END
C
C
          SUBROUTINE LOADC(A,DLX,DLY)
C=============================================================== SUBROUTINE LOADC
C
C       SUBROUTINE TO LOAD THE COVARIANCE MATRIX
C
C=============================================================================
C
          IMPLICIT REAL*8 (A-H,O-Z)
          PARAMETER(NP=100,NPR=8424)
          COMMON/DATA/ SCALEX,SCALEY,SCALET,VAR,NPTS,NPRED,IPMO,IMEAN,IPM
          COMMON/COV/ICOV,SMALLV
          REAL*16 A(NP,NP)
          REAL*8  DLX(NP),DLY(NP)
C
         COVL(X,SCALET,VAR)=VAR*(1.-(DABS(X)/SCALET))
         COVE(X,SCALET,VAR)=VAR*EXP(-(DABS(X))/SCALET)
```

```
      COVG(X,SCALET,VAR)=VAR*EXP(-(DABS(X*X))/(SCALET**2))
C
      DO 100 I=1,NPTS
         DO 200 J=1,NPTS
            DIS = DSQRT(((DLX(I)-DLX(J))**2)+((DLY(I)-DLY(J))**2))
             IF(ICOV.EQ.1)THEN
                  A(I,J)= COVG(DIS,SCALET,VAR)
             ELSEIF(ICOV.EQ.2)THEN
                  A(I,J)= COVE(DIS,SCALET,VAR)
             ELSEIF(ICOV.EQ.3)THEN
                  A(I,J)= COVL(DIS,SCALET,VAR)
             ENDIF
 200     CONTINUE
 100  CONTINUE
      RETURN
      END
C
C
        SUBROUTINE LOADB(BB,PLX,PLY,DLX,DLY)
C======================================================== SUBROUTINE LOADB
C
C     SUBROUTINE TO LOAD THE RIGHT HAND SIDE MATRIX
C
C     BB IS THE RHS COLUMN MATRIX
C     DLX IS THE LOCATION OF THE DATA POINT ON THE X AXIS
C     DLY IS THE LOCATION OF THE DATA POINT ON THE Y AXIS
C     PLX IS THE LOCATION OF THE PREDICTION POINT ON THE X AXIS
C     PLX IS THE LOCATION OF THE PREDICTION POINT ON THE Y AXIS
C
C=============================================================================
C
        IMPLICIT REAL*8 (A-H,O-Z)
        PARAMETER(NP=100,NPR=8424)
        COMMON/DATA/ SCALEX,SCALEY,SCALET,VAR,NPTS,NPRED,IPM0,IMEAN,IPM
        COMMON/COV/ICOV,SMALLV
        REAL*8 BB(NP,1),DLX(NPR),DLY(NPR)
C
      COVL(X,SCALET,VAR)=VAR*(1.-(DABS(X)/SCALET))
      COVE(X,SCALET,VAR)=VAR*EXP(-(DABS(X))/SCALET)
      COVG(X,SCALET,VAR)=VAR*EXP(-(DABS(X*X))/(SCALET**2))
C
      DO 100 I=1,NPTS
               DIS = DSQRT(((DLX(I)-PLX)**2)+((DLY(I)-PLY)**2))
               IF(ICOV.EQ.1)THEN
                    BB(I,1)= COVG(DIS,SCALET,VAR)
               ELSEIF(ICOV.EQ.2)THEN
                    BB(I,1)= COVE(DIS,SCALET,VAR)
               ELSEIF(ICOV.EQ.3)THEN
                    BB(I,1)= COVL(DIS,SCALET,VAR)
               ENDIF
 100  CONTINUE
      RETURN
      END
C
C
        SUBROUTINE LUBKSB(A,N,INDX,B)
C======================================================== SUBROUTINE LUBKSB
C
C       SOLVES A SET OF LINEAR EQUATION A*X = B
C       BACKSUBSTITUTION ALGORITM
C
C=============================================================================
C
        IMPLICIT REAL*16 (A-H,O-Z)
        PARAMETER(NP=100,NPR=8424)
        REAL*16 INDX(N),B(N),A(NP,NP)
C
        II=0
          DO 100 I=1,N
            LL=INDX(I)
            SUM=B(LL)
            B(LL)=B(I)
            IF(II.NE.0)THEN
               DO 110 J=II,I-1
                   SUM=SUM-A(I,J)*B(J)
 110           CONTINUE
```

```
            ELSEIF(SUM.NE.0)THEN
               II=I
            ENDIF
            B(I)=SUM
100       CONTINUE
          DO 130 I=N,1,-1
            SUM=B(I)
            IF(I.LT.N)THEN
                DO 140 J=I+1,N
                   SUM=SUM-A(I,J)*B(J)
140             CONTINUE
            ENDIF
            B(I)=SUM/A(I,I)
130       CONTINUE
          RETURN
          END
C
C
      SUBROUTINE LUDCMP(A,N,INDX,D)
C=======================================================    SUBROUTINE LUDCMP
C
C       ROUTINE WHICH WORKS IN CONJUNCTION WITH LUBKSB TO INVERT A MATRIX
C       OR SOLVE A SYSTEM OF EQUATIONS.
C
C=============================================================================
C
       IMPLICIT REAL*8 (A-H,O-Z)
       PARAMETER (TINY=1.E-20)
       PARAMETER(NP=100,NPR=8424)
       REAL*16 INDX(N),VV(NP),A(NP,NP)
C
       D=1.
       DO 100 I=1,N
         AAMAX=0.
           DO 110 J=1,N
               IF(QABS(A(I,J)).GT.AAMAX)  AAMAX=QABS(A(I,J))
110        CONTINUE
           IF(AAMAX.EQ.0.) PAUSE '       SINGULAR MATRIX'
           VV(I)=1./AAMAX
100    CONTINUE
       DO 130 J=1,N
         FRAC=(FLOAT(J)/FLOAT(N))*100.
         WRITE(*,1000)FRAC
          DO 140 I=1,J-1
              SUM=A(I,J)
                DO 150 K=1,I-1
                  SUM=SUM-A(I,K)*A(K,J)
150             CONTINUE
              A(I,J)=SUM
140        CONTINUE
           AAMAX=0.
           DO 160 I=J,N
              SUM=A(I,J)
                 DO 170 K=1,J-1
                    SUM=SUM-A(I,K)*A(K,J)
170              CONTINUE
              A(I,J)=SUM
              DUM=VV(I)*DABS(SUM)
              IF(DUM.GE.AAMAX)THEN
                   IMAX=I
                   AAMAX=DUM
              ENDIF
160        CONTINUE
           IF(J.NE.IMAX)THEN
               DO 180 K=1,N
                 DUM=A(IMAX,K)
                 A(IMAX,K)=A(J,K)
                 A(J,K)=DUM
180            CONTINUE
            D=-D
            VV(IMAX)=VV(J)
            ENDIF
            INDX(J)=IMAX
          IF(A(J,J).EQ.0.)A(J,J)=TINY
          IF(J.NE.N)THEN
                DUM=1./A(J,J)
```

```
                  DO 190 I=J+1,N
                      A(I,J)=A(I,J)*DUM
190               CONTINUE
            ENDIF
130       CONTINUE
1000      FORMAT(G12.3,' % COMPLETED WITH LU DECOMPOSITION')
          RETURN
          END
C
C
          SUBROUTINE MEAN(PREDF,V,INDEX,ISIGN,DLOCX,DLOCY)
C=============================================================  SUBROUTINE MEAN
C
C         SUBROUTINE TO SUBRACT THE "MEAN" FROM THE INPUT FIELD
C         IN ORDER TO ACHEIVE STATIONARY FIELD (IF THAT'S POSSIBLE!!)
C         AND THEN ADD IT BACK ON TO THE CONDITIONED OR KRIGED FIELD.
C
C         ISIGN = 1 TO ADD THE MEAN BACK TO THE FIELD
C         ISIGN = -1 TO SUBTRACT THE MEAN VALUES FROM OBSERVED
C         ISIGN = 2 TO SUBTRACT MEAN VALUES FROM THE UNCONDITIONED FIELD
C=============================================================================
C
          IMPLICIT REAL*8 (A-H,O-Z)
          PARAMETER(NP=100,NPR=8424)
          COMMON/DATA/ SCALEX,SCALEY,SCALET,VAR,NPTS,NPRED,IPM0,IMEAN,IPM
          CHARACTER *80 FILMEN
          REAL*8 MEANP(NPR),PREDF(NPR),DLOCX(NP),DLOCY(NP),V(NP,1)
          INTEGER INDEX(NP)
C
        IF(ISIGN.EQ.-1)THEN
            WRITE(*,*)' ENTER DATA FILE OF MEAN FIELD'
            READ(*,'(A)')FILMEN
            OPEN(76,FILE=FILMEN,STATUS='OLD')
C
            READ(76,1000)(MEANP(I),I=1,NPRED)
            IF(IPM.EQ.1)THEN
                  WRITE(90,*)'              MEAN FIELD'
                  WRITE(90,1004)(MEANP(I),I=1,NPRED)
              ENDIF
C
          TOTV=0.
          DO 100 I=1,NPTS
                JPT=INDEX(I)
                V(I,1)=V(I,1) - MEANP(JPT)
                TOTV=TOTV+V(I,1)
100       CONTINUE
          AVEV=TOTV/NPTS
          IF(IPM0.EQ.1)THEN
              WRITE(90,1003)AVEV
              WRITE(90,1001)
              DO 400 I=1,NPTS
                  WRITE(90,1002)I,INDEX(I),V(I,1),DLOCX(I),DLOCY(I)
400           CONTINUE
          ENDIF
        ELSEIF(ISIGN.EQ.1)THEN
          DO 200 I=1,NPRED
                PREDF(I)=PREDF(I) + MEANP(I)
200       CONTINUE
        ELSEIF(ISIGN.EQ.2)THEN
          TOT=0.
          DO 300 I=1,NPRED
                PREDF(I)=PREDF(I)-MEANP(I)
                TOT=TOT+PREDF(I)
300       CONTINUE
                AVE=TOT/NPRED
                WRITE(90,*)' MEAN OF MEAN-0 UNCOND FIELD POINTS=',AVE
        ENDIF
C
1000    FORMAT(8E10.3)
1001    FORMAT(/,10X,' "PICKED" DATA FROM THE UNCONDITIONAL FIELD',/,
     * 10X,' VALUES ARE "PICKED" VALUES MINUS RESPECTIVE MEAN VALUES',//
     *  ,T3,'#',T7,'INDEX #',T20,'VALUE',T35,'X LOCATION',T50,
     *   'Y LOCATION',/79('*')/)
1002    FORMAT(I4,I8,G15.5,T30,G15.5,T46,G15.5)
1003    FORMAT(//79('*'),/10X,' AVERAGE OF INPUT VALUES MINUS ',
```

```
     *       'RESPECTIVE MEAN VALUES  = ',G12.4)
 1004   FORMAT(8G10.3)
        RETURN
        END
C
C
        SUBROUTINE MULTIP(A,B,C,L,N,M)
C======================================================== SUBROUTINE MULTIP
C
C     SUBROUTINE TO MULTIPLY 2 MATRICES
C     MATRIX A IS L ROWS BY N COLUMNS.
C     MATRIX B IS N ROWS BY M COLUMNS.
C     MATRIX C IS L ROWS BY M COLUMNS.
C
C=============================================================================
       IMPLICIT REAL*8 (A-H,O-Z)
       PARAMETER(NP=100,NPR=8424)
       COMMON/DATA/ SCALEX,SCALEY,SCALET,VAR,NPTS,NPRED,IPMO,IMEAN,IPM
       REAL*8 A(NP,NP),B(NP,NP),C(NP,NP)
C
       DO 100 I=1,L
         DO 200 J=1,M
            C(I,J)=0.0
              DO 300 K=1,N
                 C(I,J)=C(I,J)+A(I,K)*B(K,J)
 300           CONTINUE
 200     CONTINUE
 100   CONTINUE
       RETURN
       END
C
C
       SUBROUTINE PICK(UNCOND,PUNCON,PLOCX,PLOCY,INDEX)
C=========================================================  SUBROUTINE PICK
C
C      USED IN CONDITIONAL SIMULATION TECHNIQUE
C      SUBROUTINE WHICH PICKS THE VALUES AT THE "OBSERVED" POINTS IN THE
C      UNCONDITIONED FIELD FOR USE IN THE CONDITIONING ALGORITHM
C
C=============================================================================
C
        IMPLICIT REAL*8 (A-H,O-Z)
        PARAMETER(NP=100,NPR=8424)
        COMMON/MATRX/NPX,NPY,IDIREC,XMIN,XMAX,XSKIP,YMIN,
     *              YSKIP,YMAX,XSTART,YSTART
        COMMON/FLAGS/IFLAGC,IPIN,KFLAG,IPPL,IPTRAN,IPUNC,NUNF,IPPUNC
        COMMON/DATA/ SCALEX,SCALEY,SCALET,VAR,NPTS,NPRED,IPMO,IMEAN,IPM
        REAL*8 UNCOND(NPR,1),PUNCON(NP,1),PLOCX(NPR),PLOCY(NPR)
        INTEGER INDEX(NP)
C
C
C=====  FIND OUT THE LOCATIONS OF THE DATA AND PICK DATA FROM THE SAME
C       LOCATIONS IN THE UNCONDITIONED FIELD AND PRINT IF NEEDED
C

        DO 100 I=1,NPTS
              JPT=INDEX(I)
              PUNCON(I,1)=UNCOND(JPT,1)
 100    CONTINUE
        IF(IPPUNC.EQ.1)THEN
             WRITE(90,1030)
          DO 800 I=1,NPTS
             JPT=INDEX(I)
             WRITE(90,1002)I,INDEX(I),PUNCON(I,1),PLOCX(JPT),PLOCY(JPT)
 800       CONTINUE
        ENDIF
C
 1002   FORMAT(I4,I8,G15.5,T30,G15.5,T46,G15.5)
 1030   FORMAT(//,10X,' "PICKED" DATA FROM THE UNCONDITIONAL FIELD',//,
     *   T3,'#',T7,'INDEX #',T16,'VALUE',T30,'X LOCATION',T45,
     *   'Y LOCATION',/79('*')/)
        RETURN
        END
C
C
        SUBROUTINE READD(V,PLOCX,PLOCY,DLOCX,DLOCY,UNCOND,PUNCON,INDEX)
```

```
C=================================================    SUBROUTINE READD
C
C     SUBROUTINE TO READ THE DATA AND PRINT IF NESSECARY
C
C=============================================================================
C
      IMPLICIT REAL*8 (A-H,O-Z)
      PARAMETER(NP=100,NPR=8424)
      COMMON/MATRX/NPX,NPY,IDIREC,XMIN,XMAX,XSKIP,YMIN,
     *             YSKIP,YMAX,XSTART,YSTART
      COMMON/FLAGS/IFLAGC,IPIN,KFLAG,IPPL,IPTRAN,IPUNC,NUNF,IPPUNC
      COMMON/DATA/ SCALEX,SCALEY,SCALET,VAR,NPTS,NPRED,IPMO,IMEAN,IPM
      COMMON/COV/ICOV,SMALLV
      COMMON/FILES/FILUNC(20),NCF(20),FILPD(20),NCFP(20)
      REAL*8 V(NP,1),PLOCX(NPR),PLOCY(NPR),DLOCX(NP),DLOCY(NP),
     *       UNCOND(NPR,1),PUNCON(NP,1)
      INTEGER INDEX(NP)
      CHARACTER *80 FILDAT,FILOUT,FILPRD,FILUNC,FILPD,FILMEN
      CHARACTER *12 COV(5)
C
      COV(1)='BELL SHAPED '
      COV(2)='EXPONENTIAL '
      COV(3)='LINEAR      '
      WRITE(*,*)' ENTER THE NAME OF THE INPUT FILE CONTAINING THE'
      WRITE(*,*)'     DATA FROM THE SAMPLED FIELD'
      READ(*,'(A)')FILDAT
      OPEN(50,FILE=FILDAT,STATUS='OLD')
      WRITE(*,*)' ENTER THE NAME OF THE OUTPUT FILE'
      READ(*,'(A)')FILOUT
      OPEN(90,FILE=FILOUT,STATUS='UNKNOWN',CARRIAGECONTROL='LIST')
C
C=====  READ THE COVARIANCE INFORMATION AND THEN THE DATA AND LOCATIONS ETC.
C
      READ(50,*)IFLAGC,NUNF,IPIN,KFLAG,IPPL,IPTRAN,IPUNC,ILOGV,IPPUNC,
     *          IPMO,IMEAN,IPM
      READ(50,*)ICOV,VAR,SCALEX,SCALEY
      READ(50,*)XSTART,XMIN,XSKIP,XMAX,YSTART,YMIN,YSKIP,YMAX,IDIREC
      IF(IFLAGC.EQ.2)THEN
        WRITE(90,1070)
        DO 10 II=1,NUNF
          READ(50,'(A)')FILUNC(II)
          NCF(II)=LEN(FILUNC(II))
          READ(50,'(A)')FILPD(II)
          NCFP(II)=LEN(FILPD(II))
          WRITE(90,1071)II,FILUNC(II),II,FILPD(II)
 10     CONTINUE
      ENDIF
      WRITE(90,1060)IFLAGC,NUNF,IPIN,KFLAG,IPPL,IPTRAN,IPUNC,ILOGV,
     *              IPPUNC,IMEAN,IPM,IPMO
      WRITE(90,1005)COV(ICOV),VAR,SCALEX,SCALEY
C
      SMALLV=VAR/1000.
      IF(IFLAGC.EQ.1)NUNF=1
      DO 100 I=1,500
        READ(50,*,END=101)DLOCX(I),DLOCY(I),V(I,1)
 100  CONTINUE
 101  NPTS=I-1
      IF(ILOGV.EQ.1)THEN
          DO 150 J=1,NPTS
            V(J,1)=LOG10(V(J,1))
 150      CONTINUE
      ENDIF
      IF(IPIN.EQ.1)THEN
          WRITE(90,1000)
          DO 200 I=1,NPTS
            WRITE(90,1001)I,V(I,1),DLOCX(I),DLOCY(I)
 200      CONTINUE
      ENDIF
C
C====  FIND THE POINTS AT WHICH PREDICTIONS ARE TO BE MADE
C
      IF(KFLAG.EQ.1)THEN
          WRITE(6,*)' ENTER THE NAME OF THE FILE CONTAINING'
          WRITE(6,*)'     PREDICTION LOCATIONS'
          READ(5,'(A)')FILPRD
          OPEN(70,FILE=FILPRD,STATUS='OLD')
```

```
            DO 300 I=1,8075
               READ(70,*,END=301)PLOCX(I),PLOCY(I)
300         CONTINUE
301         NPRED=I-1
       ELSEIF(KFLAG.EQ.2)THEN
            CALL GETPRED(DLOCX,DLOCY,PLOCX,PLOCY,INDEX)
       ENDIF
C
       WRITE(90,1020)XSTART,XMIN,XSKIP,XMAX,NPX,YSTART,YMIN,
     *               YSKIP,YMAX,NPY,NPRED,IDIREC
        IF(IPPL.EQ.1)THEN
            WRITE(90,1040)
            WRITE(90,*)(PLOCX(I),PLOCY(I),I=1,NPRED)
        ENDIF
C
C===== CHECK IF THE COVARIANCE STRUCTURE IS ANISOTROPIC
C
       DIFFS=DABS(SCALEX-SCALEY)
       IF(DIFFS.GT.01)THEN
           CALL SCALFAC(DLOCX,DLOCY,PLOCX,PLOCY)
       ELSE
           SCALET=SCALEX
       ENDIF
C
C
C===== PRINT PREDICTION LOCATIONS IF NEEDED
C
         IF(IPTRAN.EQ.1.AND.DIFFS.GT..01)THEN
            WRITE(90,1050)
            WRITE(90,1051)(PLOCX(I),PLOCY(I),I=1,NPRED)
         ENDIF
C
C===== SUBTRACT THE MEAN FIELD IF NESSECARY
C
       IF(IMEAN.EQ.1)CALL MEAN(UNCOND,V,INDEX,-1,DLOCX,DLOCY)
C
C
 1000  FORMAT(//,15X,' INPUT DATA FROM THE ORIGINAL FIELD',/79('*'),
     *  /T8,'#',T14,'VALUE',T30,'X LOCATION',T45,'Y LOCATION',/,
     *  79('-')/)
 1001  FORMAT(I8,G15.5,T25,G15.5,T40,G15.5)
 1002  FORMAT(I4,I8,G15.5,T25,G15.5,T40,G15.5)
 1005  FORMAT(//20X,' KRIGING INFORMATION',/79('*')/10X,
     *   'TYPE OF COVARIANCE STRUCTURE.............',A12,/
     *10X,'VARIANCE OF THE MODEL ......................',F12.5,/10X,
     *   'CORRELATION SCALE IN X DIRECTION ...........',F12.5,/10X,
     *   'CORRELATION SCALE IN Y DIRECTION ...........',F12.5,/,
     *   79('*'),/)
 1015  FORMAT(8E10.3)
 1020  FORMAT(79('*')///,T20,' INFORMATION ON PREDICTED FIELD',/,
     *   79('*'),/,
     *   10X,'STARTING POINT IN X DIRECTION            =',G10.3,/,
     *   10X,'MINIMUM GRID DISTANCE IN X DIRECTION     =',G10.3,/,
     *   10X,'GRID SPACING IN X DIRECTION              =',G10.3,/,
     *   10X,'MAXIMUM GRID DISTANCE IN X DIRECTION     =',G10.3,/,
     *   10X,'# OF PREDICTION LOCATIONS IN X DIRECTION =',I10,/,
     *   10X,'STARTING POINT IN Y DIRECTION            =',G10.3,/,
     *   10X,'MINIMUM GRID DISTANCE IN Y DIRECTION     =',G10.3,/,
     *   10X,'GRID SPACING IN Y DIRECTION              =',G10.3,/,
     *   10X,'MAXIMUM GRID DISTANCE IN Y DIRECTION     =',G10.3,/,
     *   10X,'# OF PREDICTION LOCATIONS IN Y DIRECTION =',I10,/,
     *   10X,'TOTAL NUMBER OF PREDICTIONS IN THE GRID  =',I10,/,
     *   10X,'          NUMBERING SCHEME               =',I10,/,
     *   10X,' 1=SUCCESSIVE NUMBERING IN X DIRECTION    ',/,
     *   10X,' 2=SUCCESSIVE NUMBERING IN Y DIRECTION    ',/,79('*')/)
 1040  FORMAT(//,20X,'PREDICTION LOCATIONS    X(1),Y(1),..'/,
     *          79('*'))
 1050  FORMAT(//,10X,'TRANSFORMED PREDICTION LOCATIONS   X(1),Y(1),..',
     *        /,79('*'))

 1051  FORMAT(8G10.3)
 1060  FORMAT(//,20X,'CONTROL PARAMETERS',/,79('*'),/,
     *  10X,'KRIG DATA (1) OR PERFORM CONDITIONAL SIMULATION (2)',/
     *  10X,'.........................................(IFLAGC)=',I5,
     * /10X,'NUMBER OF UNCONDITIONAL FIELDS TO CONDITION ...(NUNF)=',I5,
     * /10X,'PRINT INPUT DATA (1)  .....................(IPIN)=',I5,
```

```
     * /10X,'READ PREDICTION LOCATIONS (1) OR GENERATE (2).(KFLAG)=',I5,
     * /10X,'PRINT PREDICTION LOCATIONS (1) OR NOT (0) .....(IPPL)=',I5,
     * /10X,'PRINT TRANSFORMED PREDICTION LOCATIONS (1) ..(IPTRAN)=',I5,
     * /10X,'PRINT UNCONDITIONED FIELD (1) OR NOT (0).....(IPUNC)=',I5,
     * /10X,'TAKE LOG BASE 10 OF INPUT (1) OR NOT (0).....(ILOGV)=',I5,
     * /10X,'PRINT VALUES PICKED FROM UNCONDITIONAL FIELD (1)',
     * /10X,'.............................................(IPPUNC)=',I5,
     * /10X,'SUBTRACT THE MEAN FIELD AND THEN ADD ON AGAIN (1)'
     * /10X,'.............................................(IMEAN)=',I5,
     * /10X,'PRINT THE MEAN FIELD (1) OR NOT (0).............(IPM)=',I5,
     * /10X,'PRINT "MEAN ZERO" FIELD (1) OR NOT (0).........(IPM0)=',I5,
     * //,79('*'),/)
 1070   FORMAT(//10X,'FILES CONTAINING UNCONDITIONED FIELDS AND ',/10X,
     *       'CORRESPONDING CONDITIONED FIELDS',/79('*'),//)
 1071   FORMAT(10X,'UNCONDITIONED FIELD ',I2,' .............',A20,/10X,
     *            'CONDITIONED FIELD   ',I2,' .............',A20)
        RETURN
        END
C
C
      SUBROUTINE SCALFAC(DLOCX,DLOCY,PLOCX,PLOCY)
C=================================================== SUBROUTINE SCALFAC
C
C     SUBROUTINE TO FIND THE SCALE FACTORS IN THE X AND Y DIRECTIONS
C     FOR ANISOTROPIC MEDIA BY PERFORMING LINEAR TRANSFORMATION.
C
C     XPRIME = NEW COORDINATE TRANSFORM IF SCALEX > SCALEY
C     YPRIME = NEW COORDINATE TRANSFORM IF SCALEY > SCALEX
C
C=============================================================================
C
        IMPLICIT REAL*8 (A-H,O-Z)
        PARAMETER(NP=100,NPR=8424)
        COMMON/UNIT/NUNIT
        COMMON/DATA/ SCALEX,SCALEY,SCALET,VAR,NPTS,NPRED,IPM0,IMEAN,IPM
        REAL*8 DLOCX(NP),DLOCY(NP),PLOCX(NPR),PLOCY(NPR)
C
C===== SET TRANSFORMED ISOTROPIC SCALE EQUAL TO SMALLEST OF 2 SCALES
C
      IF(SCALEX.GT.SCALEY)THEN
          SCALET=SCALEY
          XPRIME=DSQRT(SCALEY/SCALEX)
          YPRIME=1.
      ELSEIF(SCALEX.LT.SCALEY)THEN
          SCALET=SCALEX
          YPRIME=DSQRT(SCALEX/SCALEY)
          XPRIME=1.
      ENDIF
C
C===== RESET ALL OF THE LOCATIONS ACCORDING TO THE TRANSFORMED COORDINATES
C
      DO 100 I=1,NPTS
         DLOCX(I)=XPRIME*DLOCX(I)
         DLOCY(I)=YPRIME*DLOCY(I)
 100  CONTINUE
      DO 200 I=1,NPRED
         PLOCX(I)=XPRIME*PLOCX(I)
         PLOCY(I)=YPRIME*PLOCY(I)
 200  CONTINUE

      WRITE(90,1000)XPRIME,YPRIME,SCALET
1000  FORMAT(//15X,' COVARIANCE STRUCTURE IS ANISOTROPIC',/79('*'),
     *  /10X,'DISTANCE TRANSFORMATION IN X DIRECTION.....=',F10.3,
     *  /10X,'DISTANCE TRANSFORMATION IN Y DIRECTION.....=',F10.3,
     *  /10X,'SCALE USED FOR THE TRANSFORMED DOMAIN......=',F10.3,/
     *  79('*')/)
      RETURN
      END
```

```
2 10 1 2 0 0 0 0 1 1 1 0                                                    ;IFLAGC
2  1. 850. 85.                  ;ICOV,VARIANCE,SCALEX,SCALEY
0. 0. 17. 5474. 0. 0. 17. 408. 2    ;XMIN,XSKIP,XMAX,YMIN,YSKIP,YMAX,IDIREC
KV1C850X10_01.INPUT
CONDEXP_01.INPUT
KV1C850X10_02.INPUT
CONDEXP_02.INPUT
KV1C850X10_03.INPUT
CONDEXP_03.INPUT
KV1C850X10_04.INPUT
CONDEXP_04.INPUT
KV1C850X10_05.INPUT
CONDEXP_05.INPUT
KV1C850X10_06.INPUT
CONDEXP_06.INPUT
KV1C850X10_09.INPUT
CONDEXP_07.INPUT
KV1C850X10_10.INPUT
CONDEXP_08.INPUT
KV1C850X10_11.INPUT
CONDEXP_09.INPUT
KV1C850X10_12.INPUT
CONDEXP_10.INPUT
   493.        391.0000       -5.823900
   493.        374.0000       -6.050600
   493.        357.0000       -6.080900
   493.        340.0000       -6.585000
   493.        323.0000       -6.356500
   493.        306.0000       -7.408900
   493.        289.0000       -5.853900
   493.        272.0000       -5.366500
   493.        255.0000       -3.795900
   493.        238.0000       -5.552800
   493.        221.0000       -5.853900
   493.        204.0000       -5.376700
   493.        187.0000       -4.494900
   493.        170.0000       -5.958600
   493.        153.0000       -5.920800
   493.        136.0000       -5.468500
   493.        119.0000       -6.301000
   493.        102.0000       -6.397900
   493.        85.00000       -6.346800
   2193.00       391.0000        -5.356500
   2193.00       374.0000        -4.958600
   2193.00       357.0000        -4.619800
   2193.00       340.0000        -4.638300
   2193.00       323.0000        -4.744700
   2193.00       306.0000        -5.337200
   2193.00       289.0000        -3.508600
   2193.00       272.0000        -4.136700
   2193.00       255.0000        -4.408900
   2193.00       238.0000        -3.585000
   2193.00       221.0000        -3.602100
   2193.00       204.0000        -4.229100
   2193.00       187.0000        -3.699000
   2193.00       170.0000        -3.309800
   2193.00       153.0000        -4.699000
   2193.00       136.0000        -5.221900
   2193.00       119.0000        -5.958600
   2193.00       102.0000        -6.130800
   3196.000       391.0000         -3.180500
   3196.000       374.0000         -4.124900
   3196.000       357.0000         -3.769600
   3196.000       340.0000         -3.356500
   3196.000       323.0000         -4.193800
   3196.000       306.0000         -4.823900
   3196.000       289.0000         -4.638300
   3196.000       272.0000         -3.494900
   3196.000       255.0000         -4.585000
   3196.000       238.0000         -4.958600
   3196.000       221.0000         -4.699000
   3196.000       204.0000         -3.769600
   3196.000       187.0000         -3.958600
   3196.000       170.0000         -4.065500
   3196.000       153.0000         -4.229100
   3196.000       136.0000         -4.251800
```

```
      program FFT2D
c
c     for sun system
c     library calls to new IMSL (version 10.0) are required.
c
c     This program generates random fields in two-dimensions with
c     prescribed covariance functions.  The procedure used generates
c     random fields with variance 1 and includes a variety of internal
c     covariance/spectral functions.  A more complete description is
c     contained in the program documentation available from Allan
c     Gutjahr, Math Dept., NM Tech, Socorro, NM  87801.
c
c     To compile and link:
c     f77 -o fft -f68881 fft2d.f -limsl10
c
c                                       (you must be on a machine
c                                       which has access to imsl routines
c                                       jupiter for instance)
c
c     Prompts go through standard error so output can be redirected
c     or piped as desired:
c        unit      meaning
c         0      standard error
c         5      standard input
c         6      standard output
c
c     Several different covariance functions are available internally
c     as well as the possibility of linking with a user-defined function
c     via the function g(x,y).
c
c     menu questions concerning parameters such as:
c        m -- size of field
c        scale -- correlation length for x and y
c        dx,dy -- time domain spacing dx and dy
c        sigsq -- input variance
c        itype -- type of covariance/spectral form
c        nseed -- random number seed
c
c     calculated values
c        xmean -- mean of random field
c        var -- variance of random field
c     arrays
c        zr -- real part of random field
c        zc -- complex part of random field
c        zy -- random field
c
c     quadrant structure of 2-dim array is:
c
c     II        I
c     III       IV
c
c     data is in III and II, the rest are zero
c
c     Eight types of covariance-spectral pairs are available:
c        Bell-shaped, isotropic (also called a Gaussian shaped
c           covariance function or double exponential)
c        Mizell - A ( see Mizell, et.al., WRR, 1982 )
c        Mizell - B (  "    "       "      "    "   )
c        Whittle    (  "    "       "      "    "   )
c        Telis      ( see Mantoglou and Wilson, WRR )
c        Exponential
c        Telis head
c        Bell-shaped, non-isotropic
c
c     option available whether to write out real parts, complex parts,
c     or a combination of real and complex parts for random field


c      parameter(maxn=512)
      parameter(maxn=648)
      real zy(maxn/2,maxn/2)
      real zr(maxn/2,maxn/2),zc(maxn/2,maxn/2)
      complex x(maxn,maxn),im,zz
      character*80 label(9),ifln,outfil,talk,ifl19 *19,ifl *10
      character*3 num(12)
```

```
c-----rwksp used by imsl routine
      real rwksp(900000)
c      real rwksp(529460)
      common /worksp/ rwksp
      common /corr/ itype,sigsq,alf2
      common /const/ pi,pi2

      pi=3.141592654
      pi2=2.0*pi
      im=(0.0,1.0)

      label(1)='Bell-shaped, isotropic'
      label(2)='Mizell - A'
      label(3)='Mizell - B'
      label(4)='Whittle'
      label(5)='Telis'
      label(6)='Exponential'
      label(7)='Telis head'
      label(8)='Bell-shaped, non-isotropic'
      label(9)='Exponential, non-isotropic'

      num(1)='_01'
      num(2)='_02'
      num(3)='_03'
      num(4)='_04'
      num(5)='_05'
      num(6)='_06'
      num(7)='_07'
      num(8)='_08'
      num(9)='_09'
      num(10)='_10'
      num(11)='_11'
      num(12)='_12'

      write(0,*)'Enter field size'
      write(0,*)'(a power of 2 less than or equal to 324)'
      read(5,*)m

      write(0,*)'What kind of covariance-spectral pair do you want?'
      do 20 i=1,9
         write(0,10)i,label(i)
 10      format(1x,i2,' = ',a30)
 20   continue
      read(5,*)itype

      if(itype.le.7)then
         write(0,*)'Enter the scale'
         read(5,*)scale
         clx=scale
         cly=scale
         if(itype.eq.2)alpha=pi/4.
         if(itype.eq.3)alpha=3.*pi/16.
         if(itype.eq.4)alpha=pi/2.
      else
         write(0,*)'Enter the x-scale and y-scale'
         read(5,*)xscale,yscale
         clx=xscale
         cly=yscale
      endif

      write(0,*)'Enter the spacings - dx and dy'
      read(5,*)dx,dy

      write(0,*)'Enter variance'
      read(5,*)sigsq

      write(0,*)'Enter seed for random number generator'
      read(5,*)nseed

      write(0,*)'Enter file name for the field characteristics'
      read(5,'(a)')outfil

      write(0,*)'Enter a line of chatter to identify this run'
      read(5,'(a)')talk
```

```
      write(0,*)'Type 0 to write out real and complex parts'
      write(0,*)'Type 1 to write out real part only'
      write(0,*)'Type 2 to write out complex part only'
c      read(5,*)iwrt1
      write(*,*)'       '
      write(*,*)' real part will be written'
      write(*,*)' enter the size of the matrix to be printed'
      write(*,*)'         x,y'
      read(*,*)matx,maty
      write(*,*)'               '
      write(*,*)'   RUNNING PROGRAM '
      write(*,*)' PLEASE DO NOT DISTURB'
      iwrt1=1
      n=2*m
      alf2=alpha**2
      if(clx.ne.1.0)then
         dx=dx/clx
         clx=1.0
      endif
      if(cly.ne.1.0)then
         dy=dy/cly
         cly=1.0
      endif
c-----standard normal RV
      call rnset(nseed)
      sq5=sqrt(0.5)
      dfx=2*pi/(n*dx)
      dfy=2*pi/(n*dy)

      do 40 i=1,m
         do 30 j=1,m
            x1=f(i,j,dfx,dfy)
            sdf=sqrt(x1)
            x2=f(i,-j,dfx,dfy)
            sdf2=sqrt(x2)
c-----puts data in III
            xr=rnnof()*sdf*sq5
            xc=rnnof()*sdf*sq5
            x(i,j)=cmplx(xr,xc)
c-----puts data in II
            xr=rnnof()*sdf2*sq5
            xc=rnnof()*sdf2*sq5
            x(i,n+1-j)=cmplx(xr,xc)
c-----zero I and IV
            x(m+i,j)=(0.0,0.0)
            x(m+i,m+j)=(0.0,0.0)
 30      continue
 40   continue


c-----inverse fast Fourier transform, store in x
      call iwkin(900000)
c      call iwkin(529460)
      call fft2b(n,n,x,maxn,x,maxn)
c      do 45 i=1,m
c         write(6,*)(x(i,j),j=1,m)
c 45   continue

c-----generates 2 independent fields from real and complex parts
      do 60 i=1,m
         do 50 j=1,m
            zx=float(i+j)
            zz=2*x(i,j)*cexp(im*pi*zx/float(n))
            zr(i,j)=real(zz)
            zc(i,j)=aimag(zz)
 50      continue
 60   continue

c-----store random field in zy
      total=0.0
      do 80 i=1,m
            write(*,*)' loading row # ',i,' of ',m
         do 70 j=1,m
            if(iwrt1.eq.0) zy(i,j)=(zr(i,j)+zc(m+1-i,j))/sqrt(2.)
            if(iwrt1.eq.1) zy(i,j)=zr(i,j)
            if(iwrt1.eq.2) zy(i,j)=zc(m+1-i,j)
```

```
            total=total+zy(i,j)
 70       continue
 80    continue

c-----calculate mean of random field
      xmean=total/(m*m)
      var=0.0

c-----print out random field and size
      open(unit=25,file=outfil)
c-----  check how many files are needed and get a name
      write(*,*)' how many seperate files are needed ?'
      write(*,*)' maximum = ',aint(real(m/maty))
      read(5,*)numfil
      write(*,*)' enter the base filename for files  (< 10 letters)'
      read(*,'(a)')ifln
      ifl=ifln(:10)

c
      do 150 nf=1,numfil
        mbg=(nf-1)*maty+1
        mend=nf*maty
        ifl19=ifl//num(nf)//'.input'
        write(*,*)' loading file # ',nf,'    filename   = ',ifl19
         open(unit=22,file=ifl19,status='unknown')
         write(22,*)matx,maty,talk
         write(*,*)' WRITING ',matx,' X ',maty,' FIELD'
         write(*,*)' beginning =',mbg,'  end = ',mend
         write(*,*)'     '
      do 100 i=1,matx
         write(22,*)(zy(i,k),k=mbg,mend)
 100   continue
      close (22)
 150  continue

c-----calculate variance
        var=0.0
        do 91 i=1,m
         do 90 j=1,m
            var=var+(zy(i,j)-xmean)**2
 90       continue
 91      continue
        var=var/(m*m-1)

c-----print out parameter values
      write(25,1500)talk,m,m,label(itype),dx,dy,sigsq,xscale,
     *              yscale,nseed,xmean,var
      write(22,1500)talk,m,m,label(itype),dx,dy,sigsq,xscale,
     *              yscale,nseed,xmean,var
c- covariance-spectral pair-',label(itype)
c      write(25,*)dx,dy,' = dx, dy'
c      write(25,*)sigsq,' = input variance'
c      if(itype.le.7)then
c         write(25,*)scale,' = scale'
c      else
c         write(25,*)xscale,yscale,' = xscale, yscale'
c      endif
c
c      write(25,*)nseed,' = seed'
c      write(25,*)xmean,' = mean'
c      write(25,*)var,' = calculated variance'
 1500 format(//,79('*'),//,a80,//,
     * 10x,'SIZE OF GRID GENERATED ..........',i3,' X ',i3,/,
     * 10x,'TYPE OF STRUCTURE   ..............',a30,/,
     * 10x,'DELTA X AND Y ....................',f6.4,2x,f6.4,/,
     * 10x,'INPUT VARIANCE ...................',f10.4,/
     * 10x,'X AND Y SCALE ....................',f5.1,2x,f5.1,/,
     * 10x,'SEED FOR RANDOM NUMBER GENERATOR..',i10,/
     * 10x,'CALCULATED MEAN...................',f10.4,/,
     * 10x,'CALCULATED VARIANCE ..............',f10.4,//,79('*'))
 1501  format(8e10.3)
      close(unit=25)

 999  end

c-----spectral distribution
```

```
      function f (i,j,dfx,dfy)
      f=dfx*dfy*g((i-0.5)*dfx,(j-0.5)*dfy)
      return
      end

c-----spectral density
      function g (x,y)
      common /const/ pi,pi2
      common /corr/ itype,sigsq,alf2

      xy = x**2 + y**2
      if(itype.eq.1.or.itype.eq.8)gg=(exp(-xy/4.))/(4.*pi)
      if(itype.eq.2) gg = (2.*alf2*xy)/(pi*(xy+alf2)**3)
      if(itype.eq.3) gg = (3.*alf2*xy)/(pi*(xy+alf2)**4)
      if(itype.eq.4) gg = alf2/(pi*(xy+alf2)**2)
      if(itype.eq.5.or.itype.eq.7) gg = 2.*sqrt(xy)/(pi**2*(1.+xy)**2)
      if(itype.eq.6.or.itype.eq.9) gg = 1./(pi2*sqrt((1.+xy)**3))
      if(itype.eq.7)gg = gg*(x**2)/(xy**2)
      g = sigsq*gg
      return
      end
```